Effects of Climate and Land-Use on Flooding in the Illinois River Basin of Oklahoma and Arkansas

Rheannon Hart, Edmund Howe, and Maranda Blankenship

Hydraulics and Technical Services Branch
U.S. Army Corps of Engineers – Little Rock District
700 W. Capitol Ave
Little Rock, AR 72201

DATE: MAY 3, 2023

Table of Contents

Effects of Climate and Land-Use on Flooding in the Illinois River Basin of Oklahoma and Arkansas

By Rheannon M. Hart, Edmund M. Howe, and Maranda Blankenship

Introduction

The Illinois River originates in northwest Arkansas, west of Fayetteville, Arkansas in Washington County where it flows approximately 40 miles to the Arkansas-Oklahoma border. After leaving Arkansas, the river flows southwesterly approximately 50 miles before it is impounded at Lake Tenkiller near Tahlequah, OK (Figure 1). The drainage area of the Illinois River is split near evenly between Arkansas and Oklahoma with 45 percent in Arkansas and 55 percent in Oklahoma. The Illinois River has been contentious between Arkansas and Oklahoma primarily because of nutrient concerns. In November 2018, Oklahoma and Arkansas entered an agreement designed to follow a science-based regulatory process for water quality standards.

Flooding along the Illinois River has been a regular occurrence since the mid-2000's. In fact, since 2011, the Illinois River streamgage South of Siloam Springs (near the Arkansas-Oklahoma border and operated by the U.S. Geological Survey (USGS)) has exceeded the 25-year flood level twice and exceeded a 100-year flood level once. Prior to 2011, the highest recorded peak streamflow was 50,000 cubic feet per second (since 1996) which is approximately a 5-year flood event.

Significant increases in rainfall, sedimentation in the stream, channel debris, and substantial land use changes in the basin are likely causes for the increase in flooding problems. U.S. Army Corps of Engineers (USACE) analysis of flow in the Illinois River from Prairie Grove, Arkansas, to Lake Tenkiller have indicated several reasons for the increased frequency and magnitude of flooding in the Illinois River, with the most likely being an increase in runoff from heavier precipitation into the Illinois River.

Objective and Scope

The objective of this study is to identify the major contributing factors to the increased water levels in the Illinois River in northwest Arkansas and northeast Oklahoma and to present scenarios that may identify ways to decrease the frequency and magnitude of flooding. To accomplish these tasks, the study focused on three components: 1) Illinois River gage analysis, 2) climatic variability and hydrology as it relates to a) streamflow and b) precipitation and runoff, and 3) comprehensive hydraulic analysis.

The following report sections will describe the spatial distribution and temporal trends of the annual, seasonal and monthly precipitation, streamgage data temporal trends for select streamgages, temporal and spatial variability on trends for various streamflow characteristics, model data input, results of simulating historical storm events and select scenarios within the Illinois River watershed.

Previous Investigations

The Illinois River watershed has been the location for many scientific studies, particularly for water quality. The predominant water quality concern for the Illinois River watershed has been nutrients, in particular, increased total phosphorus concentrations resulting primarily from nonpoint sources of cattle and poultry production (Oklahoma Conservation Commission, 2010; Oklahoma Department of Environmental Quality, 2018).

An assessment of the Illinois River in Arkansas from 2001 to 2005 determined this stretch of river to be impaired by turbidity. The State of Arkansas subsequently added this stretch of stream to the state's 2006 303(d) list of impaired waters for turbidity. However, implementation of best management practices has been effective in reducing turbidity concentrations in the Illinois River in Arkansas and the waterbody is now meeting turbidity standards (Arkansas Department of Environmental Quality, 2018).

The State of Oklahoma has several stretches of the Illinois River and its large tributaries (Flint Creek and Baron Fork) listed on its 303(d) list of impaired waters for Dissolved Oxygen (DO), Chlorophyll-a, Enterococcus, Escherichia coli (E-coli), and Total Phosphorus. The State of Arkansas has placed the Illinois River watershed, including Osage Creek, in a Category 3 for total phosphorus and Category 5 for pathogens (Arkansas Department of Environmental Quality, 2018). A Category 3 designation indicates potential impacts or downward trends in water quality and a Category 5 designation indicates the waterbody is impaired, or one or more water quality standards are not attained, i.e., the 303(d) list of impaired waters (Arkansas Department of Environmental Quality, 2018). Potential sources for pathogens are listed as failing septic systems, from wildlife, illicit discharges, agriculture, urban runoff, and others (Arkansas Department of Environmental Quality, 2018).

The Illinois River has been fraught with litigation, contentious dialogue, and other controversy that has led the two States to come together and combat the water quality issues. In 2003, the states signed the first "Joint Statement of Principles and Actions" to improve and protect the water quality in the Illinois River watershed. Subsequently, in 2013, a Joint Study Committee was established to reach agreement on the procurement, execution and conduct of the "Joint Study". And, most recently (2018), the States signed a MOA that outlines the formation of a Watershed Improvement Plan (WIP) for developing science-based regulatory actions and permitting.

Description of Study Area

The Illinois River watershed is situated in the Ozark Plateaus of northwest Arkansas and northeast Oklahoma. Its headwaters originate in northwest Arkansas, southwest of Fayetteville, near the communities of Hogeye and Onda and flows in a southwesterly direction until its confluence with the Arkansas River. The drainage area is approximately 1,653.4 square miles and is predominantly forested. There are primarily 4 large communities, Bentonville, Rogers, Springdale, and Fayetteville, within the drainage area that together encompass an area of 167.5 square miles with a population of approximately 280,575. These 4 communities are located in northwest Arkansas near the headwaters of the Illinois River and Osage Creek, a major tributary of the Illinois River (Figure 1).
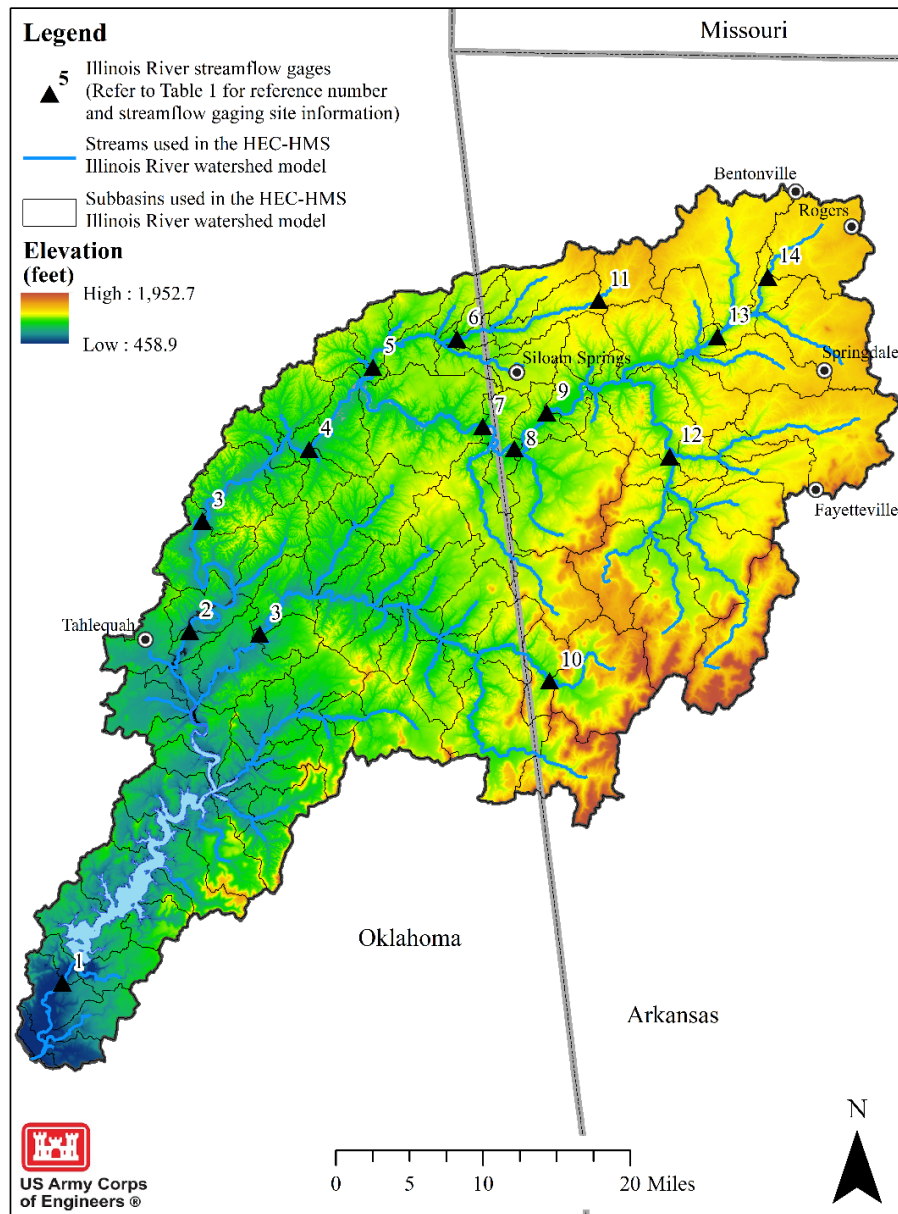
Figure 1. Study area of the Illinois River watershed.

Deemed an ecologically sensitive waterbody by Arkansas Department of Environmental Quality (Arkansas Department of Environmental Quality, 2018) and an Oklahoma State Scenic River, the Illinois River has been recognized as one of Oklahoma's most valuable water resources. As an ecologically sensitive waterbody, segments of the stream are known to provide habitat within the existing range of threatened, endangered, or endemic species of aquatic or semi-aquatic life forms (Arkansas Department of Environmental Quality, 2018). And, as a Scenic River, the Illinois River is the highest designated protected waterbody in Oklahoma (Oklahoma Department of Environmental Quality, 2018).

Trends

Trend analysis is essential for water-resources management. Methods, such as the Mann-Kendall test and the Sen's Slope estimator, are used to evaluate the presence of a statistically significant trend in climatological and hydrological time series. Statistically significant trends can be useful for parsing potential cause and effect of flooding within watersheds. The Mann-Kendall trend test and the Sen's Slope estimator are both nonparametric tests and are commonly used in hydrologic studies (Praveen et al., 2020; Feng et al., 2016). The streamflow gaging sites and sites used for calibration of the HEC-HMS watershed model and select sites used for trend analysis are given in Table 1.

Table 1. USGS stream gaging sites used for calibration of the HMS Illinois River watershed model and select sites used for trend analysis. Refer to Figure 1 for location of each within the watershed.

Label Number (refer to Figure 1)	Site Number	Site Name	Latitude	Longitude
1	07198000	Illinois River near Gore, OK	35.5731511	-95.068845
2	07196500	Illinois River near Tahlequah, OK	35.9228688	-94.923565
3	07197000	Baron Fork at Eldon, OK	35.9212003	-94.838563
4	07196090	Illinois River at Chewey, OK	36.1042527	-94.782728
5	07196000	Flint Creek near Kansas, OK	36.1864724	-94.706891
6	07195855	Flint Creek near West Siloam Springs, OK	36.2161111	-94.605277
7	07195500	Illinois River near Watts, OK	36.1300818	-94.572164
8	07195430	Illinois River South of Siloam Springs, AR	36.1086111	-94.533333
9	07195400	Illinois River at Hwy. 16 near Siloam Springs, AR	36.1447222	-94.494722
10	07196900	Baron Fork at Dutch Mills, AR	35.88	-94.486388
11	07195800	Flint Creek at Springtown, AR	36.2561111	-94.433611
12	07194800	Illinois River at Savoy, AR	36.1030555	-94.344444
13	07195000	Osage Creek near Elm Springs, AR	36.2219444	-94.288333
14	07194880	Osage Creek near Cave Springs, AR	36.2814662	-94.227983

Land-Use Trends

Land-use changes have created disturbances in streams in the Ozarks beginning at or near the time of European settlement (Jacobson and Primm, 1997). The first change in land cover was the conversion of valley-bottom forest with cultivated fields and pasture in the early 1800s followed by harvesting of shortleaf pine for sawlogs and oak for railroad ties beginning in the mid to late 1800s and continuing until early 1920s (Jacobson and Primm, 1997). The period between 1920 and 1960 has been indicated as the period when most stream disturbance occurred due to annual burning of uplands and cut-over valley-side slopes, increased grazing on open range, and increased use of marginal land for cultivated crops (Jacobson and Primm, 1997). Furthermore, historical accounts consistently recall that smaller streams had more discharge for longer periods from 1920 to 1960 than from 1960 and onward and that floods were "flashier" under then present-day (1993) conditions (Jacobson and Primm, 1997). Finally, destruction of riparian vegetation in the channels and banks by free-range livestock was probably the most destabilizing effect on Ozark streams, as well as destruction in small valleys which may have encouraged headward migration of channels, resulting in extension of the drainage network and accelerated release of gravel from storage in the small valleys (Jacobson and Primm, 1997).

The Ozarks have undergone some major land-use changes since the settlement of Europeans; however, Northwest Arkansas has seen substantial and rapid land-use changes, primarily, in the cities of Fayetteville, Springdale, and Rogers beginning in the early 1990s (Figures 2 and 3). Furthermore, the population for Benton and Washington Counties (the counties containing the aforementioned cities) has more than doubled (145.76% increase) from 1990 (210,908; U.S. Census Bureau, 2000) to 2019 (518,328) (U.S. Census Bureau, 2020; Figure 4).
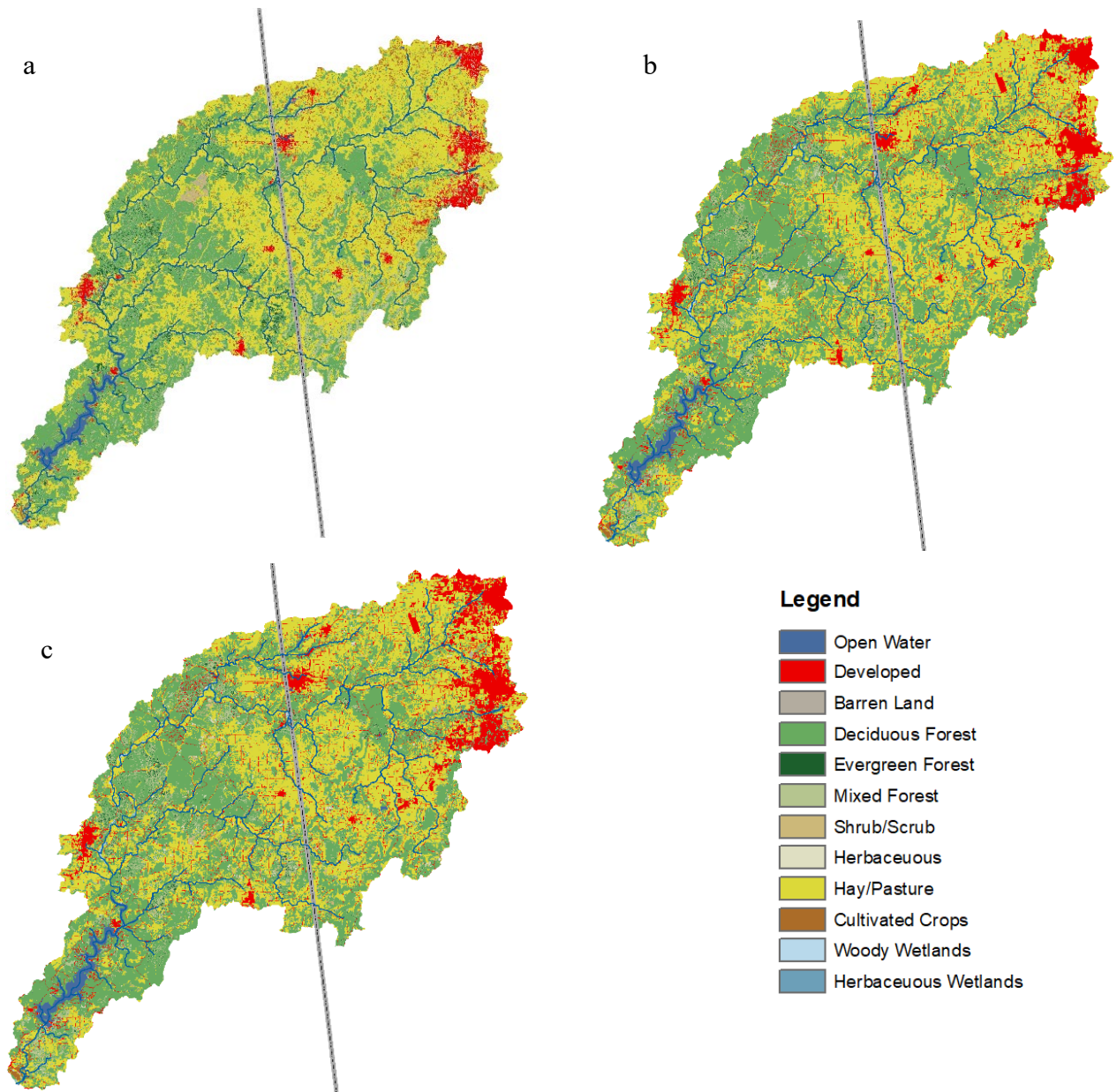
Figure 2. Land-use change through time: a, National Land Cover Database 1992; b, National Land Cover Database 2001; c, National Land Cover Database 2016 (Homer et al., 2012).
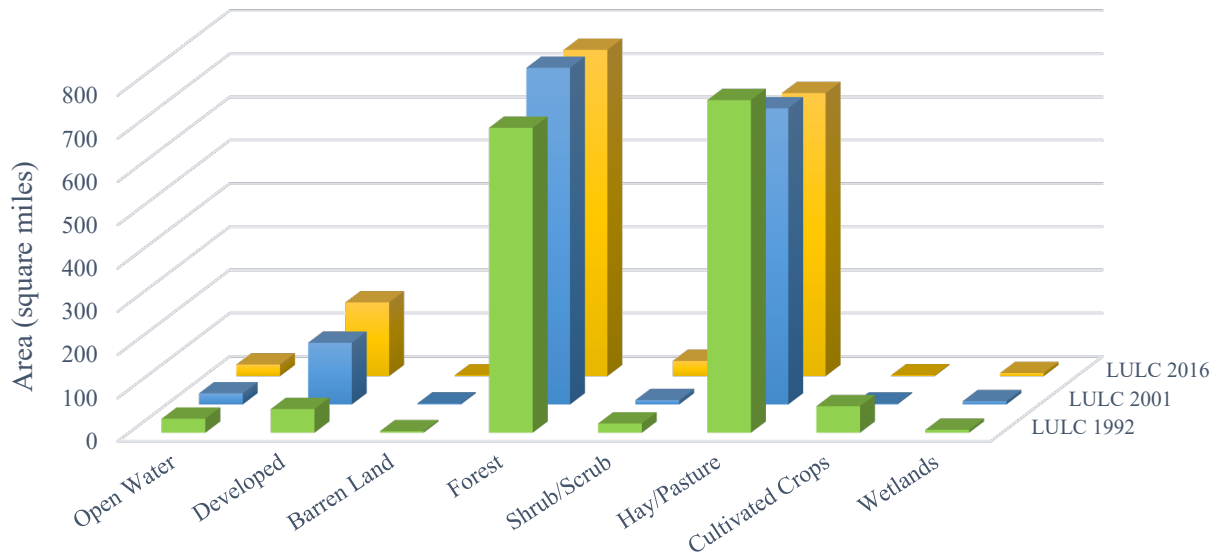
Figure 3. Land-use land-cover area change between National Land Cover Database 1992, 2001, and 2016 (Homer et al., 2012).
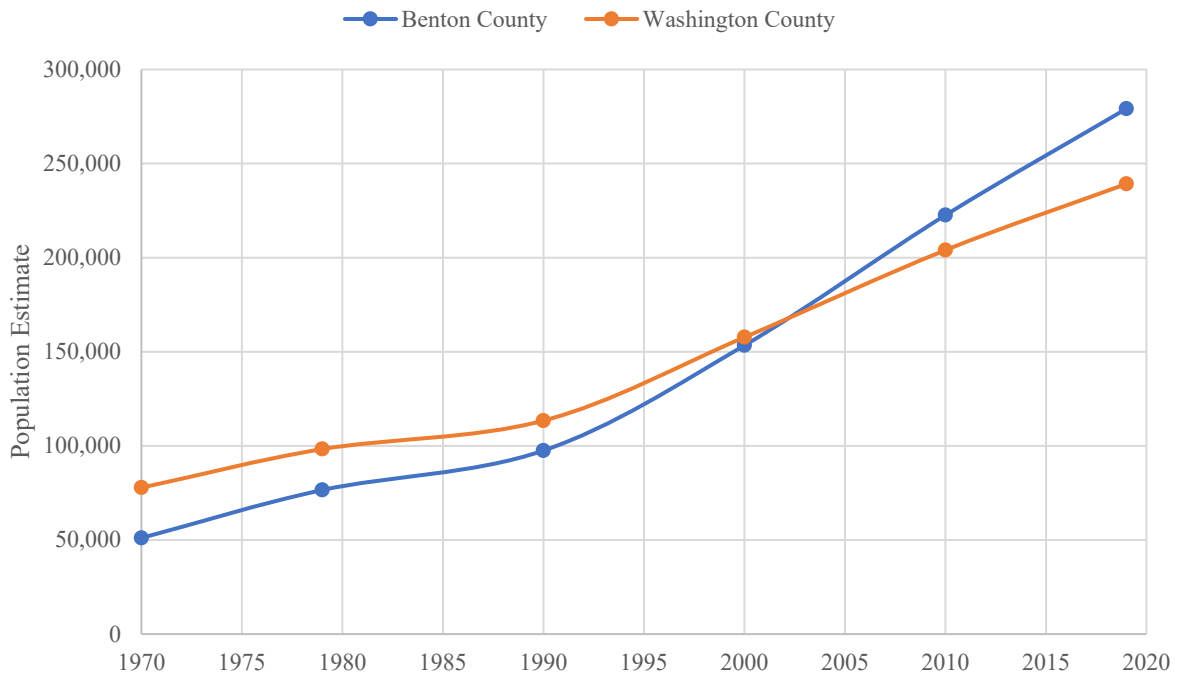
Figure 4. Population trends for Benton and Washington County, Arkansas (U.S. Census Bureau, 2021).

Land-use changes, such as urbanization, can enhance runoff generation and hence flood peaks (Merz et al., 2021) and these effects are most important in small watersheds where the fraction of land-use change can be large relative to the catchment area (Merz et al., 2021). However, Rogger et al., (2017) pointed out that it is difficult to obtain general statements on the impacts of land use changes on streamflow and floods; furthermore, land-use change impacts on floods are poorly understood at the catchment scale and the exact role of land-use change in modifying river floods is still elusive (Rogger et al., 2017). Again, at the small catchment scale, it has been demonstrated that urbanization creates higher surface runoff and river discharge rates and shortened times to achieve the peak runoff and discharge (Feng et al., 2021). Furthermore, flood-frequency models have been used to prove that urbanization has statistically significant effect on the growing magnitude and frequency of floods (Feng et al., 2021). More specifically, Feng et al., (2021) determined "urbanization leads to the increase in peak discharge and shortens the time before the peak arrives during an event and the downstream areas exhibited higher flood depth increases and larger flood extent increases than the upstream areas due to urbanization in the contributing areas". In summary, it has been shown that flooding on a local scale is affected by urbanization, but at a regional scale, land-use change impacts are not as easily understood.

Precipitation Trends

It has been well documented that climate change is causing extremes in the climate, particularly, observed increases in precipitation (Myhre et al., 2019; Blunden and Arndt, 2020). Based on the "State of the Climate in 2019" (Dunn et al., 2020), the spring Climate Extremes Index (CEI) was the highest spring value (2019) on record for the contiguous United States, with 6 of the 10 highest spring totals occurring in the 2010s. Additionally, the season also saw record CEI highs in the South and Southwest climate regions (Dunn et al., 2020). Furthermore, in general, it has been determined the largest changes in precipitation events are with the frequency rather than the magnitude of heavy precipitation (Mallakpour and Villarini, 2015; Myhre et al., 2019). However, within the Illinois River watershed, both frequency and magnitude have increased.

Statistical trends were determined both seasonally and yearly for select sites. Historical precipitation data were obtained from the Parameter-elevation Regressions on Independent Slopes Model (PRISM; PRISM, 2021). The monthly gridded data extends back to January 1895 and continues through December 2019. These monthly gridded values were extracted for select gage's subbasins and represents the monthly total for any given year. Each subbasins' monthly values were either separated into different seasons with the spring season represented by the months of March, April, May, the summer season represented by the months of June, July, and August, the fall season represented by the months of September, October, and November, and the winter season represented by the months of December, January, and February, or totaled to obtain a yearly precipitation by summing each month for that particular year.

Using daily PRISM precipitation data (PRISM, 2021), storm intensity was also examined for select sites within the Illinois River watershed. Daily PRISM gridded data begins in January 1981 and continues through December 2021. These daily gridded data were used to determine days per year where 24-hour precipitation accumulation exceeded 2 inches and annual maximum 24-hour and 48- hour precipitation accumulation. For the 24-hour precipitation accumulation, the number of days that have exceeded 2 inches has increased, overall, since 1981, and notably since

the mid-2000s (Figure 5). Furthermore, the annual maximum precipitation accumulation for both the 24- and 48-hour time periods has also increased, overall, since 1981, and notably since the mid-2000s (Figures 6 and 7). Osage Creek near Elm Springs, AR, had the largest increase in annual maximum 24-hour and 48-hour precipitation accumulation (Figures 6 and 7, respectively).
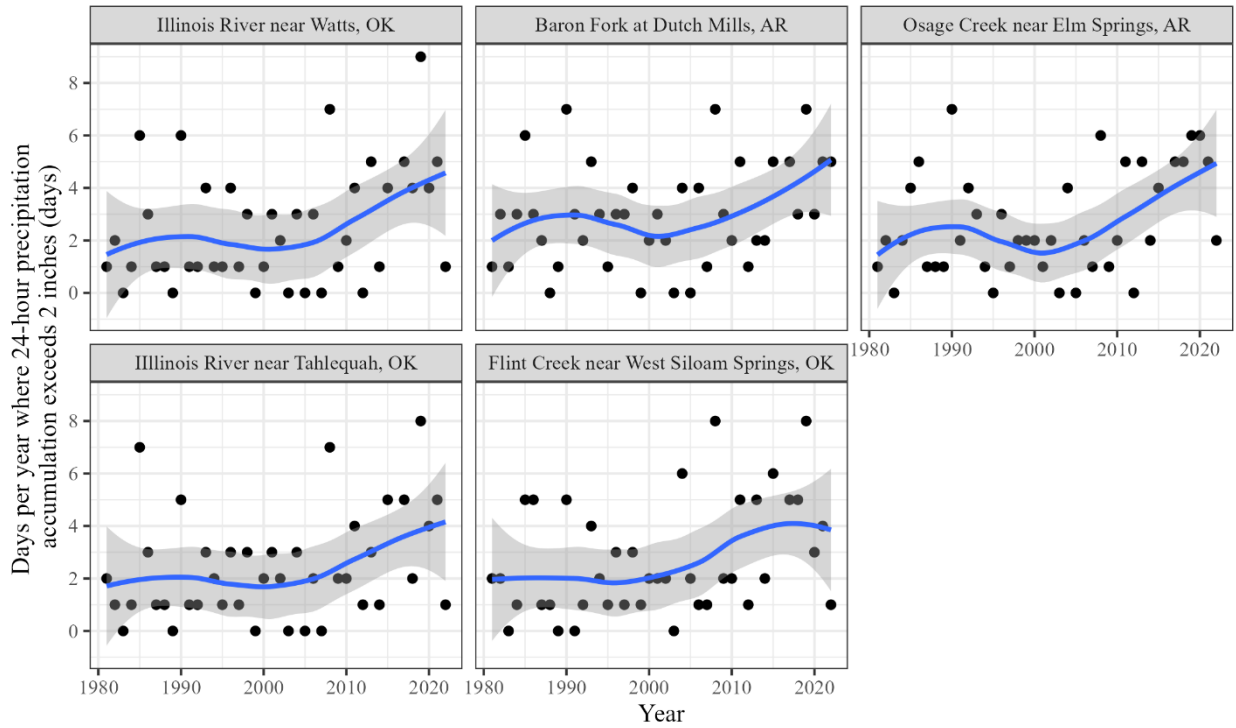
Figure 5. Days per year where 24-hour precipitation accumulation exceeds 2 inches for select sites within the Illinois River watershed (blue line is a locally estimated scatterplot smoothing (LOESS) curve with 95% confidence limits (grey area)).
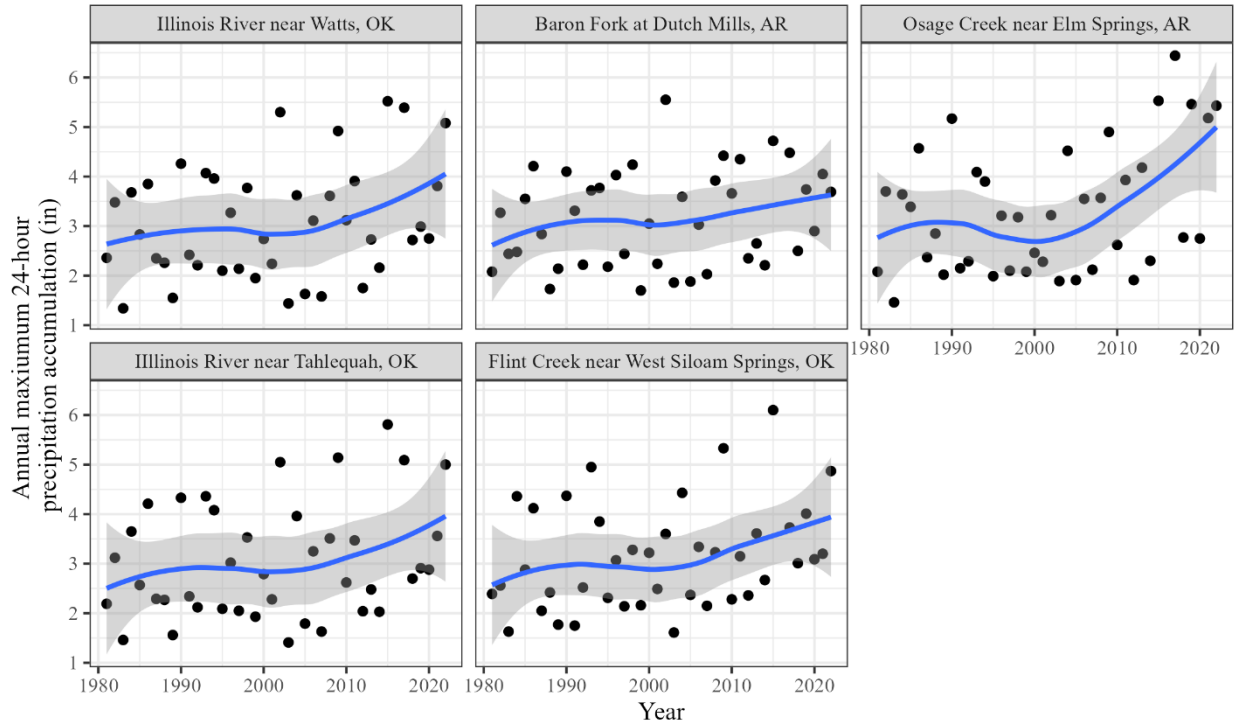
Figure 6. Annual maximum 24-hour precipitation accumulation for select sites within the Illinois River watershed (blue line is a locally estimated scatterplot smoothing (LOESS) curve with 95% confidence limits (grey area)).
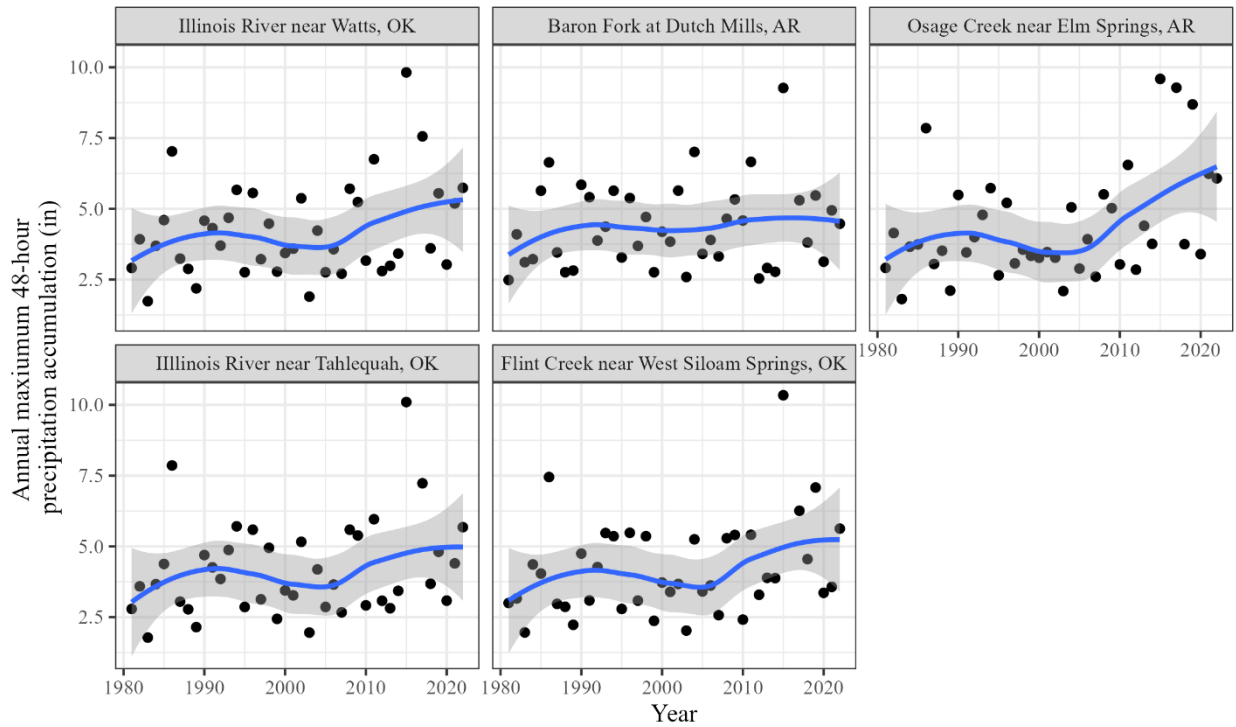
Figure 7. Annual maximum 48-hour precipitation accumulation for select sites within the Illinois River watershed (blue line is a locally estimated scatterplot smoothing (LOESS) curve with 95% confidence limits (grey area)).

10

Overall, precipitation has been increasing in the Illinois River watershed. Figures 8 to 12 show an increasing trend in total annual precipitation for several subbasins within the watershed with the greatest increase at Osage Creek near Elm Springs (Figure 8).
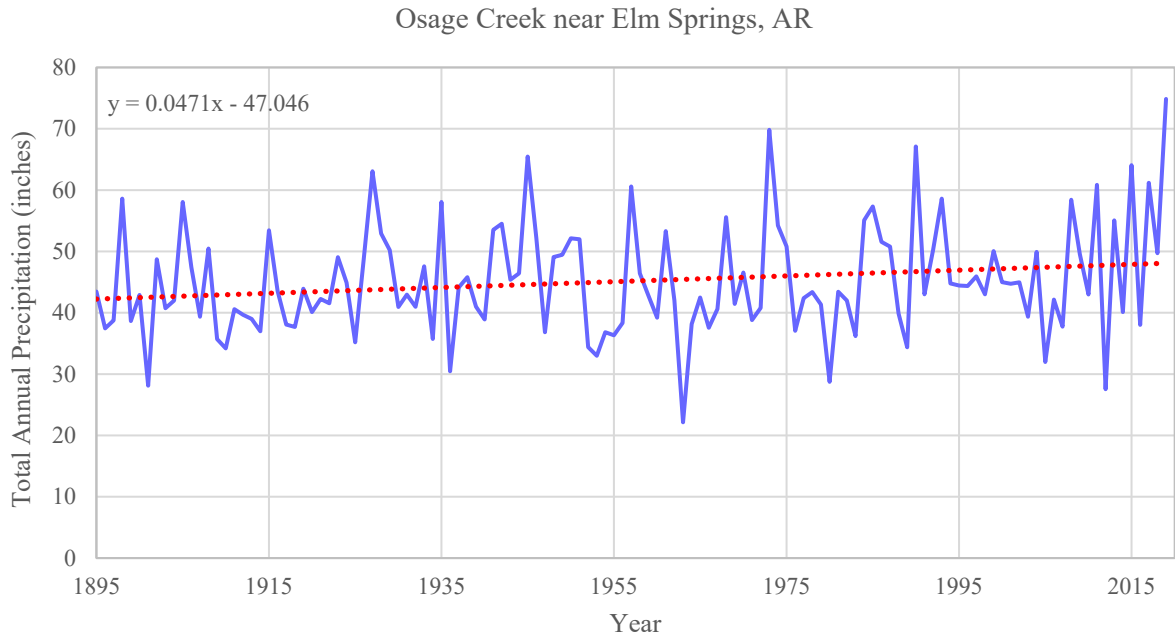
Figure 8.Total annual precipitation, in inches, for Osage Creek near Elm Springs, AR.
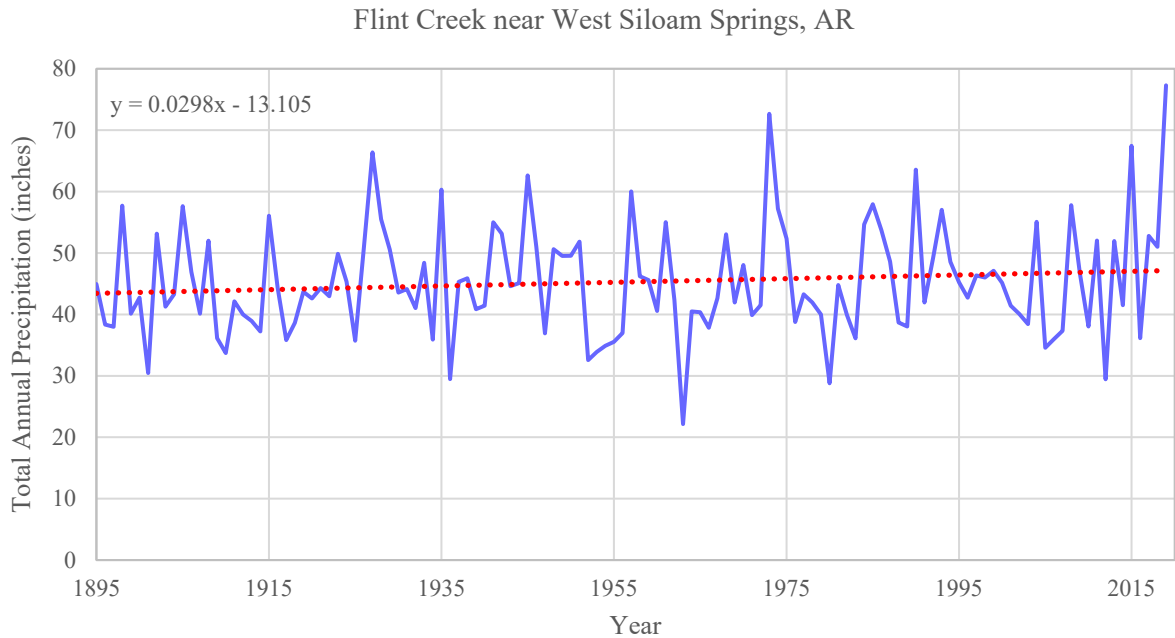
Figure 9. Total annual precipitation, in inches, for Flint Creek near West Siloam Springs, AR.

Baron Fork at Dutch Mills, AR

y = 0.0372x - 25.444
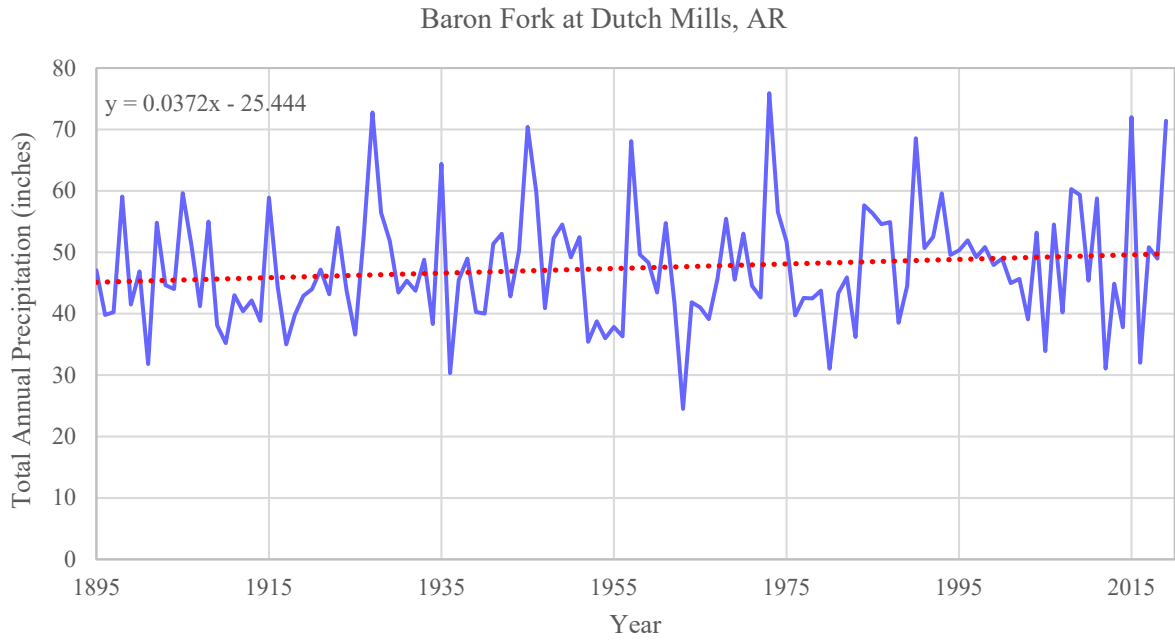
Figure 10. Total annual precipitation, in inches, for Baron Fork at Dutch Mills, AR.

Illinois River near Watts, OK

y = 0.0347x - 22.48
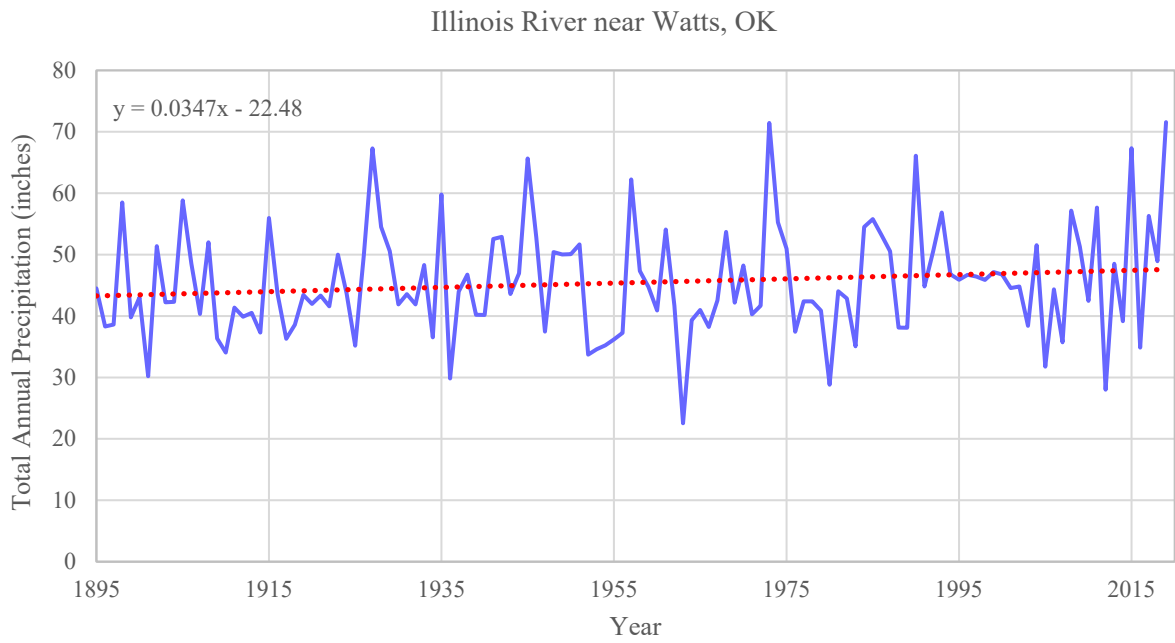
Figure 11. Total annual precipitation, in inches, for Illinois River near Watts, OK.

Illinois River near Tahlequah, OK

y = 0.0347x - 22.603
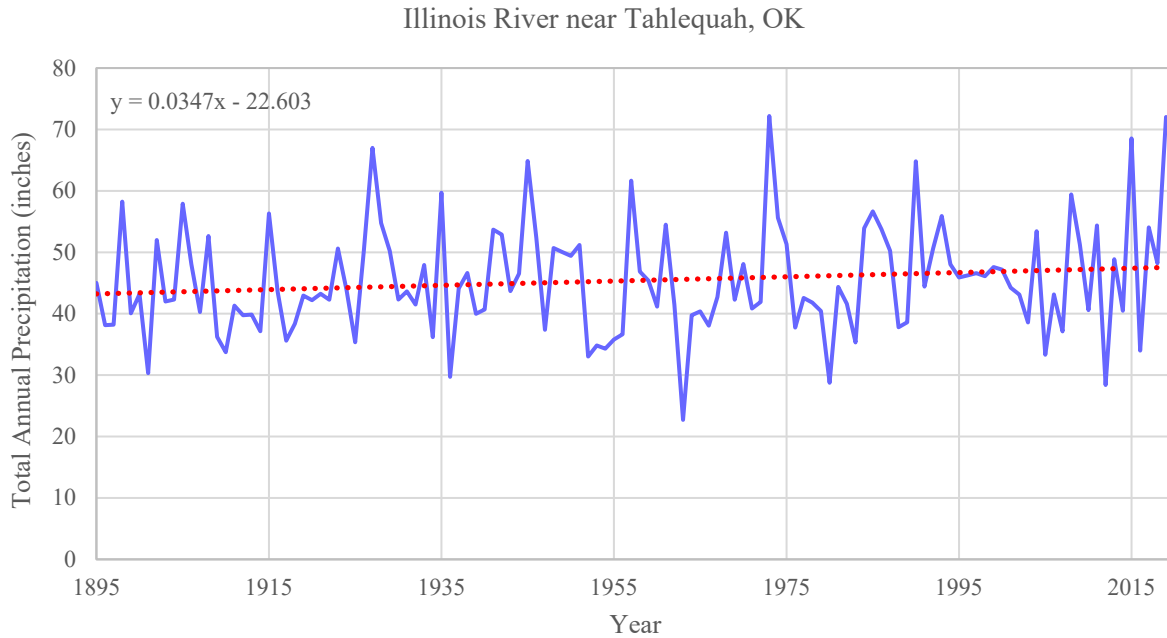
Figure 12. Total annual precipitation, in inches, for Illinois River near Tahlequah, OK.

Using the same PRISM data (PRISM, 2021), departures from the long-term average were also examined for select sites within the Illinois River watershed. For each subbasin, the average precipitation for the entire period of record (1895-2019) was calculated and the departure from that long-term average was determined. Additionally, a locally estimated scatterplot smoothing (LOESS) curve (moving regression) was fit through the data along with its 90 percent confidence limits. Departures from the long-term average help discern average, wet, and dry years and the LOESS curve reveals trends and cycles within the data. For all sites, beginning in 2008, there is an increasing trend in the long-term average precipitation and more so in the last decade (Figures 13 to 17).

Annual precipitation departure for Osage Creek near Elm Springs, AR
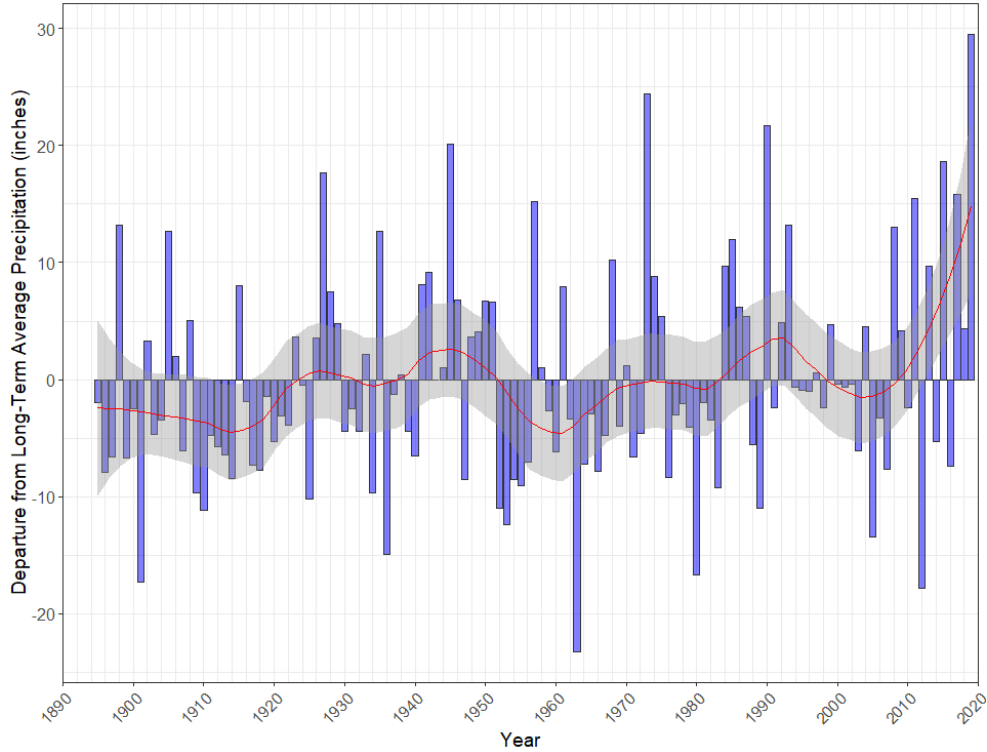
Figure 13. Annual precipitation departure, in inches, from the long-term average precipitation (1895-2019) for Osage Creek near Elm Springs, AR, (red line is a LOESS curve with 90% confidence limits (grey area)).

Annual precipitation departure for Flint Creek near West Siloam Springs, AR
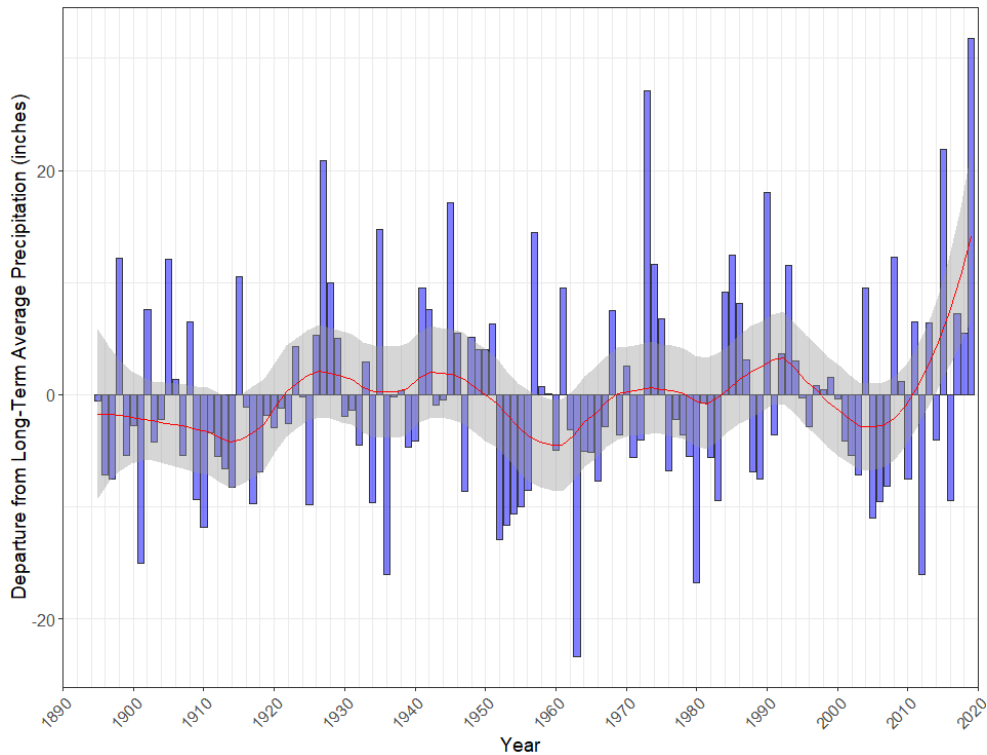
Figure 14. Annual precipitation departure, in inches, from the long-term average precipitation (1895-2019) for Flint Creek near West Siloam Springs, AR, (red line is a LOESS curve with 90% confidence limits (grey area)).

Annual precipitation departure for Baron Fork at Dutch Mills, AR
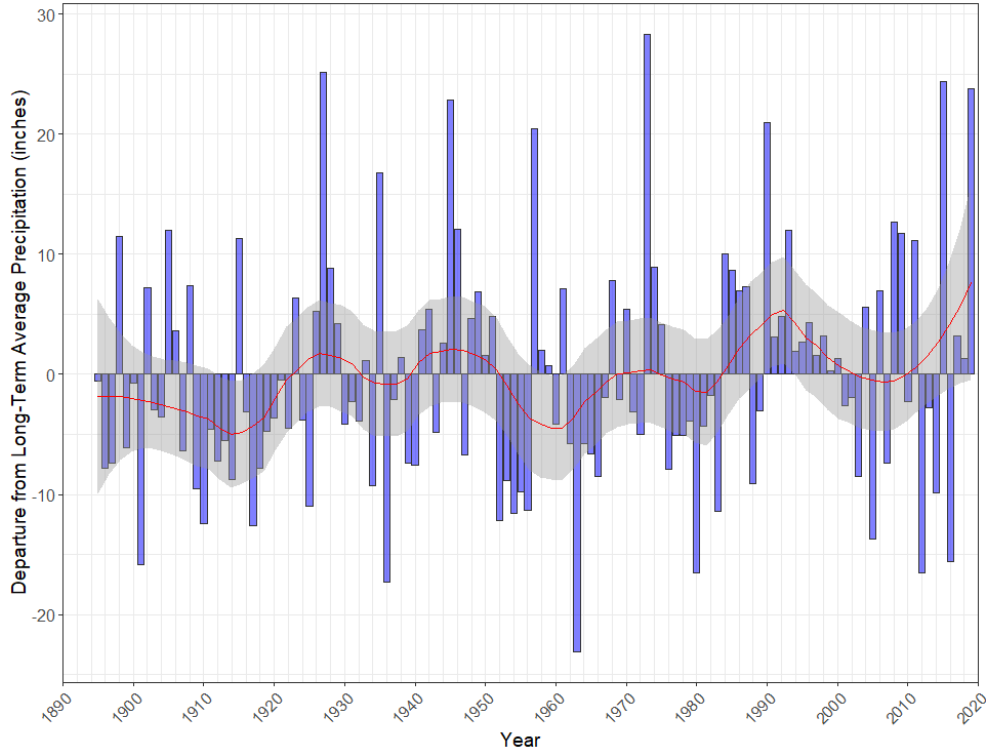
Figure 15. Annual precipitation departure, in inches, from the long-term average precipitation (1895-2019) for Baron Fork at Dutch Mills, AR, (red line is a LOESS curve with 90% confidence limits (grey area)).

Annual precipitation departure for Illinois river near Watts, OK
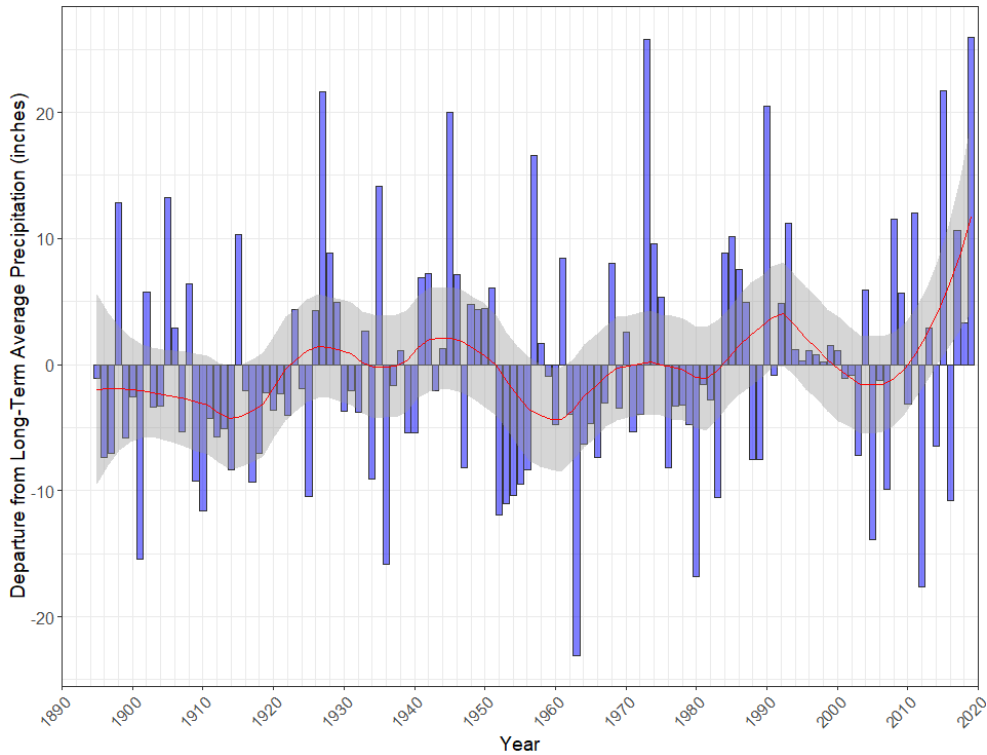
Figure 16. Annual precipitation departure, in inches, from the long-term average precipitation (1895-2019) for Illinois river near Watts, OK, (red line is a LOESS curve with 90% confidence limits (grey area)).
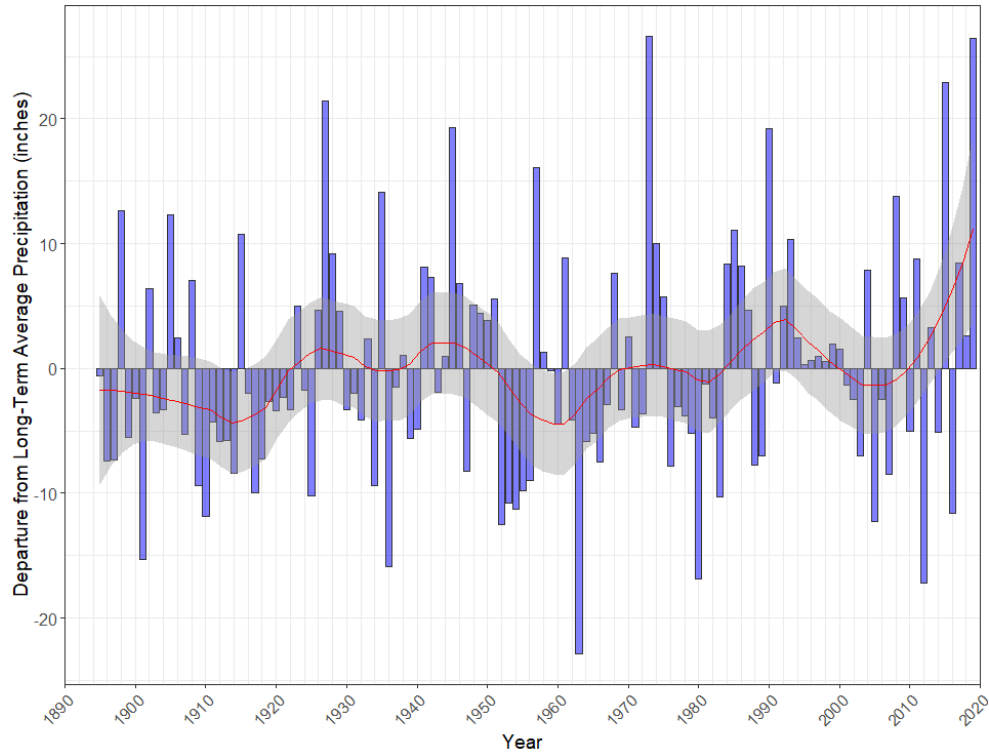
Figure 17. Annual precipitation departure, in inches, from the long-term average precipitation (1895-2019) for Illinois River near Tahlequah, OK, (red line is a LOESS curve with 90% confidence limits (grey area)).

In addition to annual trends in precipitation, seasonal trends in precipitation were also examined for select sites. Again, the most notable increasing trend occurs in approximately the last decade, beginning in 2008, particularly for the winter and spring seasons (Figure 18 to 22). However, there is also an increasing trend for summer and fall precipitation for most sites for the period beginning in 2008 (Figures 18, 19, 21, and 22), the exception being Baron Fork at Dutch Mills where there is not any notable trend in fall precipitation (Figure 20).

Winter Precipitation for 07195000

Spring Precipitation for 07195000

c
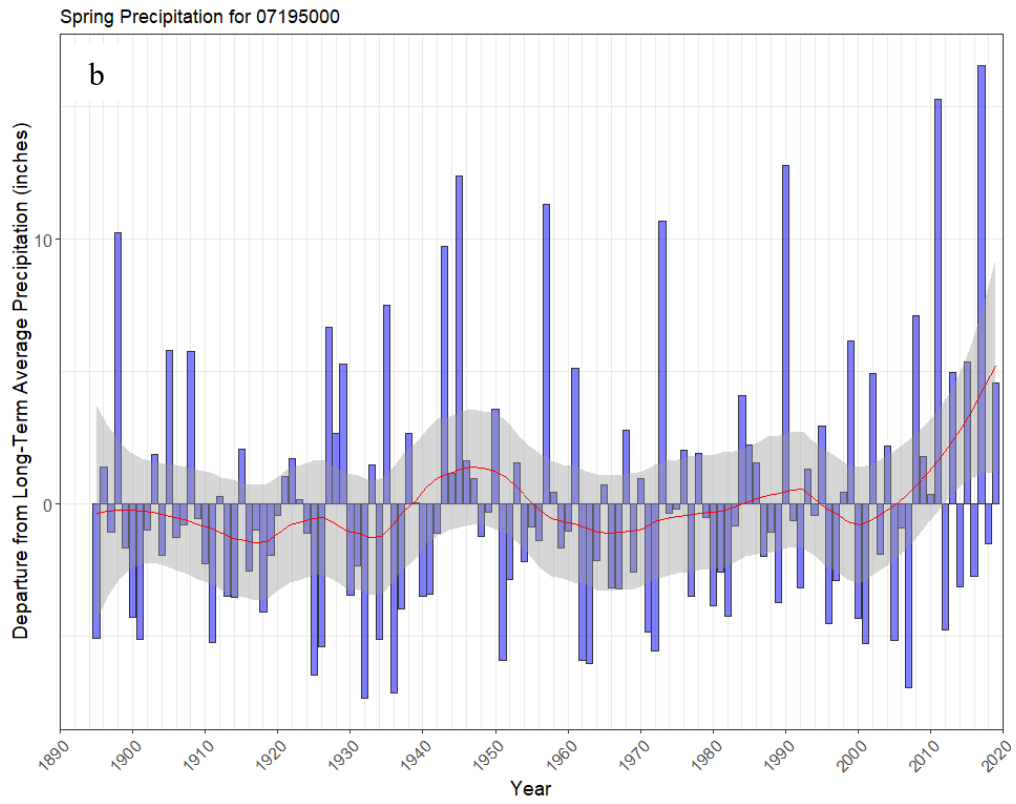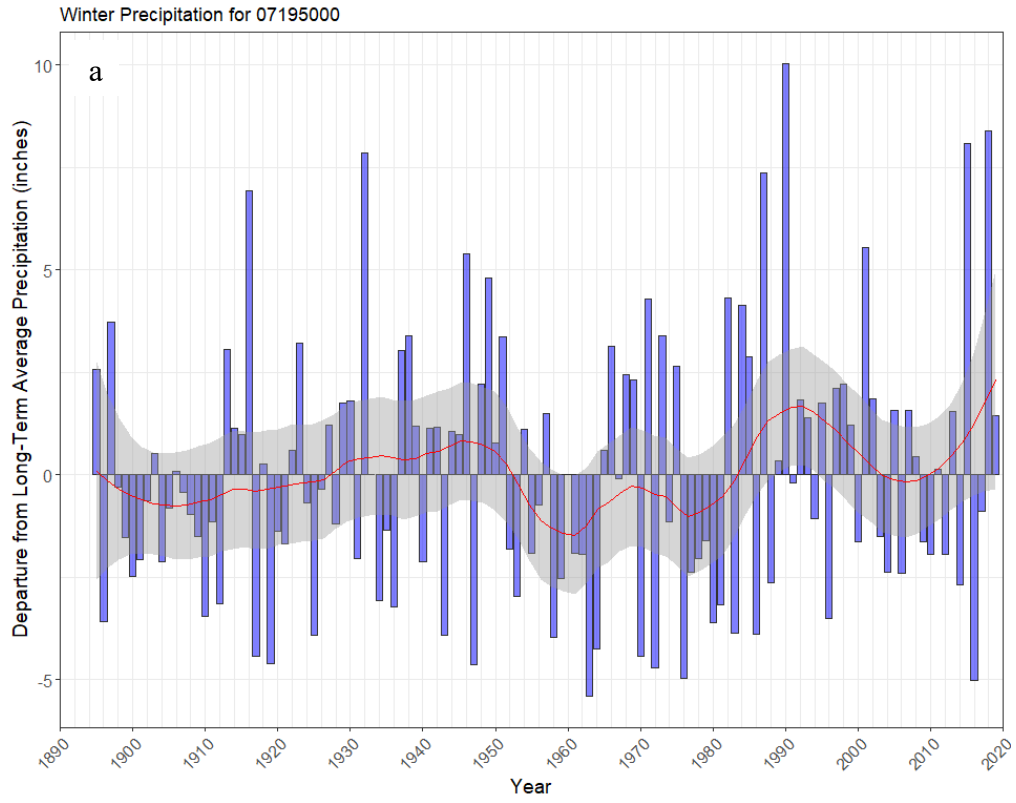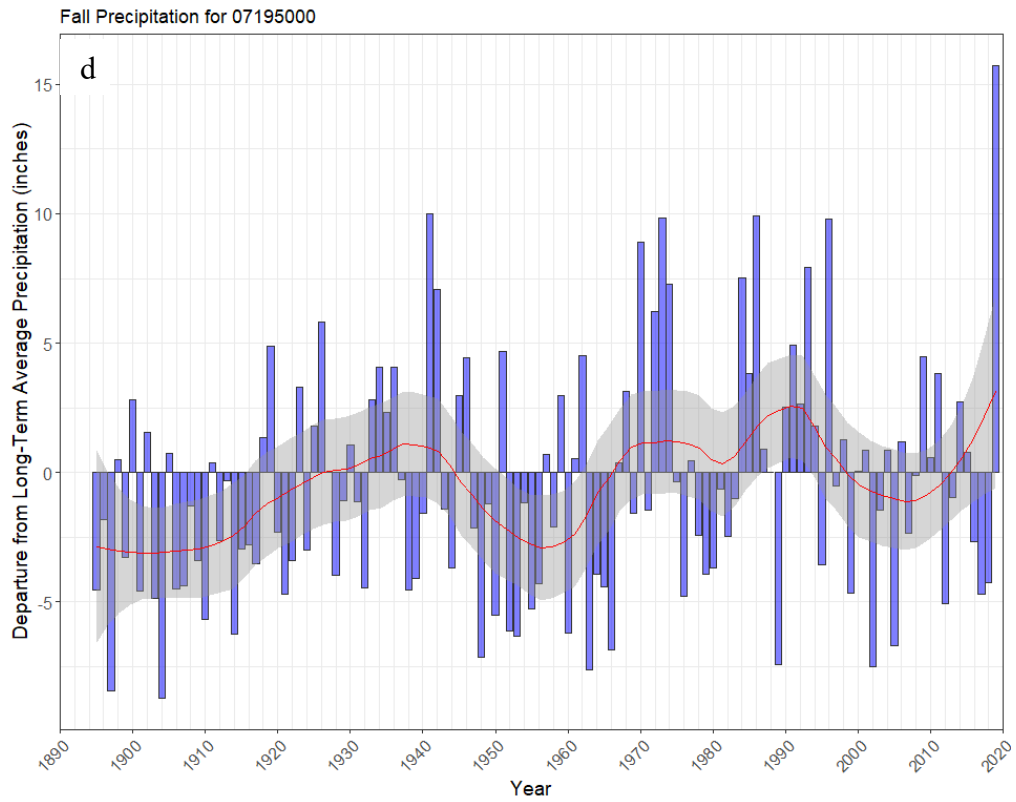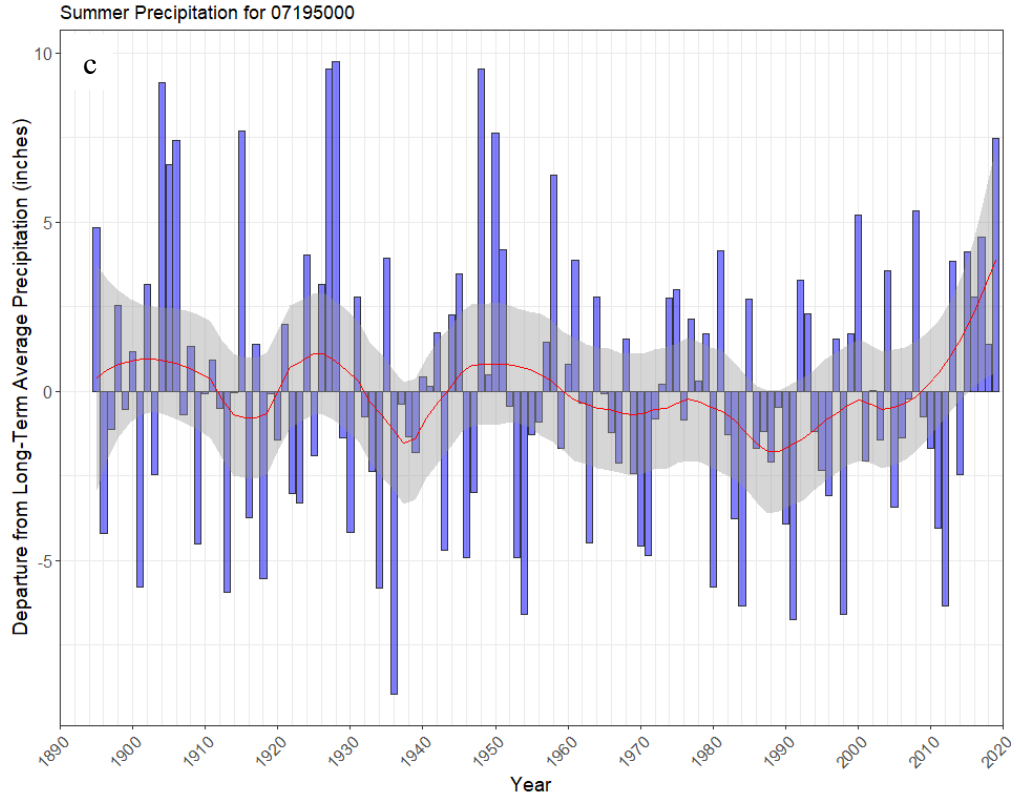
Figure 18. Precipitation departure, in inches, from the long-term average precipitation (1895-2019) for Osage Creek near Elm Springs, AR, (red line is a LOESS curve with 90% confidence limits (grey area)) for the: a, winter season; b, spring season; c, summer season; and d, fall season.

Winter Precipitation for 07195855

Spring Precipitation for 07195855

c
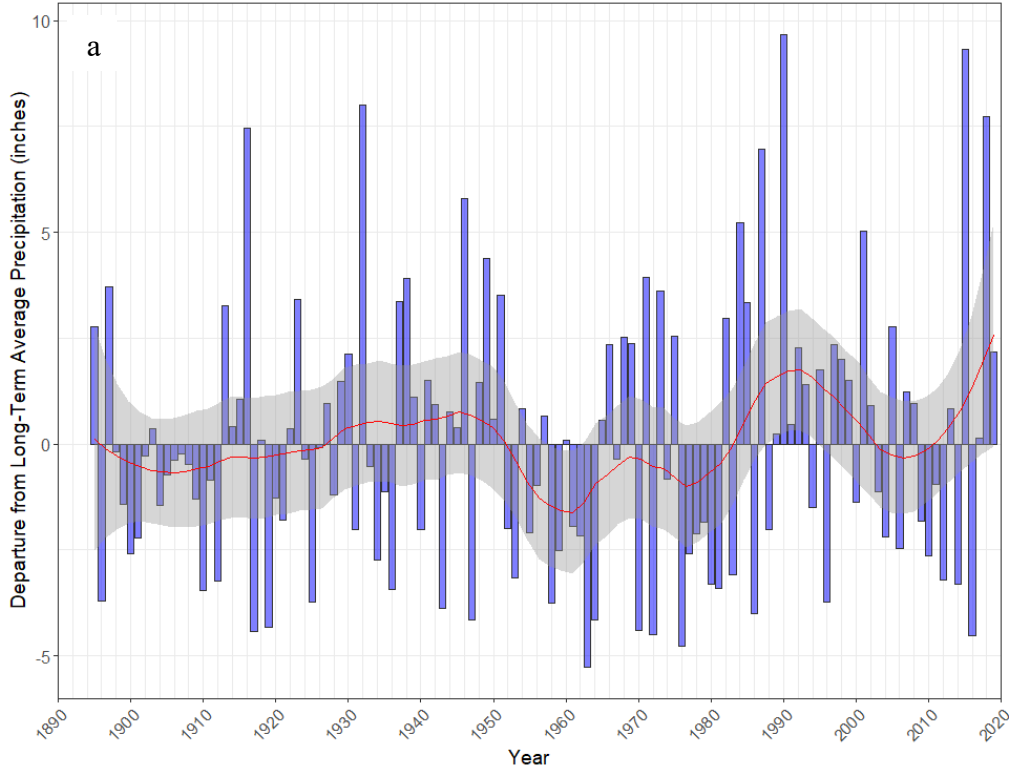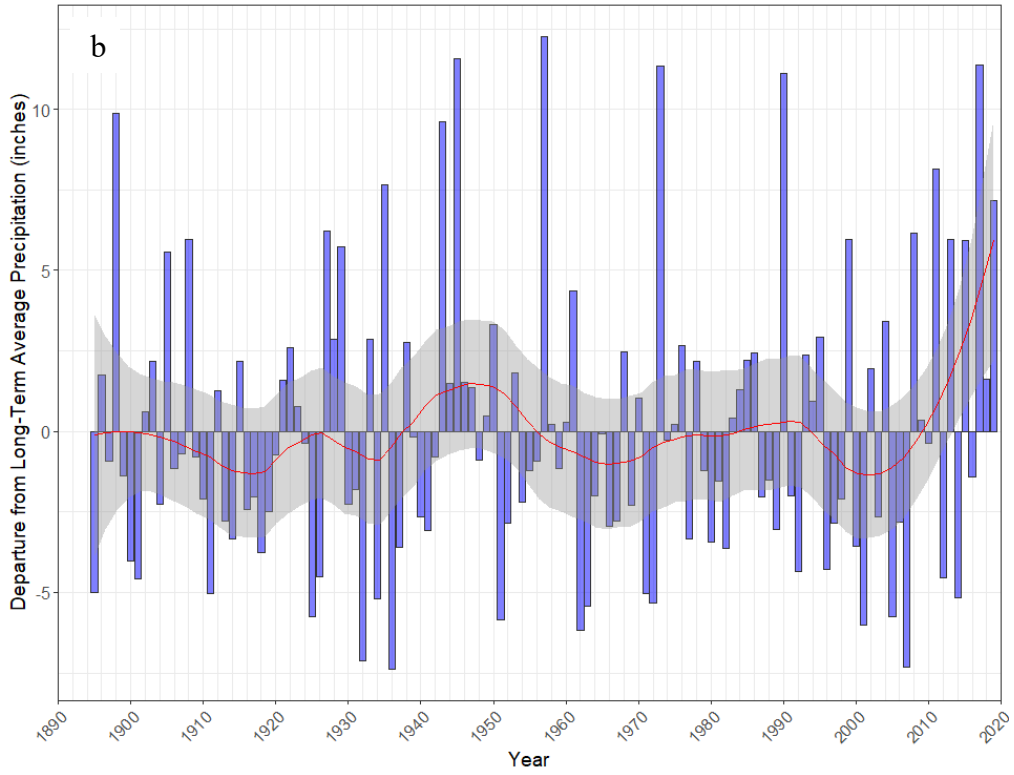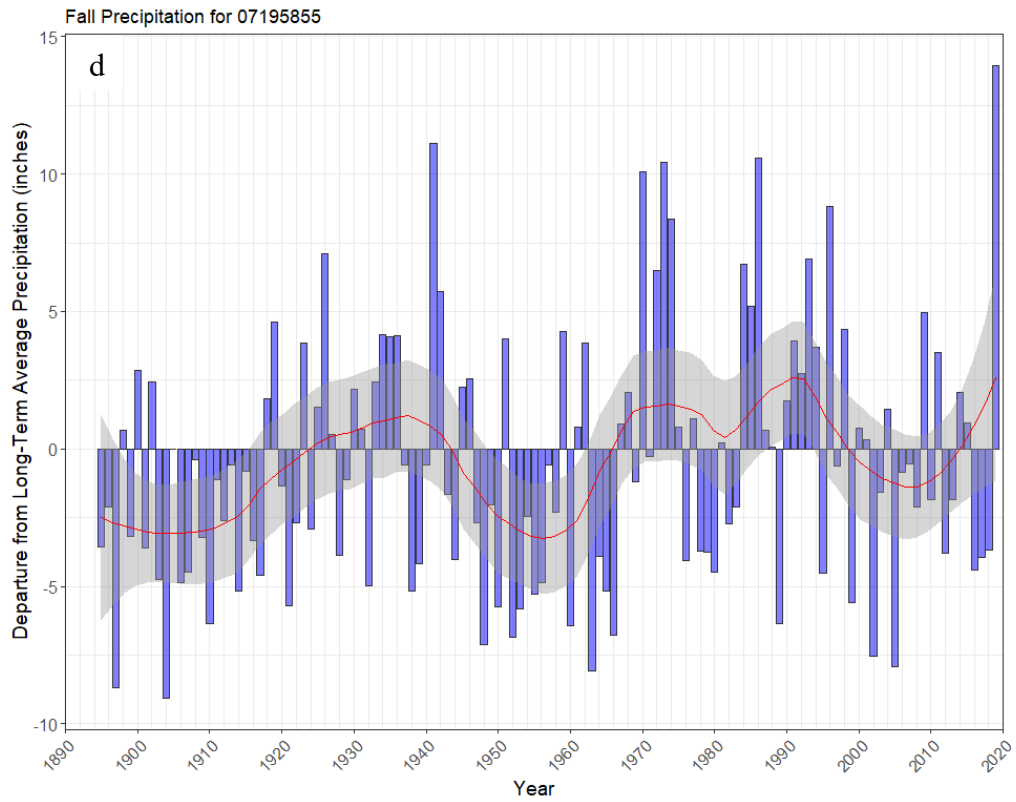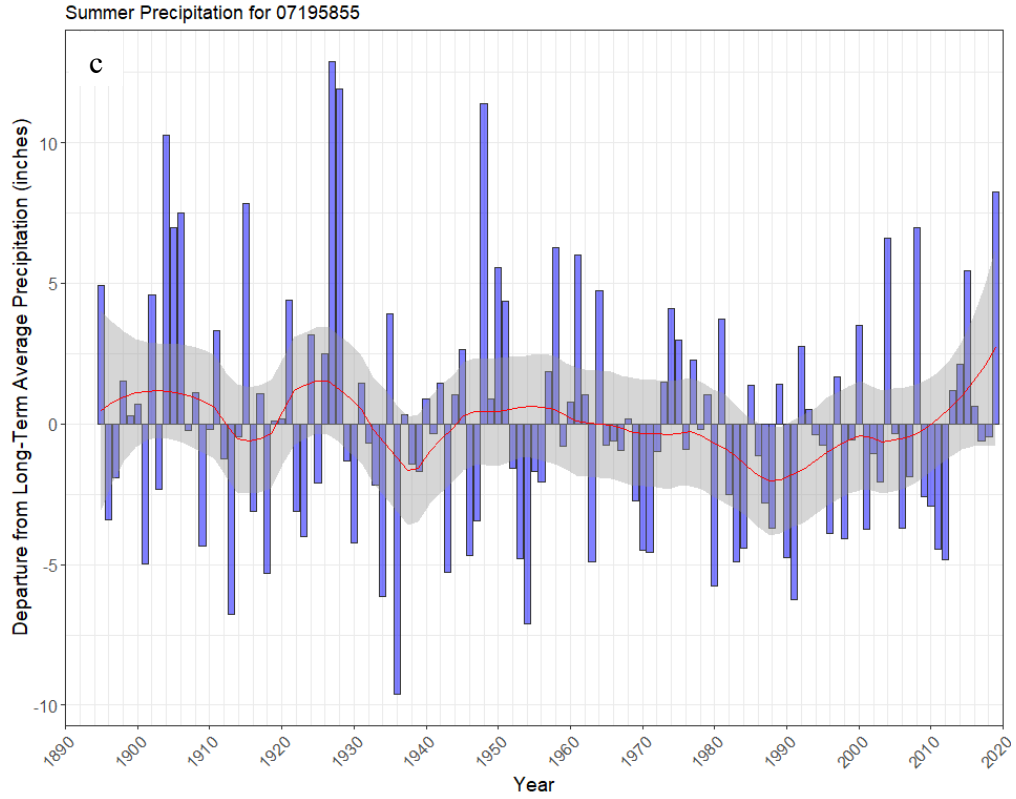
Figure 19. Precipitation departure, in inches, from the long-term average precipitation (1895-2019) for Flint Creek near West Siloam Springs, AR, (red line is a LOESS curve with 90% confidence limits (grey area)) for the: a, winter season; b, spring season; c, summer season; and d, fall season.

Winter Precipitation for 07196900
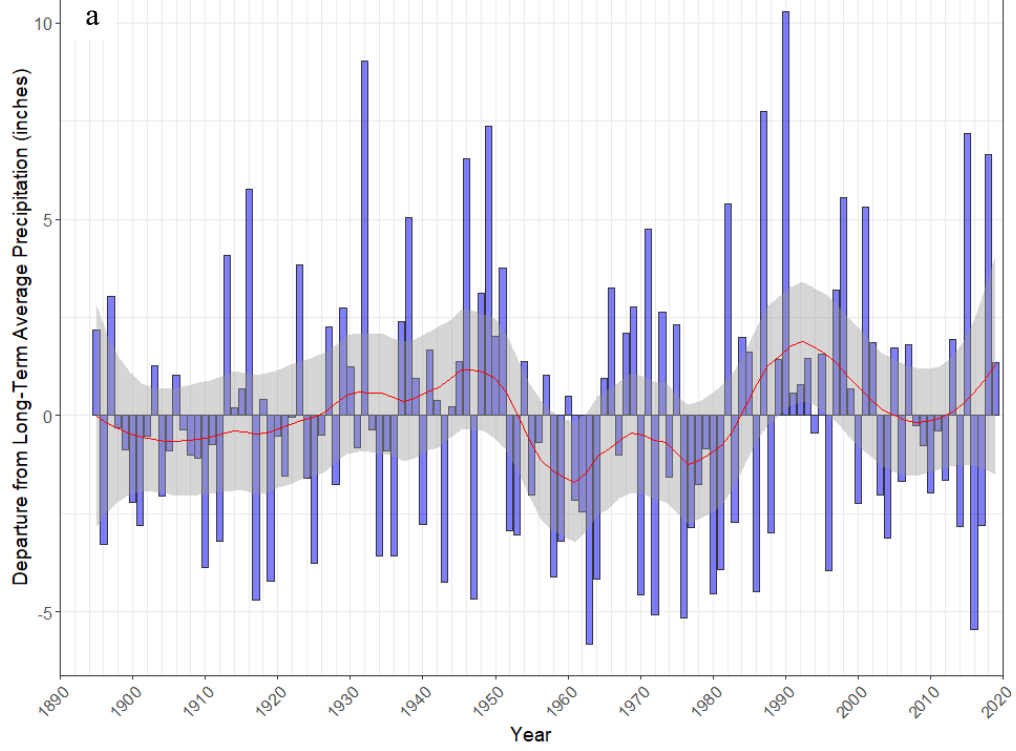
Spring Precipitation for 07196900
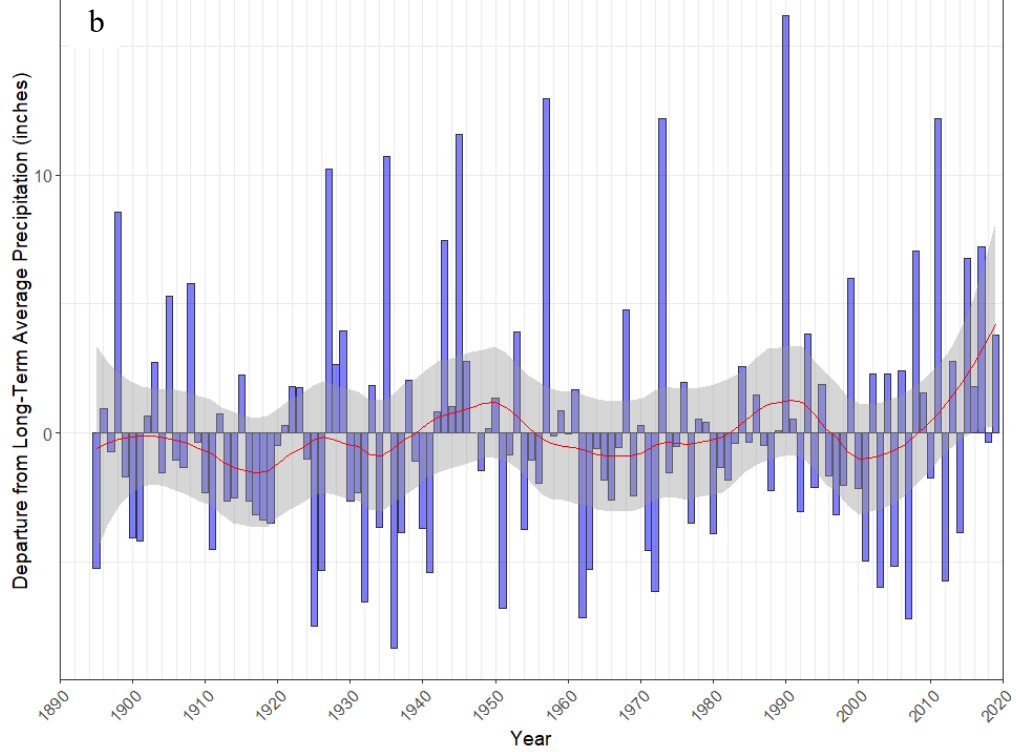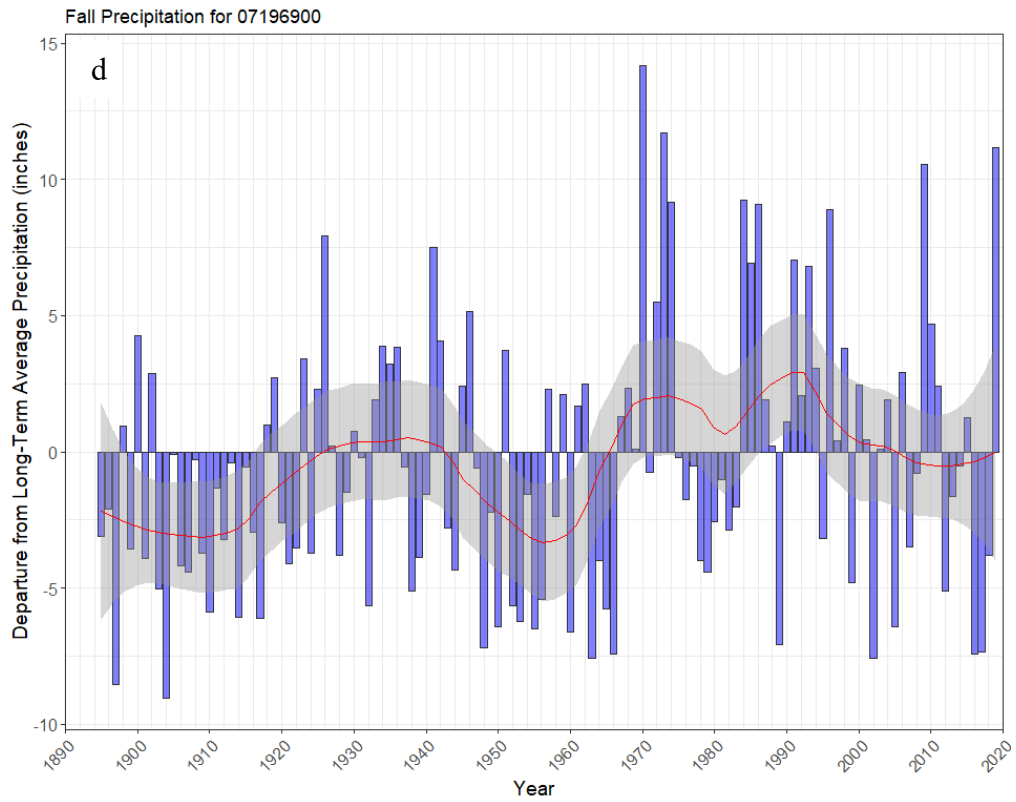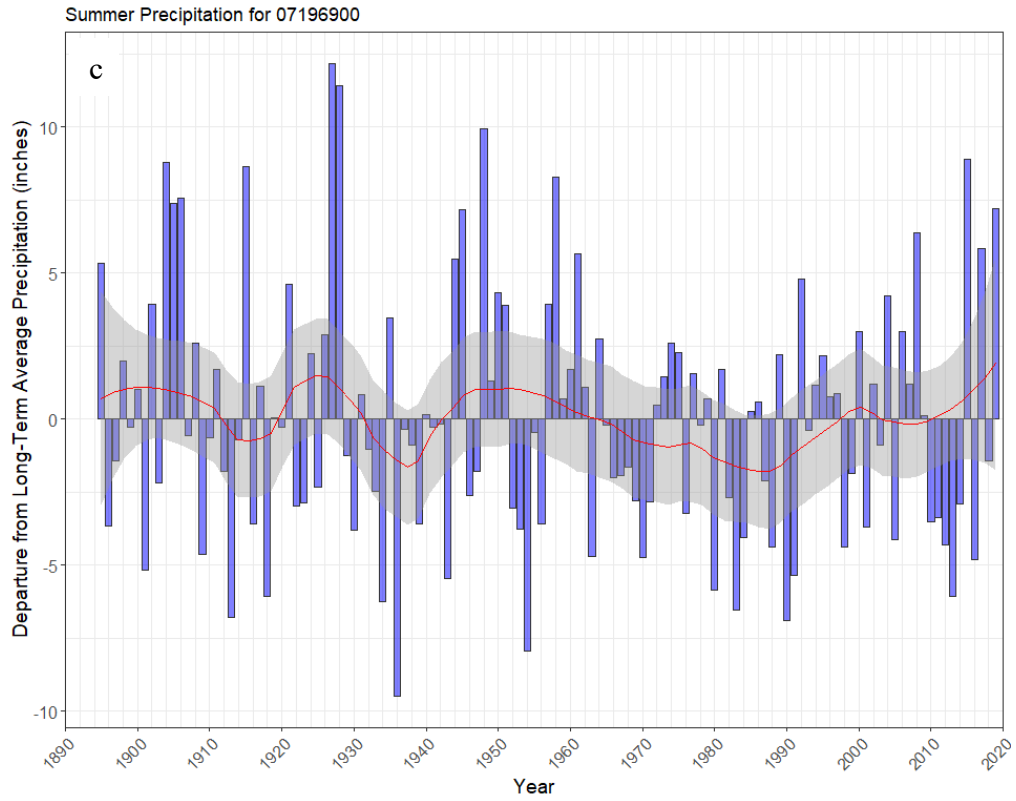
Figure 20. Precipitation departure, in inches, from the long-term average precipitation (1895-2019) for Baron Fork at Dutch Mills, AR, (red line is a LOESS curve with 90% confidence limits (grey area)) for the: a, winter season; b, spring season; c, summer season; and d, fall season.

Winter Precipitation for 07195500

Spring Precipitation for 07195500
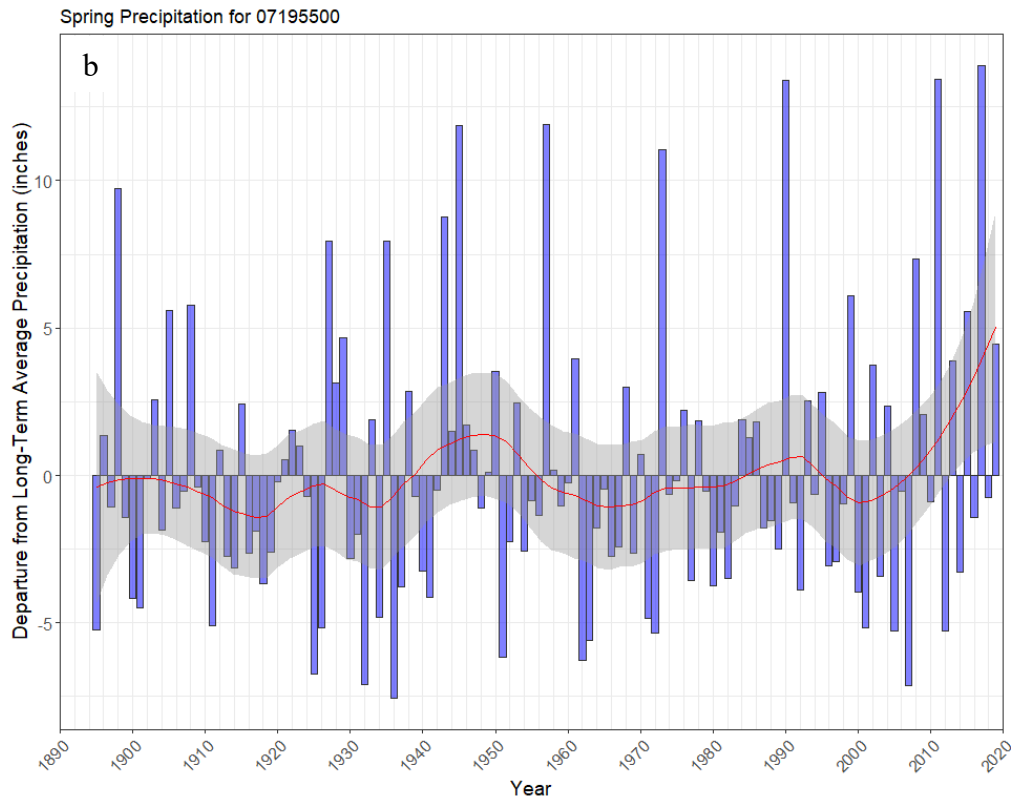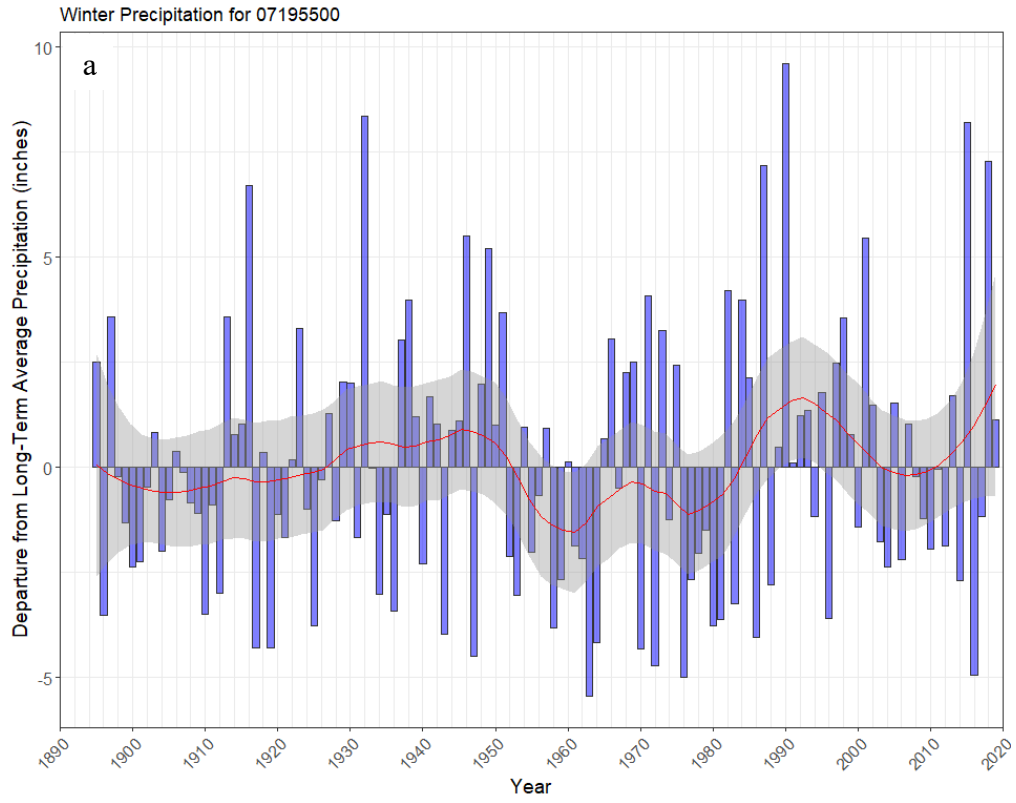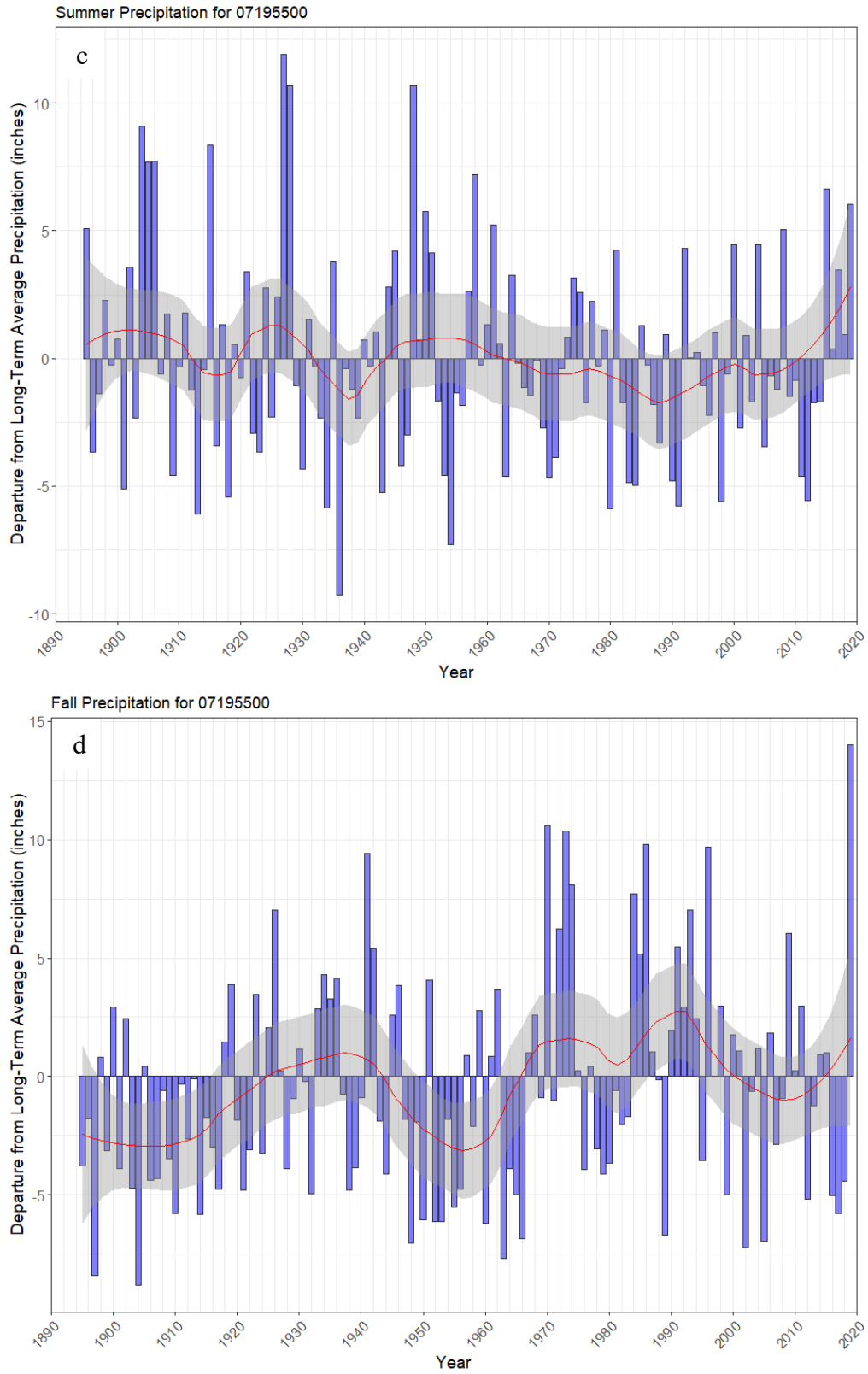
Figure 21. Precipitation departure, in inches, from the long-term average precipitation (1895-2019) for Illinois River near Watts, OK, (red line is a LOESS curve with 90% confidence limits (grey area)) for the: a, winter season; b, spring season; c, summer season; and d, fall season.

Winter Precipitation for 07196500

Spring Precipitation for 07196500
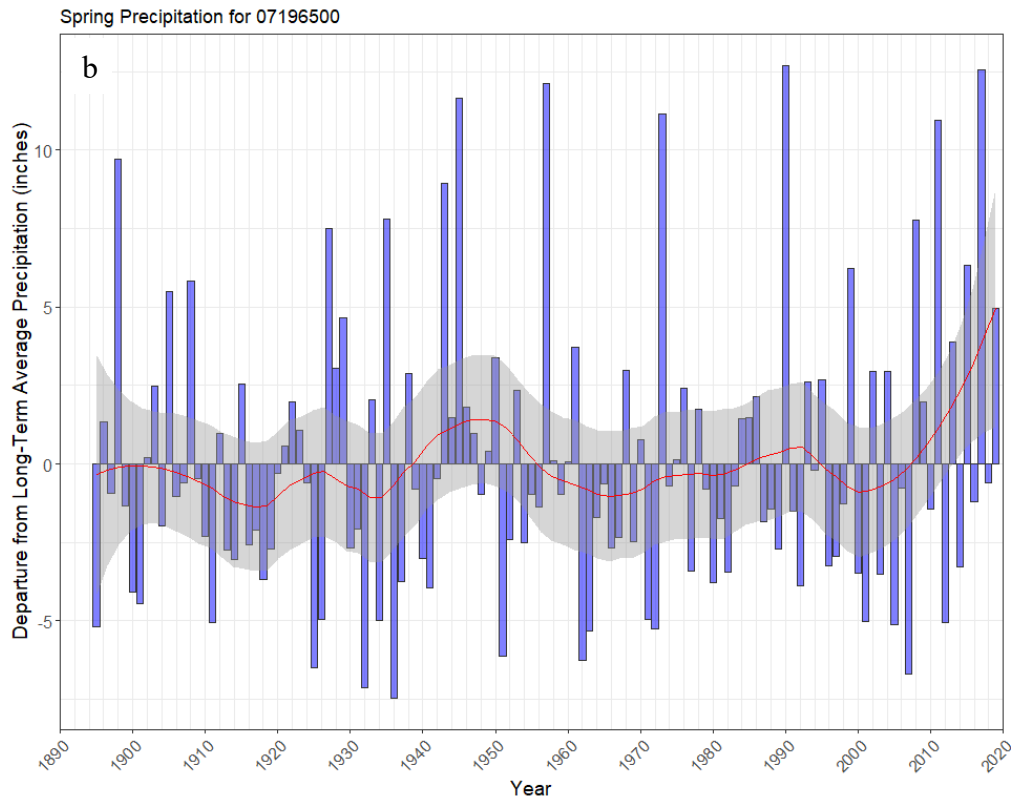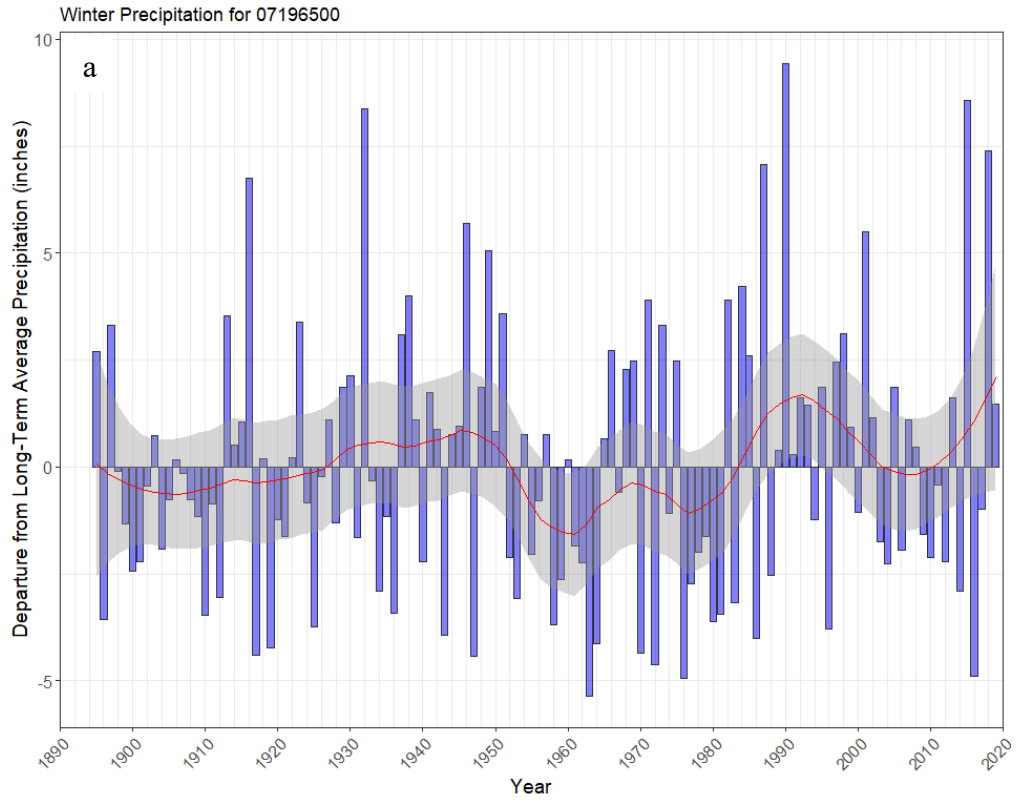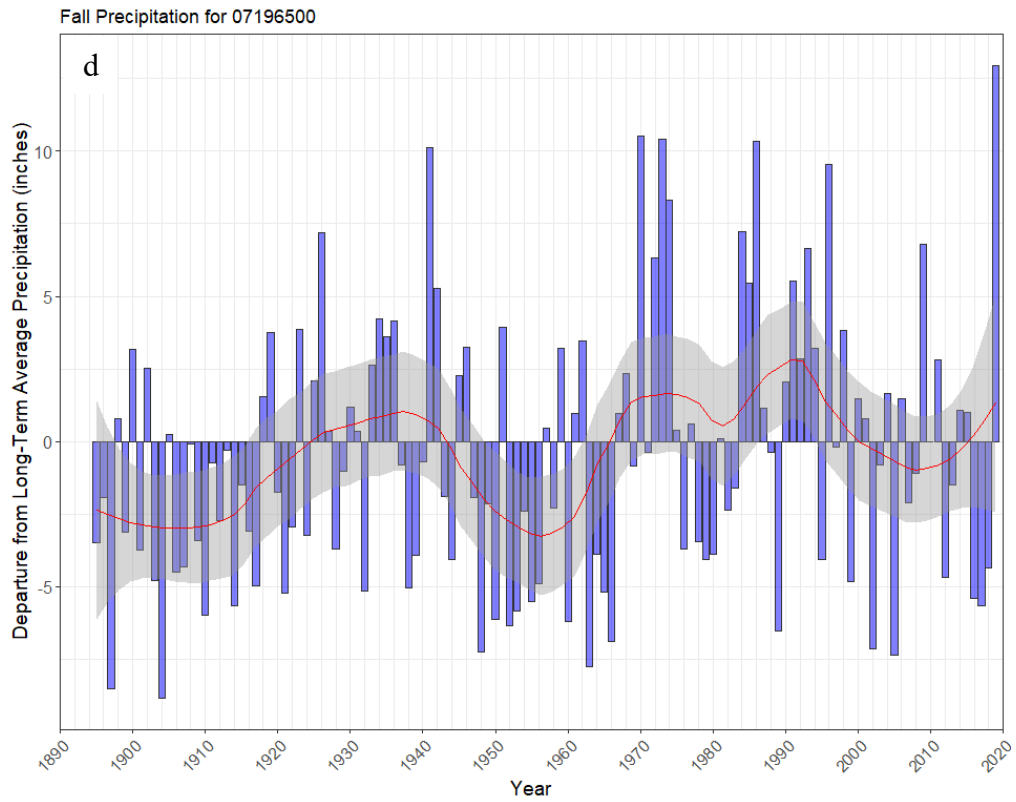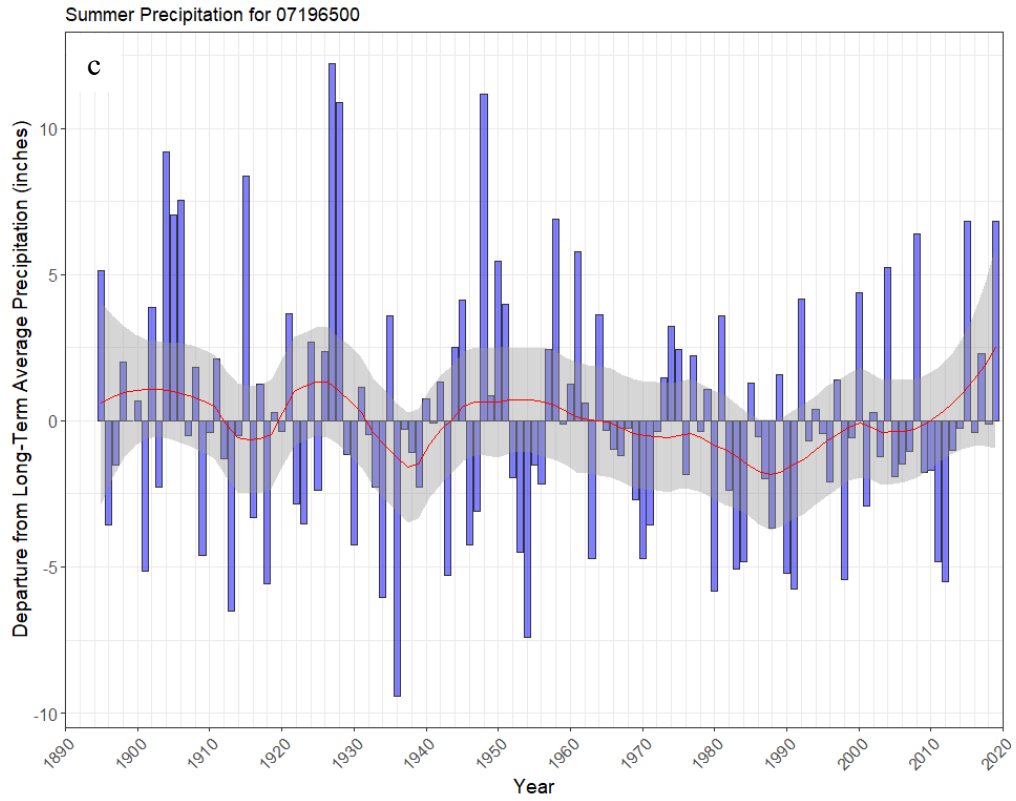
Figure 22. Precipitation departure, in inches, from the long-term average precipitation (1895-2019) for Illinois River near Tahlequah, OK, (red line is a LOESS curve with 90% confidence limits (grey area)) for the: a, winter season; b, spring season; c, summer season; and d, fall season.

Streamflow Trends

Recent studies have shown that the frequency of flood events has been generally increasing (Neri et al., 2019; Hirsch and Archfield, 2015; Mallakpour and Villarini, 2015) in the central United States due to increased precipitation (see previous section). However, there is limited evidence of significant changes in the magnitude of flood peaks (Hirsch and Archfield, 2015; Mallakpour and Villarini, 2015). Neri et al., (2019) determined that water basin wetness conditions (i.e., antecedent wetness) was the most frequently selected explanatory variable rather than a precipitation-only model when decreasing the flood event threshold from 1 to 4 events per year (i.e., higher flood threshold values to lower flood threshold values, respectively). This suggests that the largest flood events tend to be driven by storm rainfall, and that the role of basin wetness increases when encountering lower magnitude but more frequent flood events (Neri et al., 2019). Furthermore, extreme floods have been caused by extreme event rainfall and modest basin wetness or extreme basin wetness and modest rainfall (Merz et al., 2021).

Mean Annual Streamflow

Mean annual streamflow has increased overtime for sites within the Illinois River watershed. A select set of streamgaging sites were analyzed for mean annual streamflow (Figure 25 to 27), and for each site, mean annual streamflow has been increasing for the site's period of record.

Mean annual streamflow Osage Creek near Elm Springs, AR

$y = 1.7658x - 3357.5$
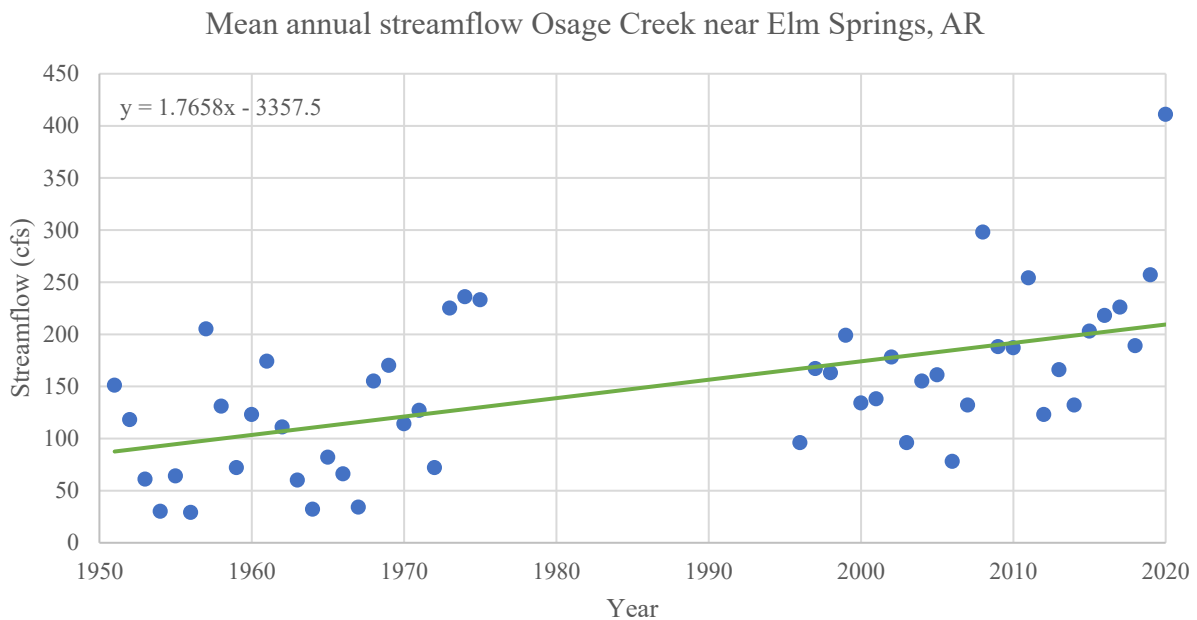
Figure 23. Mean annual streamflow for the period of record for Osage Creek near Elm Springs, AR.
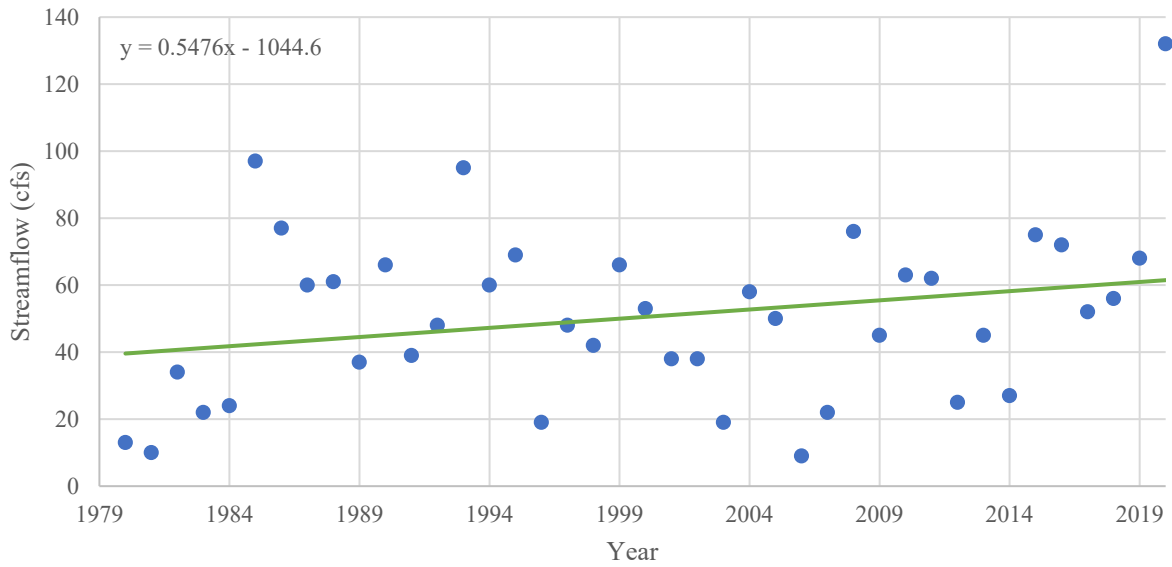
Figure 24. Mean annual streamflow for the period of record for Flint Creek near West Siloam Springs, AR.
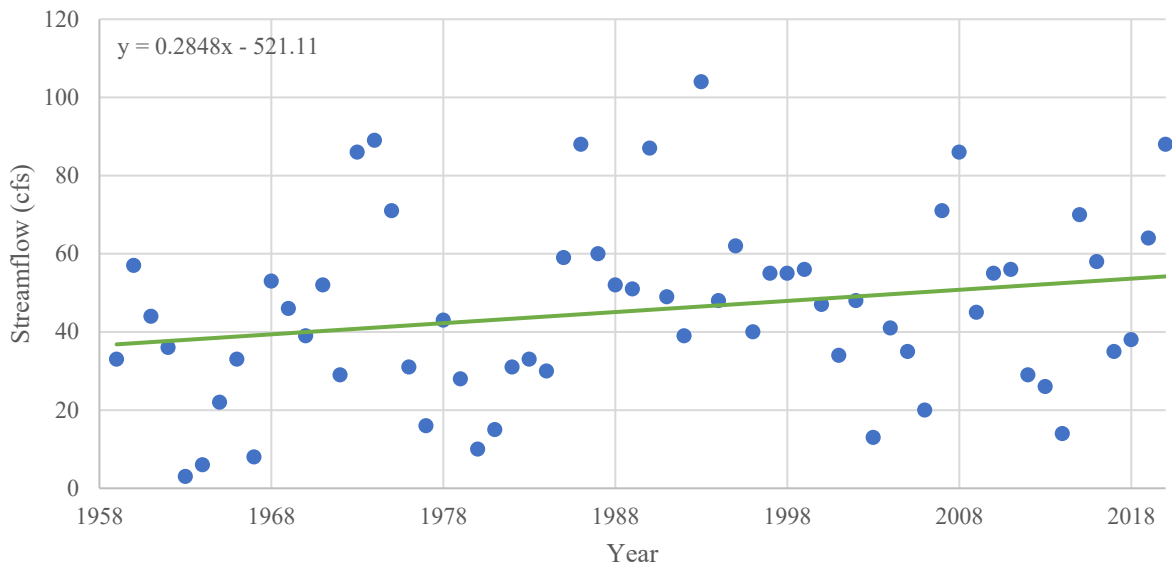
Figure 25. Mean annual streamflow for the period of record for Baron Fork at Dutch Mills, AR.
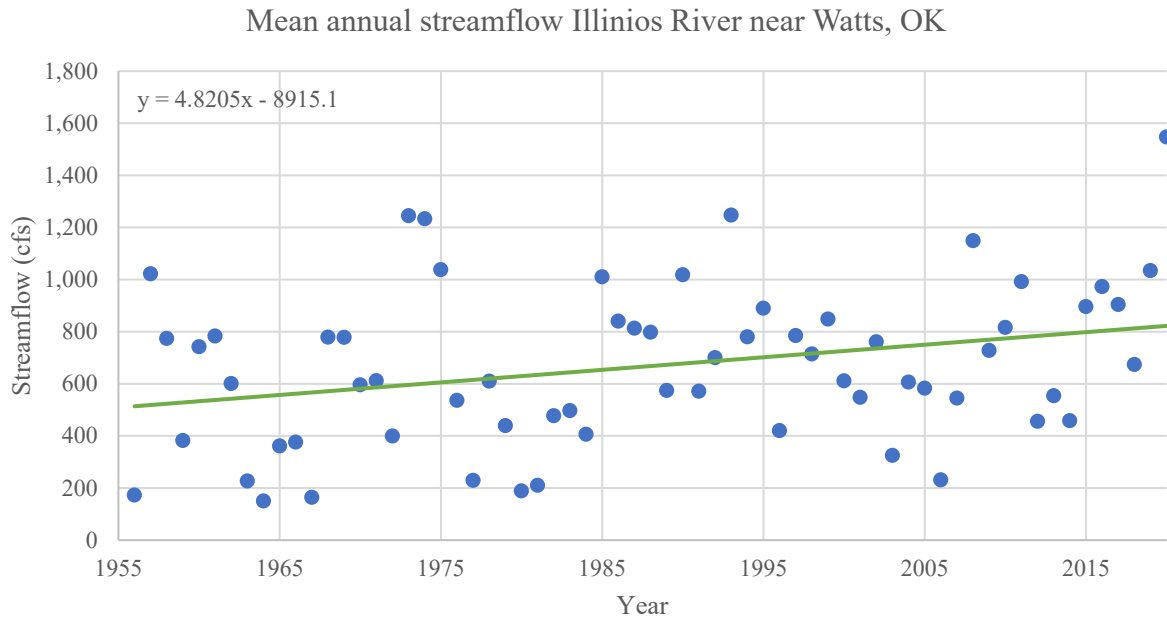
Figure 26. Mean annual streamflow for the period of record for Illinois River near Watts, OK.
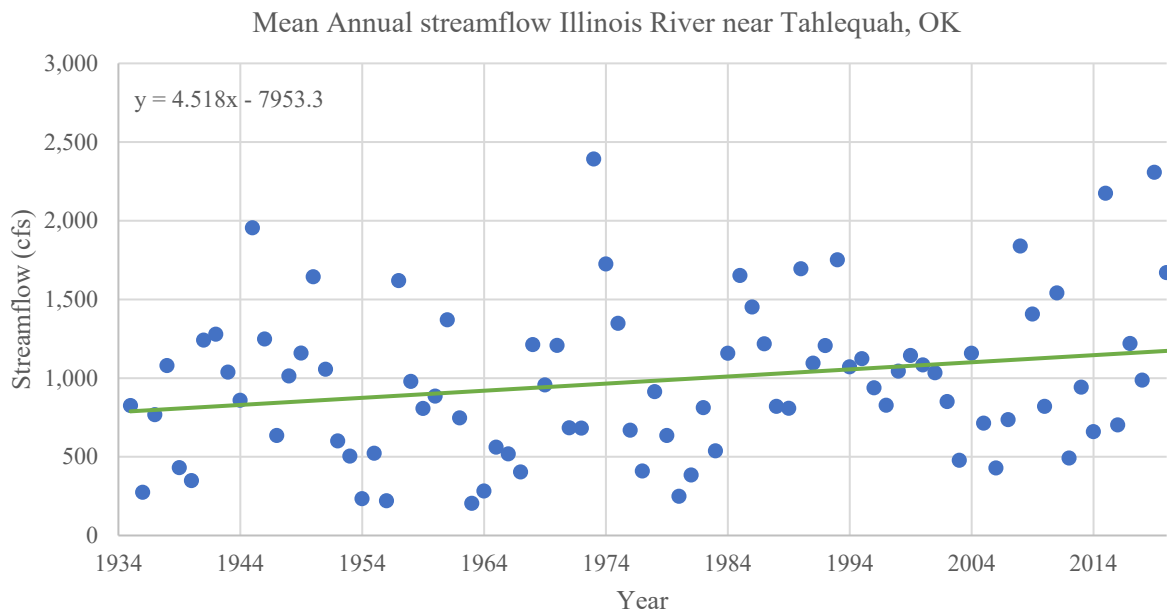
Figure 27. Mean annual streamflow for the period of record for Illinois River near Tahlequah, OK.

1% Annual Exceedance Probability

In order to examine how the largest floods have changed through time, the 1% annual exceedance probability was examined for the streamflow gaging sites with the longest period of records. Flood frequency statistics at streamgaging sites is a function of not only the magnitude of the observed data, but also the record length. The analysis iterates the Bulletin 17C methodology (England et al., 2018) by computing flood frequency using the first 20 years of record, then adding additional years up to present day to depict how sensitive the frequency flow

values are to both magnitude and record length as well as trends. The sites included in the analysis are the Illinois River near Watts, OK, and the Illinois River near Tahlequah, OK, gaging sites. The following figures (Figure 28 and Figure 29) show how the 1% exceedance (red dots) has changed through time. The grey dots are the peak flows for any given water year and the blue area are the error bounds around the calculated 1% exceedance values. For both sites, the 1% exceedance decreased during the first part of the period of record, which is a result of the fewer number of records used in the calculations, and then increased for both sites for the later, particularly in the approximate last 10 years, period of record. Furthermore, the 1% exceedance has been met or exceeded three times in the last approximate 10 years for Illinois River near Watts, OK, and once at Illinois River near Tahlequah, OK.
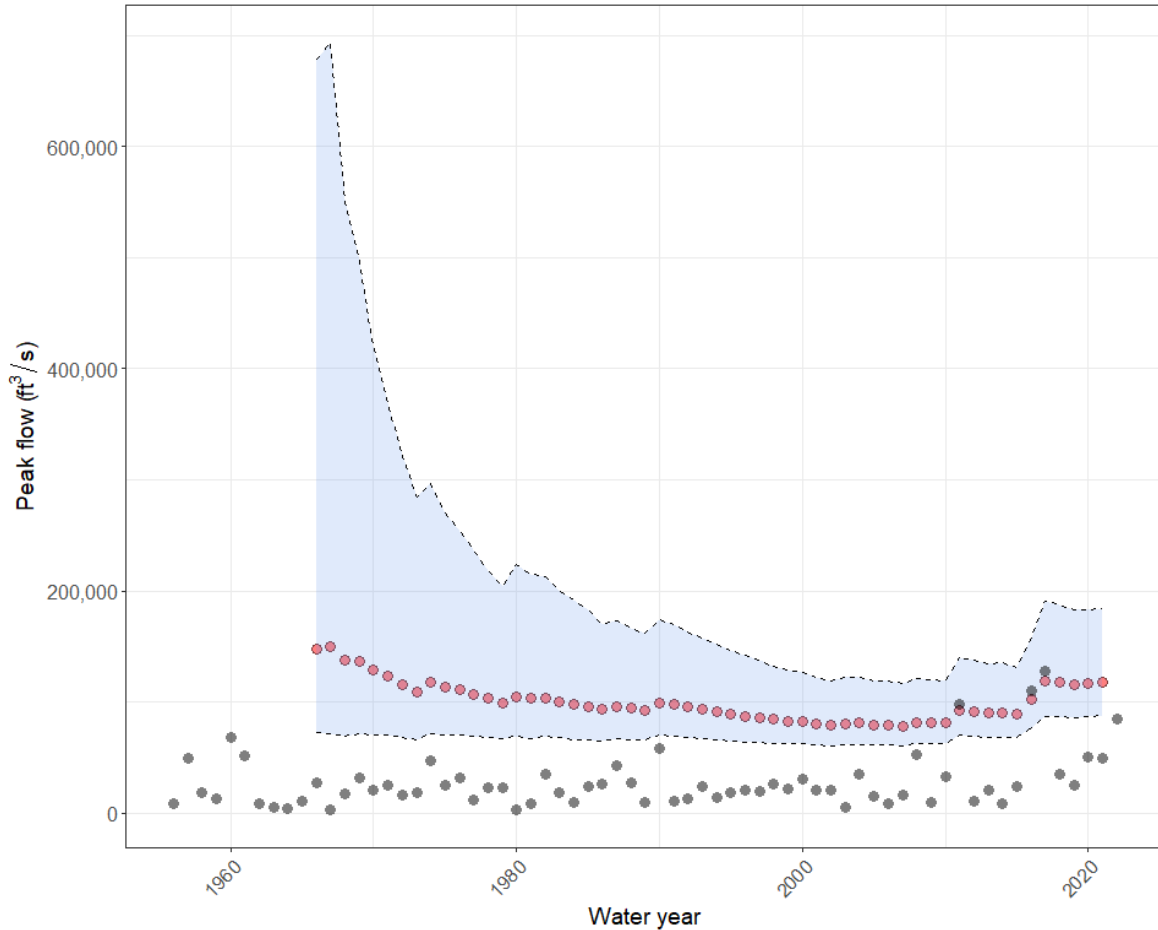
Figure 28. Illinois River near Watts, OK, 1% exceedance probability (grey dots are observed peak flows, red dots are calculated 1% exceedance values, and blue area are the error bounds).
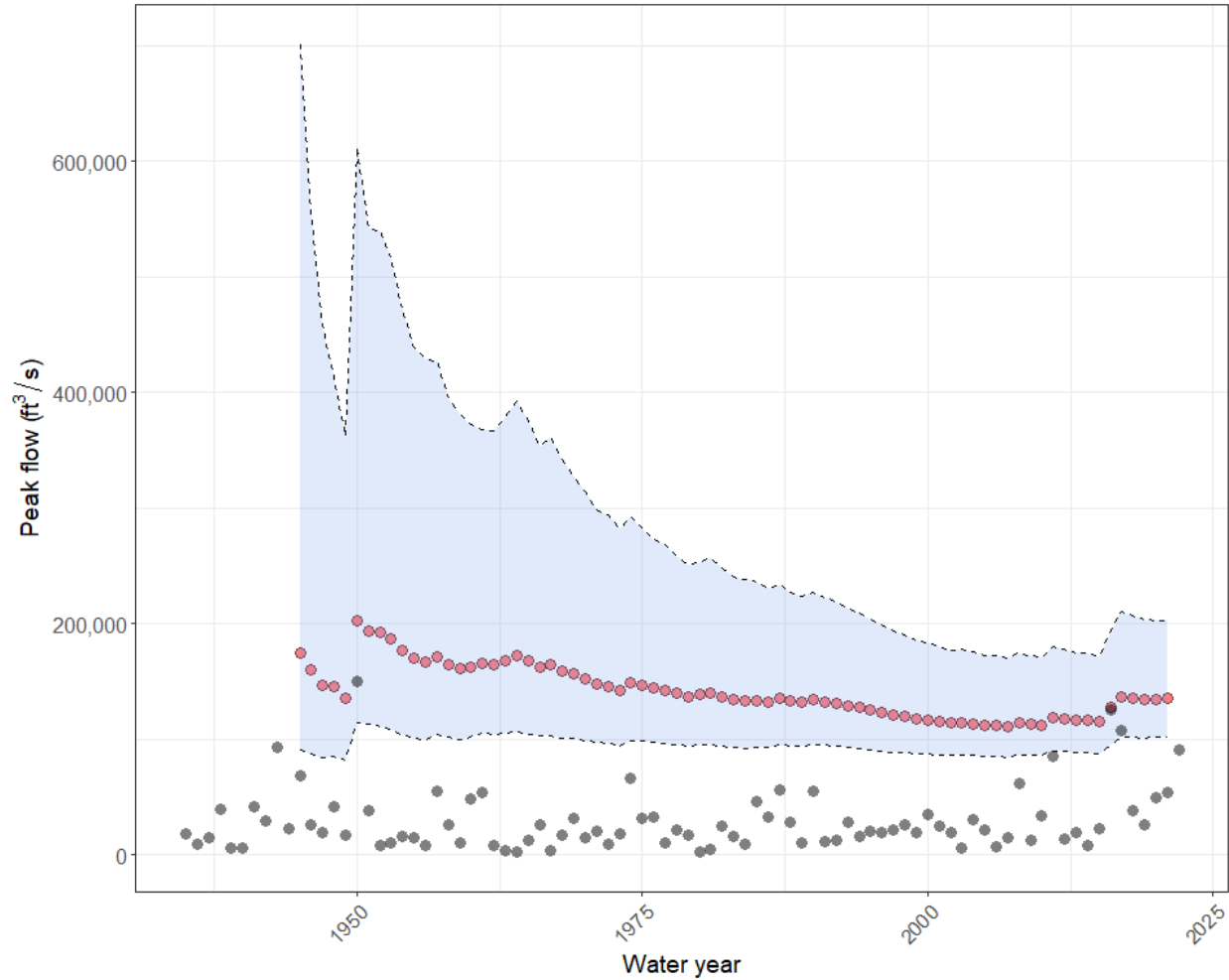
Figure 29. Illinois River near Tahlequah, OK, 1% exceedance probability (grey dots are observed peak flows, red dots are calculated 1% exceedance values, and blue area are the error bounds).

Streamflow Statistics

In order to determine whether changes in frequency, magnitude, duration, timing, and rate of change have occurred, several streamflow statistics were examined at select sites within the Illinois River watershed. Streamflow statistics were developed using the EflowStats package (Mills and Blodgett, 2017) using the R statistical computing language (R Core Team, 2020). Streamflow statistics can be used to quantify streamflow alteration, understand catchment function and processes (Archfield et al., 2013), and determine temporal and spatial variability by examining changes in hydrologic properties. The EflowStats package produces 171 hydrologic indices for stream classification analysis and 7 additional statistics used for streamflow classification referred to as the "Magnificent Seven" (MAG7, Archfield et al., 2013). Only a select number of streamflow statistics will be presented here; however, the selected statistics cover the five critical components of the flow regime: magnitude, frequency, duration, timing, and rate of change. These components can be used to characterize the entire range of flows and specific hydrologic phenomena (Poff et al., 1997).

For the select streamflow statistics, a comparison was made between the prior to 1990 time period and the post 1990 time period. The year 1990 was chosen based on population (Figure 4)

and land-use change (Figure 2) data and represents an assumed period when urbanization started increasing within the most populated area of the Illinois River watershed (northwest Arkansas; Figure 1). For the select streamflow gaging sites, the prior to 1990 period of record includes the start of the water year the record began (Table 2) to the end of water year 1989 (i.e., September 30, 1989). A water year is defined as the 12-month period beginning on October 1, for any given year, through September 30, of the following year. The post 1990 time period includes the beginning of water year 1990 (i.e., October 1, 1989) through end of water year 2020 (i.e., September 30, 2020).

Table 2. Pertinent streamflow gaging site information for select sites used for streamflow statistics within the Illinois River watershed.

USGS Site No	Station Name	Drainage Area (square miles)	Record Begin Date	Record End Date
07195000	Osage Creek near Elm Springs, AR	130.0	1950-10-01	2020-09-30
07195500	Illinois River near Watts, OK	630.0	1955-10-01	2020-09-30
07196500	Illinois River near Tahlequah, OK	950.0	1935-10-01	2020-09-30

Magnitude

Streamflow magnitude is defined as the amount of water moving past a fixed location per unit time and can refer either to absolute or to relative discharge (Poff et al., 1997). Magnitude statistics of mean daily, median daily, and annual runoff all have increased between the prior to 1990 time period to the post 1990 time period (Figure 30, Figure 31, and Figure 32). The largest percent increase for all represented magnitude statistics occurred at Osage Creek near Elm Springs. Mean daily flow had an approximate 59 percent increase between the prior to 1990 and post 1990 time periods (Figure 30); the median daily flow increased approximately 68 percent between the prior to 1990 and post 1990 time periods (Figure 31); and annual runoff increased approximately 57 percent between the prior to 1990 and post 1990 time periods (Figure 32).

Mean Daily Flow Values

Streamflow (cfs)

- Osage Creek near Elm Springs: 115 (Prior to 1990), 183 (Post 1990)
- Illinois River near Watts: 591 (Prior to 1990), 754 (Post 1990)
- Illinois River near Tahlequah: 899 (Prior to 1990), 1,128 (Post 1990)
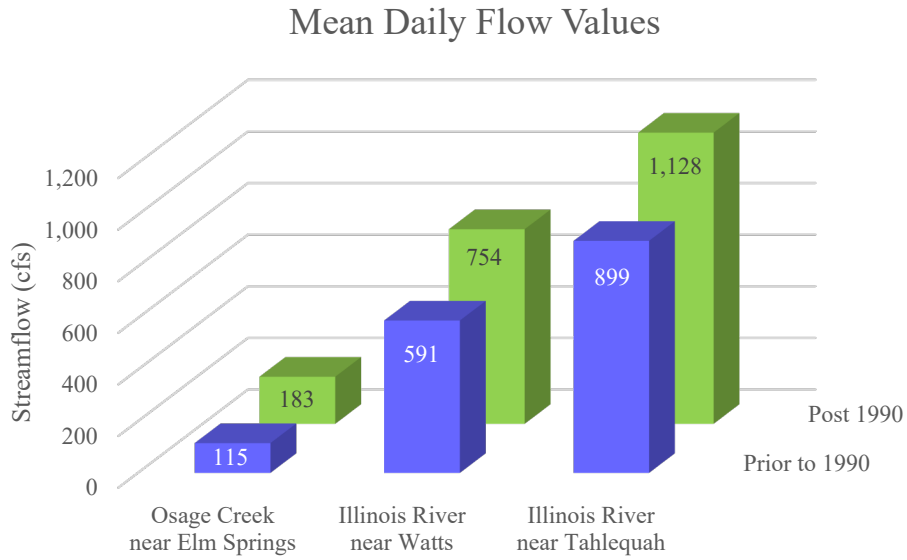
Figure 30. Mean daily streamflow values, in cubic feet per second, for select sites prior to 1990 and post 1990.

Median Daily Flow Values

Streamflow (cfs)

- Osage Creek near Elm Springs: 66 (Prior to 1990), 111 (Post 1990)
- Illinois River near Watts: 264 (Prior to 1990), 353 (Post 1990)
- Illinois River near Tahlequah: 387 (Prior to 1990), 534 (Post 1990)
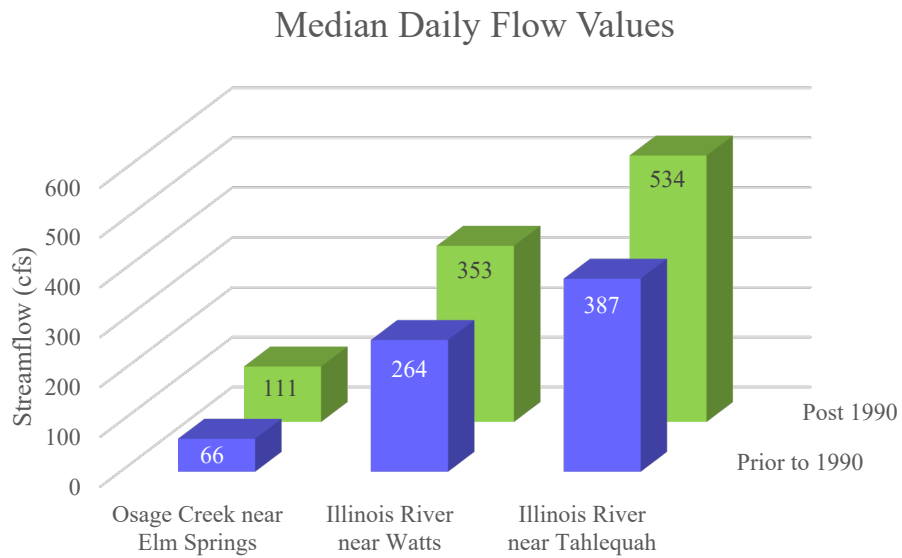
Figure 31. Median daily streamflow values, in cubic feet per second, for select sites prior to 1990 and post 1990.
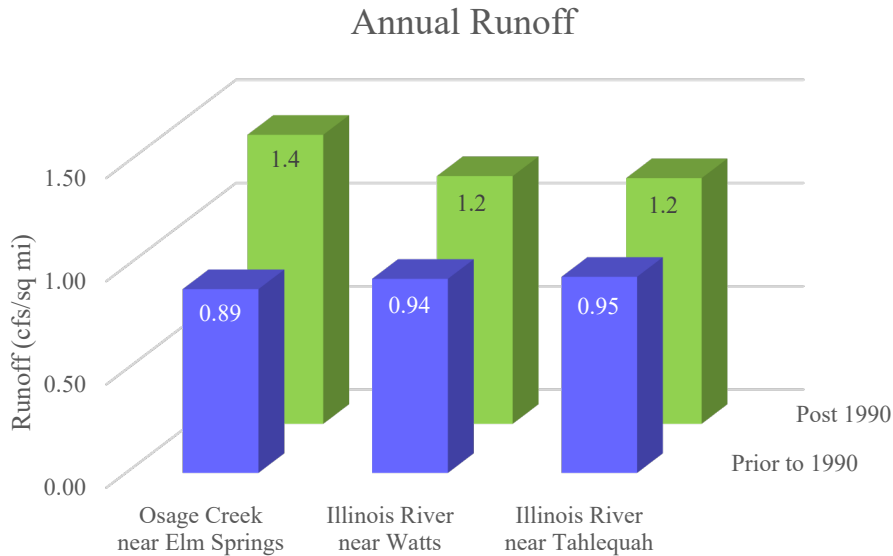
Figure 32. Average annual runoff values, in cubic feet per second per square mile, for select sites prior to 1990 and post 1990.

Frequency

Streamflow frequency is defined as how often streamflow above a given magnitude recurs over some specified time interval and is inversely related to flow magnitude (Poff et al., 1997). The number of low flow events (the average number of flow events with flows below a threshold equal to 5 percent of the mean flow value for the entire flow record) decreased for all sites between the prior to 1990 and post 1990 time periods. The largest change in number of events (from 2.3 to 0) occurred for Illinois River near Watts (Figure 33). However, all sites went to 0 number of low flow spells for the post 1990 time period (Figure 33), but this number could be misleading. It is acknowledged that there are known point dischargers in the Illinois River watershed. Without specifically knowing when these entities started discharging, it is hard to account for their effects on the streamflow, particularly on the low flows. Furthermore, this is a flood study and the effects of the point discharges on these extremely high flows are negligible and delving deeper into a low flow analysis is beyond the scope of this project. The number of flood events (the average number of flow events with flows above a threshold equal to 75 percent exceedance value for the entire flow record) doubled between the prior to 1990 and post 1990 time periods for Osage Creek near Elm Springs, increased slightly for Illinois River near Watts, and slightly for Illinois River near Tahlequah (Figure 34).
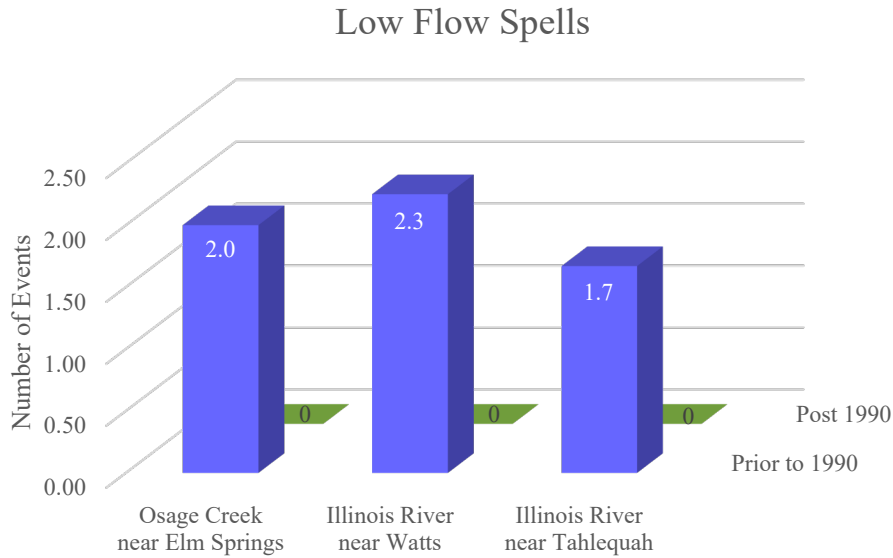
Low Flow Spells

Figure 33. Number of low flow spells for select sites prior to 1990 and post 1990.

Flood Frequency
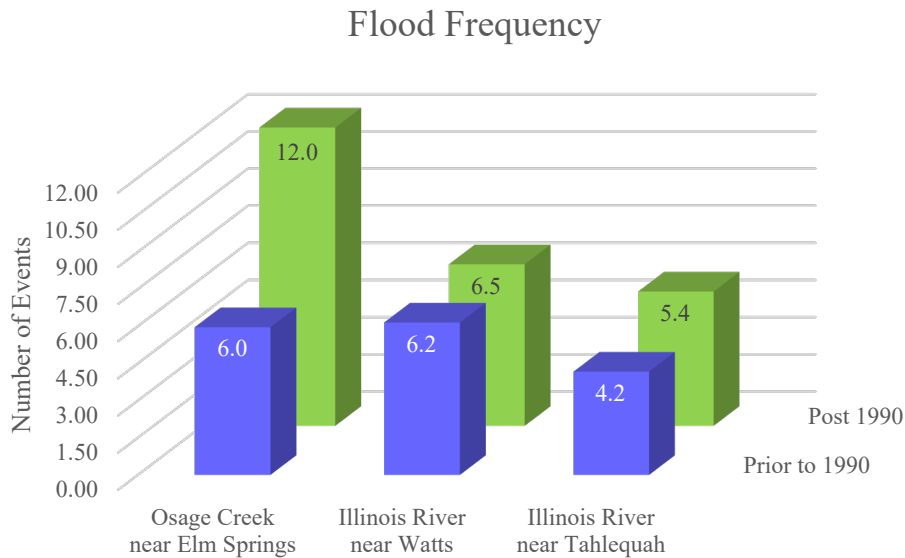
Figure 34. Number of floods for select sites prior to 1990 and post 1990.

Duration

Streamflow duration is defined as the period of time associated with a specific flow condition and can be either relative to a particular flow event or as a composite expressed over a specified time period (Poff et al., 1997). The minimum and maximum 1-day average flows increased for all sites between the prior to 1990 and post 1990 time periods (Figure 35 and Figure 36). Both Osage Creek near Elm Springs and Illinois River near Watts increased approximately 80 percent

in minimum 1-day average flow between the prior to 1990 and post 1990 time periods (Figure 35). Osage Creek near Elm Springs had a 125 percent increase in maximum 1-day average flow between the prior to 1990 and post 1990 time periods (Figure 36).

Minimum 1-day Average Flow
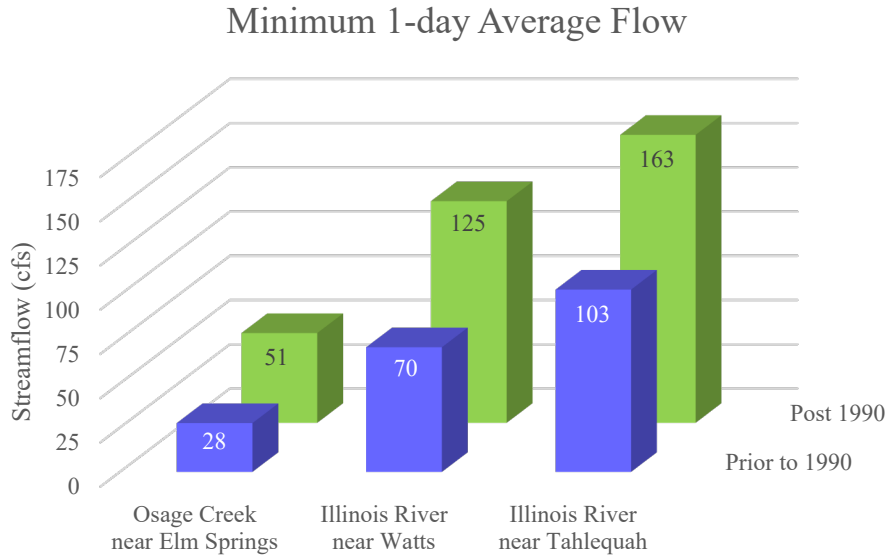
Figure 35. The minimum 1-day average flow, in cubic feet per second, for select sites prior to 1990 and post 1990.

Maximumm 1-day Average Flow
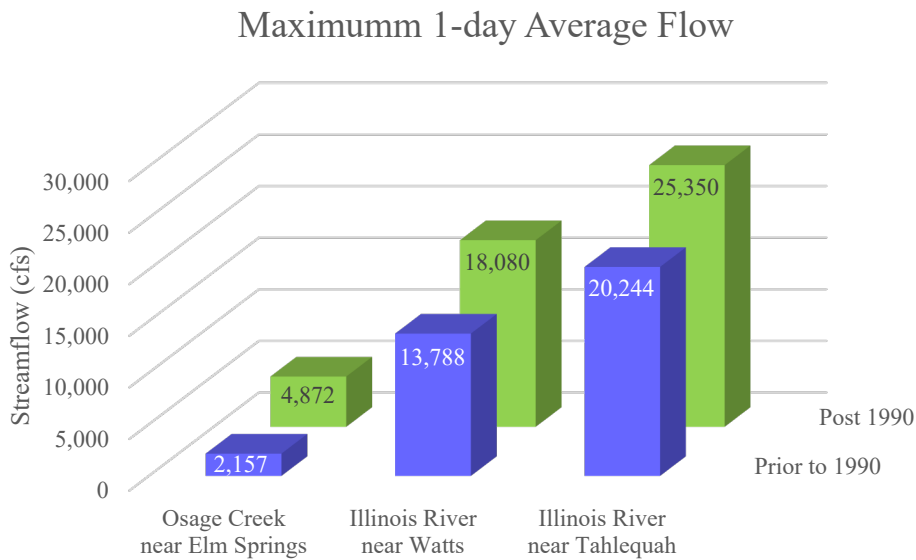
Figure 36. The maximum 1-day average flow, in cubic feet per second, for select sites prior to 1990 and post 1990.

Timing

Streamflow timing, or predictability, is defined as the regularity with which specific magnitudes occur and this regularity can be formal or informal and with reference to different time scales (Poff et al., 1997). Figure 37 shows the change in the average Julian date that the maximum flow occurs for each year. For both Osage Creek near Elm Springs and Illinois River near Tahlequah, the date for the annual maximum flow has come 9 days and 8 days sooner, respectively, post 1990 as compared to prior to 1990 (Figure 37). However, the annual maximum flow has occurred 12 days later at the Illinois River near Watts site (Figure 37). The change in dates could be an indication of how weather patterns are shifting within the Illinois River watershed.

Julian date of annual maximum flow
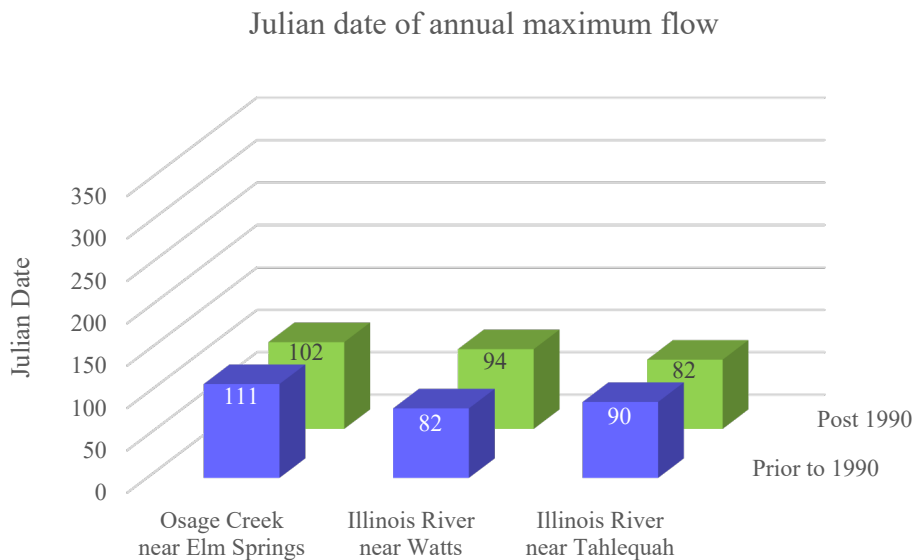
Figure 37. Julian date of annual maximum flow for select sites prior to 1990 and post 1990.

Rate of Change

Streamflow rate of change, or flashiness, is defined as how quickly flow changes from one magnitude to another (Poff et al., 1997). For all three sites, the rise and fall rate (the change in flow for days in which the change is positive and negative, respectively, for the flow record) has increased between the prior to 1990 time period and the post 1990 time period (Figure 38 and Figure 39). This is an indication of there being more streamflow on both the rising and falling limbs of the hydrograph for all three sites.

Rise Rate

Change in flow days (cfs/day)

Osage Creek near Elm Springs	Illinois River near Watts	Illinois River near Tahlequah
81 (Prior to 1990), 120 (Post 1990)	432 (Prior to 1990), 629 (Post 1990)	586 (Prior to 1990), 750 (Post 1990)

Post 1990
Prior to 1990
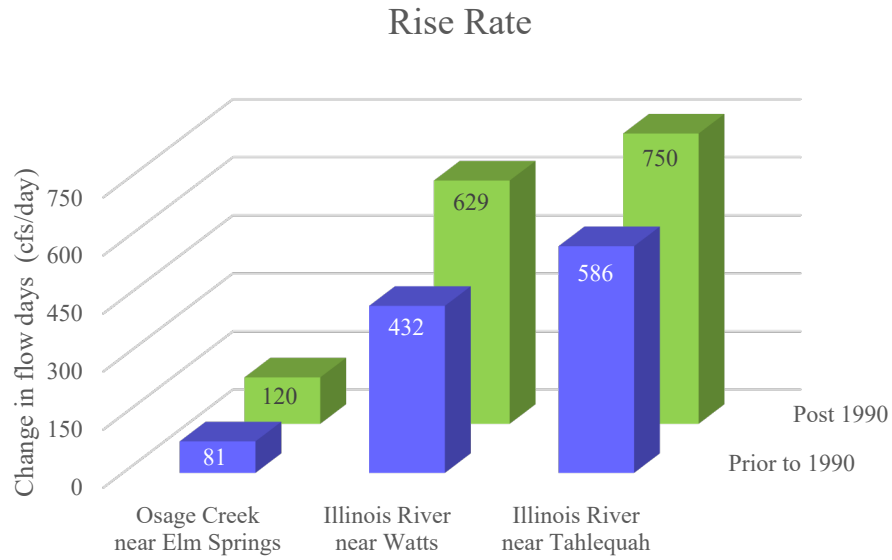
Figure 38. The rise rate, in cubic feet per second per day, for select sites prior to 1990 and post 1990.

Fall Rate

Change in flow days (cfs/day)

Osage Creek near Elm Springs	Illinois River near Watts	Illinois River near Tahlequah
31 (Prior to 1990), 56 (Post 1990)	174 (Prior to 1990), 214 (Post 1990)	221 (Prior to 1990), 266 (Post 1990)

Post 1990
Prior to 1990
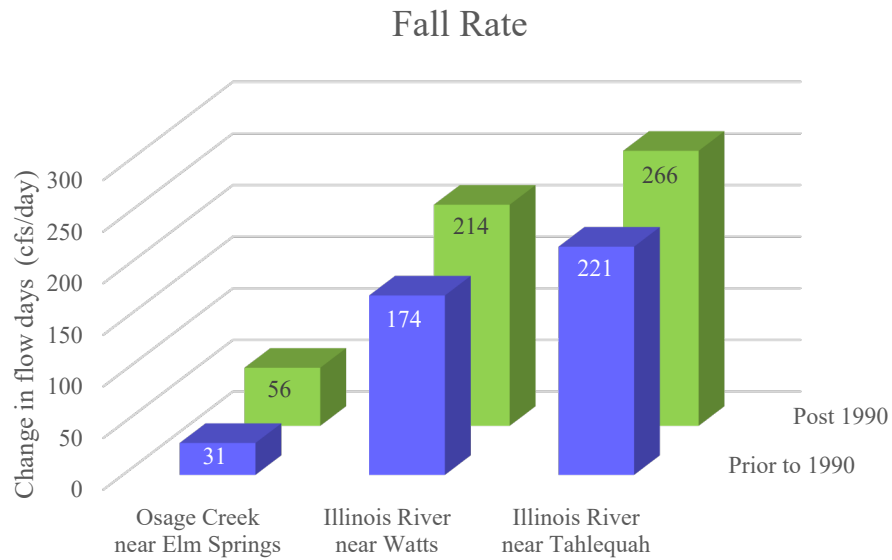
Figure 39. The fall rate, in cubic feet per second per day, for select sites prior to 1990 and post 1990.

HEC-HMS Model Development

The Hydrologic Engineering Center (HEC) watershed modeling software, Hydrologic Modeling System (HMS), was used in order to simulate infiltration, surface runoff, subsurface processes, and streamflow in gaged and ungaged basins. HEC-HMS is designed to simulate the precipitation-runoff processes, including flood hydrology and small urban or natural watershed runoff, for dendritic watershed systems (Bartles et al., 2021).

The Illinois River HMS model simulates the physical properties of the watershed through user-specified methods of infiltration, surface runoff, and subsurface processes for each subbasin (Figure 1). The process of simulating infiltration was performed using the deficit and constant loss method. This particular method conserves mass and uses a single soil layer to account for changes in moisture content (Bartles et al., 2021). The process of simulating runoff was performed using the ModClark transform method. This particular method is a linear, quasi-distributed transform method that is based on the Clark conceptual unit hydrograph (Bartles et al., 2021). The process of simulating the subsurface was performed using the recession baseflow method. This particular method is designed to approximate the typical behavior observed in watersheds when channel flow recedes exponentially after an event (Bartles et al., 2021).

Rivers and streams within the Illinois River HMS model (Figure 1), are simulated as having one or more inflows and only one outflow and all inflows are summed together before computing an outflow (Bartles et al., 2021). The routing method used to route streamflow through the Illinois River HMS model was the Muskingum routing method. The Muskingum routing method uses a simple conservation of mass approach but does not assume that the water surface is level (Bartles et al., 2021). This approach accounts for increased storage during the rising side of a flood wave and decreased storage during the falling side (Bartles et al., 2021). Additionally, attenuation was approximated within the Illinois River HMS model using the Muskingum routing method.

The main driving force in any hydrologic model is precipitation. Precipitation, in the form of rain, was input into the Illinois River HMS model as six distinct storm events. Each storm event was input as a grid that was derived from radar rainfall data, except for the 1990 event, which will be described in more detail in a later section. The gridded precipitation method, within HMS, is designed to work with the ModClark gridded transform method (Bartles et al., 2021).

HEC-HMS Modeled Storm Events

Six historical storm events were chosen to capture flood hydrology in the Illinois River watershed. Four of the historical storm events were used to calibrate the HEC-HMS model and the other two were used to validate parameter sets for the four calibration events. Table 3 lists the name and dates of the events and whether the event was used for calibration or validation.

Table 3. Modeled storm events used for calibration or validation in the Illinois River watershed HEC-HMS model.

Event Name	Event Dates	Calibration or Validation
May 1990	01May1990 - 10May1990	Calibration
Mar 2008	18Mar2008 - 21Mar2008	Validation
Apr 2011	23Apr2011 - 29Apr2011	Calibration
Dec 2015	26Dec2015 - 30Dec2015	Calibration
Apr 2017	26Apr2017 - 06May2017	Validation
Feb 2018	20Feb2018 - 01Mar2018	Calibration

The five most recent events were chosen because 1) gridded rainfall data was available and used to drive the model, and 2) four of those five (2008, 2011, 2015, 2017) were the largest events to have occurred in the Illinois River watershed since gage data began being collected. The 1990 event was also one of the largest events to have occurred; however, there was not any gridded rainfall data available and, therefore, had to be developed. This precipitation dataset and methods to create will be discussed in the next section. The precipitation data for the remaining storm events were obtained from Stage III radar data.

1990 Event

The 1990 storm event was gridded from fixed location, time-series climate measurements within and around the Illinois River watershed. In order to create the gridded precipitation data, the HEC GageInterp program was utilized (Evans, 2016). The GageInterp program creates a sequence of precipitation grids that approximates the variation of the precipitation through time and space from fixed locations to be used within HEC computer modeling programs (Evans, 2016). Once the gridded data was created, the data was used within the Illinois River HMS model like the Stage III radar data of the later events.

Calibration of the HEC-HMS Model

To obtain good agreement between simulated and observed streamflow, the Illinois River HMS model was calibrated by adjusting certain parameters within the hydrologic model. Parameters were adjusted manually by examining model fit statistics between observed and simulated streamflow. The statistics of interest include the Nash-Sutcliffe efficiency (NSE) index and percent bias (pbias). NSE and pbias are widely used statistics for assessing the goodness of fit for hydrologic models. Moriasi et al. (2015) recommend a range of NSE and pbias values that are widely accepted among the hydrologic community for assessing model performance. Furthermore, Moriasi et al. (2015) state using time series and scatter plots, for shorter time periods, are effective for data visualization and demonstration of model performance. Time series plots are provided in Appendix A.

HEC-HMS Model Parameters

As previously mentioned, the calibration of simulated streamflow was achieved by manually adjusting certain parameters within the HMS model. After model calibration was achieved, the

model parameters from each calibrated event were averaged, except for percent impervious. Percent impervious was obtained from the National Land Cover Database (NLCD; Dewitz, 2021) and each modeled storm event used the percent impervious values from the closest year NLCD percent impervious maps were published. For example, the December 2015 calibration event and the April 2017 validation event both had percent impervious values from the 2016 NLCD percent impervious surface. All other averaged parameter values were then used to assess model performance using two validation storm events that were not included during calibration.

HEC-HMS Model Results

In general, the simulated streamflows matched the observed streamflows for all calibrated streamflow gaging sites. For all calibration and validation events, only the goodness of fit statistics will be shown. All comparison graphs (simulated versus observed streamflow) will be shown in Appendix A. The goodness of fit statistics provided include mean absolute error (MAE), normalized root-mean-square error (RMSE), percent bias (PBIAS), the standard deviation of measured data (RSR), the Nash-Sutcliffe efficiency (NSE), modified NSE, the coefficient of determination (R^2), and adjusted R^2. The statistics presented here are those that are commonly used in evaluating the calibration of hydrologic models. Moriasi et al. (2015) provides greater detail (i.e., how they are calculated) for each of the goodness of fit statistics presented here and provides qualitative ratings for "very good", "good", "satisfactory", or "unsatisfactory" for each statistic; similar designations are color coded as green, yellow, orange, and red, respectively, in Table 4. In addition to calibration, two, additional storm events (2008 and 2017) were used for validation of model parameters. Validation is a necessary step in order to assess model performance.

Table 4. HEC-HMS modeling results for calibration and validation events for all sites in the Illinois River watershed.

Site Name	MAE	Normalized RMSE (%)	PBIAS (%)	RSR	NSE	Modified NSE	R^2	Adjusted R^2
May 1990 Calibration Event								
Illinois River near Tahlequah, OK	1,238.45	13.3	-6.1	0.13	0.98	0.86	0.98	0.96
Baron Fork at Eldon, OK	1,521.44	47.7	4.5	0.48	0.77	0.67	0.81	0.59
Flint Creek near Kansas, OK	555.89	50.4	-4.5	0.5	0.75	0.42	0.78	0.73
Illinois River near Watts, OK	1,266.15	20.6	-3.9	0.21	0.96	0.79	0.96	0.95
Baron Fork at Dutch Mills, AR	299.15	45.1	-4.1	0.45	0.8	0.61	0.81	0.6
April 2011 Calibration Event								

Site Name	MAE	Normalized RMSE (%)	PBIAS (%)	RSR	NSE	Modified NSE	R^2	Adjusted R^2
Illinois River near Tahlequah, OK	3,541.87	19.8	-1.3	0.2	0.96	0.84	0.97	0.9
Baron Fork at Eldon, OK	1,715.94	20.8	-2.9	0.21	0.96	0.82	0.96	0.93
Illinois River at Chewey, OK	3,677.71	19.8	-4.4	0.2	0.96	0.82	0.97	0.9
Flint Creek near Kansas, OK	443.22	31	-14.7	0.31	0.9	0.76	0.92	0.79
Flint Creek near West Siloam Springs, OK	477.22	45.3	3	0.45	0.79	0.58	0.83	0.61
Illinois River near Watts, OK	3,364.7	21.3	3.1	0.21	0.95	0.81	0.96	0.92
Illinois River South of Siloam Springs, AR	3,767.48	27.6	-1.9	0.28	0.92	0.75	0.92	0.87
Illinois River at Hwy. 16 near Siloam Springs, AR	2,761.3	21.4	-1.4	0.21	0.95	0.79	0.95	0.93
Baron Fork at Dutch Mills, AR	327.04	24.6	11.3	0.25	0.94	0.77	0.95	0.89
Flint Creek at Springtown, AR	78.75	34.7	-4	0.35	0.88	0.71	0.88	0.79
Osage Creek near Elm Springs, AR	1,142.38	38.4	-14.1	0.38	0.85	0.71	0.89	0.69
December 2015 Calibration Event								
Illinois River near Tahlequah, OK	3,819.69	15.1	-10.8	0.15	0.98	0.88	0.99	0.9
Baron Fork at Eldon, OK	872.42	9.1	-0.6	0.09	0.99	0.92	0.99	0.98
Illinois River at Chewey, OK	3,978.45	17.2	-12.2	0.17	0.97	0.85	0.98	0.89
Flint Creek near Kansas, OK	567.7	17.3	-3.7	0.17	0.97	0.88	0.97	0.97
Flint Creek near West Siloam Springs, OK	209.23	19.2	-1.1	0.19	0.96	0.86	0.97	0.96
Illinois River near Watts, OK	3,924.02	21	-15.2	0.21	0.96	0.82	0.97	0.86
Illinois River South of Siloam Springs, AR	2,707.87	17	-9.6	0.17	0.97	0.86	0.98	0.89

Site Name	MAE	Normalized RMSE (%)	PBIAS (%)	RSR	NSE	Modified NSE	R^2	Adjusted R^2
Illinois River at Hwy. 16 near Siloam Springs, AR	4,535.26	26.4	-22.5	0.26	0.93	0.77	0.97	0.83
Baron Fork at Dutch Mills, AR	257.81	20.4	1.3	0.2	0.96	0.85	0.96	0.94
Flint Creek at Springtown, AR	73.19	16.7	0.6	0.17	0.97	0.87	0.97	0.97
Illinois River at Savoy, AR	534.21	12.3	2	0.12	0.98	0.92	0.99	0.94
Osage Creek near Elm Springs, AR	813.76	31.5	14.2	0.31	0.9	0.79	0.94	0.84
Osage Creek near Cave Springs, AR	187.7	17.9	1.2	0.18	0.97	0.87	0.97	0.96
February 2018 Calibration Event								
Illinois River near Tahlequah, OK	1,287.35	22.7	4	0.23	0.95	0.74	0.95	0.93
Baron Fork at Eldon, OK	683.67	33.1	4.6	0.33	0.89	0.65	0.92	0.86
Illinois River at Chewey, OK	1,072.23	18.4	6.3	0.18	0.97	0.77	0.97	0.95
Flint Creek near Kansas, OK	166.26	27.6	6.7	0.28	0.92	0.77	0.94	0.89
Flint Creek near West Siloam Springs, OK	96.95	50.8	-2.2	0.51	0.74	0.46	0.85	0.78
Illinois River near Watts, OK	980.25	19.6	1.5	0.2	0.96	0.74	0.96	0. 92
Illinois River South of Siloam Springs, AR	1,003.85	28.7	11.2	0.29	0.92	0.66	0.95	0.86
Illinois River at Hwy. 16 near Siloam Springs, AR	833.25	23	6.1	0.23	0.95	0.72	0.96	0.9
Baron Fork at Dutch Mills, AR	155.74	41.1	-6.5	0.41	0.83	0.62	0.83	0.72
Flint Creek at Springtown, AR	41.38	63	20.1	0.63	0.6	0.21	0.75	0.68
Illinois River at Savoy, AR	291.73	24.4	1.9	0.24	0.94	0.75	0.96	0.9
Osage Creek near Elm Springs, AR	272.11	26	5.7	0.26	0.93	0.64	0.94	0.9

Site Name	MAE	Normalized RMSE (%)	PBIAS (%)	RSR	NSE	Modified NSE	R^2	Adjusted R^2
Osage Creek near Cave Springs, AR	83.44	25	2.8	0.25	0.94	0.67	0.96	0.89

<table>

			March 2008 Validation Event					
Illinois River near Tahlequah, OK	1,856.17	16.5	-18.8	0.17	0.97	0.78	0.99	0.92
Baron Fork at Eldon, OK	655.8	14.5	-17.6	0.14	0.98	0.81	0.99	0.9
Flint Creek near Kansas, OK	440.45	41.8	7.2	0.42	0.82	0.59	0.9	0.79
Flint Creek near West Siloam Springs, OK	148.48	38.4	17.3	0.38	0.85	0.6	0.97	0.76
Illinois River near Watts, OK	1,516.56	24.4	-17	0.24	0.94	0.75	0.96	0.81
Illinois River at Hwy. 16 near Siloam Springs, AR	1,424.19	28.4	-9.3	0.28	0.92	0.74	0.94	0.78
Baron Fork at Dutch Mills, AR	159.27	26.2	-15.5	0.26	0.93	0.71	0.94	0.84
Flint Creek at Springtown, AR	99.54	81.7	8.7	0.82	0.33	0.06	0.93	0.64
Illinois River at Savoy, AR	572.47	25.7	2.9	0.26	0.93	0.72	0.97	0.85
Osage Creek near Elm Springs, AR	326.19	18.7	-25.5	0.19	0.96	0.71	0.98	0.9
Osage Creek near Cave Springs, AR	113.41	28.7	-33.5	0.29	0.92	0.72	0.99	0.74

			April 2017 Validation Event					
Illinois River near Tahlequah, OK	7,544.38	54	3.3	0.54	0.71	0.47	0.85	0.75
Baron Fork at Eldon, OK	1,927.06	53.4	4.6	0.53	0.71	0.42	0.84	0.74
Illinois River at Chewey, OK	6,427.33	52.1	1.7	0.52	0.73	0.51	0.83	0.76
Flint Creek near Kansas, OK	1,158.57	85.5	41.4	0.85	0.27	0.22	0.82	0.56
Flint Creek near West Siloam Springs, OK	590.07	168.9	115.1	1.69	-1.86	-0.4	0.9	0.38

</table>

Site Name	MAE	Normalized RMSE (%)	PBIAS (%)	RSR	NSE	Modified NSE	R^2	Adjusted R^2
Illinois River near Watts, OK	5,330.06	45.8	-3.6	0.46	0.79	0.55	0.81	0.76
Illinois River South of Siloam Springs, AR	4,949.53	46.2	3	0.46	0.79	0.51	0.82	0.82
Illinois River at Hwy. 16 near Siloam Springs, AR	4,689.64	45.4	-4.2	0.45	0.79	0.56	0.8	0.68
Baron Fork at Dutch Mills, AR	237.71	34.6	39.9	0.35	0.88	0.63	0.93	0.82
Flint Creek at Springtown, AR	231.27	169.9	176.5	1.7	-1. 9	-1.04	0.76	0.35
Illinois River at Savoy, AR	2,395.78	65	52.9	0.65	0.58	0.27	0.79	0.65
Osage Creek near Elm Springs, AR	2,674.06	136.9	-21.2	1.37	-0.88	-0.06	0.53	0.49
Osage Creek near Cave Springs, AR	297.52	60.6	26.6	0.61	0.63	0.56	0.96	0.66

May 1990 Calibration Event

For the May 1990 calibration event, only five sites had observed data to calibrate against. All sites had good agreement between simulated and observed represented by the goodness of fit statistics presented in Table 4 and by the time series plots presented in Appendix A.

April 2011 Calibration Event

For the April 2011 calibration event, the Illinois River at Savoy, AR, and the Osage Creek near Cave Springs, AR, gages were not functioning during the time of the event. Therefore, those gages were not able to be calibrated. All other sites had good agreement between simulated and observed represented by the goodness of fit statistics presented in Table 4 and by the time series plots presented in Appendix A.

December 2015 Calibration Event

For the December 2015 calibration event, most sites had good agreement between simulated and observed represented by the goodness of fit statistics and time series plots (Table 4 and Appendix A). The Illinois River at Hwy. 16 near Siloam Springs, AR, had the PBIAS values that were determined to be unsatisfactory; however, all other statistics were deemed to be very good.

February 2018 Calibration Event

For the February 2018 calibration event, all sites had good agreement between simulated and observed represented by the goodness of fit statistics presented in Table 4 and by the time series plots presented in Appendix A. One site, Flint Creek at Springtown, AR, had a "satisfactory" to "good" rating for all statistics (Table 4).

March 2008 Validation Event

For the 2008 validation event, the averaged parameters performed reasonably well for most sites (Table 4 and Appendix A). The sites with the lowest performance were Flint Creek at Springtown, AR, Osage Creek near Elm Springs, AR, and Osage Creek near Cave Springs, AR, but not with every statistic (Table 4).

April 2017 Validation Event

The 2017 validation event was the lowest performing event, overall. In general, the sites with the poorest statistics were the headwater and/or the tributaries (Table 4 and Appendix A). However, the mainstem of the Illinois River, excluding the headwater site of Illinois River at Savoy, AR, validated fairly well (Table 4).

HEC-RAS Model Development

The Hydrologic Engineering Center's River Analysis System software (HEC-RAS) version 5.0.7 was used to build the hydraulic model for the Illinois River basin, and final updates to the model were run in HEC-RAS v 6.1. HEC-RAS is designed to perform one-dimensional and two-dimensional hydraulic calculations for a full network of natural and constructed channels, overbank/floodplain areas, etc. This model utilizes the one-dimensional approach with the output from the HEC-HMS model as flow hydrograph input for the Illinois River and its tributaries to compute expected water surface elevations associated with the various flow scenarios. Output for the HEC-RAS model includes profile plots for streams, cross sections, and structures along the reaches, as well as computed rating curves and hydrographs at individual cross section locations and inundation mapping via the RAS Mapper feature. Most reaches were modeled as cross sections, although some of the smaller tributaries were modeled as storage areas. Larger bridges were included as bridge structures using the bridge data editor. The dams at Lake Tenkiller and Siloam Springs Lake were modeled as inline structures, while smaller low water structures found on various reaches were modeled using blocked obstructions on a cross section.

Storm events were modeled using an unsteady flow simulation and the calibrated flow results from the HEC-HMS model. The gate operations at Tenkiller Dam were set using the parameters from the 2014 Mapping and Modeling Consequences (MMC) dam break model of Tenkiller Dam.

The April 2011 and December 2015 events were used as calibration events, and the April 2017 event was included as a verification event. All events were modeled using the unsteady flow analysis option in HEC-RAS. The simulation time windows for the events are given below in Table 5. The April 2017 event remains the largest single event in the basin, with several locations reaching record flows during that event.

Table 5. Simulation time windows for the Illinois River HEC-RAS model.

Storm Event	Simulation Start Date	Simulation Start Time	Simulation End Date	Simulation End Time
April 2011	24 Apr 2011	0000	29 Apr 2011	2400
December 2015	25 Dec 2015	0000	30 Dec 2015	1200
April 2017	22 Apr 2017	1200	03 May 2017	2400

All three events used HEC-HMS output in the form of DSS files for the unsteady flow data. Subbasin breakouts were matched with cross sections, and the corresponding flows set as flow hydrographs (at the most upstream cross section of a reach) or lateral inflow hydrographs (at cross sections that fall within the reach) for those locations. The downstream boundary condition for the entire basin is set to Normal Depth at a slope of 0.0007.

In addition to the calibration and verification events, thirteen (13) other unsteady flow files were developed with output hydrographs from the HEC-HMS model: the current 50, 20, 10, 2, and 1 percent annual exceedance probability (AEP) events, the 1 percent AEP frequency event with future A1B land use projections, the 1 percent AEP frequency event with future B2 land use projections, the 2017 event with future A1B land use projections, and the 2017 event with future B2 land use projections. Please see section on Combination Land Use and Climate for more information on the land use projection description and methodology. Each of the future projection scenarios were also simulated with hypothetical detention basins.

The model contains two geometries: one which models current hydraulic conditions in the basin and one which models riparian zones along the upstream tributaries. Differences between the two conditions were modeled primarily by changing Manning's n-values throughout the basin. The flows resulting from projected future land use conditions from the hydrologic model were simulated on the current conditions geometry because the majority of the land use changes are in the headwaters of the watershed and are represented outside the hydraulic model domain by the hydrologic model. It is recognized that some future development could occur close to the rivers (inside the hydraulic model domain), but the overall projection of future development is better represented in the lump-sum hydrologic model. A sensitivity to lower Manning's n-values at some possible future land-use locations within the upstream portions of the hydraulic model domain indicated little impact to flows along the mainstem reach of the Illinois River.

Manning's n-values for the current-conditions geometry range from 0.03 in the channel downstream of Tenkiller Lake to 0.085 for wooded overbanks areas. Typical channel values throughout the model are between 0.04-0.05.

Riparian zones were represented by horizontally varied n-values, in bands of approximately 100 feet on either side of the channel in affected zones. Tributaries in the upstream portion of the basin were included, as well as certain zones along the downstream tributaries and the main stem of the Illinois River, as identified in an HEC-HMS analysis. Manning's n-values in riparian zones were set to 0.15.

Calibration of the HEC-RAS Model

Model calibration is the process of adjusting model parameters to reproduce observed data for a fixed period of time. Model verification is simulating the model over a different time period without further adjustment to the model parameters in order to test the accuracy of the predictive ability of the model. The HEC-RAS model was calibrated and validated by making comparisons to the latest ratings curves for the existing USGS gages as well as the time series comparisons of stage and flow for the respective events. Additionally, the flow computations in the hydraulic model were compared to the flow computations from the HMS model at the USGS gage locations. While the hydraulic model was not calibrated to the HMS model, the comparison between the two models was made to ensure proper linkage between the hydrologic model outputs and the hydraulic model inputs as well. The following sites were used to make calibration and validation comparisons. Fourteen (14) USGS streamgages with gage datum information available were included in the model for calibration purposes. They are listed below in Table 6.

Table 6. US Geological Survey stream gaging locations used for calibration of the Illinois River HEC-RAS model.

USGS Site Number	USGS Site Name	HMS Site Name	HEC-RAS Cross Section	HEC-RAS River Name	HEC-RAS Reach Name
07197000	Baron Fork at Eldon, OK	BRNFRKELDN	9.009231	Baron Fork	Main
07196900[1]	Baron For at Dutch Mills, AR	BRNFRKDTCHML	36.51449	Baron Fork	Main
07196000	Flint Creek near Kansas, OK	FLNTCRKKS	1.683396	Flint Creek	Main
07195800	Flint Creek at Springtown, AR	FLNTCRKSPRGTWN	23.42009	Flint Creek	Main
07195855	Flint Creek near West Siloam Springs, OK	FLNTCRKWSS	10.82928	Flint Creek	Main
07196090	Illinois River at Chewey, OK	ILLCHEWEY	76.19955	Illinois River	DS_FlintCr
07198000	Illinois River at Gore, OK	ILLGORE	8.009267	Illinois River	DS_CaneyCr
07195400	Illinois River at Hwy. 16 near Siloam Springs AR	ILLHWY16	107.3044	Illinois River	DS_OsageCr
07194800	Illinois River at Savoy, AR	ILLSAVOY	124.9029	Illinois River	DS_MuddyFork
07195430	Illinois River South of Siloam Springs, AR	ILLSSS	102.0608	Illinois River	DS_OsageCr

USGS Site Number	USGS Site Name	HMS Site Name	HEC-RAS Cross Section	HEC-RAS River Name	HEC-RAS Reach Name
07195500	Illinois River near Watts, OK	ILLWATTS	97.13998	Illinois River	DS_BallardCr
07195000	Osage Creek near Elm Springs, AR	OSAGEELMSPGS	9.985327	Osage Creek	Main
07196500	Illinois River near Tahlequah, OK	ILLTLQUAH	45.07397	Illinois River	DS_FlintCr
07194880	Osage Creek near Cave Springs, AR	OSAGECVESPG	16.77052	Osage Creek	Main

[1]The gage datum for Baron Fork at Dutch Mills is inaccurate and the USGS was notified, but flow comparisons were still valid.

Channel inverts were set at cross sections with known (or recently known) channel bed elevations. These were almost exclusively at bridges, although existing bathymetric survey data for the Tenkiller reservoir area was incorporated. Much of the channel cross sections were estimated. Results can be improved with more detailed channel elevation data gathered by future surveys.

The main parameter adjusted in the RAS model for calibration was the Manning's Roughness Coefficient, or Manning's n. Manning's n values in channels in this model range from 0.04 to 0.05 for most reaches, with higher values around 0.08 in the cross sections immediately upstream and downstream of Tenkiller Dam. Typical overbank values range from 0.06 to 0.07. A lower Manning's n value corresponds to little resistance to flow, such as a concrete channel or other smooth flow area, while a higher *n*-value corresponds to a higher resistance, such as a channel that is very rocky or clogged with reeds. Flow roughness factors, which scale the roughness coefficients for specified areas for specified flow ranges, are included for several locations throughout the model to improve calibrations.

Contraction and expansion coefficients are 0.1 and 0.3, respectively, for typical cross sections throughout the model. Contraction and expansion coefficients around bridges are 0.3 and 0.5, respectively.

HEC-RAS Model Calibration Results

Observed rating curves for USGS gage locations were used to calibrate the model as well a time series data for observed stage and flow. These gage locations, along with their corresponding cross section location in the model, are listed in Table 6. Calibration results were checked by comparing the observed rating curve with the computed rating curve at that location within the RAS model, comparing the observed time series with the computed time series, and statistical goodness of fit metrics were performed for each location for each event. Table 7 summarizes the goodness of fit metrics at each location for each event. A selection of rating curves is shown below in Figure 40 through 53 that includes the last 10 years of USGS measurements, the current USGS rating, and the modeled rating results with the compute Root Mean Square Error (RMSE).

The RMSE at for the flow-stage rating relationship on the mainstem Illinois River range from 0.3 at Tahlequah and Chewey up to 1.82 at Savoy. The Savoy gage is near the confluence with Clear Creek and may experience different backwater conditions which lends itself to possibly needing a more complex rating than the published single-valued rating. The model comparison at Savoy is still in reasonable agreement with measurements made in 2011 and 2004. The time series comparisons for each event can be found in Appendix B.

Table 7. HEC-RAS modeling results for calibration and validation events for all sites in the Illinois River watershed. Qualitative color coding is explained in "HEC-HMS Model Results".

Site Name	Parameter	Maximum Simulated (feet or cfs)	Maximum Observed (feet or cfs)	Normalized RMSE (%)	PBIAS (%)	RSR	NSE	R^2
April 2011 Calibration Event								
Illinois River near Tahlequah, OK	Elevation	690.5	691.1	33.0	0.2	0.33	0.89	0.94
Illinois River near Tahlequah, OK	Flow	76,752	85,400	25.7	-4.5	0.26	0.93	0.95
Baron Fork at Eldon, OK	Elevation	729.7	729.7	24.2	0.0	0.24	0.94	0.95
Baron Fork at Eldon, OK	Flow	64,644	62,900	22.6	-3.8	0.23	0.95	0.95
Illinois River at Chewey, OK	Elevation	828.5	830.4	21.7	-0.1	0.22	0.95	0.97
Illinois River at Chewey, OK	Flow	78,078	91,500	21.1	-4.6	0.21	0.96	0.97
Flint Creek near Kansas, OK	Elevation	868.7	867.4	74.7	0.0	0.75	0.44	0.83
Flint Creek near Kansas, OK	Flow	12,240	13,500	39.1	7.1	0.39	0.85	0.85
Flint Creek near West Siloam Springs, OK	Elevation	970.7	970	61.1	0.1	0.61	0.62	0.79
Flint Creek near West Siloam Springs, OK	Flow	8,748	15,700	60.2	0.9	0.6	0.64	0.67
Illinois River near Watts, OK	Elevation	920.1	922.6	54.6	-0.3	0.55	0.7	0.88
Illinois River near Watts, OK	Flow	80,719	974,00	27.1	2.3	0.27	0.93	0.93
Illinois River South of Siloam Springs, AR	Elevation	937.9	940.8	36.0	0.0	0.36	0.87	0.87

Site Name	Parameter	Maximum Simulated (feet or cfs)	Maximum Observed (feet or cfs)	Normalized RMSE (%)	PBIAS (%)	RSR	NSE	R^2
Illinois River South of Siloam Springs, AR	Flow	76,975	105,000	33.4	-2.1	0.33	0.89	0.89
Illinois River at Hwy. 16 near Siloam Springs, AR	Elevation	958.5	959.3	48.3	0.1	0.48	0.77	0.87
Illinois River at Hwy. 16 near Siloam Springs, AR	Flow	78,636	871,00	19.4	-3.6	0.19	0.96	0.96
Baron Fork at Dutch Mills, AR	Elevation	968.7	1001.3	1432.8	-3.4	14.33	-205.6	0.75
Baron Fork at Dutch Mills, AR	Flow	18,996	19,300	48.2	12.2	0.48	0.77	0.8
Flint Creek at Springtown, AR	Elevation	1,185.7	1,182.2	137.7	0.2	1.38	-0.91	0.83
Flint Creek at Springtown, AR	Flow	2,397	2,170	37.4	-1.2	0.37	0.86	0.86
Illinois River at Savoy, AR	Elevation	1,028.2	1,029.2	65.7	0.0	0.66	0.56	0.6
Illinois River at Savoy, AR	Flow	3505	2910	149.0	58.3	1.49	-1.25	0.83
Osage Creek near Elm Springs, AR	Elevation	1,070.8	1,072.8	71.1	-0.2	0.71	0.49	0.87
Osage Creek near Elm Springs, AR	Flow	22,071	38,000	40.5	-13.1	0.4	0.83	0.88

December 2015 Calibration Event

Site Name	Parameter	Maximum Simulated (feet or cfs)	Maximum Observed (feet or cfs)	Normalized RMSE (%)	PBIAS (%)	RSR	NSE	R^2
Illinois River near Tahlequah, OK	Elevation	693.3	695.8	25.4	-0.1	0.25	0.93	0.95
Illinois River near Tahlequah, OK	Flow	99,702	126,000	36.0	-13.1	0.36	0.87	0.91
Baron Fork at Eldon, OK	Elevation	726.4	726.7	18.4	0.0	0.18	0.97	0.97
Baron Fork at Eldon, OK	Flow	47,648	48,100	10.6	0.5	0.11	0.99	0.99
Illinois River at Chewey, OK	Elevation	830.5	833.2	26.0	-0.1	0.26	0.93	0.95

Site Name	Parameter	Maximum Simulated (feet or cfs)	Maximum Observed (feet or cfs)	Normalized RMSE (%)	PBIAS (%)	RSR	NSE	R^2
Illinois River at Chewey, OK	Flow	91,939	120,000	32.6	-13.0	0.33	0.89	0.93
Flint Creek near Kansas, OK	Elevation	869.5	871	20.1	0.0	0.2	0.96	0.97
Flint Creek near Kansas, OK	Flow	14,485	18,100	32.5	-19.6	0.32	0.89	0.95
Flint Creek near West Siloam Springs, OK	Elevation	969.2	970.2	36.8	0.0	0.37	0.86	0.89
Flint Creek near West Siloam Springs, OK	Flow	6,175	7,020	29.7	-3.0	0.3	0.91	0.92
Illinois River near Watts, OK	Elevation	920.5	922.6	64.6	-0.5	0.65	0.58	0.9
Illinois River near Watts, OK	Flow	84,267	110,000	32.1	-12.1	0.32	0.9	0.91
Illinois River South of Siloam Springs, AR	Elevation	938	940	28.0	-0.1	0.28	0.92	0.93
Illinois River South of Siloam Springs, AR	Flow	77,203	93,900	26.2	-6.7	0.26	0.93	0.94
Illinois River at Hwy. 16 near Siloam Springs, AR	Elevation	957.9	959	19.2	0.0	0.19	0.96	0.96
Illinois River at Hwy. 16 near Siloam Springs, AR	Flow	71,270	83,700	31.8	-21.5	0.32	0.9	0.95
Baron Fork at Dutch Mills, AR	Elevation	964.3	996.3	1394.1	-3.5	13.94	-195.2	0.87
Baron Fork at Dutch Mills, AR	Flow	8,376	8,490	22.5	3.1	0.22	0.95	0.95
Flint Creek at Springtown, AR	Elevation	1,186.3	1,182.2	183.6	0.3	1.84	-2.4	0.91
Flint Creek at Springtown, AR	Flow	3,145	2,980	21.1	3.7	0.21	0.95	0.96
Illinois River at Savoy, AR	Elevation	1,035.3	1,038.6	48.0	-0.1	0.48	0.77	0.87
Illinois River at Savoy, AR	Flow	20,972	30,200	37.2	-22.6	0.37	0.86	0.97

Site Name	Parameter	Maximum Simulated (feet or cfs)	Maximum Observed (feet or cfs)	Normalized RMSE (%)	PBIAS (%)	RSR	NSE	R^2
Osage Creek near Elm Springs, AR	Elevation	1,070.8	1,070.9	30.0	-0.1	0.3	0.91	0.97
Osage Creek near Elm Springs, AR	Flow	22,000	23,300	32.1	16.4	0.32	0.9	0.94
Osage Creek near Cave Springs, AR	Elevation	1,142	1,142.5	19.8	0.0	0.2	0.96	0.97
Osage Creek near Cave Springs, AR	Flow	6,347	5,820	21.0	2.9	0.21	0.96	0.96
April 2017 Validation Event								
Illinois River near Tahlequah, OK	Elevation	694.1	694.4	45.7	0.2	0.46	0.79	0.86
Illinois River near Tahlequah, OK	Flow	106,792	108,000	45.0	24.9	0.45	0.8	0.88
Baron Fork at Eldon, OK	Elevation	27.2	726.4	73.2	0.0	0.73	0.46	0.79
Baron Fork at Eldon, OK	Flow	51,559	46,600	47.0	24.7	0.47	0.78	0.91
Illinois River at Chewey, OK	Elevation	832.2	833.5	33.1	0.1	0.33	0.89	0.93
Illinois River at Chewey, OK	Flow	105,100	124,000	41.7	23.8	0.42	0.83	0.88
Flint Creek near Kansas, OK	Elevation	872.1	873.3	68.5	0.0	0.68	0.53	0.75
Flint Creek near Kansas, OK	Flow	22,268	19,400	62.5	47.4	0.62	0.61	0.83
Flint Creek near West Siloam Springs, OK	Elevation	972	969.3	77.7	0.1	0.78	0.39	0.9
Flint Creek near West Siloam Springs, OK	Flow	12,753	5,560	152.4	145.6	1.52	-1.33	0.85
Illinois River near Watts, OK	Elevation	922.1	924.1	58.8	-0.2	0.59	0.65	0.87
Illinois River near Watts, OK	Flow	103,695	128,000	38.5	18.8	0.39	0.85	0.87
Illinois River South of Siloam Springs, AR	Elevation	940.2	941.7	41.2	0.2	0.41	0.83	0.9

Site Name	Parameter	Maximum Simulated (feet or cfs)	Maximum Observed (feet or cfs)	Normalized RMSE (%)	PBIAS (%)	RSR	NSE	R^2
Illinois River South of Siloam Springs, AR	Flow	100,811	106,000	52.3	36.4	0.52	0.72	0.84
Illinois River at Hwy. 16 near Siloam Springs, AR	Elevation	960.3	961.8	47.3	0.2	0.47	0.78	0.9
Illinois River at Hwy. 16 near Siloam Springs, AR	Flow	101,191	149,000	41.1	13.8	0.41	0.83	0.84
Baron Fork at Dutch Mills, AR	Elevation	967.9	999.5	1900.2	-3.5	19	-361.9	0.68
Baron Fork at Dutch Mills, AR	Flow	15,539	14,900	46.2	44.9	0.46	0.79	0.85
Flint Creek at Springtown, AR	Elevation	1,186.8	1,183.4	289.4	0.3	2.89	-7.42	0.63
Flint Creek at Springtown, AR	Flow	4,801	3,090	173.4	235.6	1.73	-2.02	0.77
Illinois River at Savoy, AR	Elevation	1,039.3	1,044.8	44.2	0.1	0.44	0.8	0.92
Illinois River at Savoy, AR	Flow	38,232	66,500	42.0	13.9	0.42	0.82	0.87
Osage Creek near Elm Springs, AR	Elevation	1,070.7	1,068.8	85.4	-0.1	0.85	0.26	0.92
Osage Creek near Elm Springs, AR	Flow	21,858	11,100	132.8	64.9	1.33	-0.78	0.92
Osage Creek near Cave Springs, AR	Elevation	1,143.4	1,143.5	35.4	0.0	0.35	0.87	0.94
Osage Creek near Cave Springs, AR	Flow	586	6810	61.8	41.7	0.62	0.62	0.95
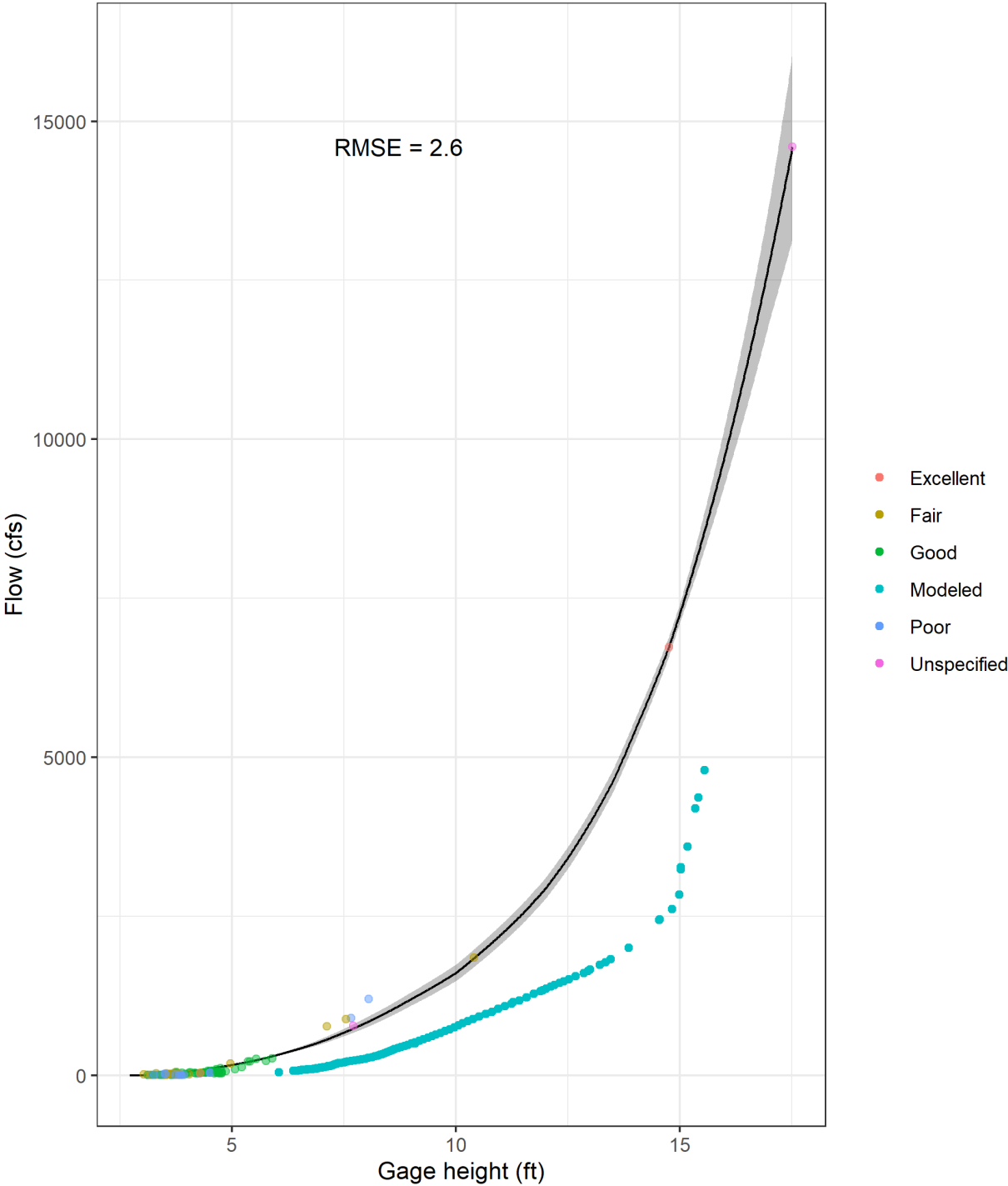
*Figure 40. USGS 07195800 – Flint Creek at Springtown, AR, calibration results for the Illinois River HEC-RAS model.*
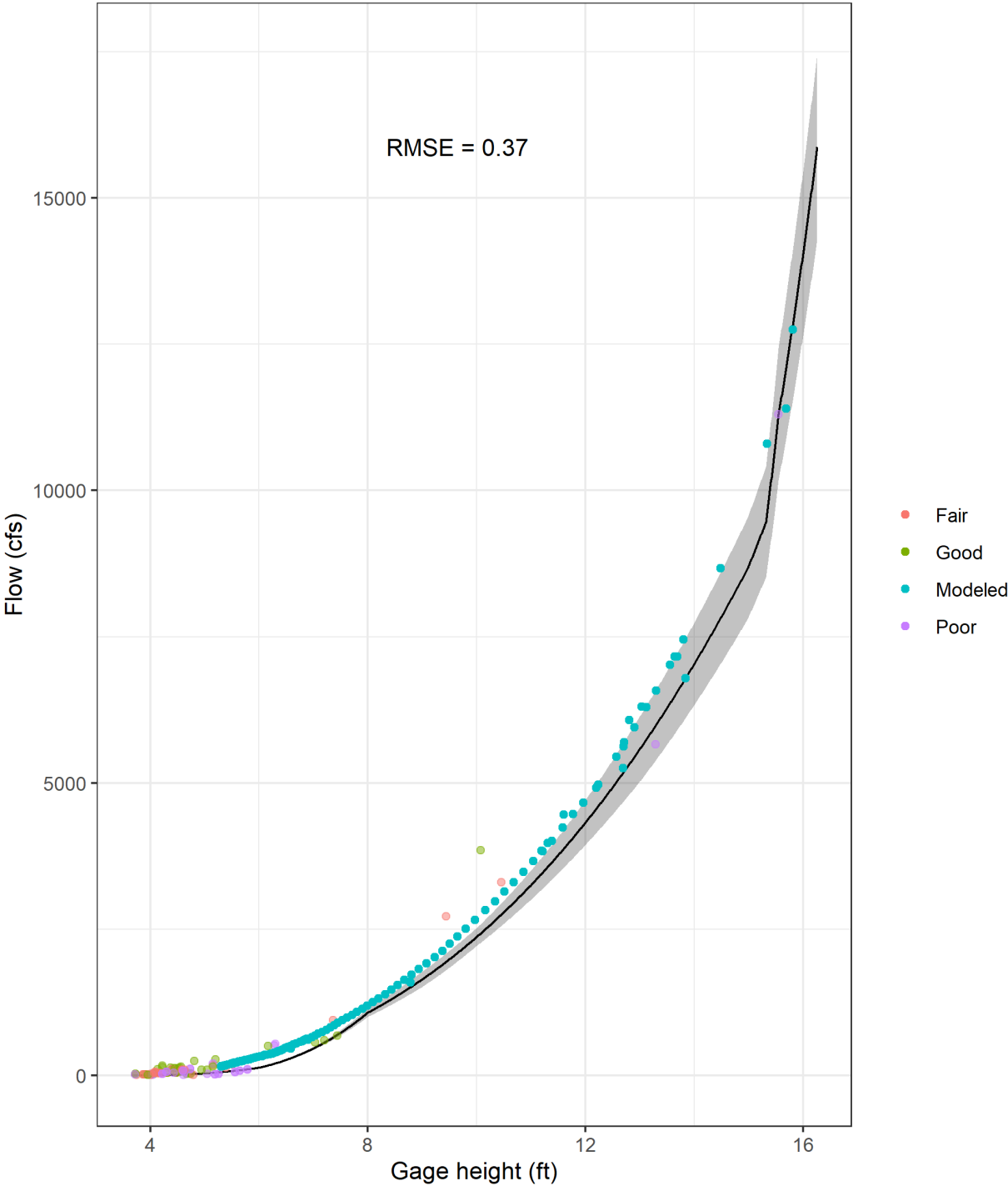
Figure 41. USGS 07195855 – Flint Creek near West Siloam Springs, OK, calibration results for the Illinois River HEC-RAS model.
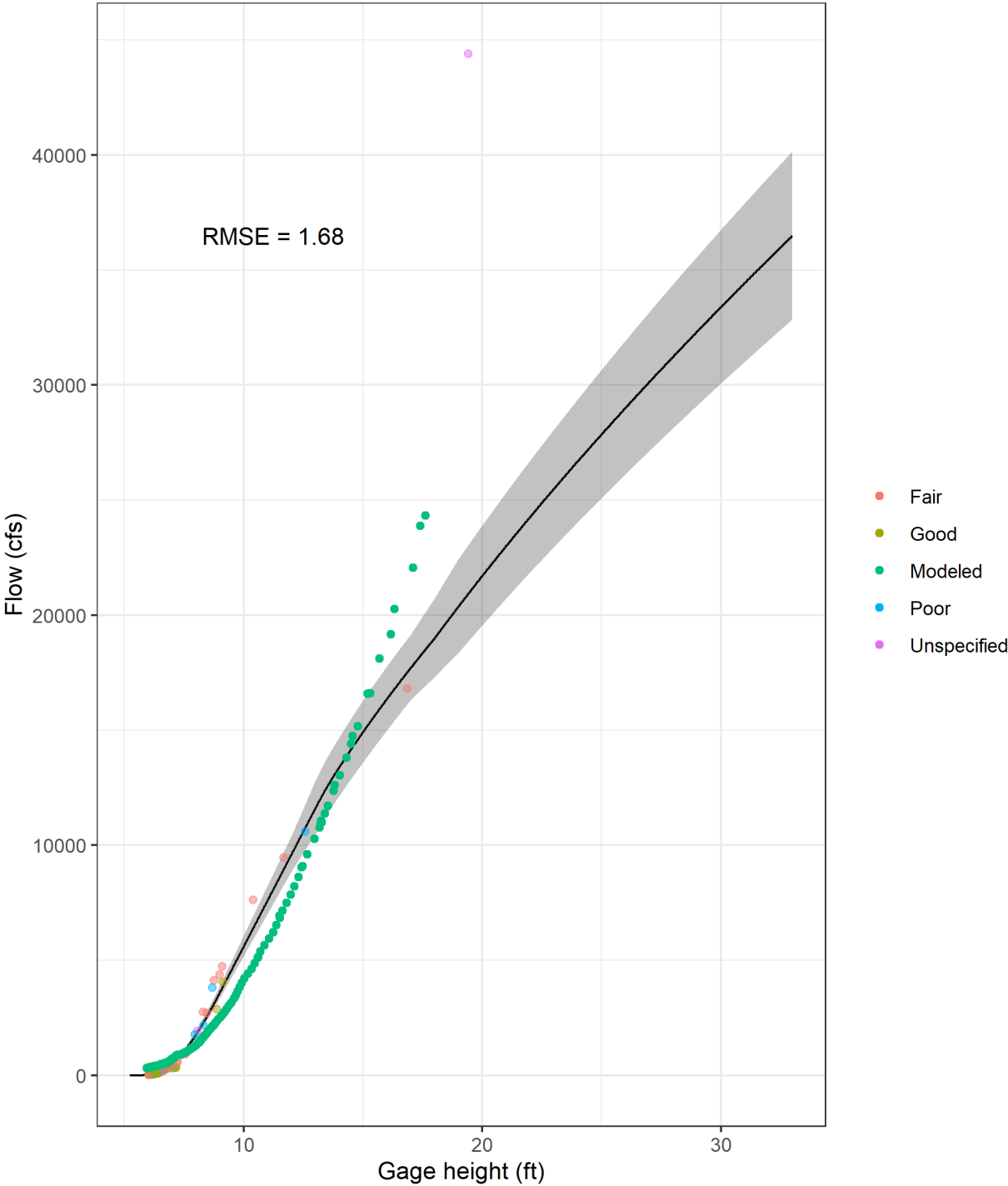
Figure 42. USGS 07196000 – Flint Creek near Kansas, OK, calibration results for the Illinois River HEC-RAS model.
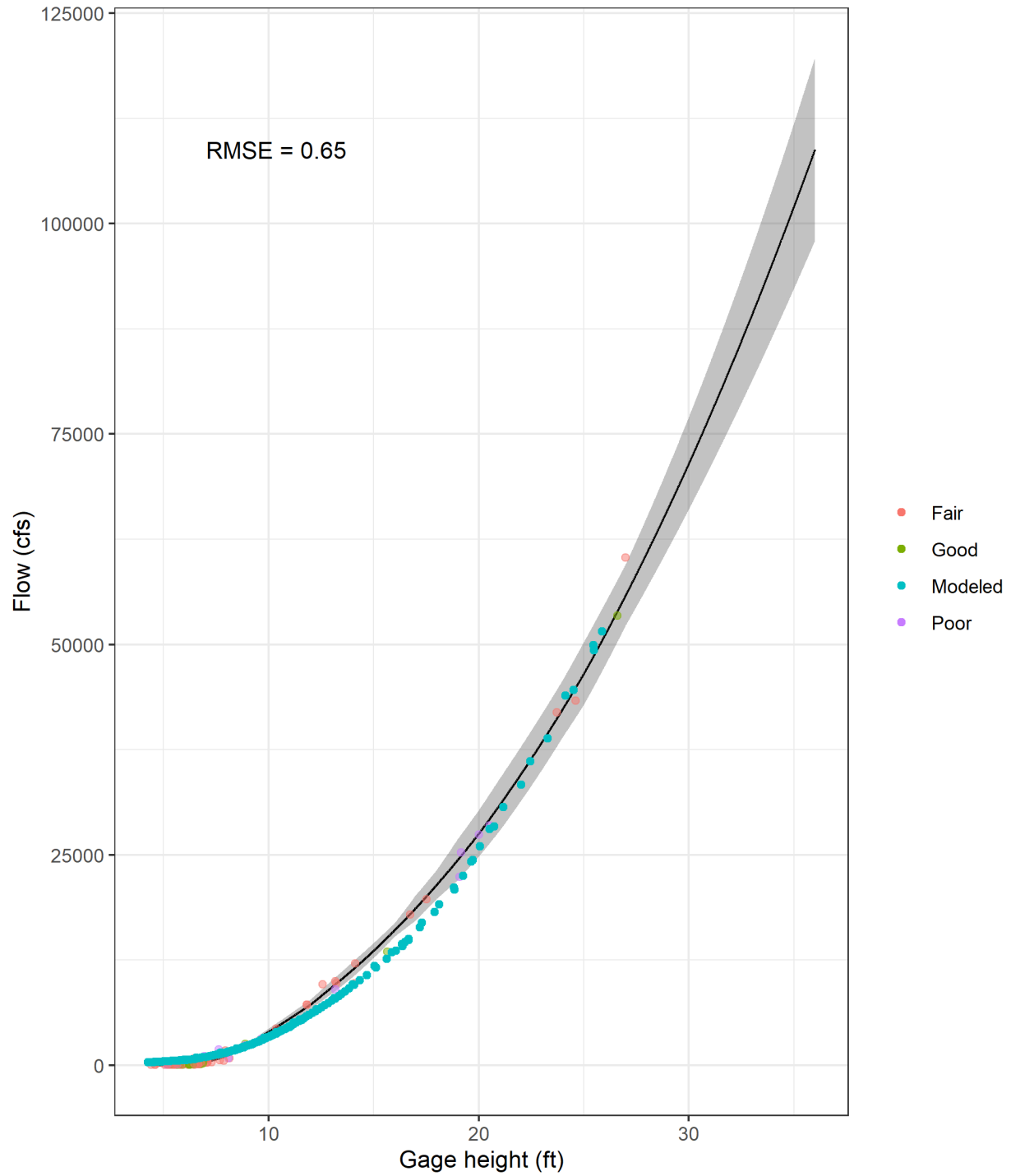
Figure 43. USGS 07197000 – Baron Fork at Eldon, OK, calibration results for the Illinois River HEC-RAS model.
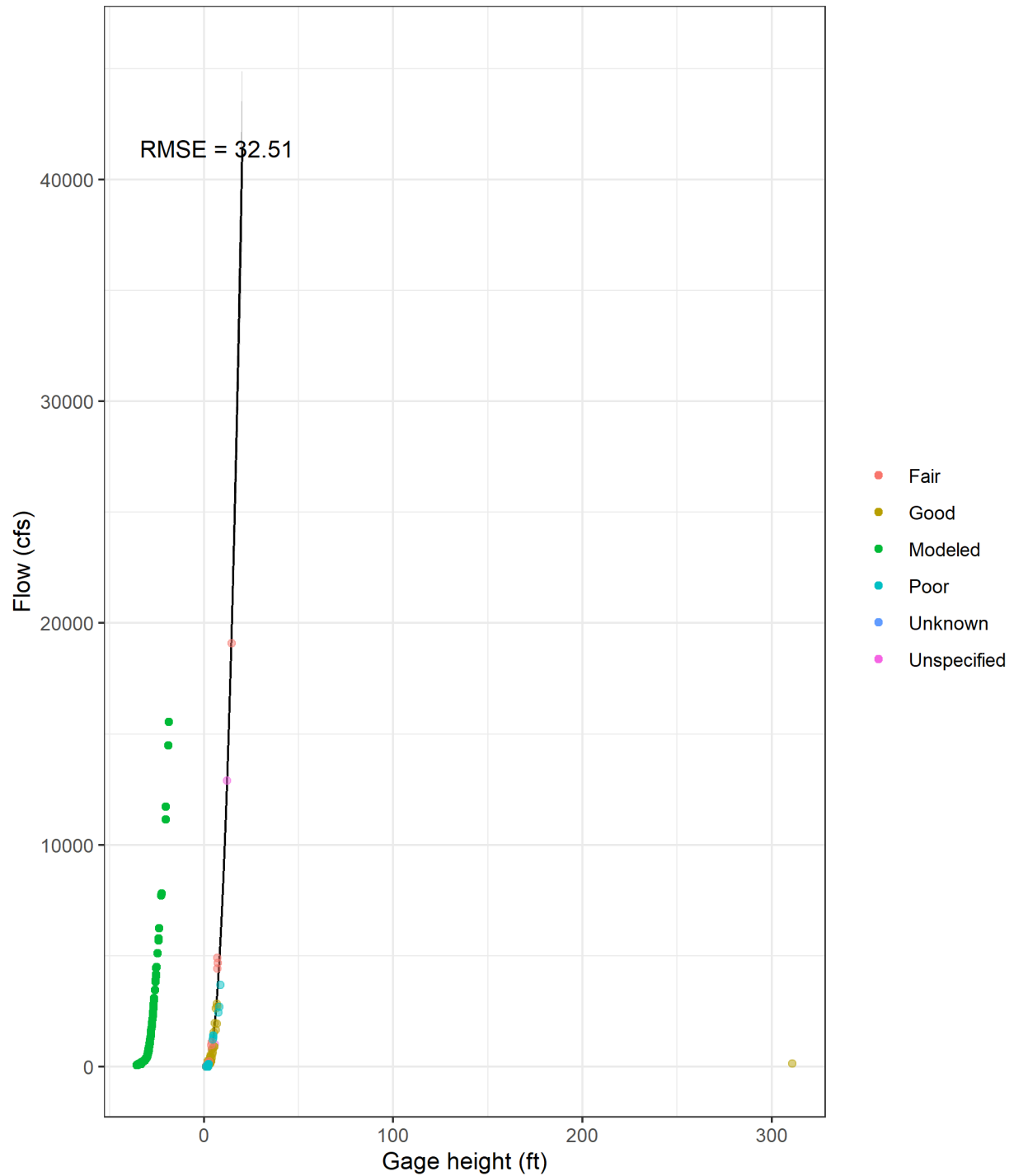
Figure 44. USGS 07196900 – Baron Fork at Dutch Mills, AR, calibration results for the Illinois River HEC-RAS model (incorrect USGS Gage Datum to be resolved by USGS).

Figure 45. USGS 07195400 – Illinois River at Hwy. 16 near Siloam Springs, AR, calibration results for the Illinois River HEC-RAS model.

Figure 46. USGS 07194800 – Illinois River at Savoy, AR, calibration results for the Illinois River HEC-RAS model.

07195430; Illinois River South of Siloam Springs, AR


RMSE = 0.83
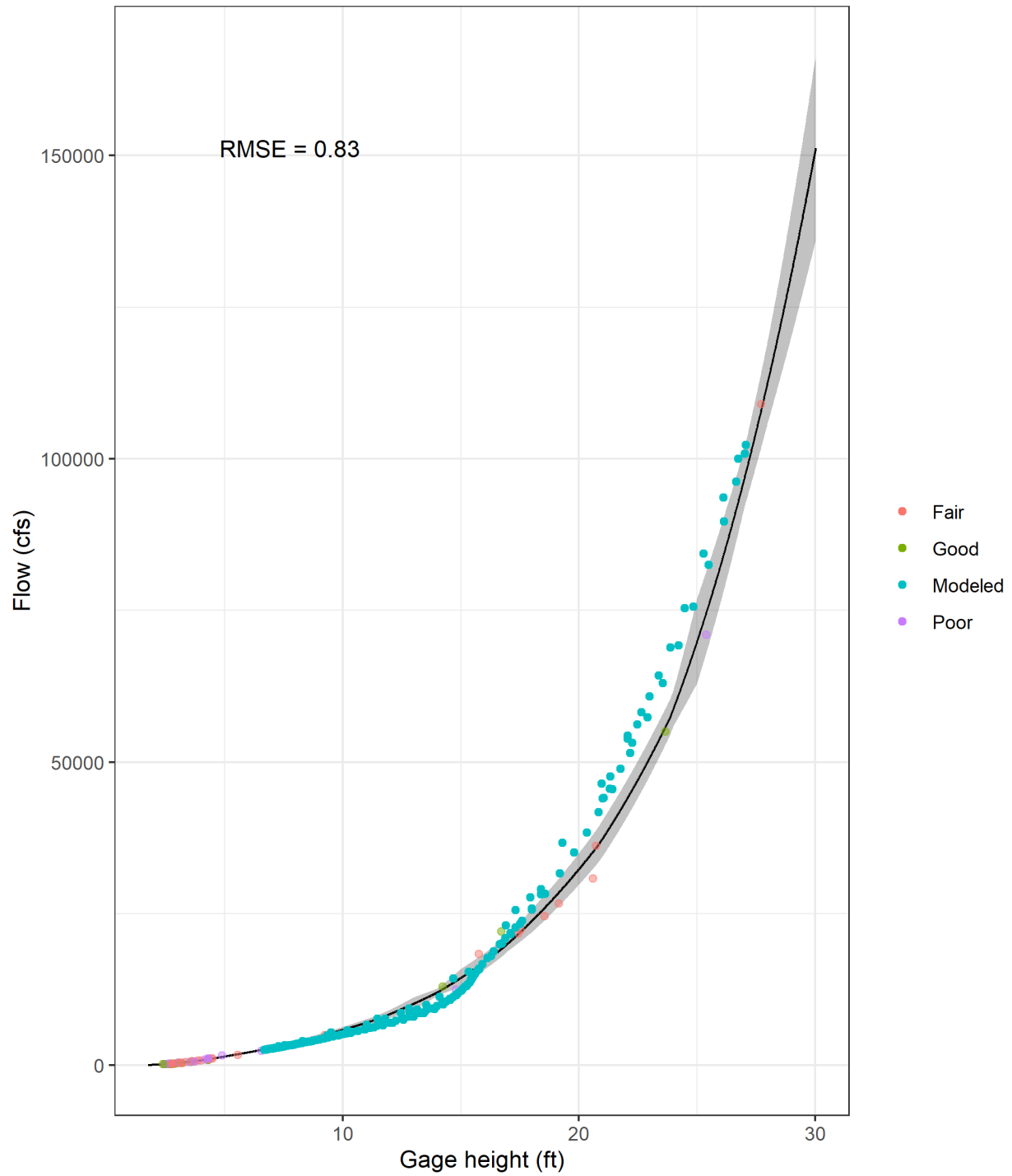
Figure 47. USGS 07195430 – Illinois River south of Siloam Springs, AR, calibration results for the Illinois River HEC-RAS model.
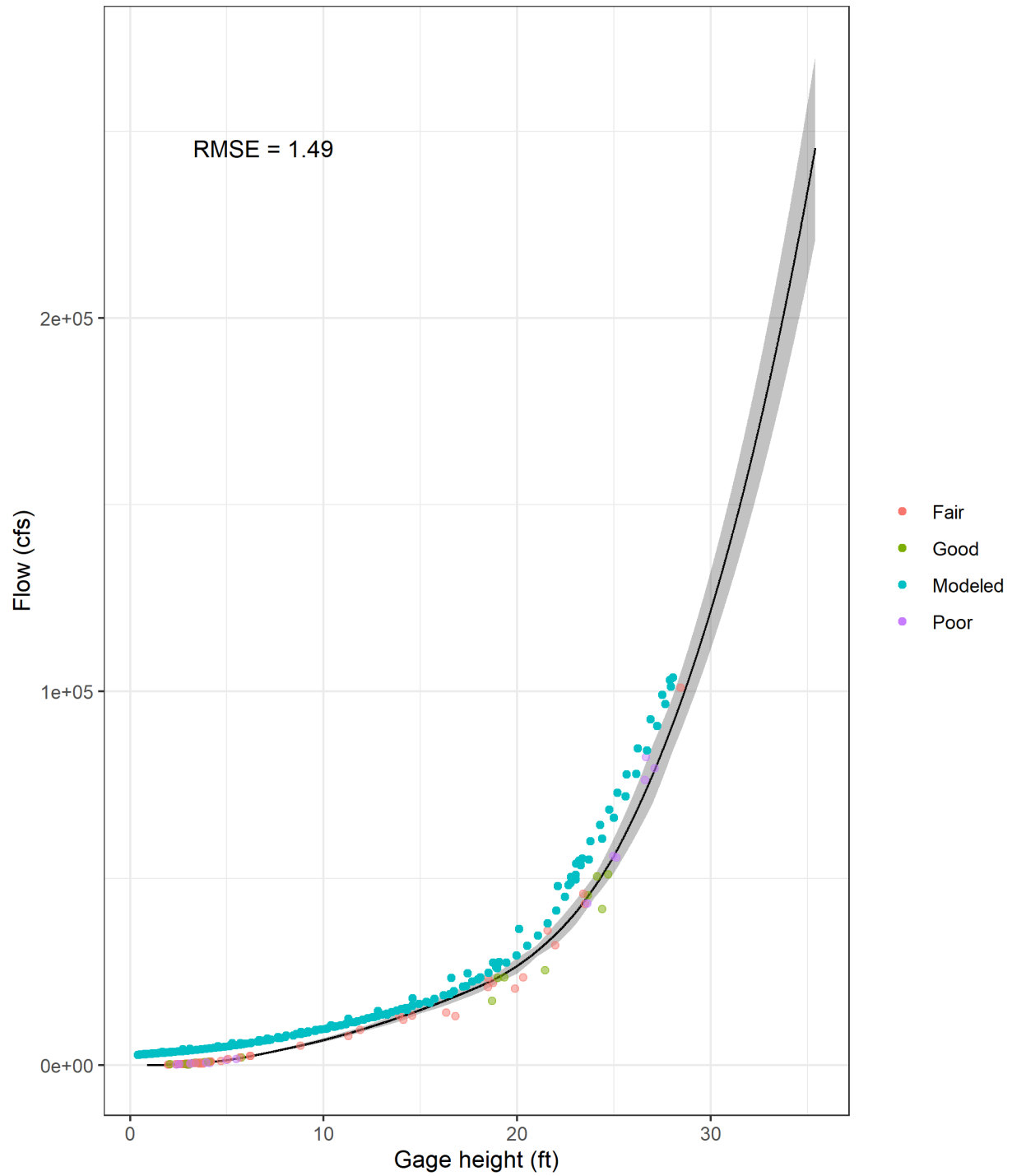
Figure 48. USGS 07195500 – Illinois River near Watts, OK, calibration results for the Illinois River HEC-RAS model.
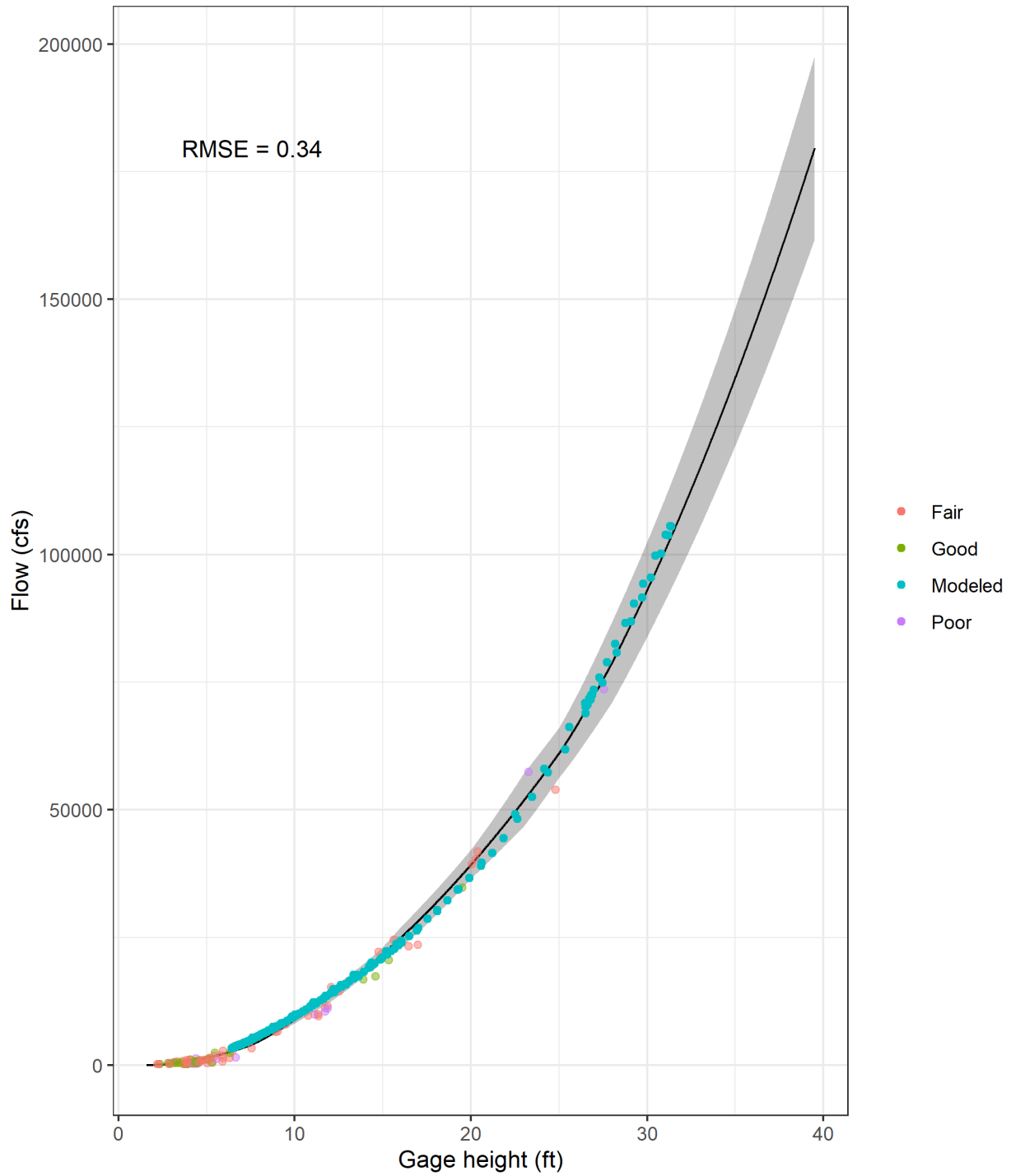
Figure 49. USGS 07196090 – Illinois River at Chewey, OK, calibration results for the Illinois River HEC-RAS model.
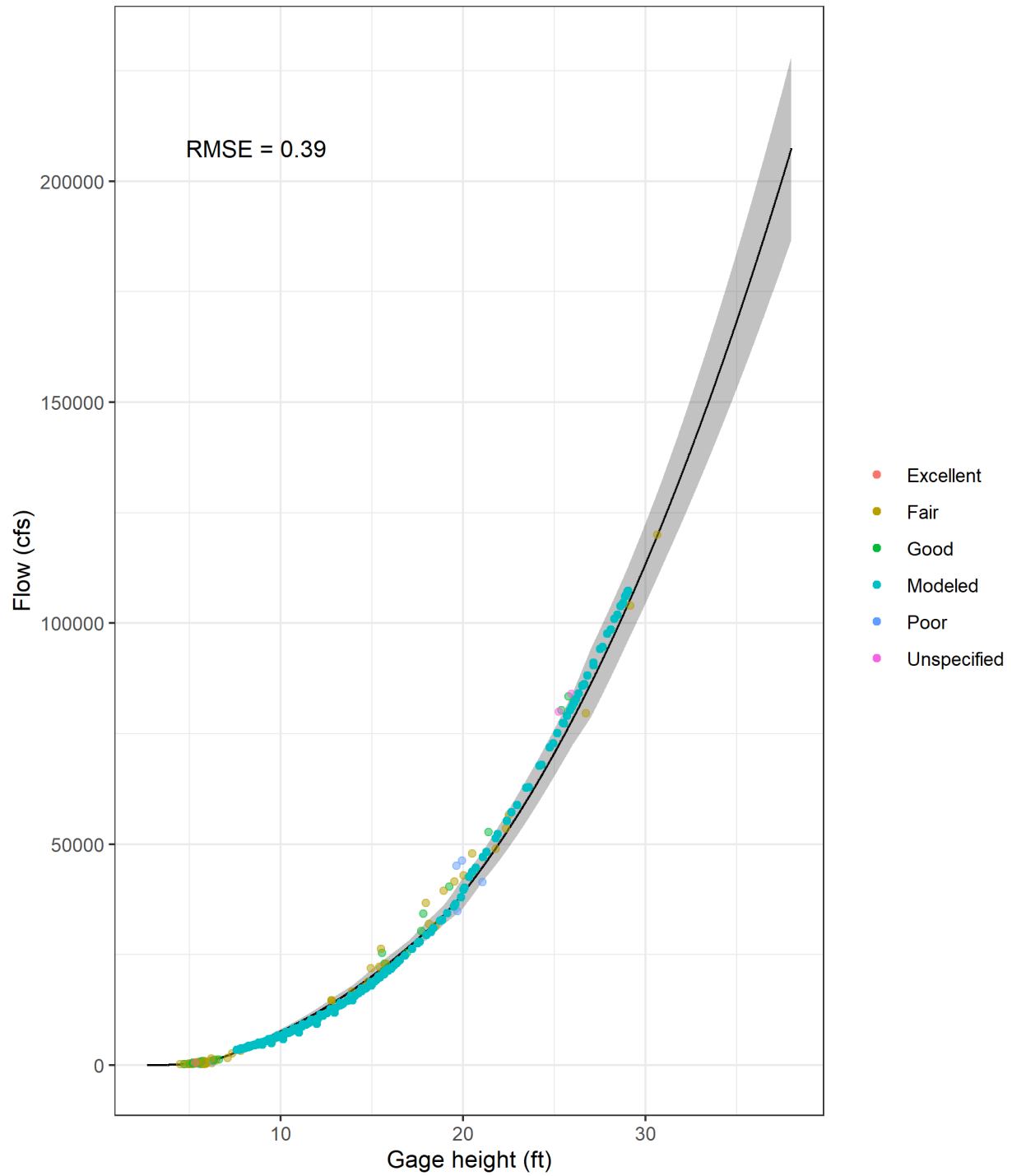
Figure 50. USGS 07196500 – Illinois River near Tahlequah, OK, calibration results for the Illinois River HEC-RAS model.
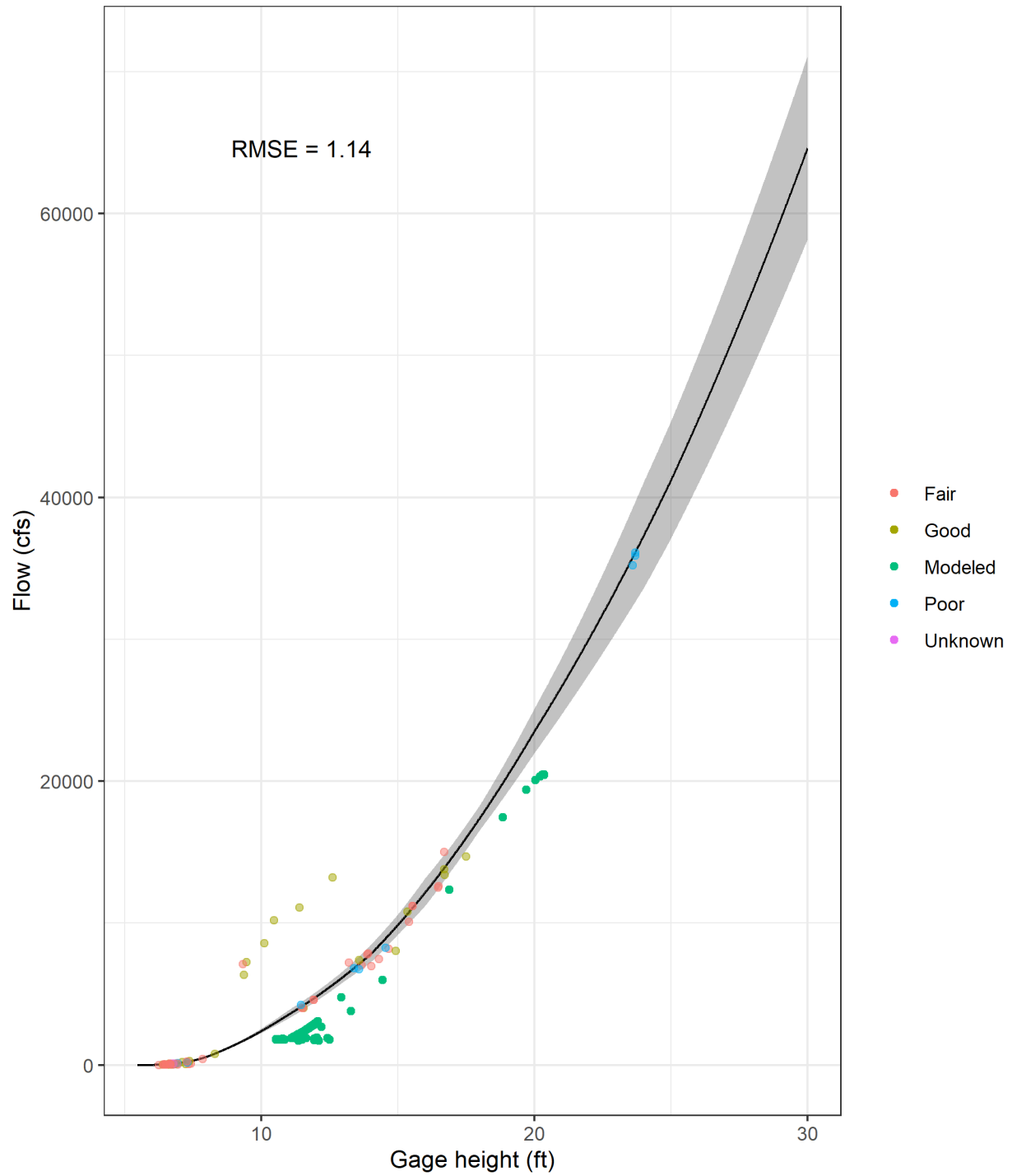
Figure 51. USGS 07198000 – Illinois River near Gore, OK, calibration results for the Illinois River HEC-RAS model.
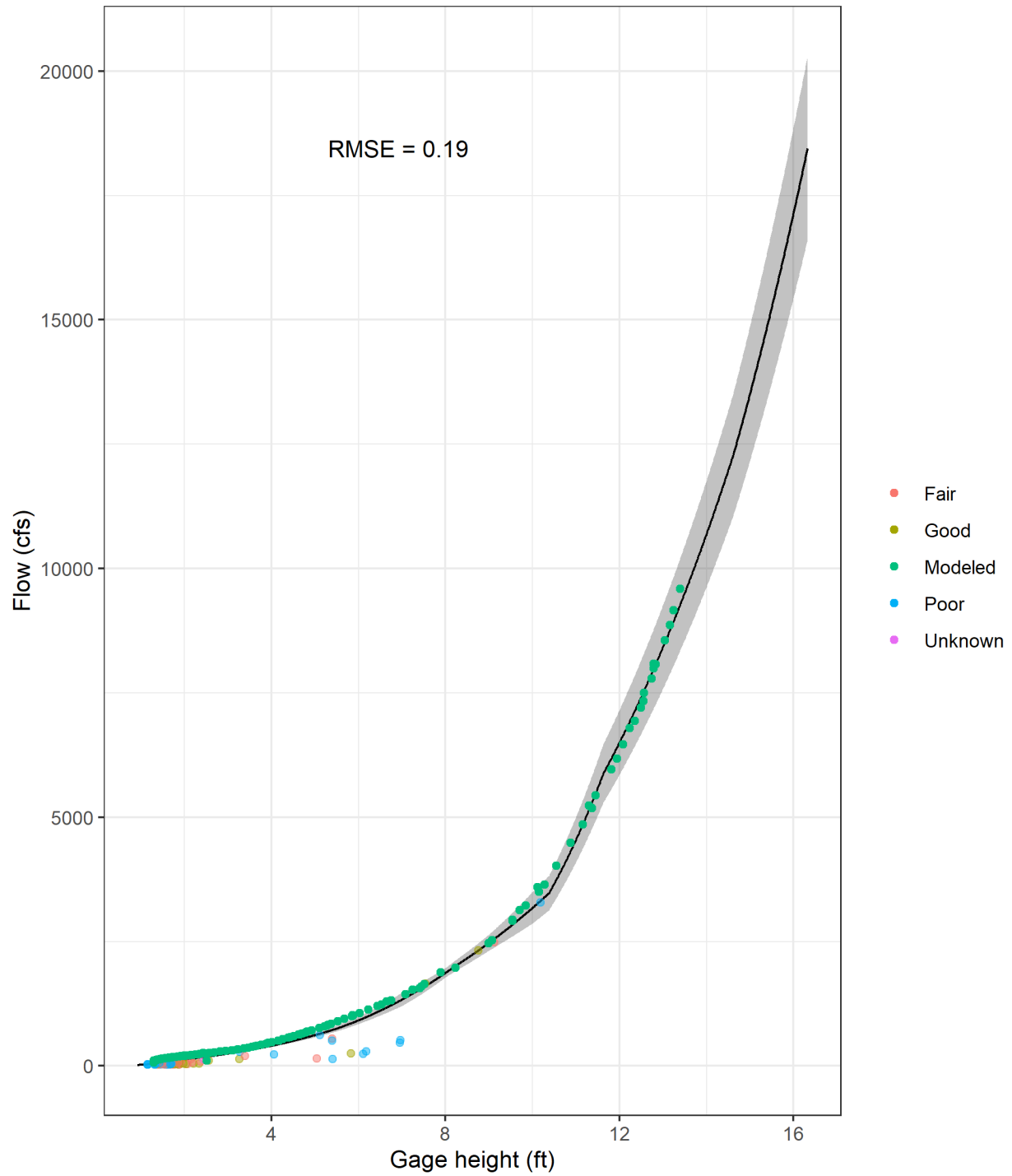
*Figure 52. USGS 07194880 – Osage Creek near Cave Springs, AR, calibration results for the Illinois River HEC-RAS model.*
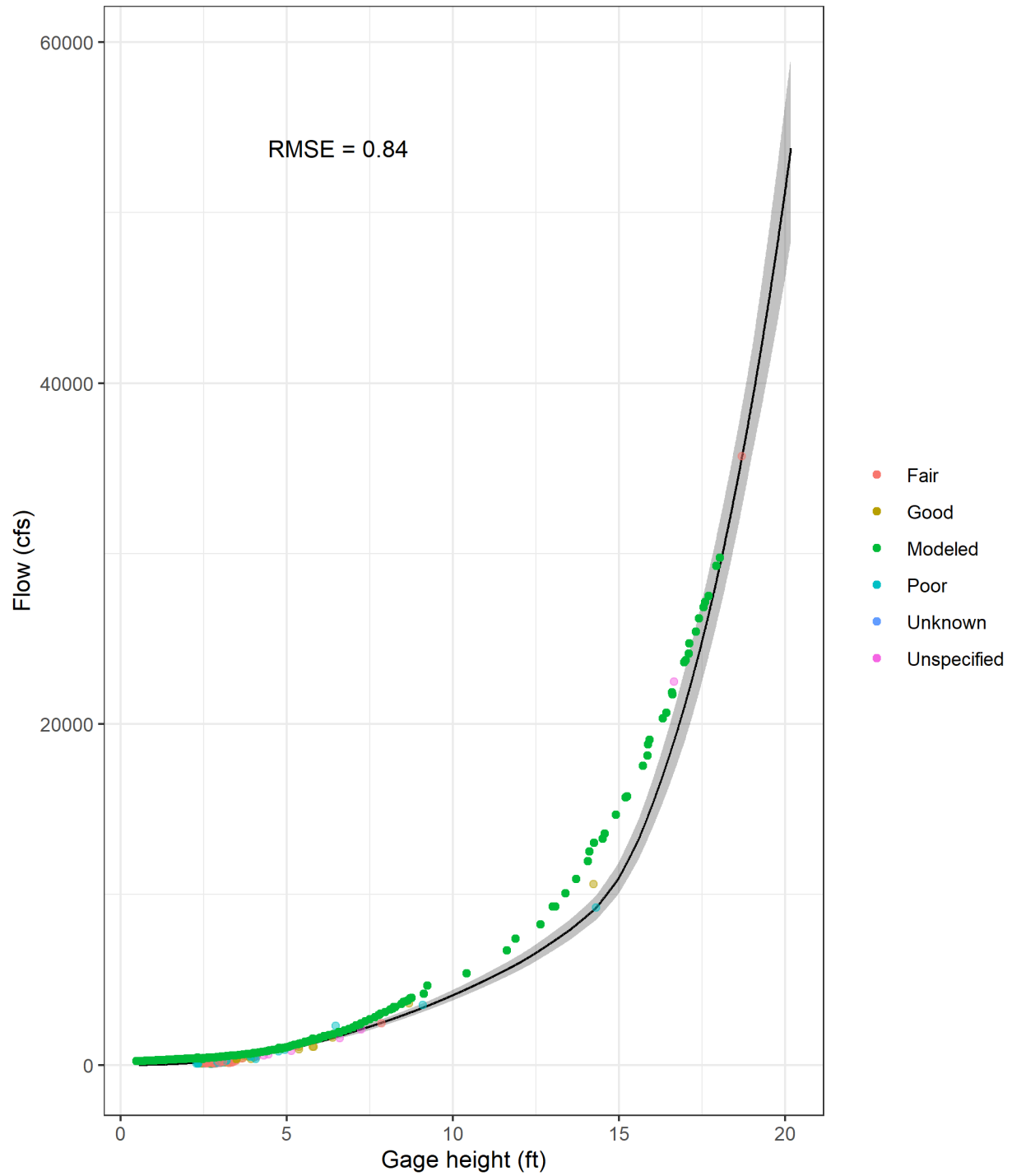
Figure 53. USGS 07195000 – Osage Creek near Elm Springs, AR, calibration results for the Illinois River HEC-RAS model.

Scenarios

Using the 2017 validated model, several climate and land-use scenarios were developed to guide policy makers in the future of the Illinois River Watershed. The scenarios presented are only a select few of the number of potential scenarios that could have been simulated and were chosen based on proven flood reduction methods and potential climate and land-use changes. Climate scenarios included developing frequency events from National Oceanic and Atmospheric Administration (NOAA) Atlas 14 Precipitation Frequency Estimates (Sanja et al., 2013). The 2-, 5-, 10-, 25-, 50-, and 100-year events were simulated within the HEC-HMS model with the resulting output provided to the HEC-RAS model. Land-use scenarios included changing the percent impervious and other associated land-use parameters to represent a historical time period, prior to any major land use change and future time periods with varying degrees of development.

The 2017 validated model was used as the basis for all scenarios. The 2017 model was chosen because it used the averaged parameters from the calibrated models (validation parameter set) and because it encompassed a relatively recent model simulation, i.e., represents a current time period of both land use and climate. Using validated model parameters is important because it indicates that model predictions are consistent with observational data and that the model is an accurate representation of physical reality (Eker et al., 2018). Furthermore, for all scenarios, excluding the precipitation frequency events, the 2017 precipitation event was used as the meteorological input. Therefore, all scenario results will be compared to the 2017 validated model that simulated either the 2017 precipitation event or the 100-year frequency event.

Frequency Events

Precipitation Frequency Estimates were obtained from NOAA's Precipitation Frequency Data Server (http://hdsc.nws.noaa.gov/hdsc/pfds) for the 2-, 5-, 10-, 25-, 50-, and 100-year events. A value was retrieved near the Arkansas-Oklahoma border (latitude: 36.1331 and longitude: -94.5625) and was applied as a constant across all subwatersheds (Table 8). The events were simulated using the 2017 validated parameter set and results are shown for Illinois River near Tahlequah (Figure 54). The 100-year meteorological frequency event was also used as an extreme for the climate land-use scenarios (see "Results").

Table 8. Precipitation Frequency Estimates for the 2-, 5-, 10-, 25-, 50-, and 100-year events used in the HMS Illinois River Watershed model (NOAA, 2013).

AMS-based point precipitation frequency estimates with 90% confidence intervals (in inches)[1]									
Duration	Annual exceedance probability (1/years)								
	1/2	**1/5**	**1/10**	**1/25**	**1/50**	**1/100**	**1/200**	**1/500**	**1/1000**
5-min	0.449 (0.360-0.545)	0.565 (0.453-0.688)	0.653 (0.521-0.797)	0.770 (0.596-0.952)	0.858 (0.653-1.07)	0.946 (0.700-1.20)	1.03 (0.741-1.33)	1.15 (0.799-1.50)	1.24 (0.843-1.63)
10-min	0.657 (0.528-0.798)	0.827 (0.663-1.01)	0.956 (0.763-1.17)	1.13 (0.873-1.39)	1.26 (0.956-1.57)	1.39 (1.03-1.75)	1.52 (1.09-1.94)	1.69 (1.17-2.19)	1.82 (1.23-2.38)
15-min	0.801 (0.643-0.974)	1.01 (0.808-1.23)	1.17 (0.930-1.42)	1.37 (1.06-1.70)	1.53 (1.17-1.91)	1.69 (1.25-2.13)	1.85 (1.32-2.37)	2.06 (1.43-2.68)	2.22 (1.51-2.91)
30-min	1.17 (0.943-1.43)	1.49 (1.19-1.81)	1.72 (1.37-2.10)	2.04 (1.58-2.52)	2.28 (1.73-2.84)	2.52 (1.86-3.18)	2.76 (1.97-3.53)	3.07 (2.13-4.00)	3.31 (2.25-4.35)
60-min	1.57 (1.26-1.90)	2.01 (1.61-2.44)	2.35 (1.87-2.87)	2.81 (2.18-3.48)	3.16 (2.41-3.95)	3.52 (2.61-4.45)	3.88 (2.78-4.99)	4.37 (3.04-5.70)	4.75 (3.23-6.23)
2-hr	1.96 (1.59-2.36)	2.53 (2.05-3.05)	2.98 (2.40-3.60)	3.58 (2.81-4.41)	4.05 (3.12-5.02)	4.53 (3.39-5.68)	5.01 (3.64-6.39)	5.67 (3.99-7.33)	6.18 (4.25-8.05)
3-hr	2.21 (1.81-2.65)	2.87 (2.34-3.44)	3.39 (2.75-4.07)	4.10 (3.24-5.03)	4.66 (3.61-5.75)	5.23 (3.95-6.54)	5.82 (4.25-7.38)	6.62 (4.69-8.53)	7.25 (5.02-9.39)
6-hr	2.69 (2.22-3.19)	3.45 (2.84-4.10)	4.06 (3.33-4.84)	4.92 (3.94-5.99)	5.60 (4.41-6.87)	6.32 (4.83-7.84)	7.06 (5.23-8.90)	8.09 (5.81-10.3)	8.91 (6.25-11.4)
12-hr	3.21 (2.68-3.77)	4.02 (3.35-4.73)	4.69 (3.89-5.53)	5.64 (4.58-6.82)	6.41 (5.11-7.80)	7.23 (5.60-8.90)	8.08 (6.07-10.1)	9.29 (6.76-11.8)	10.2 (7.28-13.1)
24-hr	3.76 (3.17-4.37)	4.71 (3.96-5.48)	5.48 (4.59-6.40)	6.57 (5.39-7.86)	7.45 (5.99-8.96)	8.37 (6.56-10.2)	9.33 (7.09-11.6)	10.7 (7.86-13.4)	11.8 (8.45-14.8)
2-day	4.32 (3.69-4.98)	5.56 (4.74-6.42)	6.54 (5.54-7.56)	7.88 (6.52-9.30)	8.93 (7.26-10.6)	10.0 (7.92-12.1)	11.1 (8.54-13.6)	12.7 (9.41-15.7)	13.8 (10.1-17.3)
3-day	4.71 (4.05-5.39)	6.07 (5.20-6.96)	7.14 (6.09-8.20)	8.61 (7.17-10.1)	9.76 (7.99-11.5)	11.0 (8.73-13.1)	12.2 (9.41-14.8)	13.8 (10.4-17.1)	15.2 (11.1-18.9)
4-day	5.04 (4.35-5.75)	6.45 (5.55-7.36)	7.56 (6.48-8.66)	9.10 (7.62-10.6)	10.3 (8.48-12.1)	11.6 (9.26-13.8)	12.8 (9.98-15.6)	14.6 (11.0-18.0)	16.0 (11.8-19.8)
7-day	5.90 (5.14-6.67)	7.37 (6.40-8.34)	8.53 (7.38-9.68)	10.1 (8.56-11.8)	11.4 (9.46-13.3)	12.7 (10.3-15.0)	14.0 (11.0-16.9)	15.9 (12.1-19.5)	17.3 (12.9-21.4)
10-day	6.64 (5.82-7.47)	8.17 (7.14-9.21)	9.37 (8.15-10.6)	11.0 (9.38-12.7)	12.3 (10.3-14.3)	13.7 (11.1-16.1)	15.0 (11.9-18.0)	16.9 (13.0-20.6)	18.4 (13.8-22.6)
20-day	8.74 (7.75-9.73)	10.6 (9.34-11.8)	12.0 (10.5-13.4)	13.9 (11.9-15.8)	15.4 (13.0-17.7)	16.9 (13.9-19.7)	18.4 (14.7-21.8)	20.5 (15.9-24.7)	22.1 (16.8-26.9)
30-day	10.5 (9.39-11.6)	12.7 (11.3-14.1)	14.4 (12.7-16.0)	16.6 (14.3-18.7)	18.3 (15.5-20.8)	19.9 (16.5-23.1)	21.6 (17.4-25.5)	23.9 (18.7-28.6)	25.6 (19.6-31.0)
45-day	12.8 (11.5-14.1)	15.6 (14.0-17.2)	17.6 (15.7-19.5)	20.3 (17.6-22.7)	22.2 (19.0-25.1)	24.1 (20.1-27.7)	26.1 (21.1-30.4)	28.5 (22.4-33.9)	30.4 (23.5-36.5)
60-day	14.9 (13.4-16.3)	18.1 (16.3-19.9)	20.5 (18.4-22.6)	23.6 (20.5-26.2)	25.8 (22.1-29.0)	27.9 (23.4-31.9)	30.0 (24.4-34.9)	32.7 (25.8-38.6)	34.6 (26.9-41.5)

[1] Precipitation frequency (PF) estimates in this table are based on frequency analysis of annual maxima series (AMS).

Numbers in parenthesis are PF estimates at lower and upper bounds of the 90% confidence interval. The probability that precipitation frequency estimates (for a given duration and annual exceedance probability) will be greater than the upper bound (or less than the lower bound) is 5%. Estimates at upper bounds are not checked against probable maximum precipitation (PMP) estimates and may be higher than currently valid PMP values.

Please refer to NOAA Atlas 14 document for more information.

07196500 Illinois River near Tahlequah, OK
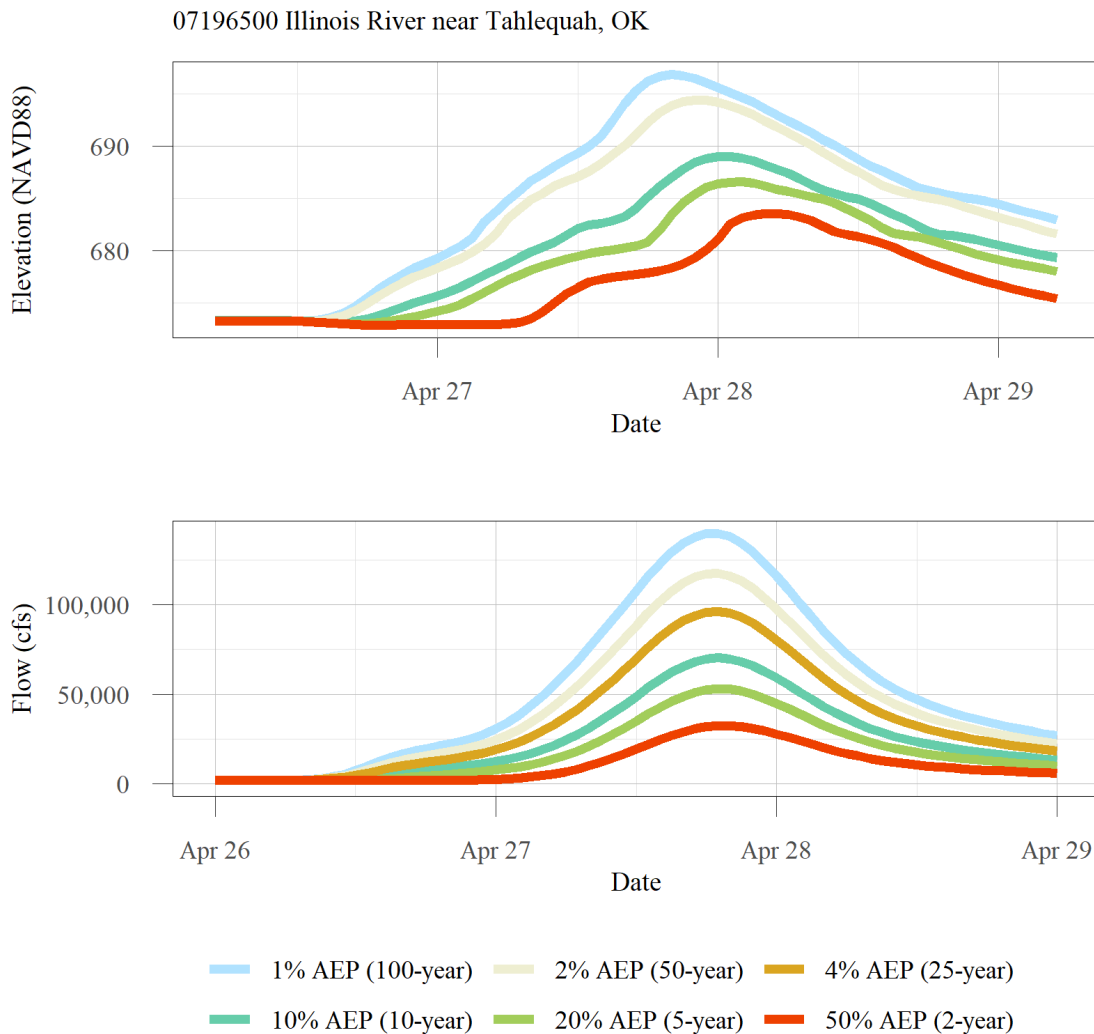
Figure 54. Illinois River near Tahlequah precipitation frequency events.

Historical and Future Land Use

Percent impervious was calculated from the NLCD for the historical land use, and for the future land use, percent impervious was calculated from the USGS Earth Resources Observation and Science (EROS) Center (Sohl et al., 2018) by applying impervious coefficients to each land use category developed by the USGS (Tilley and Slonecker, 2006). Once the percent impervious was determined for each land use category, the total percent impervious was calculated for each subwatershed. In order to consider other future land-use change processes, time of concentration (Tc) and storage (R) parameters were also adjusted by the difference in percent between the 2016 NLCD used in the 2017 Validation Event and the future land use (Figure 55). To represent possible historical time periods, a 0 percent impervious and a 75 percent of the 1990 percent impervious scenarios were developed (Figure 55). Tc and R were also adjusted (increased) by the change in percent impervious between 0 percent of the 2016 percent impervious and the 75 percent of the 1990 percent impervious and the 2016 percent impervious. For example, the 2016 NLCD percent impervious for the Ballard Creek subwatershed (located in the center of the

watershed) is 1.5 percent. The 75 percent value of the 1990 percent impervious for the Ballard Creek subwatershed is 0.89 percent. The difference between the 75 percent of the 1990 percent impervious and the 2016 percent impervious is -0.61 percent. That value was then converted to a decimal fraction (i.e., -0.0061) and subtracted from 1 to obtain a multiplier. This multiplier was then applied to the Tc and R parameters. These same methods were used to develop the multipliers and subsequent Tc and R parameter values for the future land-use scenarios.
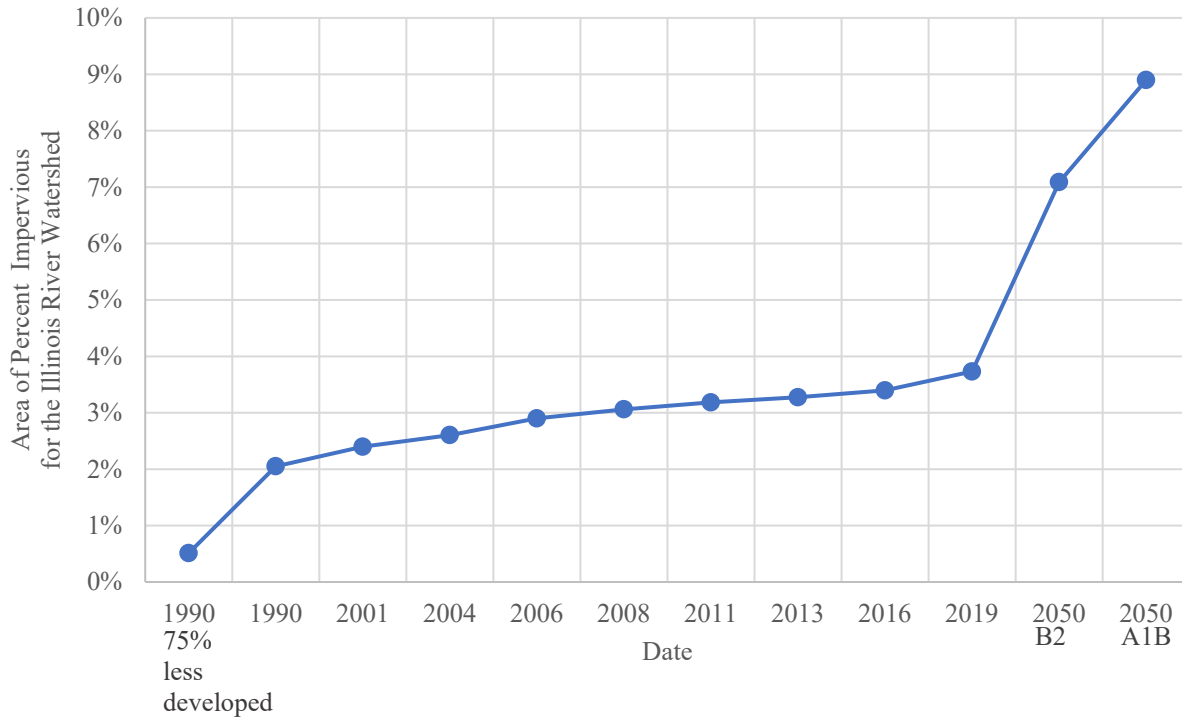

Figure 55. Area of percent impervious, by year, for the Illinois River Watershed.

Results

Results are given for several scenarios that encompass changes in current, historical, and future land use and climate and combinations of all. As mentioned previously, scenario results will be compared to the 2017 validated model.

Several scenarios were simulated: the addition of riparian buffers along the mainstem of the Illinois River and along major tributaries to the Illinois River; the addition of detention basins placed throughout the watershed above Tenkiller Lake to attenuate and lessen peak flows; the use of future-cast land-use grids to represent a "building out of the watershed"; the use of a historical land-use grid to represent a "less developed" time period; use of an extreme precipitation event, i.e., the 100-year frequency event; and combinations of each of these scenarios. The peak streamflow and stage are given in Table 9.

Table 9. Peak streamflow and stage for Illinois River near Tahlequah for each of the scenarios simulated for the Illinois River Watershed HEC-HMS and HEC-RAS model.

Scenario/Event	Land Use	Precipitation	Peak Streamflow (cubic feet per second)	Peak Stage (elevation in feet)
2-year Frequency Event	2016 NLCD	2-year Frequency Event	32,439.3	683.5
2-year Frequency Event w/Riparian Buffers	2016 NLCD	2-year Frequency Event	27,293.6	682.7
5-year Frequency Event	2016 NLCD	5-year Frequency Event	53,079.0	686.5
5-year Frequency Event w/Riparian Buffers	2016 NLCD	5-year Frequency Event	41,235.3	685.4
10-year Frequency Event	2016 NLCD	10-year Frequency Event	70,324.1	689.0
10-year Frequency Event w/Riparian Buffers	2016 NLCD	10-year Frequency Event	53,547.5	687.5
25-year Frequency Event	2016NLCD	25-year Frequency Event	96,216.7	692.1
25-year Frequency Event w/Riparian Buffers	2016 NLCD	25-year Frequency Event	71,897.6	690.3
50-year Frequency Event	2016 NLCD	50-year Frequency Event	117,495.3	694.4
50-year Frequency Event w/Riparian Buffers	2016 NLCD	50-year Frequency Event	87,617.2	692.4
100-year Frequency Event	2016 NLCD	100-year Frequency Event	139,794.5	696.9
100-year Frequency Event w/Riparian Buffers	2016 NLCD	100-year Frequency Event	104,545.8	694.3
100-year Frequency Event w/B2 Land-use Scenario	2050 SRES B2	100-year Frequency Event	147,911.8	697.4
100-year Frequency Event w/B2 Land-use Scenario and Detention Basins	2050 SRES B2 w/Detention Basins	100-year Frequency Event	107,826.7	693.1

Scenario/Event	Land Use	Precipitation	Peak Streamflow (cubic feet per second)	Peak Stage (elevation in feet)
100-year Frequency Event w/A1B Land-use Scenario	2050 SRES A1B	100-year Frequency Event	153,017.8	697.7
100-year Frequency Event w/A1B Land-use Scenario and Detention Basins	2050 SRES A1B w/Detention Basins	100-year Frequency Event	112,189.3	693.4
April 2017 Validation Event	2016 NLCD	April 2017 Event	110,557.7	694.1
0 Percent Less Developed	0% Impervious Values	April 2017 Event	106,246.8	693.7
75 Percent Less Developed	75% 1990 Impervious Values	April 2017 Event	107,240.8	693.9
B2 Land-use Scenario	2050 SRES B2	April 2017 Event	116,030.2	694.6
B2 Land-use Scenario w/Detention Basins	2050 SRES B2 w/Detention Basins	April 2017 Event	89,476.5	691.5
A1B Land-use Scenario	2050 SRES A1B	April 2017 Event	118,933.1	694.9
A1B Land-use Scenario w/Detention Basins	2050 SRES A1B w/Detention Basins	April 2017 Event	92,237.7	691.8

Riparian Buffers

Riparian buffers are vegetated areas that are adjacent to streams and rivers that play an important role in protecting and preserving water quality and ecosystems. These areas can help to filter out pollutants and sediments from entering the water, provide habitat for wildlife, and reduce erosion by stabilizing stream banks. For this study, the focus was on quantifying the impact riparian buffers might have on flood damage reduction. Flood damage reduction was analyzed by comparing current condition flow and water surface elevation to conditions with riparian buffers as well as potential reductions in velocities.

Riparian zones were represented by horizontally varied n-values, in bands of approximately 100 feet on either side of the channel in affected zones. Tributaries in the upstream portion of the basin were included, as well as certain zones along the downstream tributaries and the main stem of the Illinois River, as identified in an HEC-HMS analysis. Manning's n-values in riparian zones were set to 0.15. It is imperative to understand that the results represent conceptual expectations as no detailed layout of the zones from a logistical design perspective was completed. The conceptual changes to the system as a result of riparian buffer zones can be valuable in determining key reaches to potential pursue a more detailed design. The results are an

aggregate of how zones were represented in the model; therefore, results compound in the downstream direction as more riparian zones have a cumulative effect.

Reductions in velocity were analyzed by each frequency event and averaged by each reach to reasonably communicate potential expectations. Areas that did not experience overbank velocities were not included in the averaging. These overbank areas were not included such that averages would not be skewed by minute model differences. Additionally, areas that experienced channel velocities less than three (3) feet per second (fps) were not included in the averaging because 3 fps is recognized a velocity that will transport and erode clay, silt, sand, and some gravel and cause damages. A mean reduction in channel velocity less than 0.5 fps was also eliminated as any value less than that was deemed outside the accuracy of the model. Table 10 describes rivers and reaches for the different events that would most likely see some measurable reductions in velocities.

Table 10. Average velocity reductions by reach with riparian buffers for the Illinois River HEC-RAS model.

River	Reach	Frequency Event	Mean Channel Velocity Reduction (fps)
Baron Fork	Main	2-year	-1.4
Baron Fork	Main	5-year	-0.9
Baron Fork	Main	10-year	-1.4
Baron Fork	Main	25-year	-0.8
Baron Fork	Main	50-year	-0.9
Baron Fork	Main	100-year	-0.9
Clear Creek	Main	2-year	-1.4
Clear Creek	Main	5-year	-1.6
Clear Creek	Main	10-year	-1.9
Clear Creek	Main	25-year	-2.1
Clear Creek	Main	50-year	-2.2
Clear Creek	Main	100-year	-2.3
Illinois River	DS_BallardCr	2-year	-1
Illinois River	DS_BallardCr	5-year	-1.2
Illinois River	DS_BallardCr	10-year	-1.2
Illinois River	DS_BallardCr	25-year	-1.6
Illinois River	DS_BallardCr	50-year	-1.5
Illinois River	DS_BallardCr	100-year	-1.4
Illinois River	DS_BaronFork	2-year	-0.6
Illinois River	DS_BaronFork	5-year	-2.2
Illinois River	DS_BaronFork	10-year	-2.4
Illinois River	DS_BaronFork	25-year	-0.5
Illinois River	DS_BaronFork	50-year	-0.6
Illinois River	DS_ClearCr	2-year	-1.8
Illinois River	DS_ClearCr	5-year	-0.7
Illinois River	DS_ClearCr	10-year	-0.6

River	Reach	Frequency Event	Mean Channel Velocity Reduction (fps)
Illinois River	DS_ClearCr	25-year	-0.8
Illinois River	DS_ClearCr	50-year	-0.9
Illinois River	DS_ClearCr	100-year	-0.8
Illinois River	DS_FlintCr	2-year	-0.8
Illinois River	DS_FlintCr	5-year	-0.8
Illinois River	DS_FlintCr	10-year	-0.9
Illinois River	DS_FlintCr	25-year	-1
Illinois River	DS_FlintCr	50-year	-1
Illinois River	DS_FlintCr	100-year	-1.1
Illinois River	DS_MuddyFork	2-year	-1.2
Illinois River	DS_MuddyFork	5-year	-0.5
Illinois River	DS_MuddyFork	10-year	-0.6
Illinois River	DS_MuddyFork	50-year	-0.5
Illinois River	DS_MuddyFork	100-year	-0.7
Illinois River	DS_OsageCr	2-year	-0.8
Illinois River	DS_OsageCr	5-year	-1.1
Illinois River	DS_OsageCr	10-year	-1.1
Illinois River	DS_OsageCr	25-year	-1.1
Illinois River	DS_OsageCr	50-year	-1.1
Illinois River	DS_OsageCr	100-year	-1.2
Illinois River	Main	2-year	-0.9
Illinois River	Main	5-year	-1
Illinois River	Main	10-year	-1.1
Illinois River	Main	25-year	-1.3
Illinois River	Main	50-year	-1.3
Illinois River	Main	100-year	-1.3
Muddy Fork	DS_MooresCr	2-year	-0.9
Muddy Fork	DS_MooresCr	5-year	-1.2
Muddy Fork	DS_MooresCr	10-year	-1.3
Muddy Fork	DS_MooresCr	25-year	-1.5
Muddy Fork	DS_MooresCr	50-year	-1.7
Muddy Fork	DS_MooresCr	100-year	-1.6
Osage Creek	Main	2-year	-2.2
Osage Creek	Main	5-year	-1.3
Osage Creek	Main	10-year	-1.4
Osage Creek	Main	25-year	-1.7
Osage Creek	Main	50-year	-1.7
Osage Creek	Main	100-year	-1.6

Changes in water surface elevation and flow were analyzed by each frequency event and averaged by each reach to reasonably communicate potential expectations. A mean change in

76

water surface less than 0.5 feet was eliminated as any value less than that was deemed outside the accuracy of the model. Upstream reaches tended to see an increase in water surface elevation with smaller changes in flow as the riparian zones attenuate the energy of the water. Downstream reaches tended to see a decrease in water surface elevation with a larger decrease in flow as the riparian zones have a cumulative effect. Table 11 lists the rivers and reaches with the greatest average change in water surface elevation along with the corresponding average change in flow in the reach for each event.

Table 11. Average change in water surface and flow by reach with riparian buffers for the Illinois River HEC-RAS model.

River	Reach	Frequency Event	Mean Change in Water Surface Elevation (ft)	Mean Change in Flow (cfs)
Ballard Creek	Main	25-year	0.5	-458.8
Ballard Creek	Main	50-year	0.9	-784
Ballard Creek	Main	100-year	1.3	-879.2
Baron Fork	Main	2-year	0.5	-117.2
Baron Fork	Main	100-year	0.5	-336.1
Clear Creek	Main	2-year	1	-527.2
Clear Creek	Main	5-year	1.2	-958
Clear Creek	Main	10-year	1.5	-1,577.90
Clear Creek	Main	25-year	1.9	-2,455.70
Clear Creek	Main	50-year	2.3	-2,973.30
Clear Creek	Main	100-year	2.7	-3,576.30
Illinois River	DS_BallardCr	2-year	-0.7	-7,027.60
Illinois River	DS_BallardCr	5-year	-0.7	-12,145.40
Illinois River	DS_BallardCr	10-year	-0.5	-15,569.10
Illinois River	DS_BaronFork	2-year	-0.7	-5,279.40
Illinois River	DS_BaronFork	5-year	-0.8	-22,382.30
Illinois River	DS_BaronFork	10-year	-0.8	-30,779.90
Illinois River	DS_ClearCr	2-year	1.2	-2,537.20
Illinois River	DS_ClearCr	5-year	1.5	-4,317.80
Illinois River	DS_ClearCr	10-year	1.9	-5,785.20
Illinois River	DS_ClearCr	25-year	2.3	-7,764.90
Illinois River	DS_ClearCr	50-year	2.7	-9,490.20
Illinois River	DS_ClearCr	100-year	3.1	-10,984.90
Illinois River	DS_FlintCr	2-year	-1	-5,363.30
Illinois River	DS_FlintCr	5-year	-1.3	-9,912
Illinois River	DS_FlintCr	10-year	-1.4	-13,864.60
Illinois River	DS_FlintCr	25-year	-1.7	-19,179.80
Illinois River	DS_FlintCr	50-year	-1.8	-24,391.30
Illinois River	DS_FlintCr	100-year	-1.8	-30,710.50
Illinois River	DS_MuddyFork	2-year	1	-933

River	Reach	Frequency Event	Mean Change in Water Surface Elevation (ft)	Mean Change in Flow (cfs)
Illinois River	DS_MuddyFork	5-year	1.6	-1,775.70
Illinois River	DS_MuddyFork	10-year	1.9	-2,567.70
Illinois River	DS_MuddyFork	25-year	2.4	-3,716.50
Illinois River	DS_MuddyFork	50-year	2.7	-4,573.30
Illinois River	DS_MuddyFork	100-year	3.1	-4,994
Illinois River	DS_OsageCr	2-year	1.3	-6,890
Illinois River	DS_OsageCr	5-year	1.7	-12,276.50
Illinois River	DS_OsageCr	10-year	2	-16,001.20
Illinois River	DS_OsageCr	25-year	2.4	-21,481.80
Illinois River	DS_OsageCr	50-year	2.8	-25,727.10
Illinois River	DS_OsageCr	100-year	3	-30,461.60
Illinois River	Main	2-year	0.9	-201
Illinois River	Main	5-year	1.2	-343
Illinois River	Main	10-year	1.6	-551.3
Illinois River	Main	25-year	1.7	-918.6
Illinois River	Main	50-year	2	-1,125.30
Illinois River	Main	100-year	1.9	-49.8
Muddy Fork	DS_MooresCr	2-year	1	-457.8
Muddy Fork	DS_MooresCr	5-year	1	-946.2
Muddy Fork	DS_MooresCr	10-year	1.3	-1,459.70
Muddy Fork	DS_MooresCr	25-year	1.6	-1,932.30
Muddy Fork	DS_MooresCr	50-year	1.9	-2,402.60
Muddy Fork	DS_MooresCr	100-year	1.9	-2,775
Osage Creek	Main	2-year	0.9	-1,727.90
Osage Creek	Main	5-year	1.2	-3,392.60
Osage Creek	Main	10-year	1	-3,143.50
Osage Creek	Main	25-year	1.2	-4,252.90
Osage Creek	Main	50-year	1.4	-5,149.90
Osage Creek	Main	100-year	1.4	-5,567.90

Detention Basins

The proposed detention basins were digitized in a Geographical Information System by looking at terrain and aerial imagery to achieve maximum benefit with minimal impact to the local population. This was accomplished by avoiding infrastructure and heavily populated areas, as much as possible, when determining locations. Once the process of digitizing the detention basins was complete, the detention basin feature was overlain on a Digital Elevation Model (DEM) to determine the elevation-storage curve for the proposed basin. The elevation-storage curve for the detention basin was then input into the HEC-HMS model and ran with various frequency events (2-year, 10-year, 25-year, etc.) to determine elevations at which the reservoirs could hold back flow without releases and when or if said structure would overtop.

The elevations and inflows for the various events were then used to size and place representative outlets for the reservoir to release flows that reduce impact downstream and do not overtop the structure. This was done by placing the hypothetical culvert invert at the elevation of a no-release 10-year frequency-event rise in the reservoir to simulate a system that can hold back and attenuate releases for smaller frequency storms and reduce damages downstream. Culvert rating curves were generated to quickly estimate an approximate pipe size to release the required flow. The representative culvert rating curve for each proposed reservoir was then input into the HMS model to simulate the reservoir operation. If there were issues with overtopping at lower frequency events, the culvert rating curves would be iterated by either increasing the size or lowering the intake of the pipe.

Initially, 20 locations were chosen to represent detention basins, mostly located in headwater areas of tributaries and one in the headwaters of the Illinois River mainstem. However, in order to maximize the volume of water that could be retained, eight more detention basins were added for a total of 28 (Figure 56). The total volume retained by the proposed detention basins is approximately 796,274.5 acre-feet. It is important to note that in no way does Figure 56 and associated results of adding detention basins reflect actual intention on building such basins. They were merely used to illustrate how adding in 796,274.5 acre-feet of storage catchment can reduce streamflows in the Illinois River.
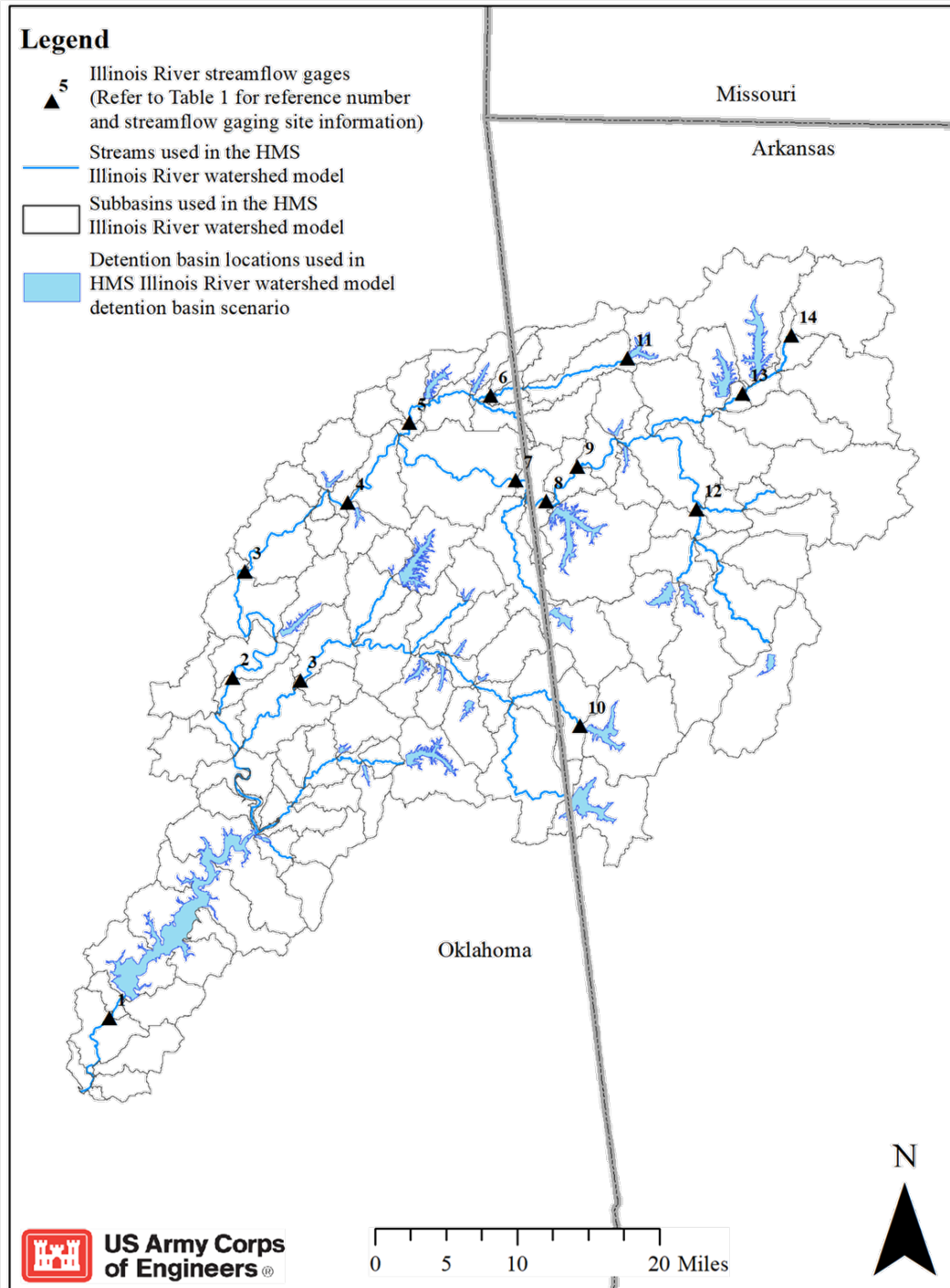
Figure 56. Location of detention basins used in the Illinois River watershed HEC-HMS model detention basin scenarios.

Combination Land Use and Climate

The first combination scenario used a current storm event, the April 2017 validation event, with two land-use changes that represent a possible, less developed, historical time period: percent impervious at 75 percent of 1990 and percent impervious at 0 percent. These scenarios were developed to help isolate development impacts versus rainfall impacts. The scenario results

indicate that changing the land use to represent a less developed time had little change on the timing or peak of the April 2017 climate event compared to the 2016 land use that was used in the April 2017 modeling event (Figure 57 and Figure 58). For all scenario results, only the Illinois River near Tahlequah, OK and the Illinois River near Watts, OK, sites (number 2 on Figure 56 and number 7 on Figure 56, respectively) will be given in the main text body. Results for all other gages will be presented in Appendix B.

The second combination scenario included "building out the watershed" using future-cast land-use grids developed by EROS. The two future land use projections that were chosen were for the year 2050 and represent the A1B and B2 Intergovernmental Panel on Climate Change (IPCC) Special Report on Emissions Scenarios (SRES) (Sohl et al., 2018). Please see Sohl et al. (2018) for a detailed explanation on how these land-use grids were developed. Briefly, the A1B scenario represents very rapid economic growth, global population that peaks in mid-century and declines thereafter, and the rapid introduction of new and more efficient technologies with a "balance" across all energy sources, i.e., not relying too heavily on one particular energy source (IPCC, 2000). The B2 scenario places an emphasis on local solutions to economic, social, and environmental sustainability; continuously increasing global population at a slower rate than other scenarios, intermediate levels of economic development, and less rapid and more diverse technological change (IPCC, 2000). Therefore, the A1B land use represents a more aggressive building out of the watershed and the B2 a more conservative build out. Figure 59 shows the land use for the B2 scenario.

For the "building out the watershed" scenario results, changing the land use (percent impervious and associated parameters) resulted in an increase in the peak flow and earlier attenuation. The more aggressive land-use change, A1B, resulted in a greater peak flow and an earlier attenuation than the less aggressive land-use change, B2 (Figure 57 and Figure 58). Additionally, these same land-use scenarios were simulated with the 28 detention basins, as described previously, and, with the addition of the detention basins, the peak flows were reduced below the original 2017 event for both the A1B and B2 land-use (Figure 57 and Figure 58).

Figure 57. Scenario results for the Illinois River near Tahlequah, OK, site using the 2017 validation event as the basis for comparison.
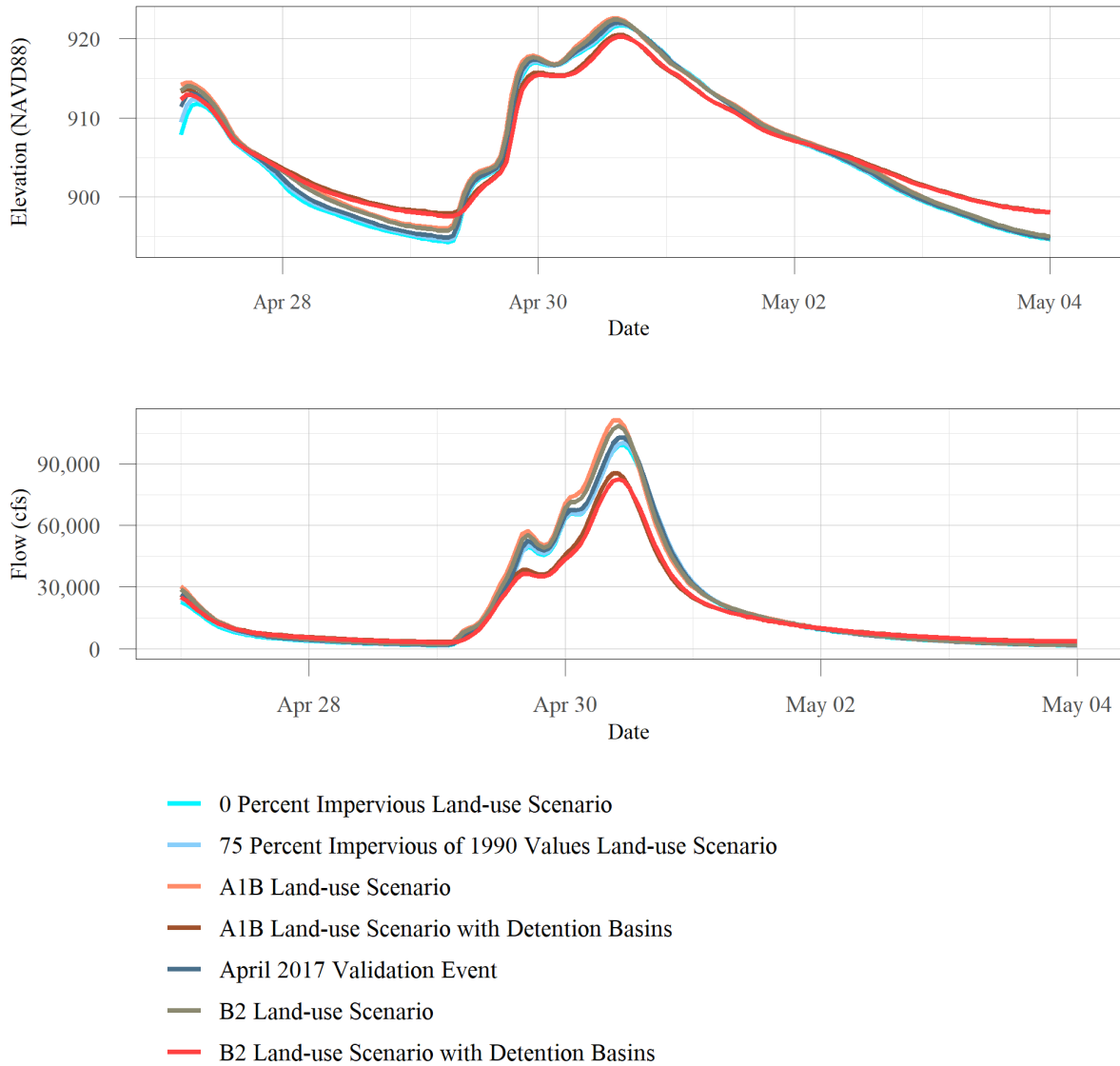
Figure 58. Scenario results for the Illinois River near Watts, OK, site using the 2017 validation event as the basis for comparison.
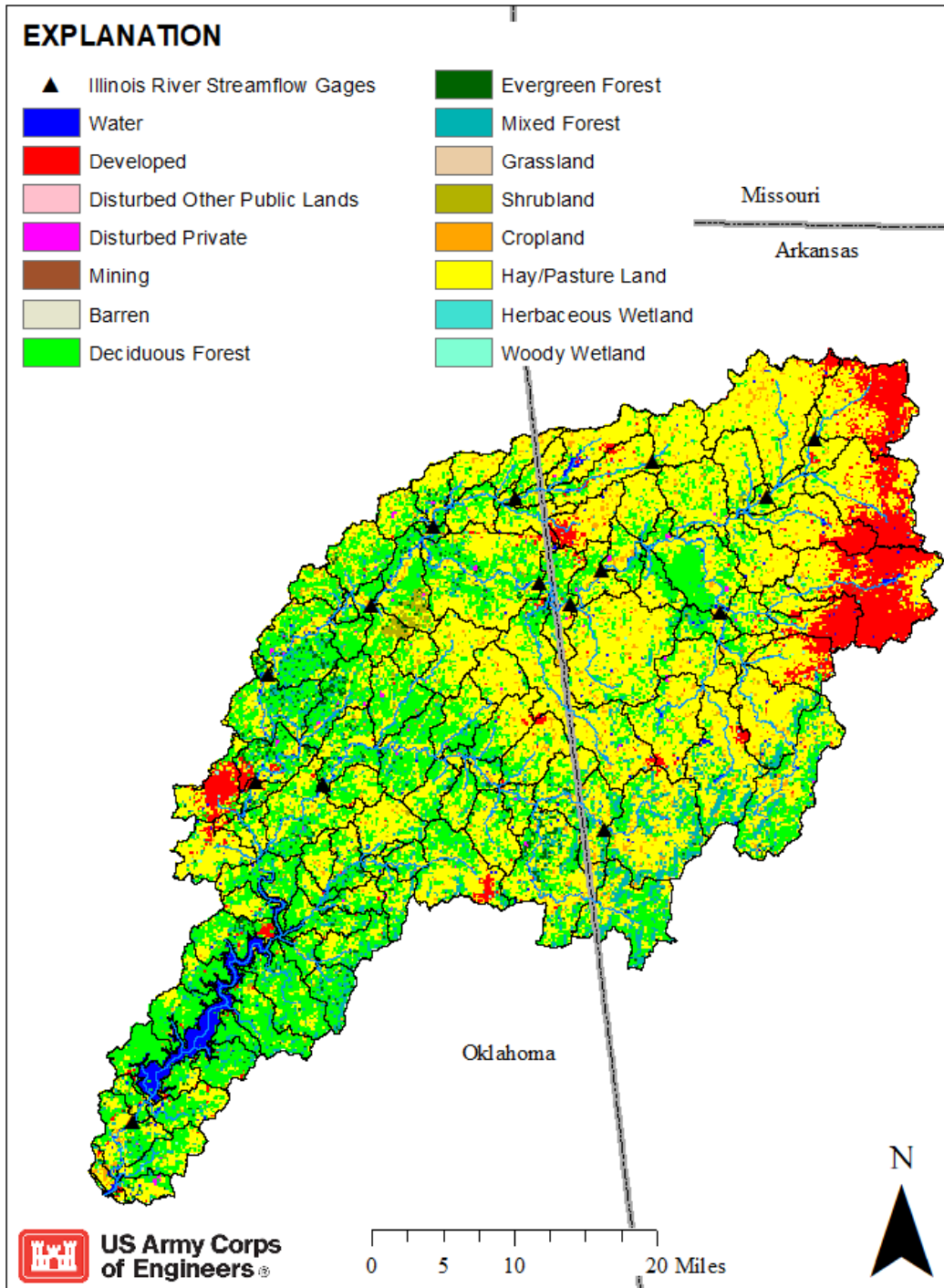
Figure 59. Land-use and land-cover projections for the year 2050 developed from the Intergovernmental Panel on Climate Change (IPCC) Special Report on Emissions Scenarios (SRES) B2 scenario.

The third combination scenario included using the future-cast A1B and B2 land-use grids developed by EROS and an extreme precipitation event. These same scenarios were also simulated using the 28 detentions basins. The more aggressive land-use change, A1B, resulted in a greater peak flow and an earlier attenuation than the less aggressive land-use change, B2 (Figure 60 and Figure 61). However, both land-use change scenarios resulted in greater peak

flows than the 100-year frequency event that used the current (2016 NLCD) land use. Additionally, the A1B and B2 future land-use scenarios were simulated with the 28 detention basins and, with the addition of the detention basins, the peak flows were reduced below the original 100-year frequency event for both the A1B and B2 land-use (Figure 60 and Figure 61).
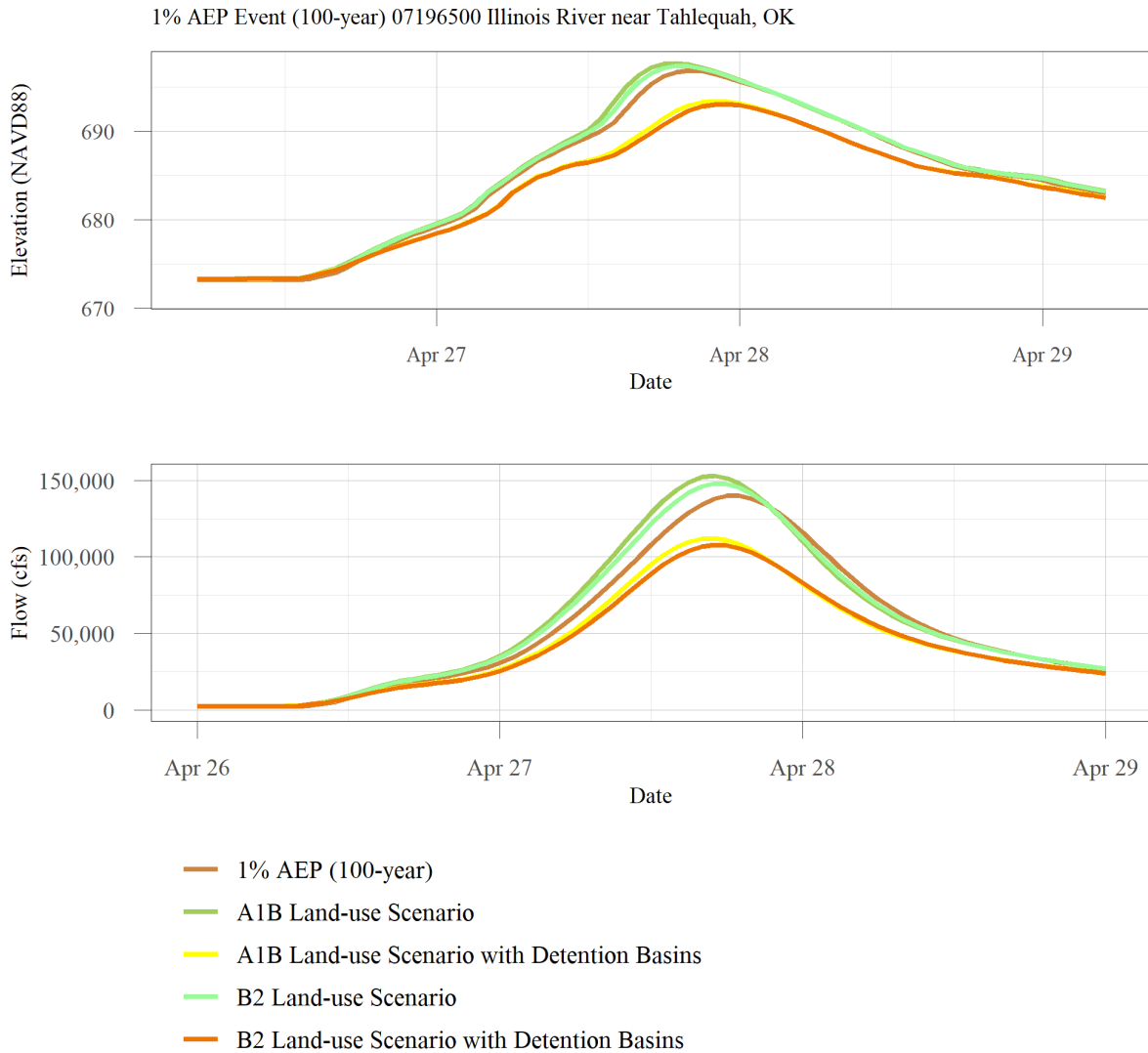
Figure 60. Scenario results for the Illinois River near Tahlequah, OK, site using the 100-year frequency event as the basis for comparison.
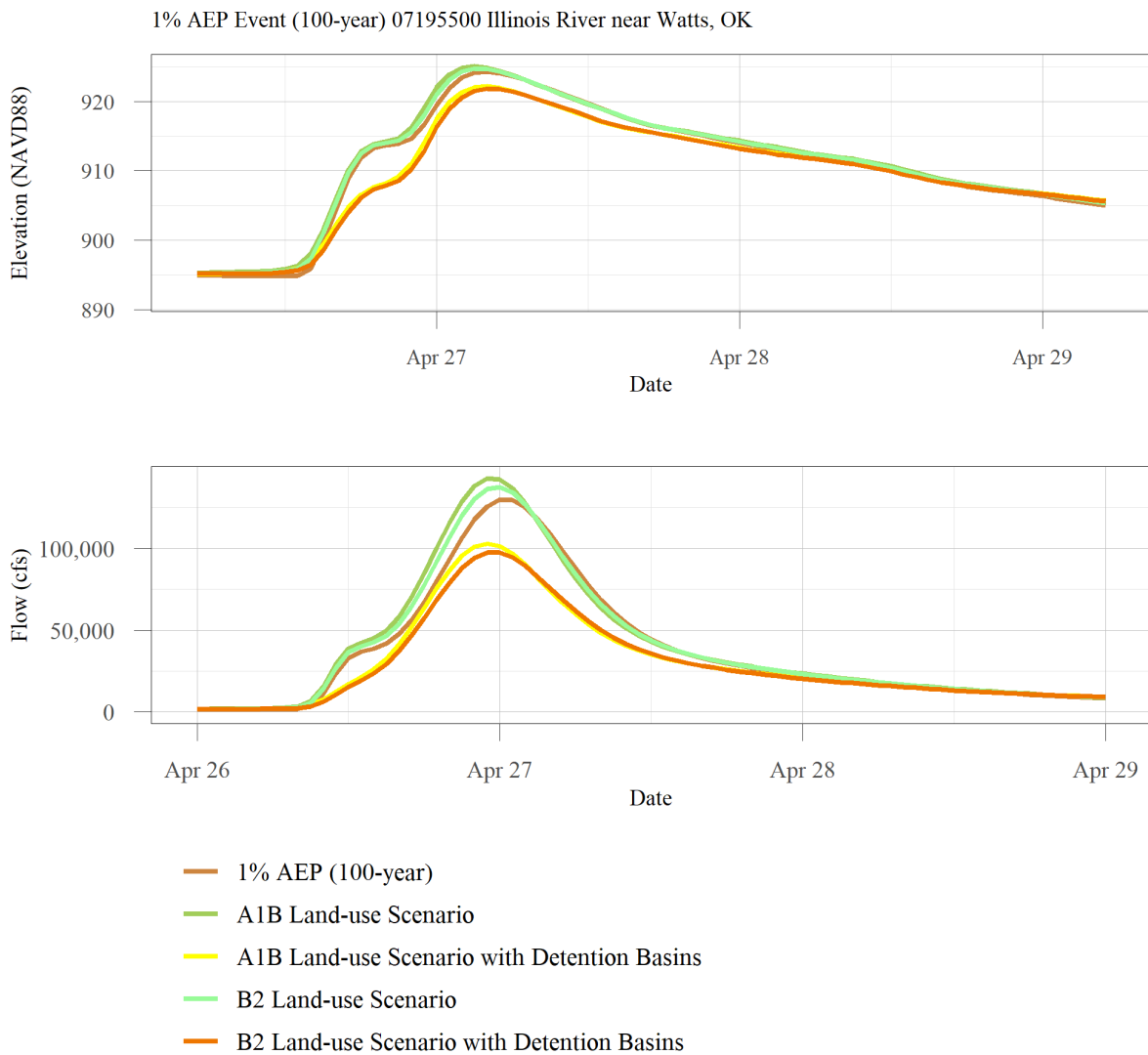
Figure 61. Scenario results for the Illinois River near Watts, OK, site using the 100-year frequency event as the basis for comparison.

Model Assumptions and Limitations

For the HEC-HMS model, potential limitations include (1) estimation of subsurface contributions to runoff, (2) errors attributed to inaccurate input climate data (historical climate datasets used for calibration and validation), (3) errors inherent within the streamflow data that are used to calibrate the model, (4) errors attributed to the subjective nature of the model calibration acceptance criteria, and (5) errors that arise from the inability to account for heterogeneity in the model parameters at a scale that is smaller than a subbasin. With respect to climate data, Behnke et al. (2016) demonstrated that while gridded input temperature data generally matched corresponding weather station records closely, the gridded input precipitation data generally did not compare as well to the weather station records. With respect to the calibration of streamflows, the model was calibrated to hourly streamflow at several streamgaging locations. However, these locations are relatively sparse, compared to the size of

86

the overall watershed and only represent one particular time in space. With respect to heterogeneity, certain hydrologic parameters were lumped over an entire subbasin, and the properties of each subbasin were assumed to be homogeneous and isotropic. As a result, detailed small-scale heterogeneity in the spatial distribution of these parameters was not accounted for.

Model limitations are primarily related to accuracy and availability of bathymetric data. In general, the terrain file is comprised of LiDAR information, which is unable to sufficiently penetrate the water surface. Bathymetry was included where available, but other locations relied on elevations given in profile cuts from bridge plans.

Because the model is calibrated to streamgage rating curves, accuracy of the calibrations also depends upon accuracy of the published rating curves, which are occasionally updated as site conditions change. To maintain proper calibration of the model, rating curves should be checked periodically to ensure the most recent information is being used.

Finally, even though the detentions basins reduce streamflow peaks, the model assumed these detention basins as new structures. In other words, there had not been any infilling of sediment and represent their highest function possible, i.e., the largest volume retained, for these structures. Furthermore, if ever a reality and because of their size, these types of structures would require periodic dam inspections, which includes regular maintenance, and development of emergency action plans, which would include inundation mapping for dam failure and risks to population and infrastructure below each dam. Finally, to achieve maximum flood reduction capacity, a reservoir sediment management plan would need to be in place for each structure.

The same limitations for the HEC-HMS model are also directly applicable to the HEC-RAS model because the HEC-RAS model uses flow computations from HEC-HMS to perform the open channel hydraulic computations. The flow comparisons at internal points in the HEC-RAS model will not exactly match the HEC-HMS model because the HEC-RAS model considers more physical dynamics of water in a channel with HEC-HMS considers the overall water balance in a watershed.

The lack of and the age of existing channel surveys impact the accuracy of the hydraulic computations; however, model prediction is reasonable to compare scenarios by relative difference that are largely focused on changes in watershed flows.

The physical representation of the detention basins was not modeled in the HEC-RAS hydraulic model as that would require more detailed elements of design and operation. As such, the hydraulic model results will give indications of changes in stage and flow, but the possible inundation extents representing the detention basis will not be mapped. The conceptual approach taken to develop dam sizes and outflow leveraging known "rules of thumb" and basic outflow rating equations is adequate to depict proof of concept.

The HEC-RAS model was not calibrated to velocity data. Collecting and calibrating the model to that data would increase the confidence in any conclusions related to modeled velocities. Additionally, the 1D model averages velocities in a cross section by conveyance area within each section, a 2D model would provide more detailed representation of the fluid dynamics.

Summary

In summary, streamflow in the Illinois River has increased in the recent past, particularly in the last decade. This is predominantly due to the fact that precipitation has also increased in the recent past. And, although land use has also changed during the same time period, it has been shown by others that urbanization effects flooding at the local scale and land-use change impacts are not as easily explained or understood at a regional scale (the scale of this modeling effort). Although it might be difficult to parse out which change (i.e., increase in the precipitation or the increase in developed land) has the most effect on flooding in the Illinois River at a local scale, the scenario results can help with mitigation efforts at a larger scale. Illinois River stakeholders can use the resulting changes in peak streamflows and/or peak stages to make informed decisions on where best to put forth resources to decrease flooding in the Illinois River.

Calibration of the models are good, overall, and can be used to model scenarios in order to gain an understanding of future land-use changes and potential remediations. Several scenarios were simulated for the Illinois River watershed and include: the addition of riparian buffers along the mainstem of the Illinois River and along major tributaries to the Illinois River; the addition of small detention basins placed throughout the watershed above Tenkiller Lake to attenuate and lessen peak flows; the use of future land-use grids to represent a "building out of the watershed"; the use of a historical land-use grid to represent a "less developed" time period; use of an extreme precipitation event, i.e., the 100-year frequency event; and combinations of each of these scenarios. Scenario results indicated that the addition of detention basins helps to attenuate and reduce peak flows. Furthermore, adding riparian buffers decreases velocities but increases elevations from flow "build-up".

Although these scenarios, and subsequent results, are conceptual in nature, they provide valuable insights into understanding the impacts of future land-use changes and potential remediations thereof. For instance, adding in riparian buffers had the greatest effect on peak streamflow and subsequent peak stage for the 5- and 10-year frequency events for the Illinois River near Tahlequah, OK, site. The addition of riparian buffers resulted in an approximate 52 percent decrease in streamflow and an approximate 0.8-foot decrease in stage for the 5-year frequency event and an approximate 24 percent decrease in streamflow and an approximate 1.5-foot decrease in stage for the 10-year frequency event (Figure 62). For the 25-, 50-, and 100-year frequency events, the addition of riparian buffers resulted in an approximate 25 percent decrease in streamflow for all three frequency events (Figure 63). Furthermore, the addition of riparian buffers resulted in an approximate 1.8-foot, 2-foot, and 2.6-foot decrease in stage for the 25-, 50-, and 100-year frequency events, respectively, for the Illinois River near Tahlequah, OK, site (Figure 64). Other notable results include an approximate 7.6 percent increase in peak streamflow and an approximate 0.8-foot increase in peak stage for the more extreme A1B land use and the 2017 precipitation event and an approximate 9.5 percent increase in peak streamflow and an approximate 0.8-foot increase in peak stage for the more extreme A1B land use and the 100-year frequency event precipitation for the Illinois River near Tahlequah, OK, site (Figure 65 and Figure 66, respectively). However, adding in detention basins decreased the peak streamflow by an approximate 22.5 percent and decreased the peak stage an approximate 3.1 feet for the more extreme A1B land use and the 2017 precipitation event and decreased the peak streamflow by an approximate 27 percent and decreased the peak stage an approximate 4.3 feet for the more

extreme A1B land use and the 100-year frequency event precipitation (Figure 65 and Figure 66, respectively). Furthermore, the reduction in velocities, which is important for streambank erosion, decreased for all frequency events. Figure 67 gives the mean change in velocity by reach within the Illinois River watershed for the 2-, 10-, 25-, and 100-year frequency events.
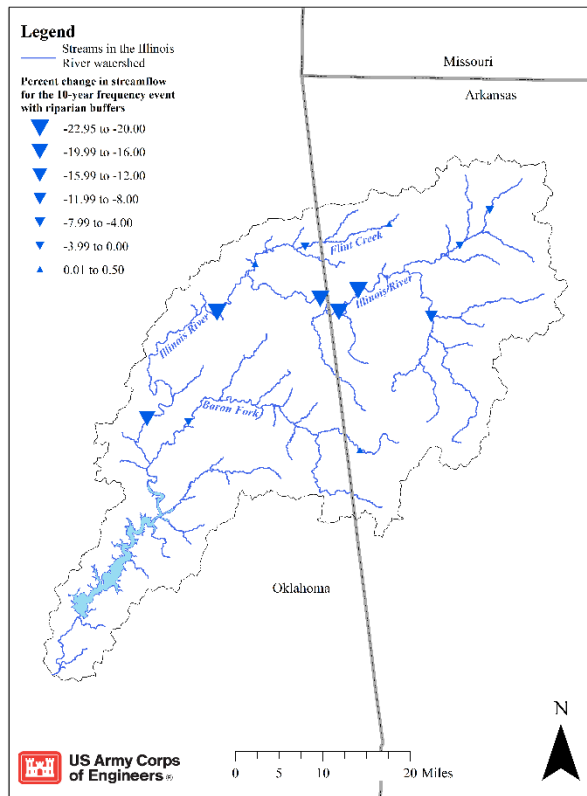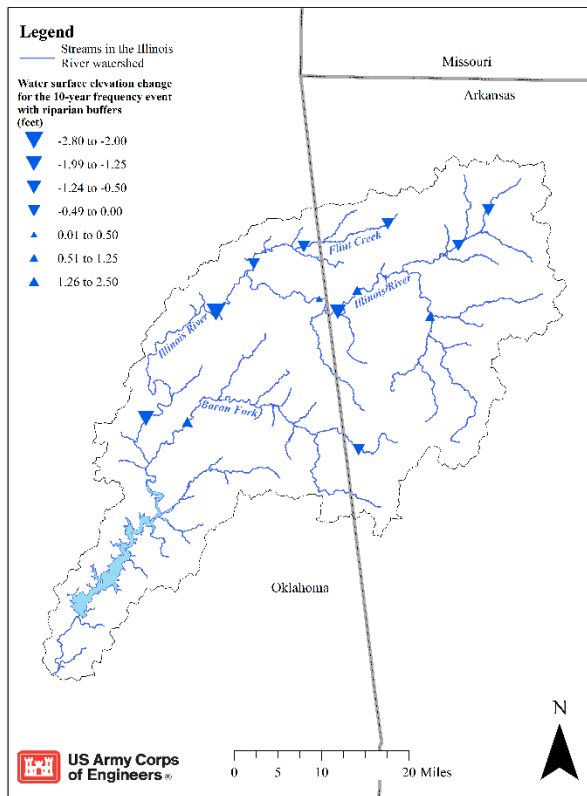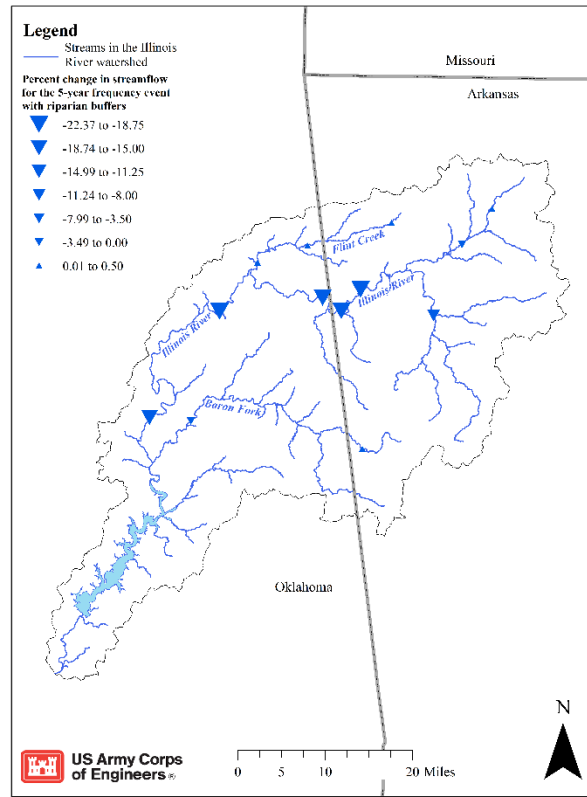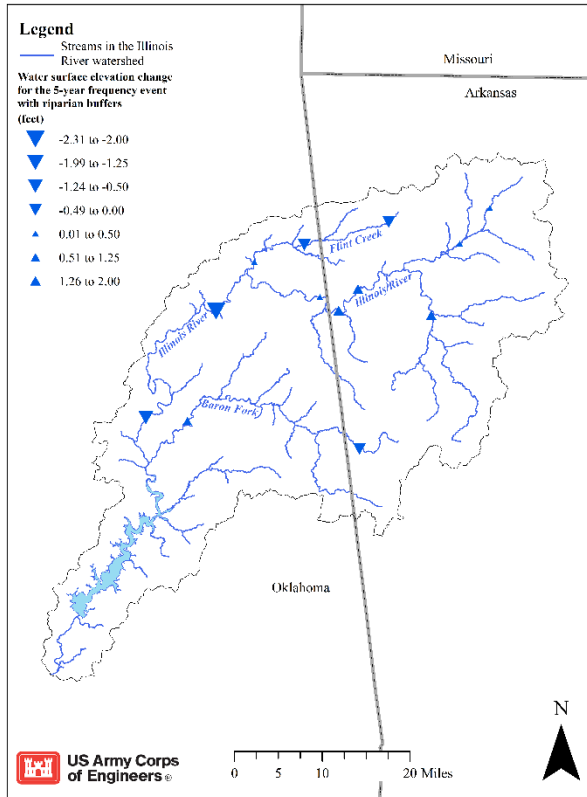
Figure 62. Water surface elevation change and percent change in streamflow for the 5-year and 10-year frequency events with the addition of riparian buffers.
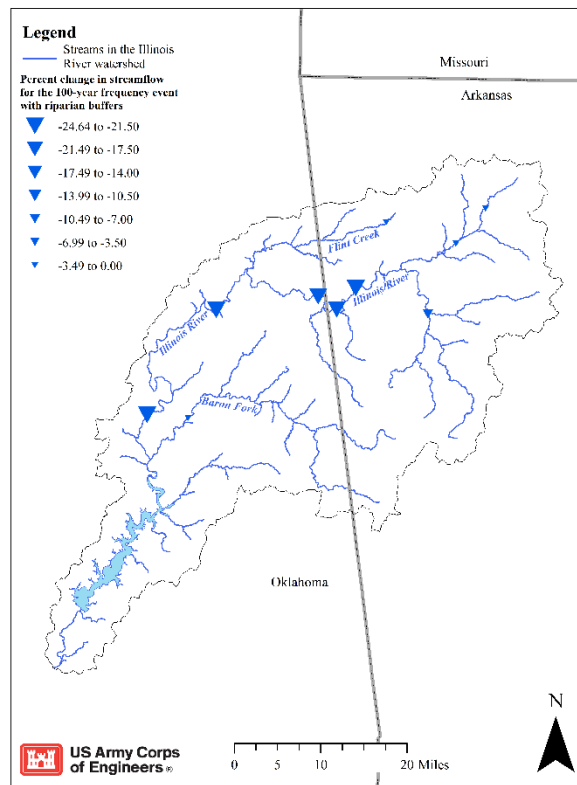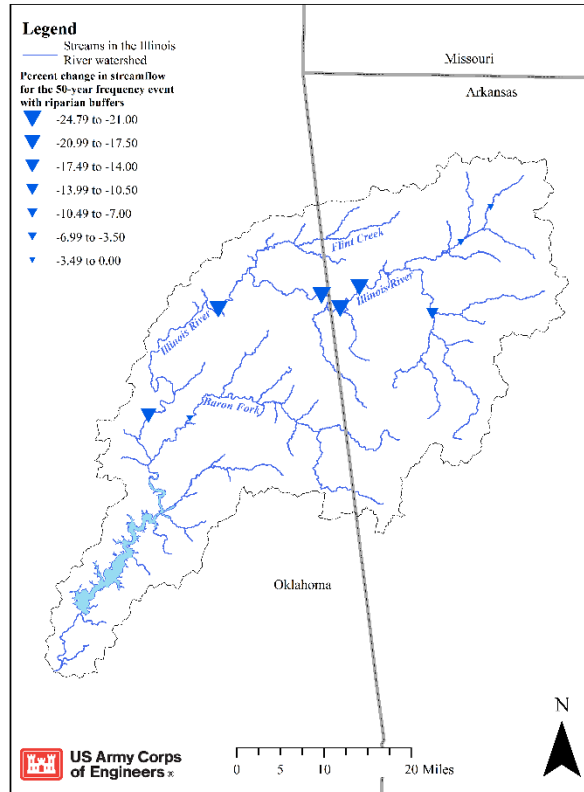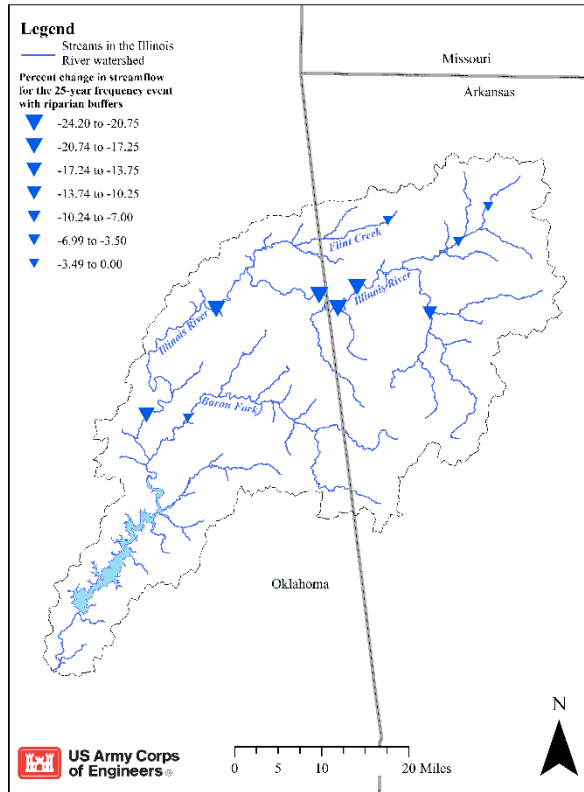
Figure 63. Percent change in streamflow for the 25-year, 50-year, and 100-year frequency events with the addition of riparian buffers.
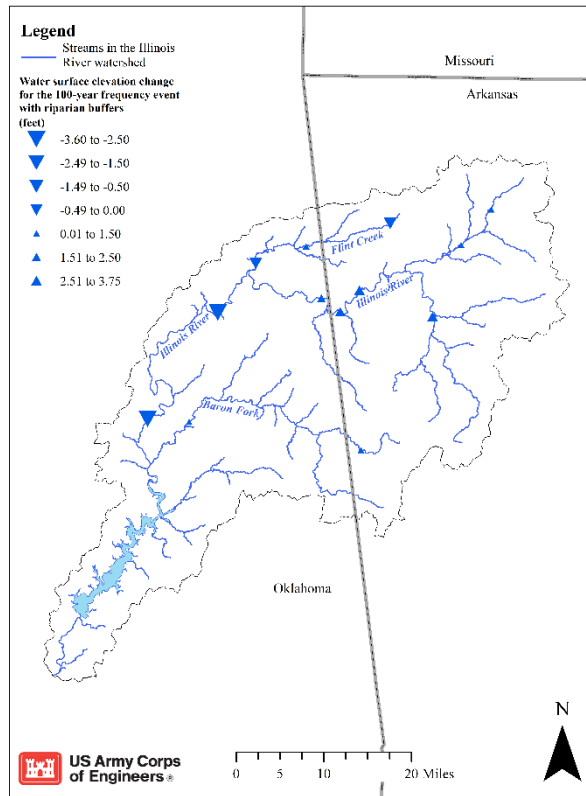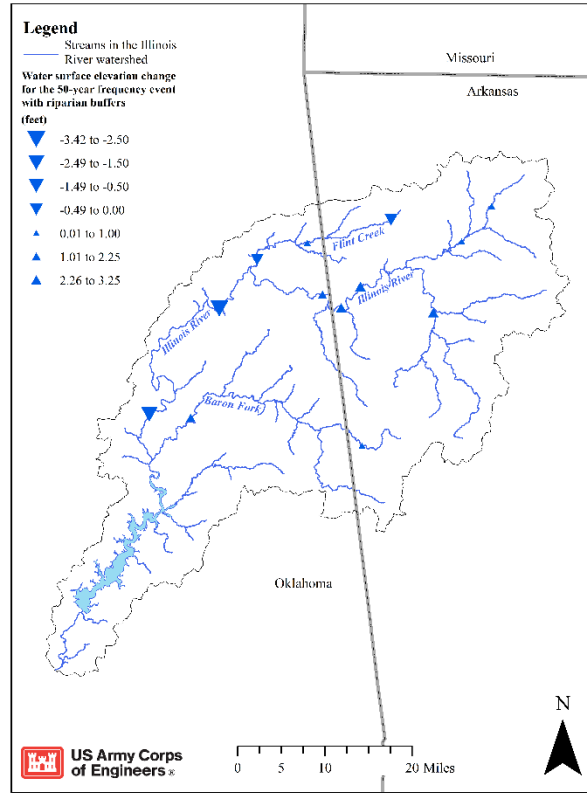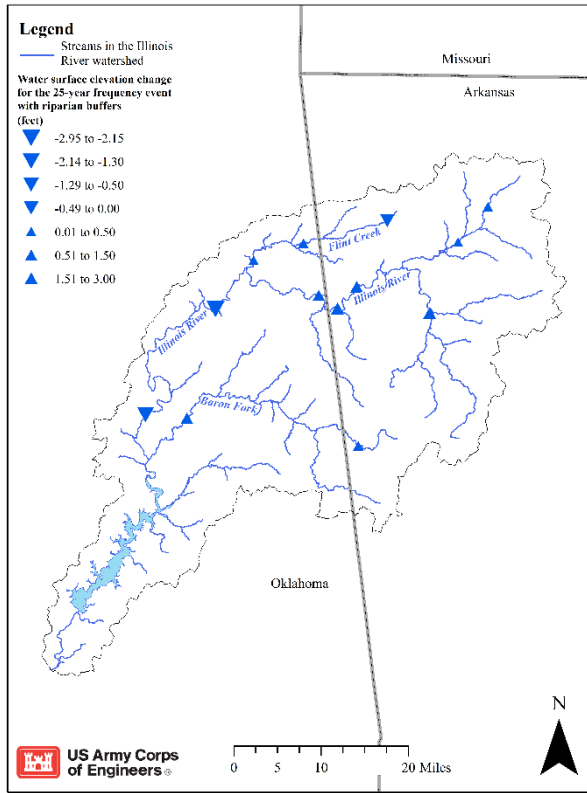
Figure 64. Water surface elevation change for the 25-year, 50-year, and 100-year frequency events with the addition of riparian buffers.
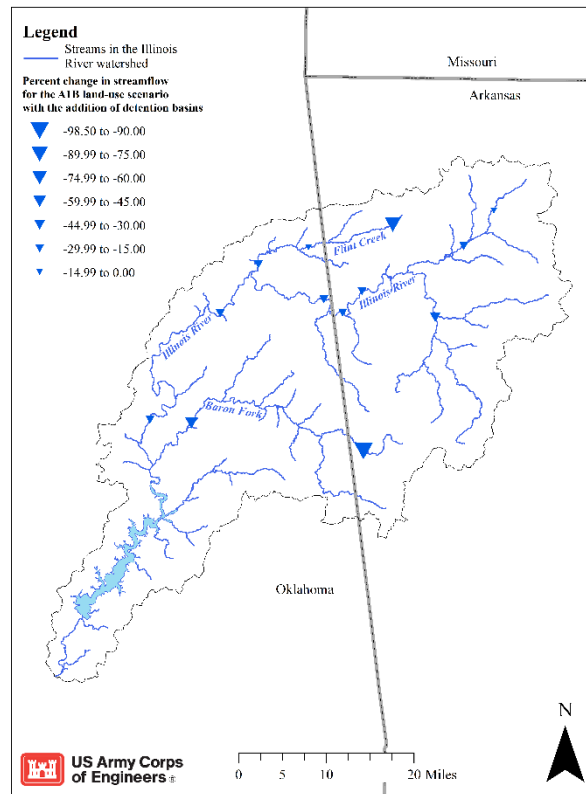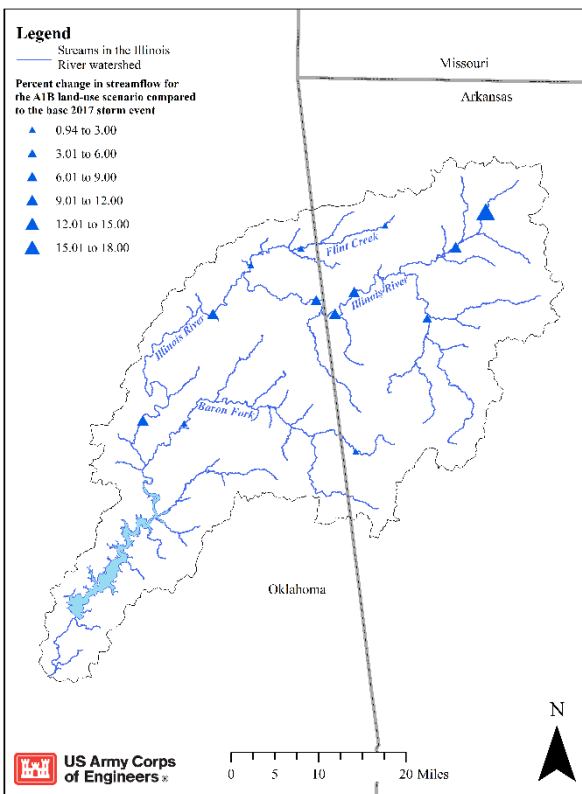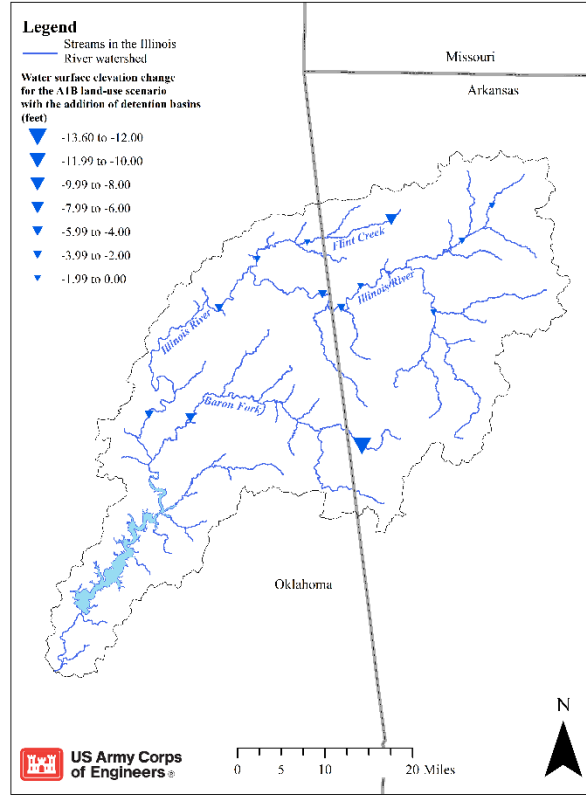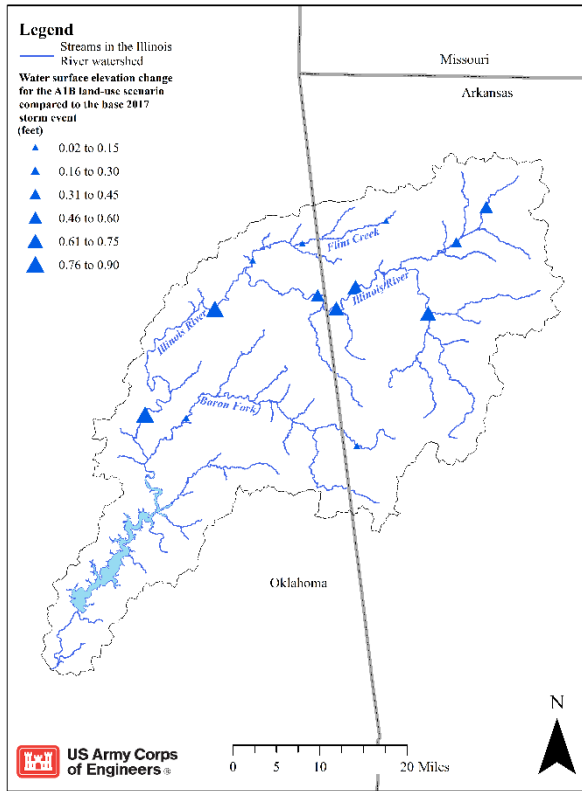
Figure 65. Water surface elevation change and percent change in streamflow for the A1B land use compared to the 2017 event and with the addition of detention basins.
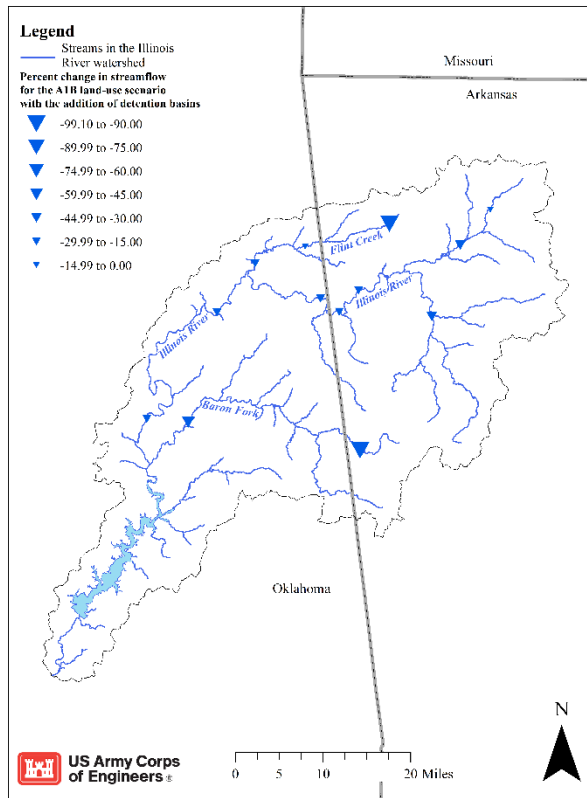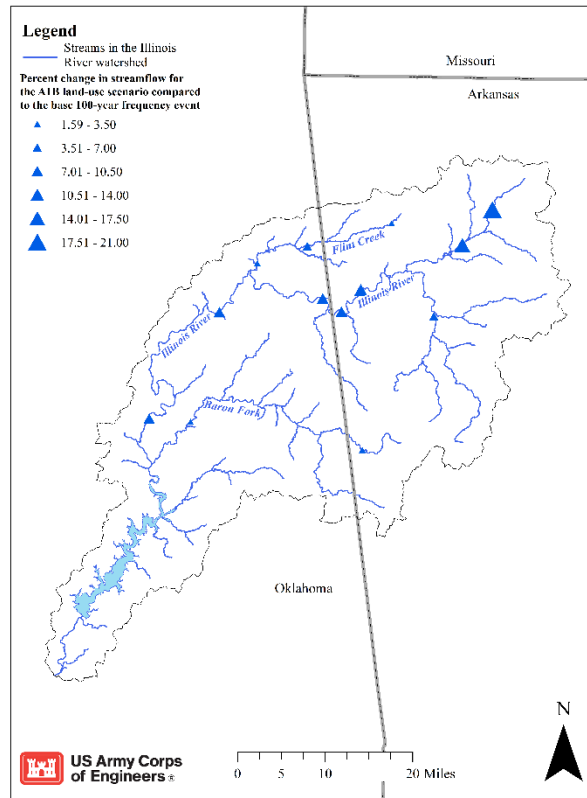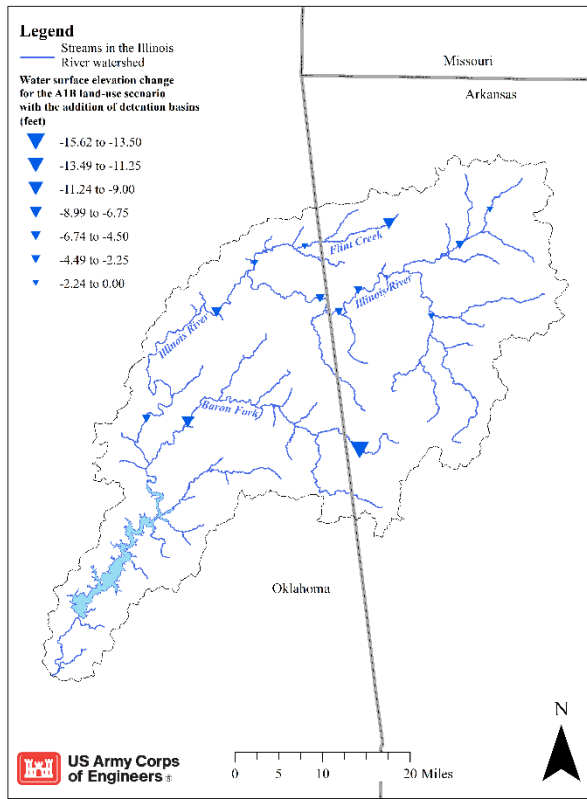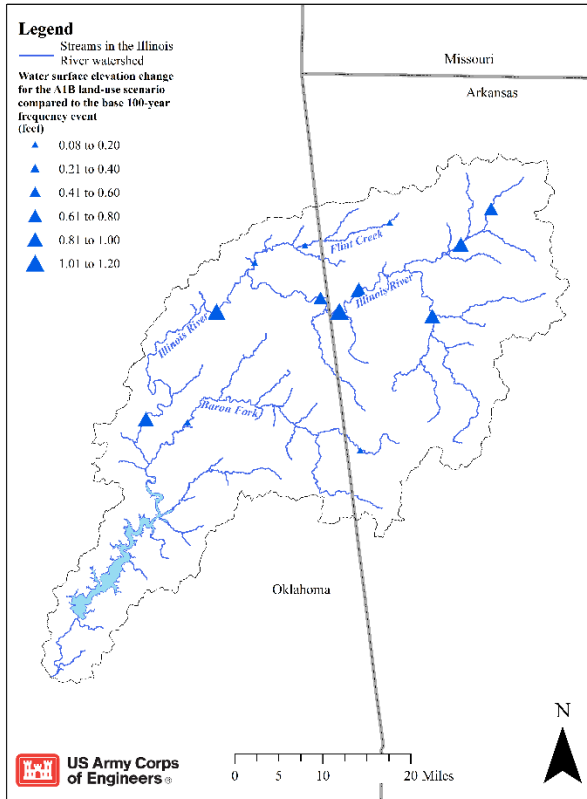
Figure 66. Water surface elevation change and percent change in streamflow for the A1B land use compared to the 100-year frequency event and with the addition of detention basins.
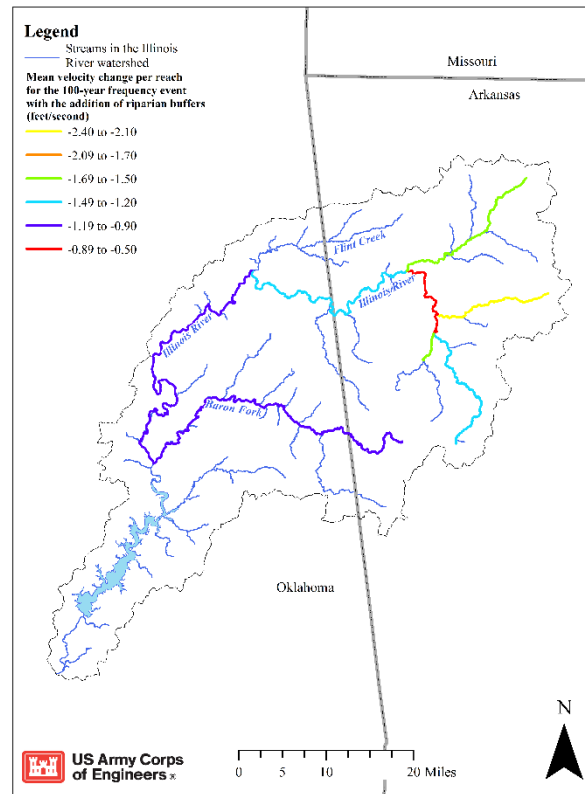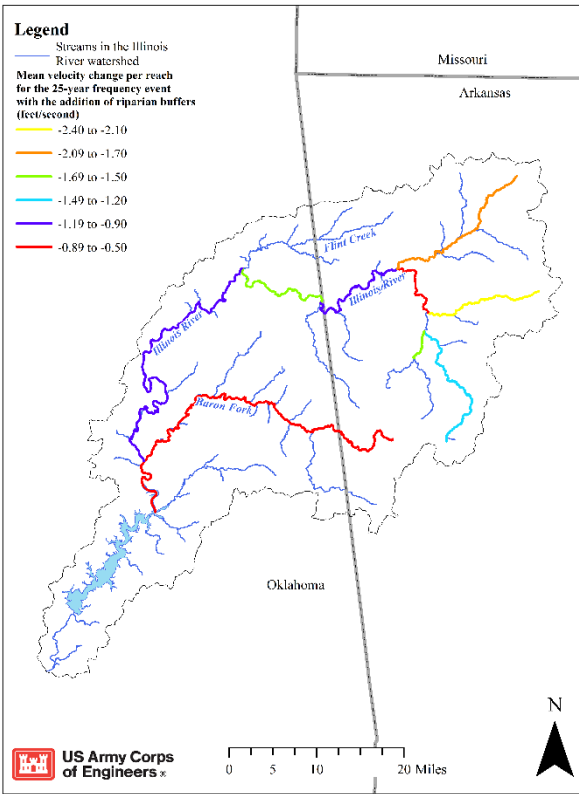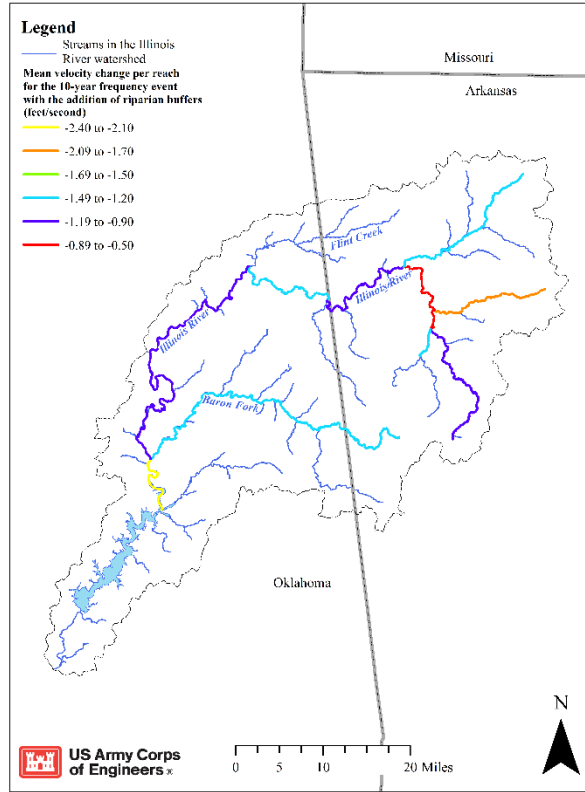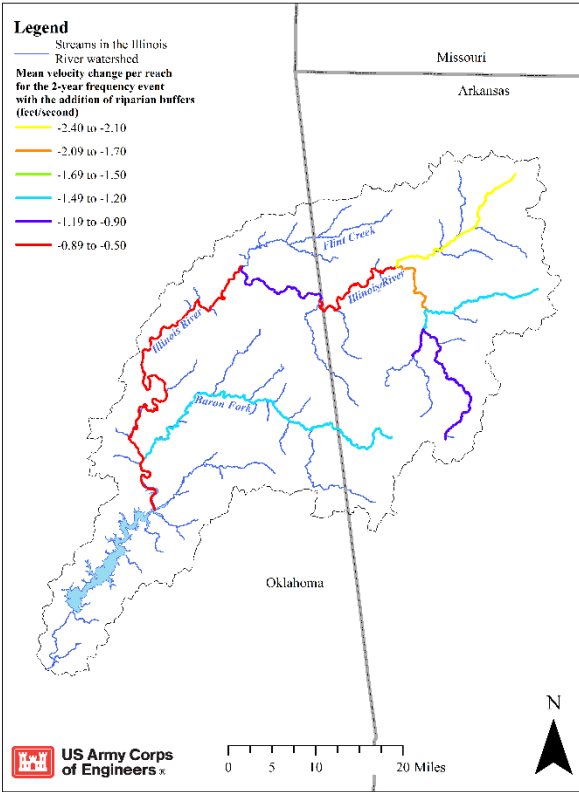
Figure 67. Mean change in velocity per reach for the 2-, 10-, 25-, and 100-year frequency events with the addition of riparian buffers.

References

Archfield, S.A., Kennen, J.G., Carlisle, D.M., and Wolock, D.M., 2013, An Objective and Parsimonious Approach for Classifying Natural Flow Regimes at a Continental Scale: RRA 30 (9), November 2014, pp. 1166-1183, https://doi.org/10.1002/rra.2710.

Arkansas Department of Environmental Quality, 2018, Integrated Water Quality Monitoring Assessment Report: Prepared Pursuant to Section 305(b) and Section 303(d) and of the Federal Pollution Control Act by Arkansas Department of Environmental Quality, 255 p., https://www.adeq.state.ar.us/water/planning/integrated/303d/pdfs/2018/final-2018-305b-report.pdf.

Bartles, M., Brauer, T., Ho, D., Fleming, M., Karlovits, G., Pak, J., Van, N., and Willis, J., 2021, Hydrologic Modeling System HEC-HMS User's Manual: U.S. Army Corps of Engineers Institute for Water Resources Hydrologic Engineering Center (CEIWR-HEC), accessed June 16, 2021 at https://www.hec.usace.army.mil/confluence/hmsdocs/hmsum/latest.

Behnke, R., Vavrus, S., Allstadt, A., Albright, T., Thogmartin, W.E., and Radeloff, V.C., 2016, Evaluation of downscaled, gridded climate data for the conterminous United States: Ecological Applications, v. 26, no. 5, p. 1338–1351.

Blunden, J. and Arndt, D.S., Eds., 2020, State of the Climate in 2019: Bull. Amer. Meteor., 101 (8), Si–S429. doi:10.1175/2020BAMSStateoftheClimate.1.

Dewitz, J., and U.S. Geological Survey, 2021, National Land Cover Database (NLCD) 2019 Products (ver. 2.0, June 2021): U.S. Geological Survey data release, https://doi.org/10.5066/P9KZCM54.

Dunn, R.J.H., Stanitski, D.M., Gobron, N., and Willett, K.M., Eds., 2020, Global Climate [in "State of the Climate in 2019"]: Bull. Amer. Meteor., 101 (8), S9–S127, https://doi.org/10.1175/BAMS-D-20-0104.1.

England, J.F., Jr., Cohn, T.A., Faber, B.A., Stedinger, J.R., Thomas, W.O., Jr., Veilleux, A.G., Kiang, J.E., and Mason, R.R., Jr., 2018, Guidelines for determining flood flow frequency—Bulletin 17C (ver. 1.1, May 2019): U.S. Geological Survey Techniques and Methods, book 4, chap. B5, 148 p., https://doi.org/10.3133/tm4B5.

Eker, S., Rovenskaya, E., Obersteiner, M., Langan, S., 2018, Practice and perspectives in the validation of resource management models: Nat Commun. Dec 18; 9(1):5359. doi: 10.1038/s41467-018-07811-9.

Evans, T.A., 2016, GageInterp User's Manual: A Program for Creating a Sequence of HEC-DSS Grids from Time-Series Measurements: US Army Corps of Engineers Institute of Water Resources Hydrologic Engineering Center, Version 1.6.

Feng, G., Cobb, S., Abdo, Z., Fisher, D.K., Ouyang, Y., Adeli, A., and Jenkins, J.N., 2016, Trend Analysis and Forecast of Precipitation, Reference Evapotranspiration, and Rainfall Deficit in the Blackland Prairie of Eastern Mississippi: Journal of Applied Meteorology and Climatology, 55 (7), pp 1425-1439, https://doi.org/10.1175/JAMC-D-15-0265.1.

Feng, B., Zhang, Y. and Bourke, R., 2021, Urbanization impacts on flood risks based on urban growth data and coupled flood models: Nat Hazards 106, 613–627, https://doi.org/10.1007/s11069-020-04480-0.

Hirsch, R.M. and Archfield, S.A., 2015, Flood trends: not higher but more often: Nat. Clim. Chang. 5, 198–199, https://doi.org/10.1038/nclimate2551.

Homer, C.H., Fry, J.A., and Barnes C.A., 2012, The National Land Cover Database, U.S. Geological Survey Fact Sheet 2012-3020, 4 p., https://doi.org/10.3133/fs20123020.

IPCC, 2000, Emissions Scenarios, Nebojsa Nakicenovic and Rob Swart (Eds.): Cambridge University Press, UK, pp 570, https://www.ipcc.ch/site/assets/uploads/2018/03/emissions_scenarios-1.pdf.

Jacobson, R.B. and Primm, A.T., 1997, Historical land-use changes and potential effects on stream disturbance in the Ozark Plateaus, Missouri: U.S. Geological Survey water-supply paper, 2484, 85 p.

Mallakpour, I., and Villarini, G., 2015, The changing nature of flooding across the central United States: Nat. Clim. Chang. 5, 250–254, https://doi.org/10.1038/nclimate2516.

Merz, B., Blöschl, G., Vorogushyn, S., Dottori, F., Aerts, J.C.J.H., Bates, P., Bertola, M., Kemter, M., Kreibich, H., Lall, U., and Macdonald, E., 2021, Causes, impacts and patterns of disastrous river floods: Nat Rev Earth Environ (2021), https://doi.org/10.1038/s43017-021-00195-3.

Mills, J., and Blodgett, D., 2017, EflowStats: Hydrologic Indicator and Alteration Stats: R package version 5.0.1.

Myhre, G., Alterskjær, K., Stjern, C.W., 2019, Frequency of extreme precipitation increases extensively with event rareness under global warming: Sci Rep 9, 16063, https://doi.org/10.1038/s41598-019-52277-4.

Neri, A., Villarini, G., Slater, L.J., and Napolitano, F., 2019, On the statistical attribution of the frequency of flood events across the U.S. Midwest: Advances in Water Resources 127, 225–236, https://doi.org/10.1016/j.advwatres.2019.03.019.

Oklahoma Conservation Commission, 2010, Watershed Based Plan for the Illinois River Watershed: Oklahoma Conservation Commission Water Quality Division, Oklahoma City, OK, 171 p., http://www.conservation.ok.gov.

Oklahoma Department of Environmental Quality, 2018, Water Quality in Oklahoma—2018 Integrated Report: Prepared Pursuant to Section 303(D) and Section 305(B) of the Clean Water Act by Oklahoma Department of Environmental Quality, 83 p., https://www.deq.ok.gov/water-quality-division/watershed-planning/integrated-report/.

Poff, N.L., Allan, J.D., Bain, M.B., Karr, J.R., Prestegaard, K.L., Richter, B.D., Sparks, R.E., and Stromberg, J.C., 1997, The Natural Flow Regime: A paradigm for river conservation and restoration: BioScience Vol. 47 No. 11, pp. 769-784.

Praveen, B., Talukdar, S., Shahfahad, Mondal, J., Sharma, P., Islam, A.R., and Rahman, A., 2020, Analyzing trend and forecasting of rainfall changes in India using non-parametrical and machine learning approaches: Sci Rep 10, 10342, https://doi.org/10.1038/s41598-020-67228-7.

PRISM Climate Group, 2021, Oregon State University, http://prism.oregonstate.edu, created 22 Jun 2021.

R Core Team, 2020, R: A language and environment for statistical computing: R Foundation for Statistical Computing, Vienna, Austria, https://www.R-project.org/.

Rogger, M., Agnoletti, M., Alaoui, A., Bathurst, J.C., Bodner, G., Borga, M., Chaplot, V., Gallart, F., Glatzel, G., Hall, J., Holden, J., Holko, L., Horn, R., Kiss, A., Kohnová, S., Leitinger, G., Lennartz, B., Parajka, J., Perdigão, R., Peth, S., Plavcová, L., Quinton, J. N., Robinson, M., Salinas, J. L., Santoro, A., Szolgay, J., Tron, S., van den Akker, J. J. H., Viglione, A., and Blöschl, G., 2017, Land use change impacts on floods at the catchment scale: Challenges and opportunities for future research: Water Resources Research 53 (7), pp. 5209-5219, https://doi.org/10.1002/2017WR020723.

Sanja, P., Martin, D., Pavlovic, S., Roy, I., St. Laurent, M., Trypaluk, C., Unruh, D., Yekta, M., Bonnin, G., 2013, NOAA Atlas 14 Volume 9 Version 2, Precipitation-Frequency Atlas of the United States, Southeastern States: NOAA, National Weather Service, Silver Spring, MD, https://www.weather.gov/media/owp/oh/hdsc/docs/Atlas14_Volume9.pdf.

Sohl, T.L., Sayler, K.L., Bouchard, M.A., Reker, R.R., Freisz, A.M., Bennett, S.L., Sleeter, B.M., Sleeter, R.R., Wilson, T., Soulard, C., Knuppe, M., and Van Hofwegen, T., 2018, Conterminous United States Land Cover Projections - 1992 to 2100: U.S. Geological Survey data release, https://doi.org/10.5066/P95AK.

Tilley, J.S., and Slonecker, E.T., 2006, Quantifying the Components of Impervious Surfaces: U.S. Geological Survey Open-File Report 2006-1008, 33 p.

U.S. Census Bureau, 2000, County Population Estimates for July 1, 1999 and Population Change for April 1, 1990 to July 1, 1999: Washington, D.C., U.S. Bureau of the Census, accessed June 1, 2021, at https://www2.census.gov/programs-surveys/popest/tables/1990-2000/counties/totals/99c2_05.txt.

U.S. Census Bureau, 2020, Annual Estimates of the Resident Population for Counties in Arkansas: April 1, 2010 to July 1, 2019: Washington, D.C., U.S. Census Bureau, Population Division, accessed June 1, 2021, at https://www.census.gov/data/tables/time-series/demo/popest/2010s-counties-total.html.

Appendix A: Simulated versus observed streamflow plots and goodness of fit statistics for the Illinois River HEC-HMS model calibration and validation events

May 1990 Calibration Event
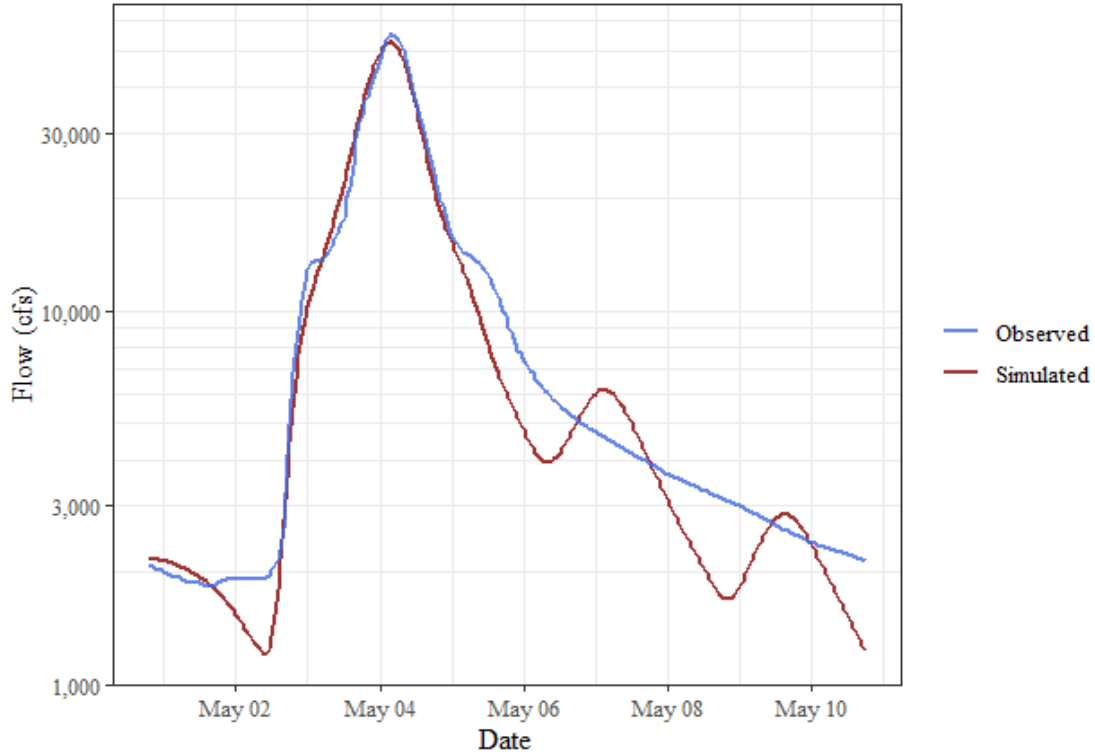
Illinois River near Tahlequah, OK, Time Series Comparison

Goodness of Fit Table

| Time Step	MAE	Normalized RMSE (%)	PBIAS (%)	RSR	NSE	Modified NSE	R^2	Adjusted R^2
Hourly	1,238.45	13.3	-6.1	0.13	0.98	0.86	0.98	0.96
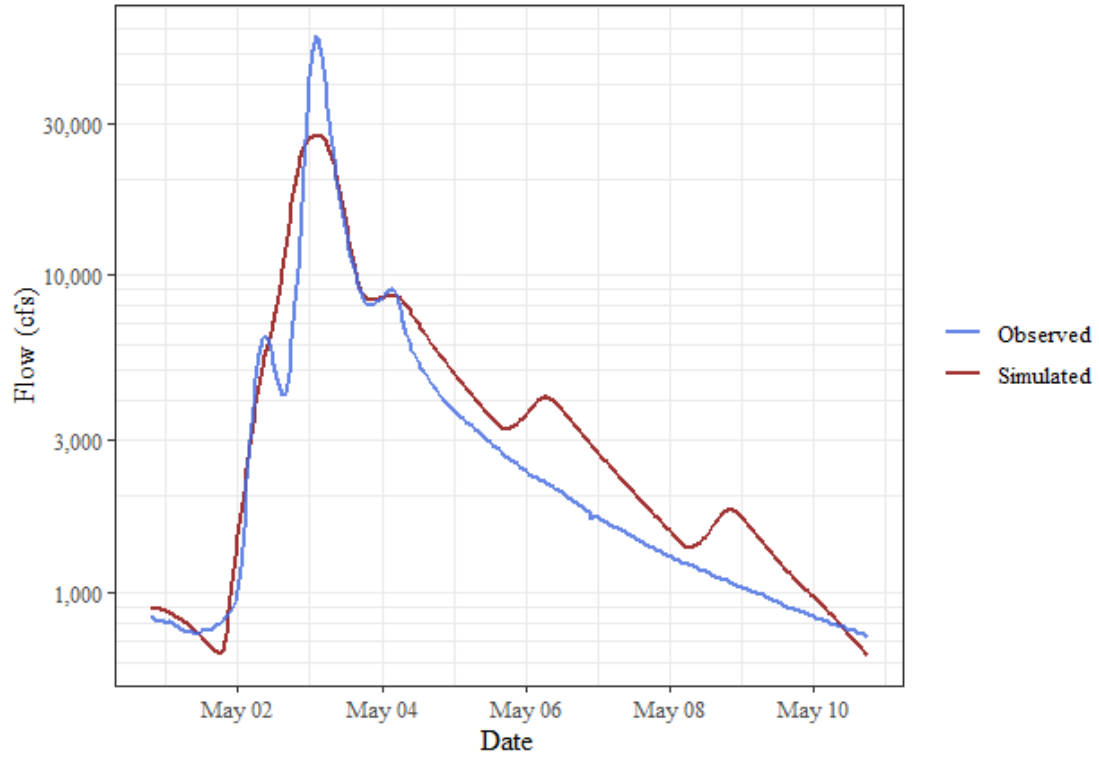
Baron Fork at Eldon, OK, Time Series Comparison

Goodness of Fit Table

Time Step	MAE	Normalized RMSE (%)	PBIAS (%)	RSR	NSE	Modified NSE	R^2	Adjusted R^2
Hourly	1,521.44	47.7	4.5	0.48	0.77	0.67	0.81	0.59
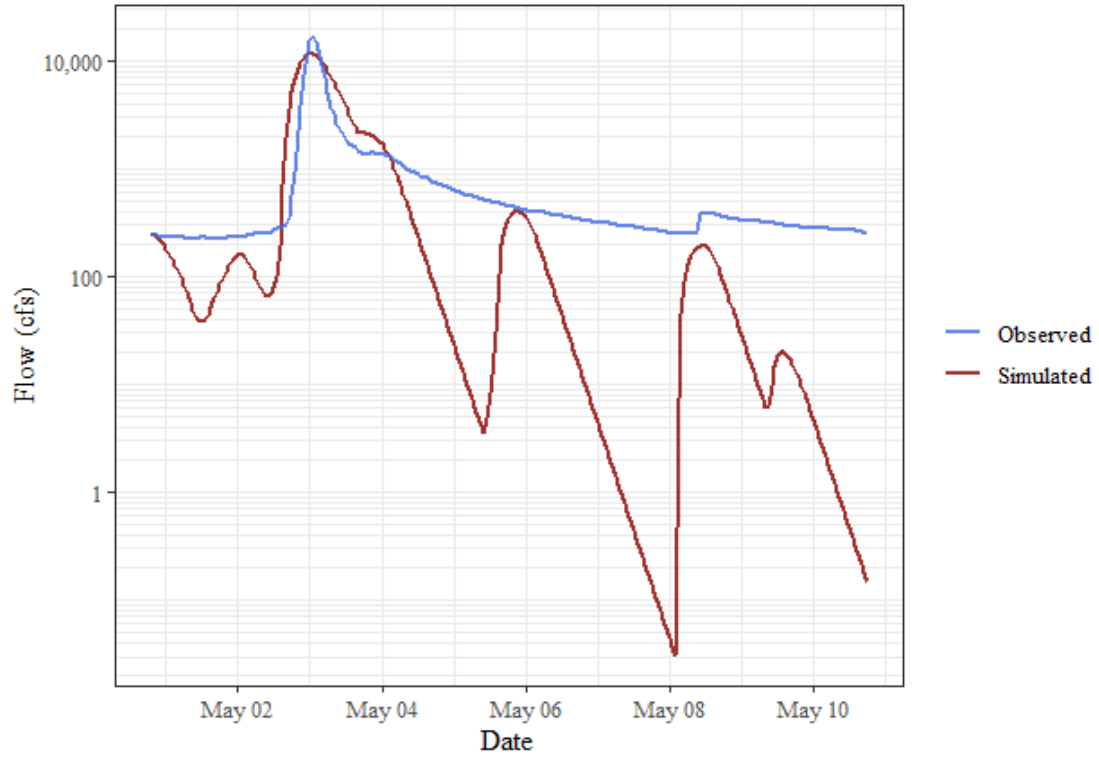
Flint Creek near Kansas, OK, Time Series Comparison

Goodness of Fit Table

Time Step	MAE	Normalized RMSE (%)	PBIAS (%)	RSR	NSE	Modified NSE	R^2	Adjusted R^2
Hourly	555.89	50.4	-4.5	0.5	0.75	0.42	0.78	0.73
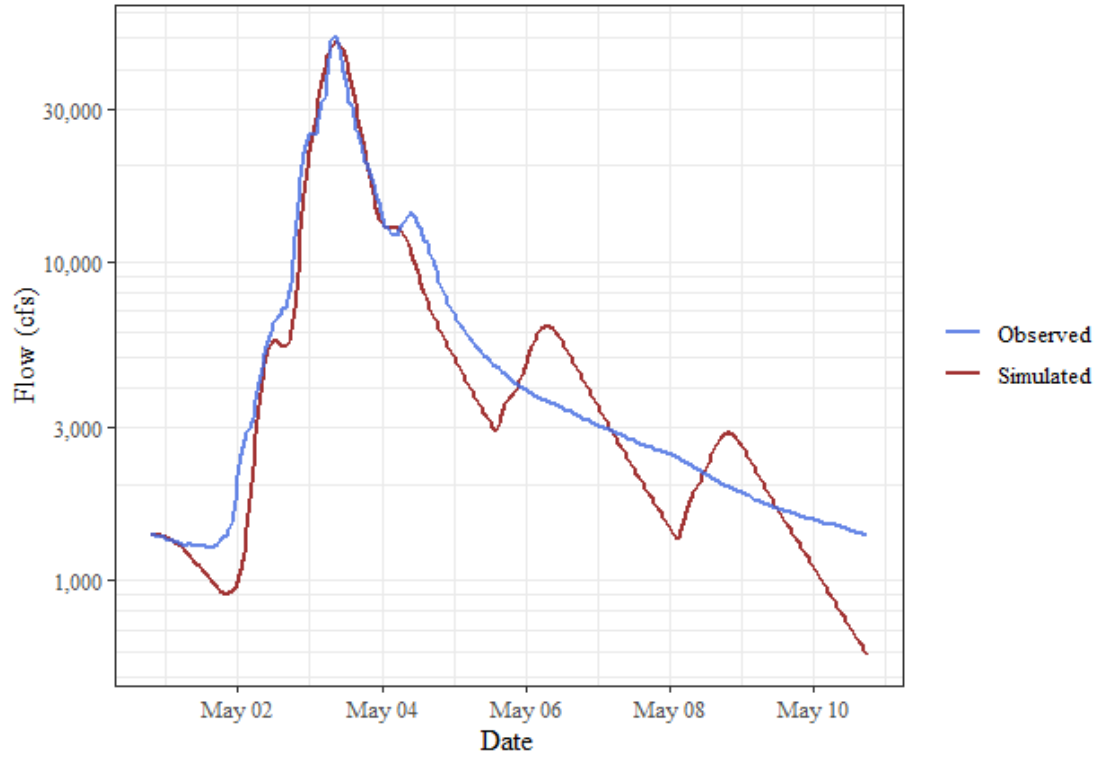
Illinois River near Watts, OK, Time Series Comparison

Goodness of Fit Table

Time Step	MAE	Normalized RMSE (%)	PBIAS (%)	RSR	NSE	Modified NSE	R^2	Adjusted R^2
Hourly	1,266.15	20.6	-3.9	0.21	0.96	0.79	0.96	0.95
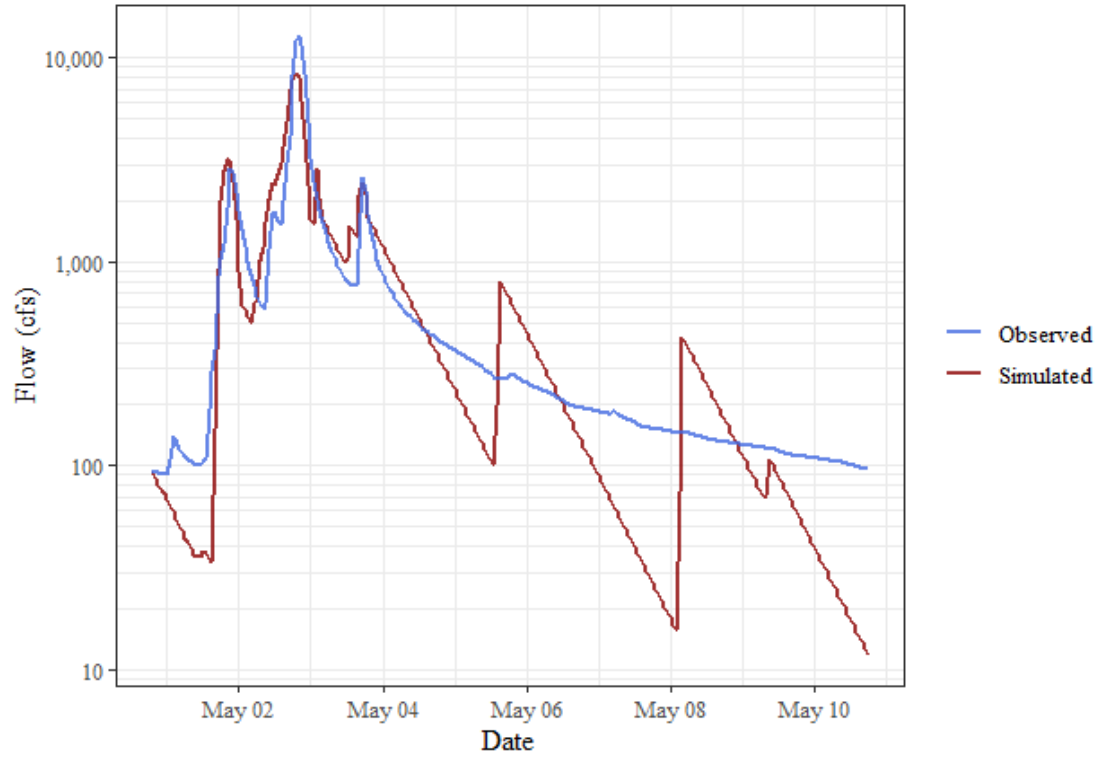
Baron Fork at Dutch Mills, AR, Time Series Comparison

Goodness of Fit Table

Time Step	MAE	Normalized RMSE (%)	PBIAS (%)	RSR	NSE	Modified NSE	R^2	Adjusted R^2
Hourly	299.15	45.1	-4.1	0.45	0.8	0.61	0.81	0.6

April 2011 Calibration Event

Illinois River near Tahlequah, OK, Time Series Comparison
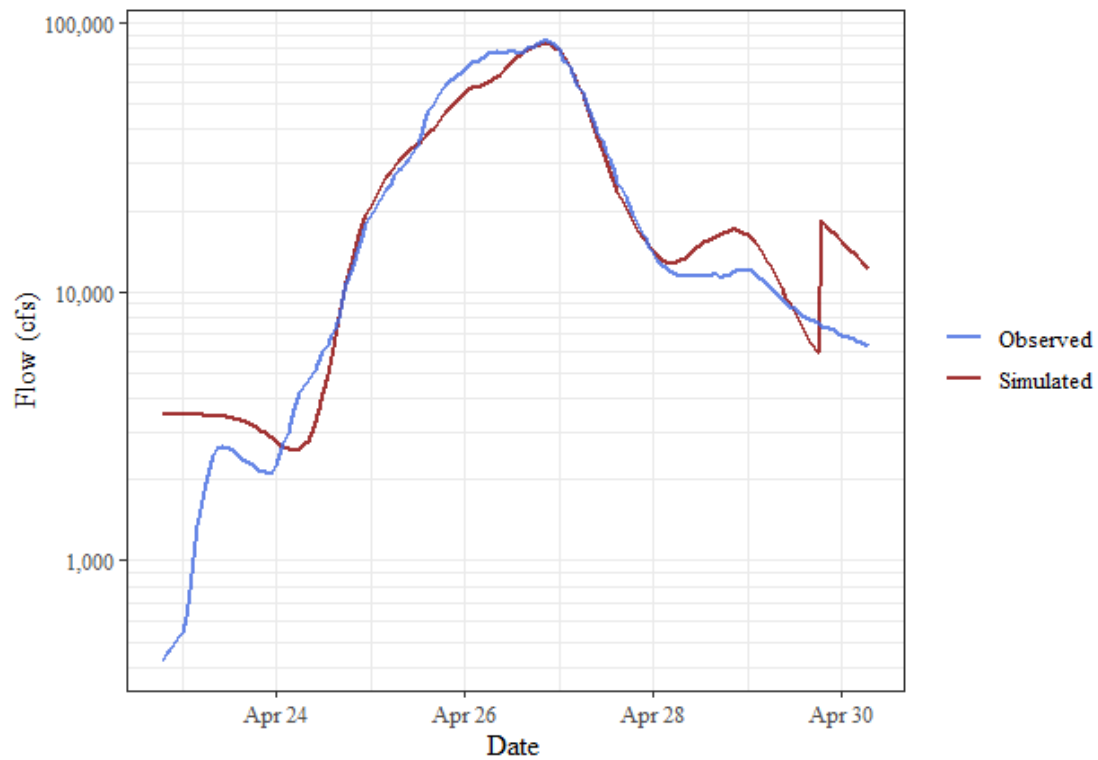
Goodness of Fit Table

Time Step	MAE	Normalized RMSE (%)	PBIAS (%)	RSR	NSE	Modified NSE	R^2	Adjusted R^2
Hourly	3,541.87	19.8	-1.3	0.2	0.96	0.84	0.97	0.9
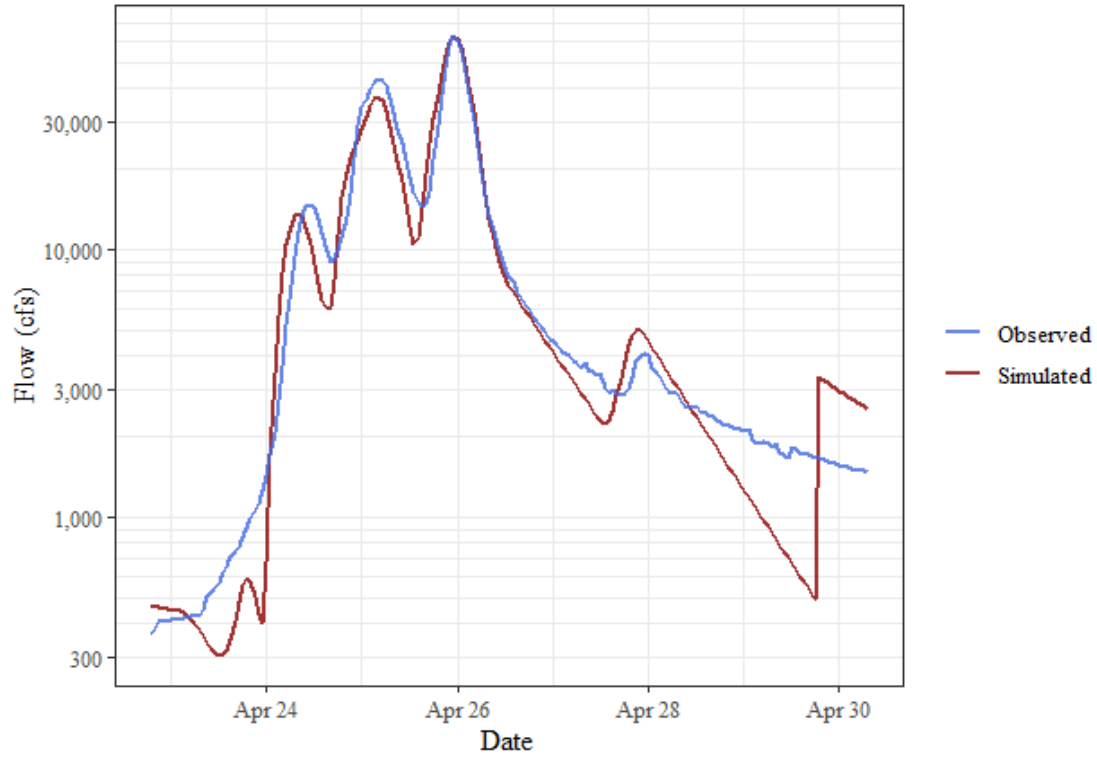
Baron Fork at Eldon, OK, Time Series Comparison

Goodness of Fit Table

Time Step	MAE	Normalized RMSE (%)	PBIAS (%)	RSR	NSE	Modified NSE	R^2	Adjusted R^2
Hourly	1,715.94	20.8	-2.9	0.21	0.96	0.82	0.96	0.93
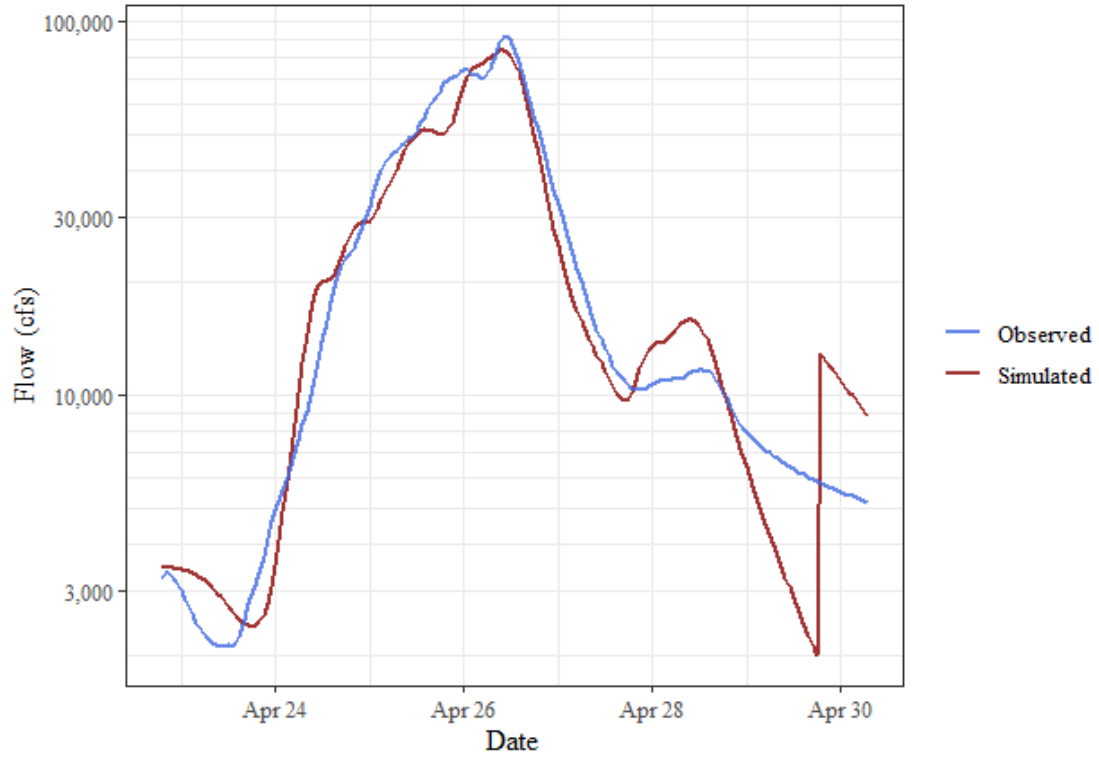
Illinois River at Chewey, OK, Time Series Comparison

Goodness of Fit Table

Time Step	MAE	Normalized RMSE (%)	PBIAS (%)	RSR	NSE	Modified NSE	R^2	Adjusted R^2
Hourly	3,677.71	19.8	-4.4	0.2	0.96	0.82	0.97	0.9
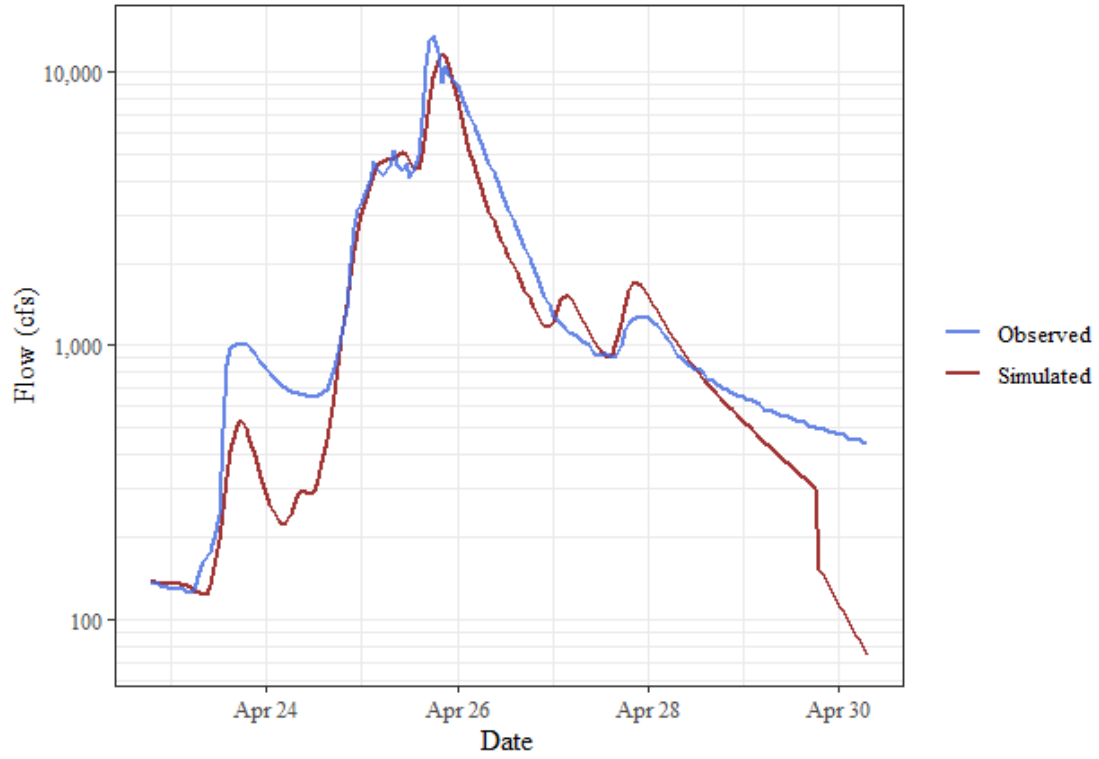
Flint Creek near Kansas, OK, Time Series Comparison

Goodness of Fit Table

Time Step	MAE	Normalized RMSE (%)	PBIAS (%)	RSR	NSE	Modified NSE	R^2	Adjusted R^2
Hourly	443.22	31	-14.7	0.31	0.9	0.76	0.92	0.79

Flint Creek near West Siloam Springs, OK, Time Series Comparison
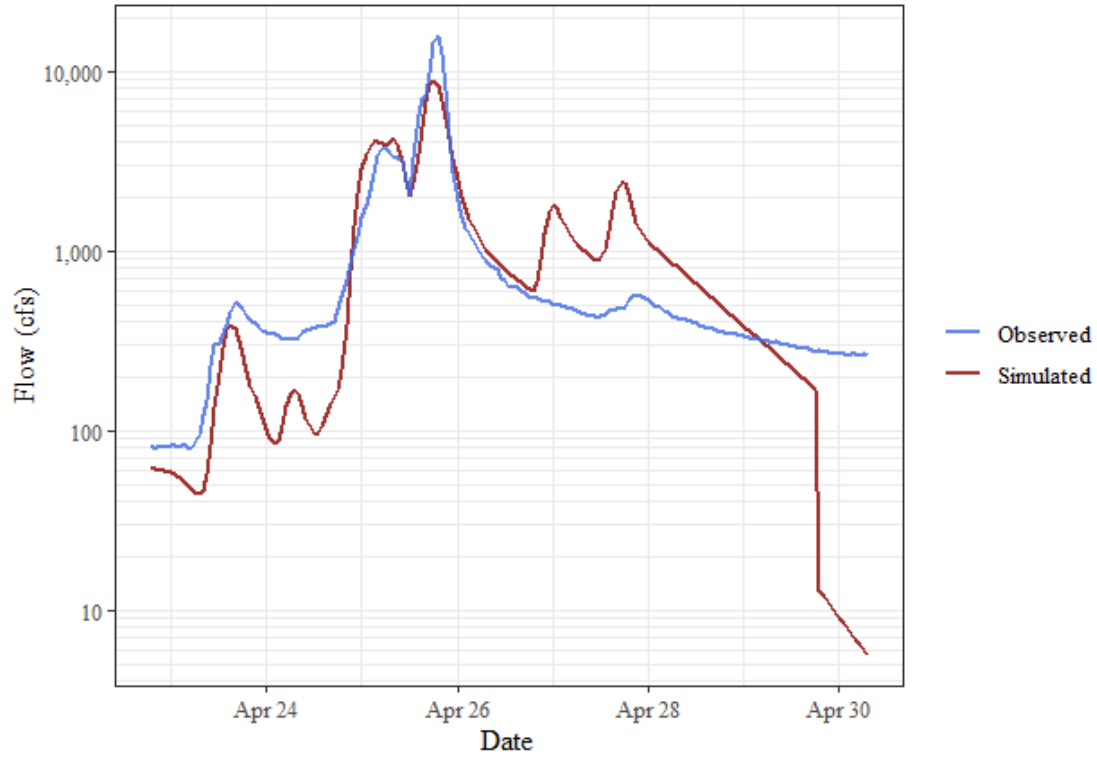
Goodness of Fit Table

Time Step	MAE	Normalized RMSE (%)	PBIAS (%)	RSR	NSE	Modified NSE	R^2	Adjusted R^2
Hourly	477.22	45.3	3	0.45	0.79	0.58	0.83	0.61
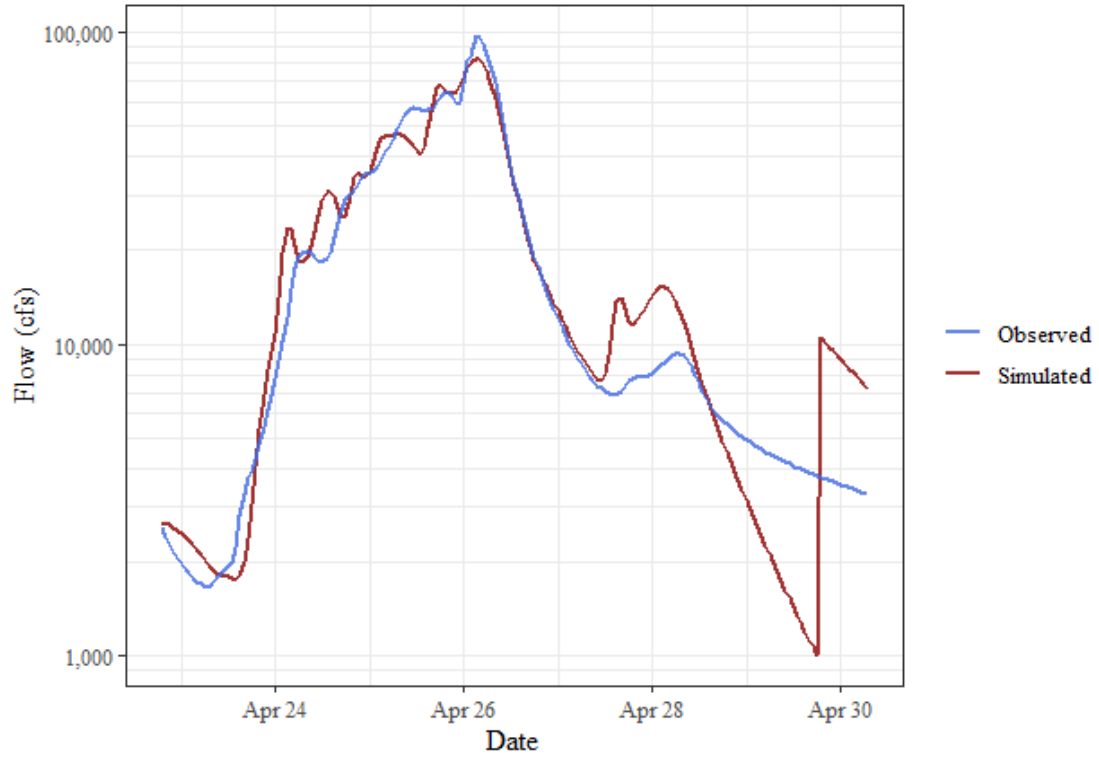
Illinois River near Watts, OK, Time Series Comparison

Goodness of Fit Table

Time Step	MAE	Normalized RMSE (%)	PBIAS (%)	RSR	NSE	Modified NSE	R^2	Adjusted R^2
Hourly	3,364.7	21.3	3.1	0.21	0.95	0.81	0.96	0.92

Illinois River South of Siloam Springs, AR, Time Series Comparison
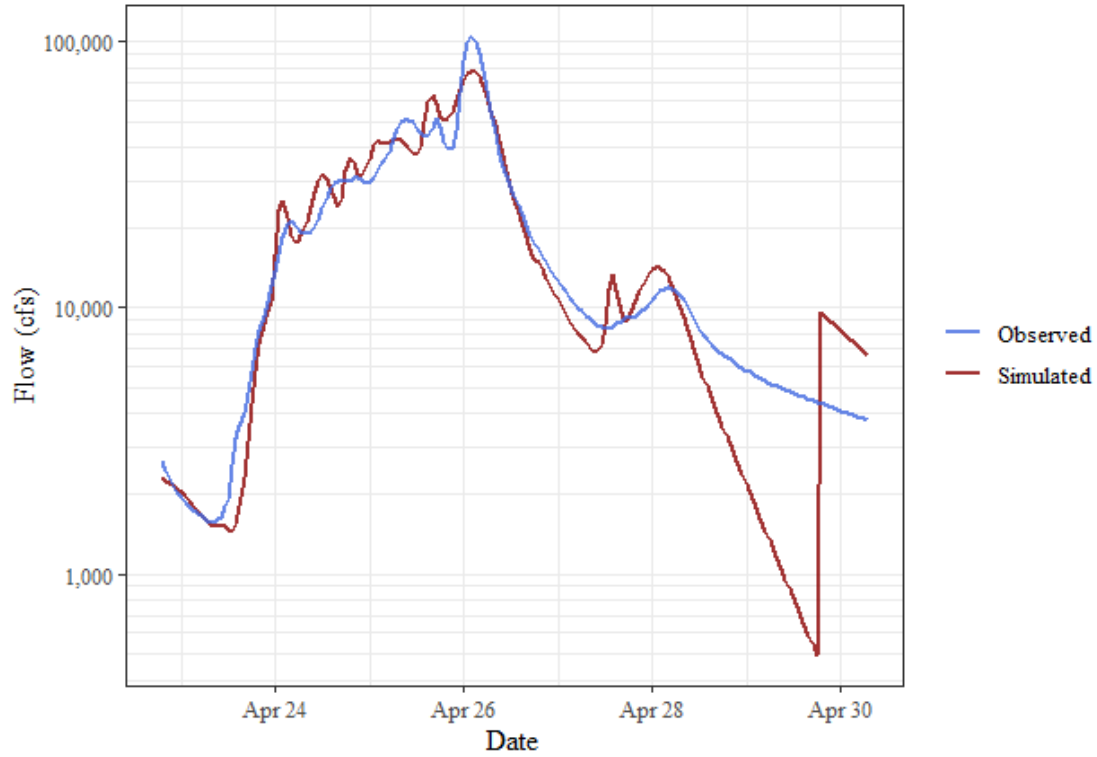
Goodness of Fit Table

Time Step	MAE	Normalized RMSE (%)	PBIAS (%)	RSR	NSE	Modified NSE	R^2	Adjusted R^2
Hourly	3,767.48	27.6	-1.9	0.28	0.92	0.75	0.92	0.87

Illinois River at Hwy. 16 near Siloam Springs, AR, Time Series Comparison
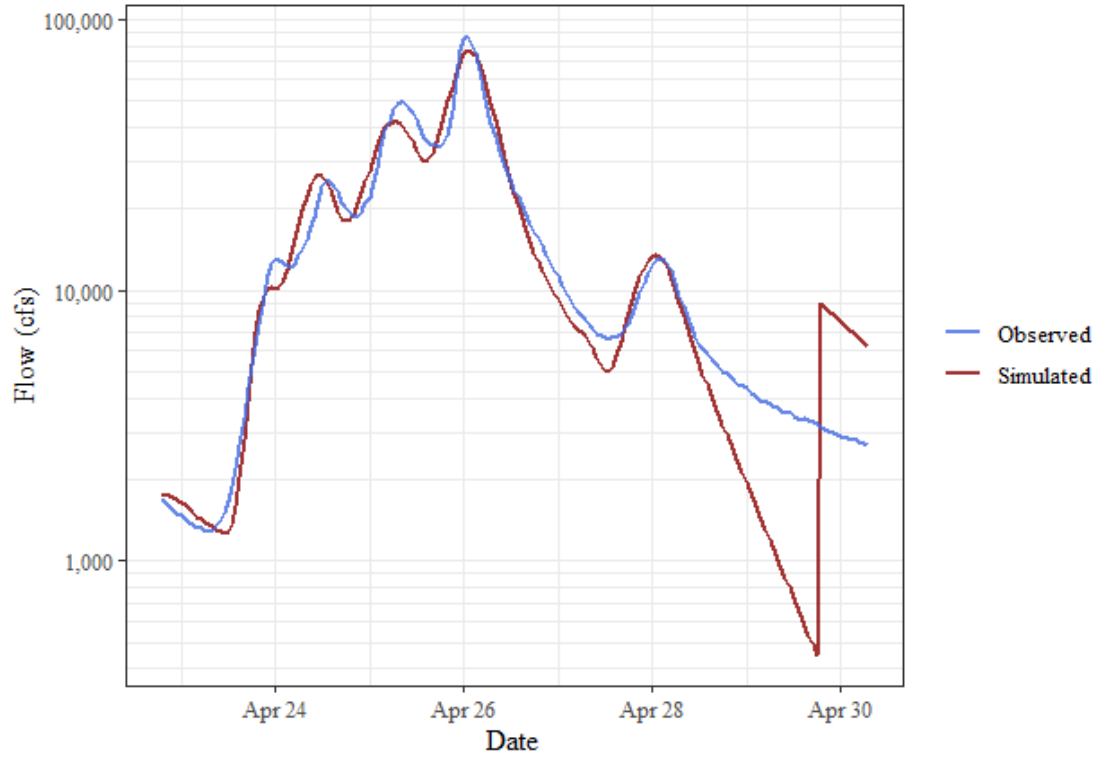
Goodness of Fit Table

Time Step	MAE	Normalized RMSE (%)	PBIAS (%)	RSR	NSE	Modified NSE	R^2	Adjusted R^2
Hourly	2,761.3	21.4	-1.4	0.21	0.95	0.79	0.95	0.93
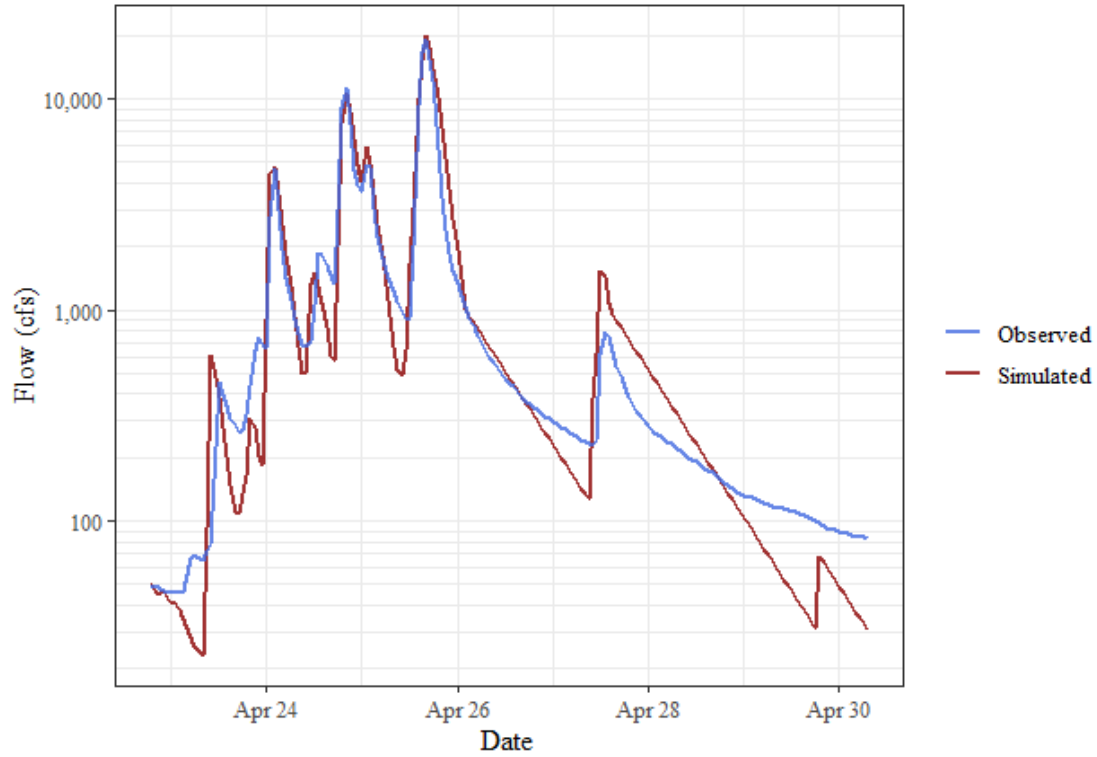
Baron Fork at Dutch Mills, AR, Time Series Comparison

Goodness of Fit Table

Time Step	MAE	Normalized RMSE (%)	PBIAS (%)	RSR	NSE	Modified NSE	R^2	Adjusted R^2
Hourly	327.04	24.6	11.3	0.25	0.94	0.77	0.95	0.89
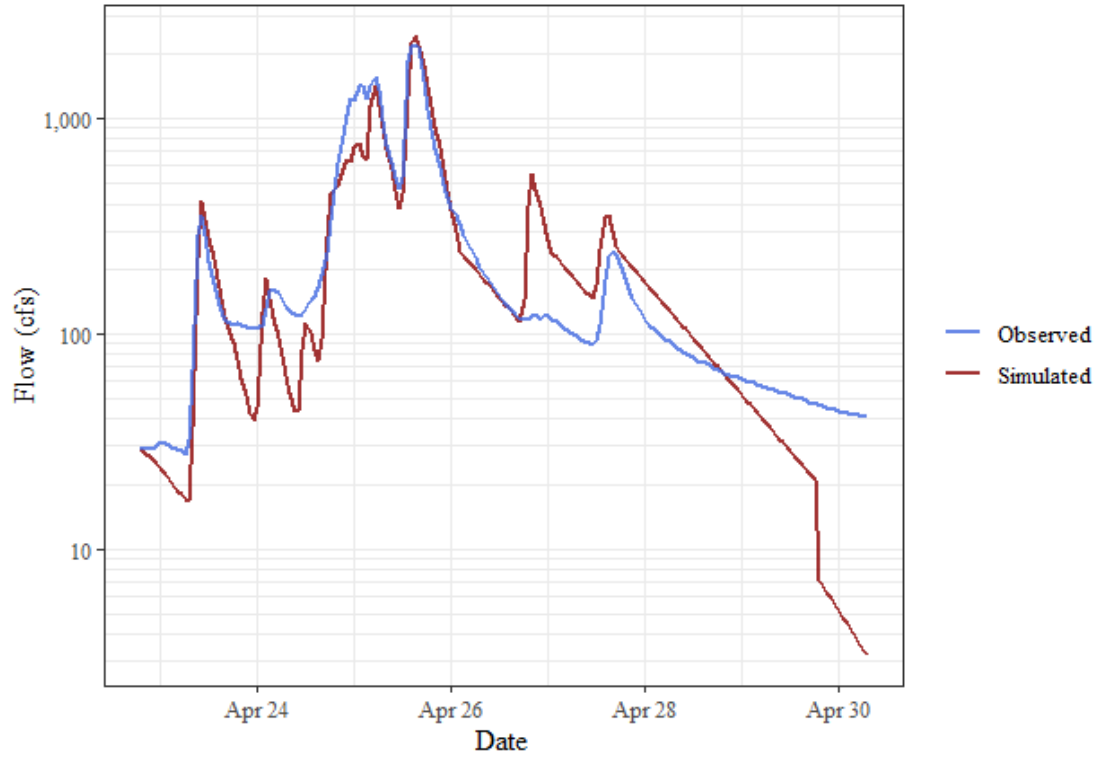
Flint Creek at Springtown, AR, Time Series Comparison

Goodness of Fit Table

Time Step	MAE	Normalized RMSE (%)	PBIAS (%)	RSR	NSE	Modified NSE	R^2	Adjusted R^2
Hourly	78.75	34.7	-4	0.35	0.88	0.71	0.88	0.79
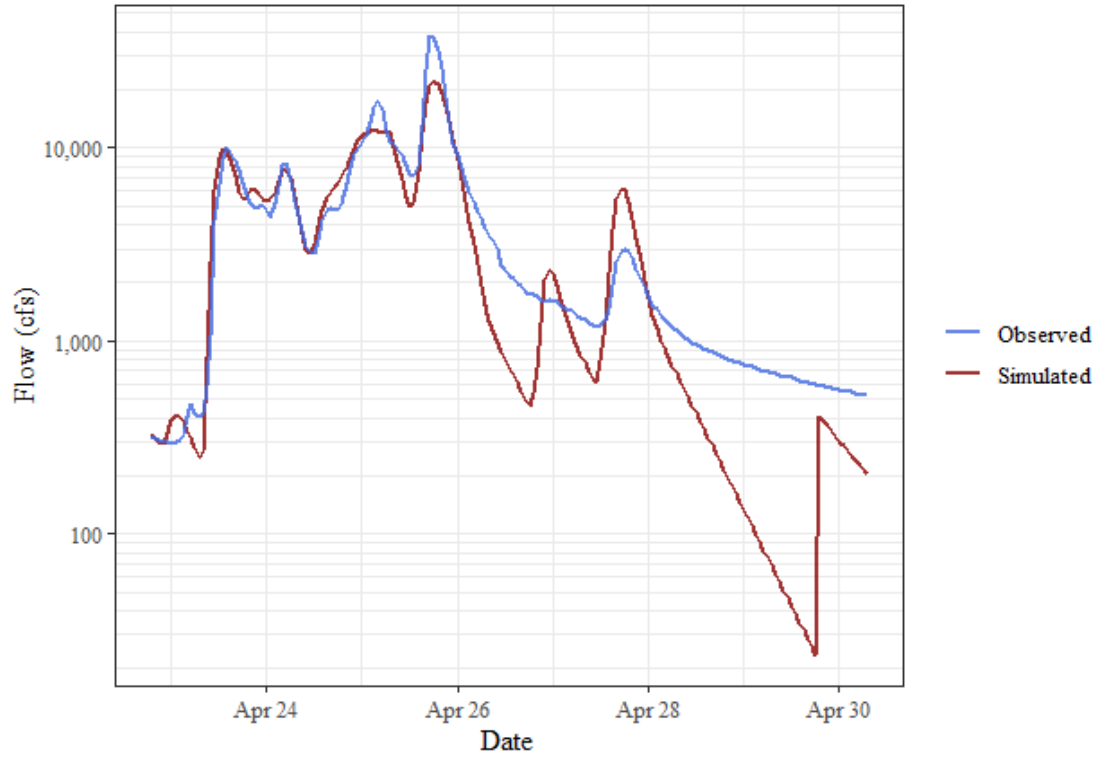
Osage Creek near Elm Springs, AR, Time Series Comparison

Goodness of Fit Table

Time Step	MAE	Normalized RMSE (%)	PBIAS (%)	RSR	NSE	Modified NSE	R^2	Adjusted R^2
Hourly	1,142.38	38.4	-14.1	0.38	0.85	0.71	0.89	0.69

December 2015 Calibration Event

Illinois River near Tahlequah, OK, Time Series Comparison
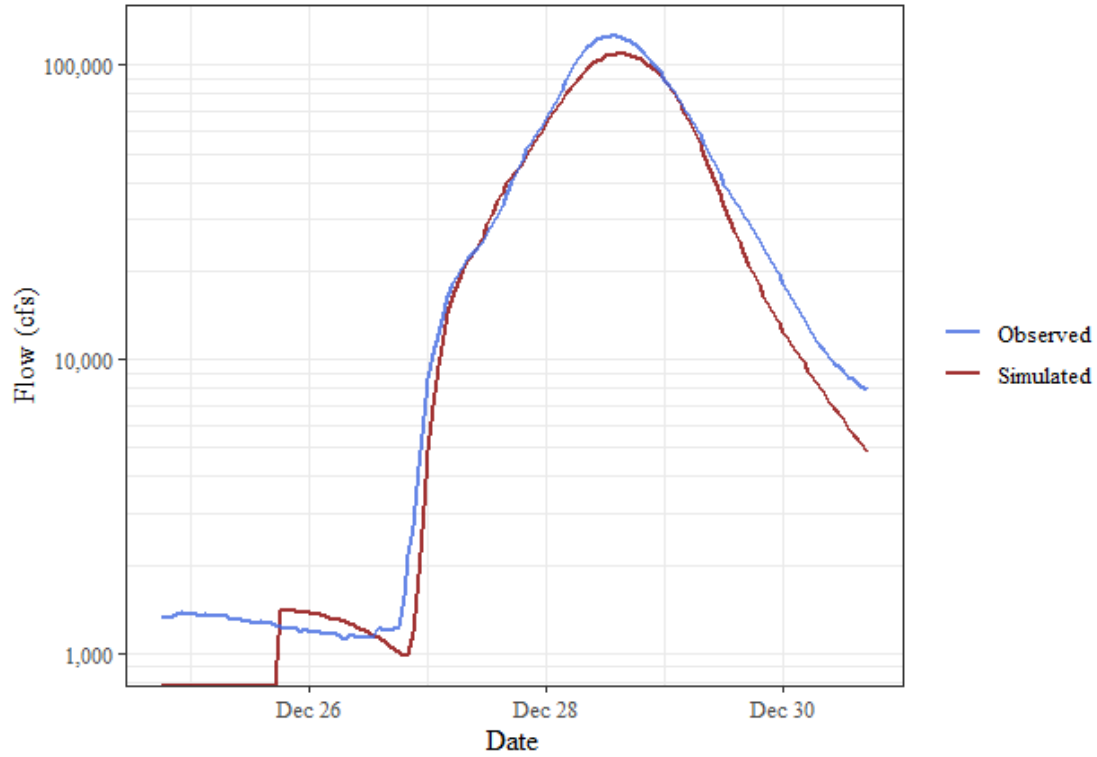
Goodness of Fit Table

Time Step	MAE	Normalized RMSE (%)	PBIAS (%)	RSR	NSE	Modified NSE	R^2	Adjusted R^2
Hourly	3,819.69	15.1	-10.8	0.15	0.98	0.88	0.99	0.9
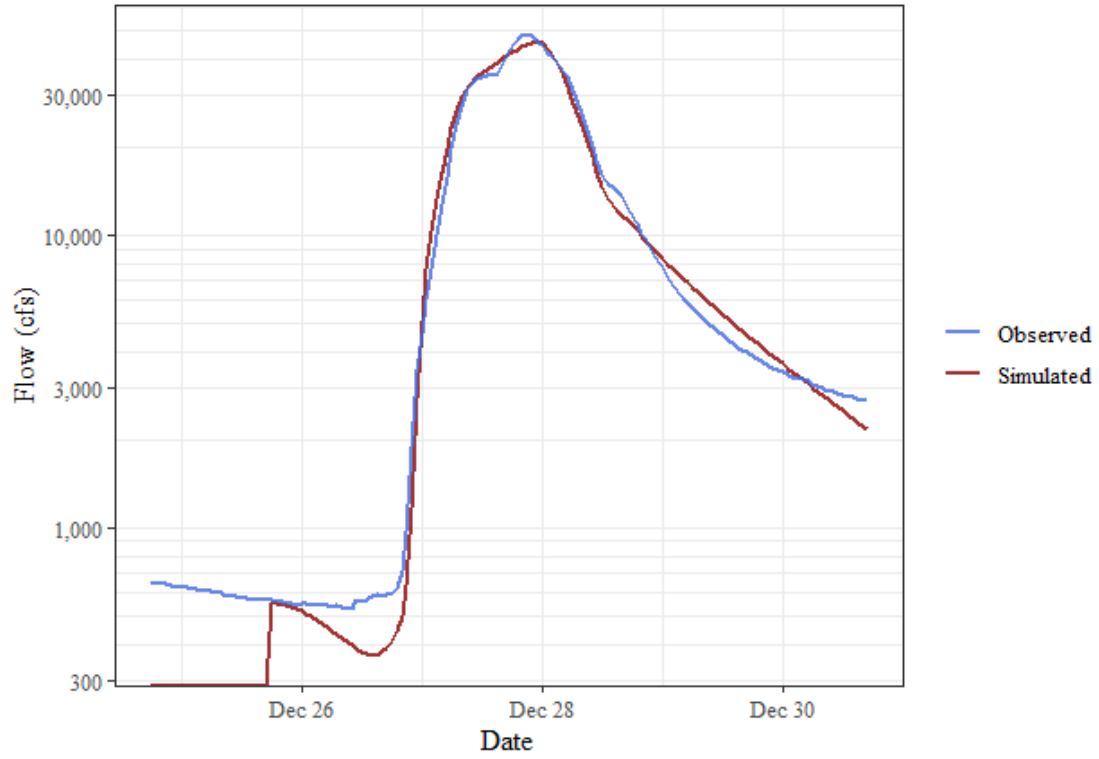
Baron Fork at Eldon, OK, Time Series Comparison

Goodness of Fit Table

Time Step	MAE	Normalized RMSE (%)	PBIAS (%)	RSR	NSE	Modified NSE	R^2	Adjusted R^2
Hourly	872.42	9.1	-0.6	0.09	0.99	0.92	0.99	0.98
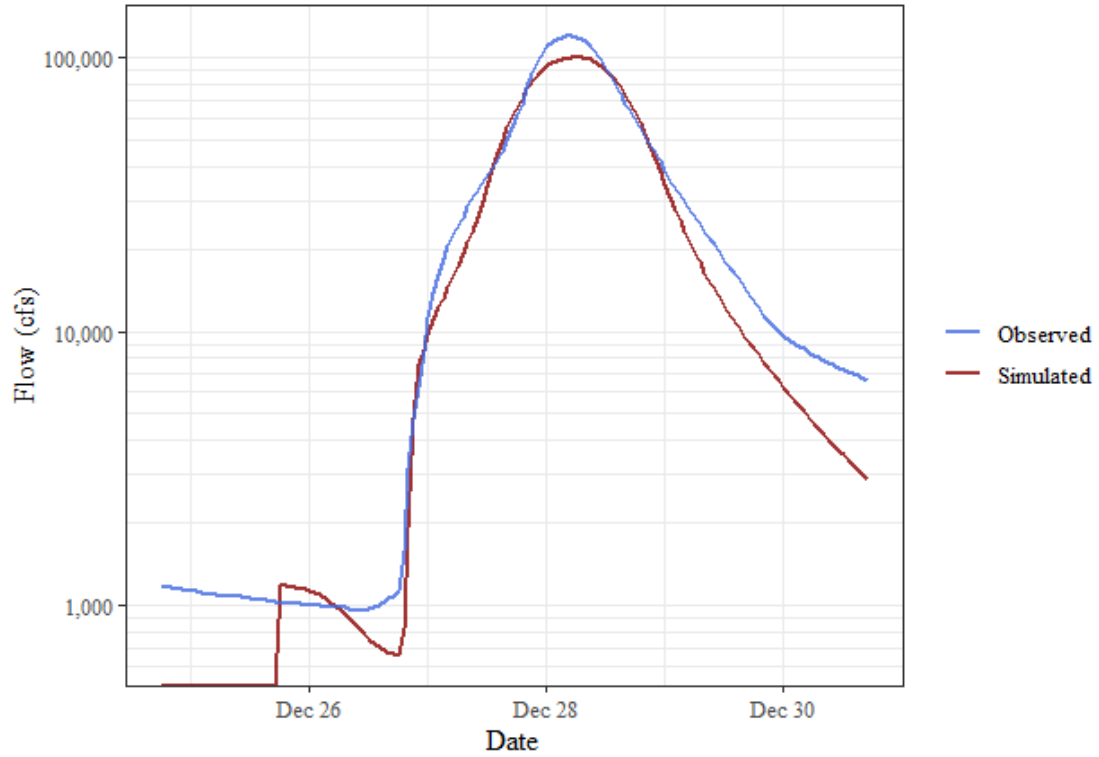
Illinois River at Chewey, OK, Time Series Comparison

Goodness of Fit Table

Time Step	MAE	Normalized RMSE (%)	PBIAS (%)	RSR	NSE	Modified NSE	R^2	Adjusted R^2
Hourly	3,978.45	17.2	-12.2	0.17	0.97	0.85	0.98	0.89
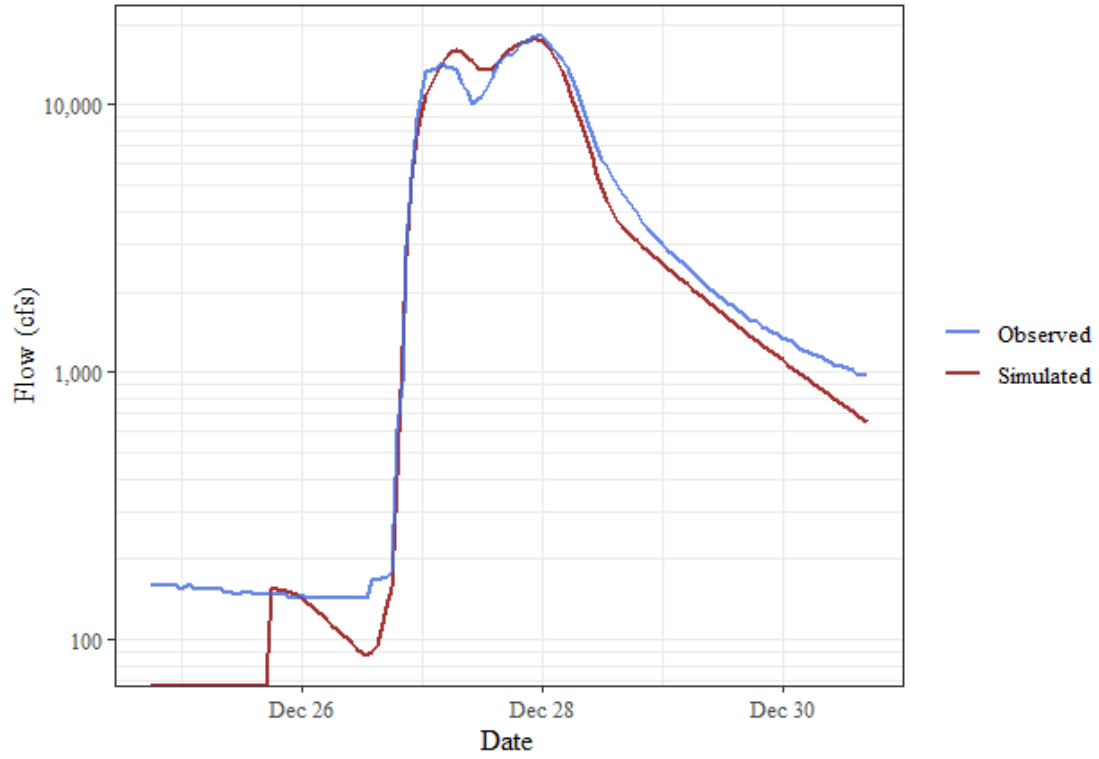
Flint Creek near Kansas, OK, Time Series Comparison

Goodness of Fit Table

Time Step	MAE	Normalized RMSE (%)	PBIAS (%)	RSR	NSE	Modified NSE	R^2	Adjusted R^2
Hourly	567.7	17.3	-3.7	0.17	0.97	0.88	0.97	0.97

Flint Creek near West Siloam Springs, OK, Time Series Comparison
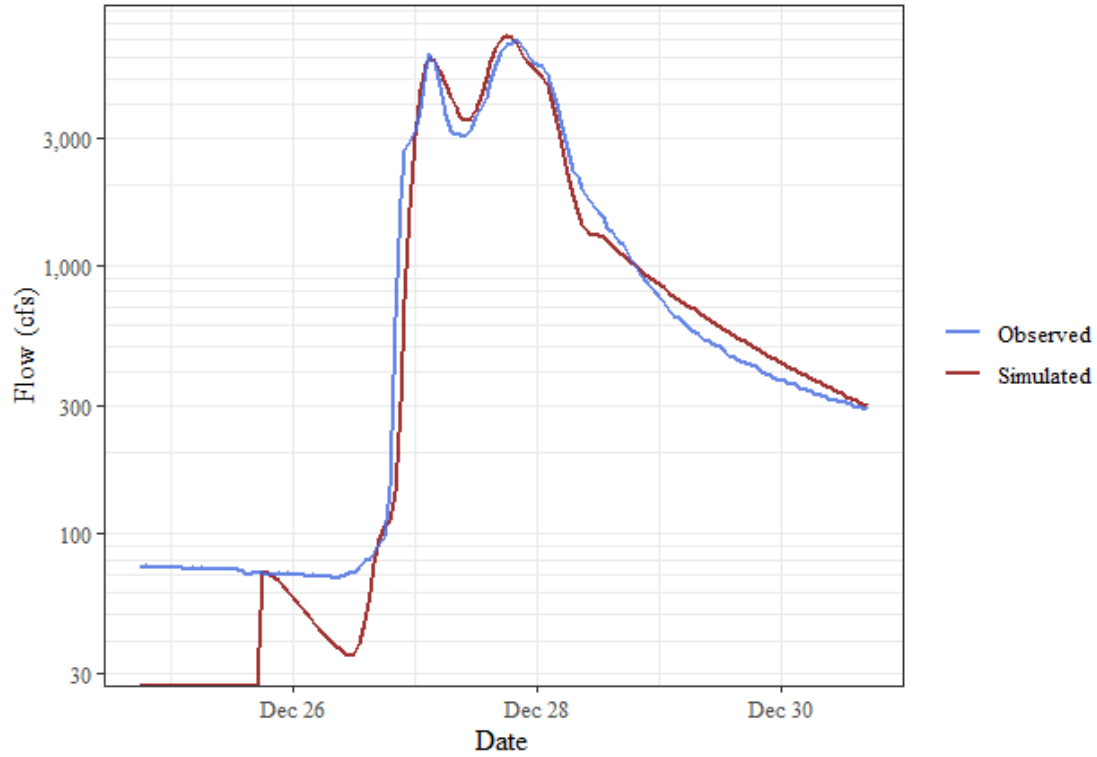
Goodness of Fit Table

Time Step	MAE	Normalized RMSE (%)	PBIAS (%)	RSR	NSE	Modified NSE	R^2	Adjusted R^2
Hourly	209.23	19.2	-1.1	0.19	0.96	0.86	0.97	0.96
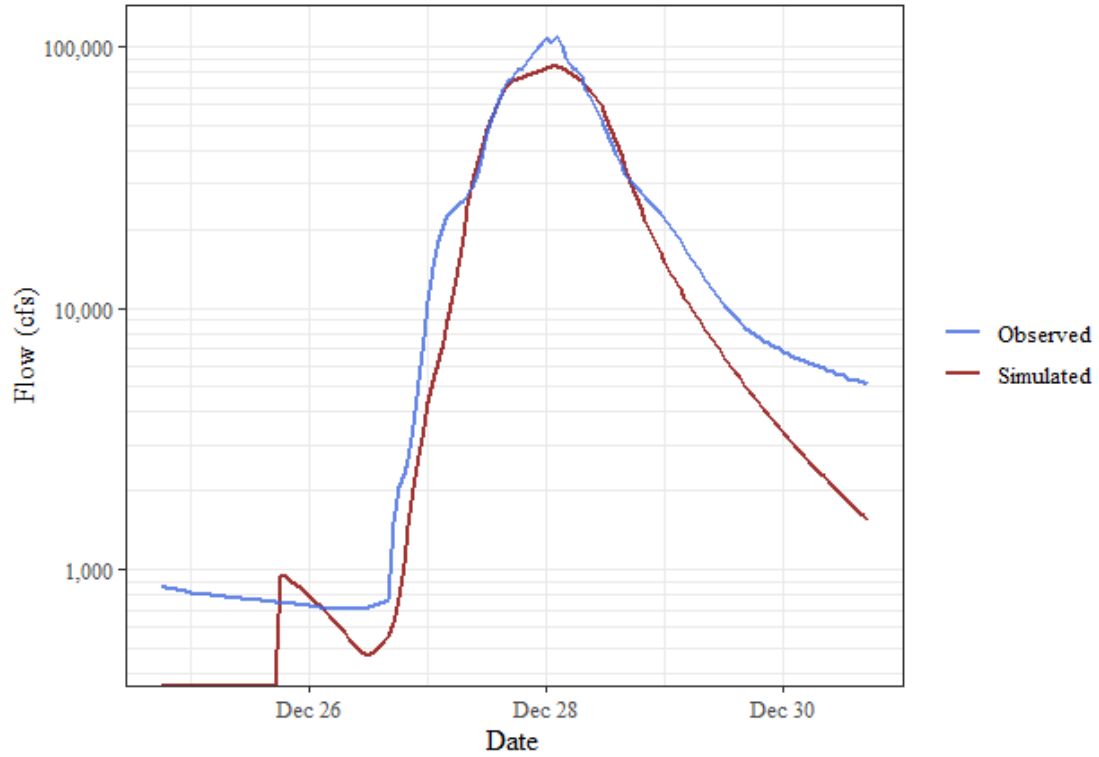
Illinois River near Watts, OK, Time Series Comparison

Goodness of Fit Table

Time Step	MAE	Normalized RMSE (%)	PBIAS (%)	RSR	NSE	Modified NSE	R^2	Adjusted R^2
Hourly	3,924.02	21	-15.2	0.21	0.96	0.82	0.97	0.86

Illinois River South of Siloam Springs, AR, Time Series Comparison
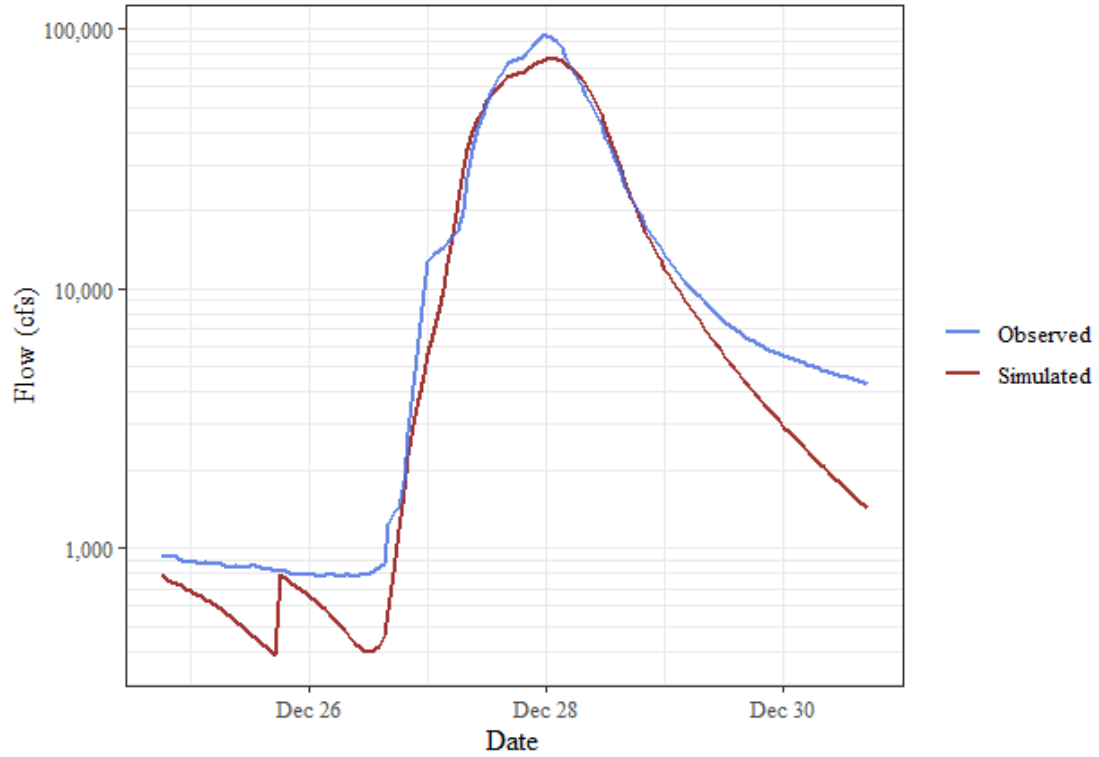
Goodness of Fit Table

Time Step	MAE	Normalized RMSE (%)	PBIAS (%)	RSR	NSE	Modified NSE	R^2	Adjusted R^2
Hourly	2,707.87	17	-9.6	0.17	0.97	0.86	0.98	0.89

Illinois River at Hwy. 16 near Siloam Springs, AR, Time Series Comparison
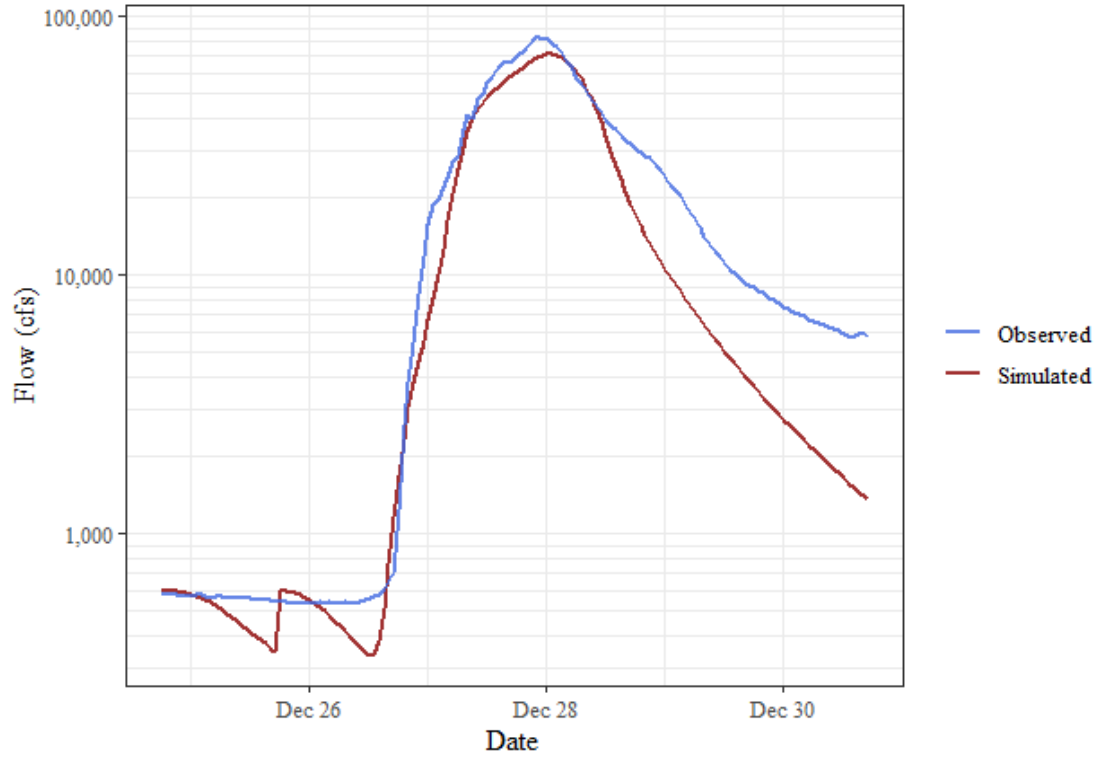
Goodness of Fit Table

Time Step	MAE	Normalized RMSE (%)	PBIAS (%)	RSR	NSE	Modified NSE	R^2	Adjusted R^2
Hourly	4,535.26	26.4	-22.5	0.26	0.93	0.77	0.97	0.83
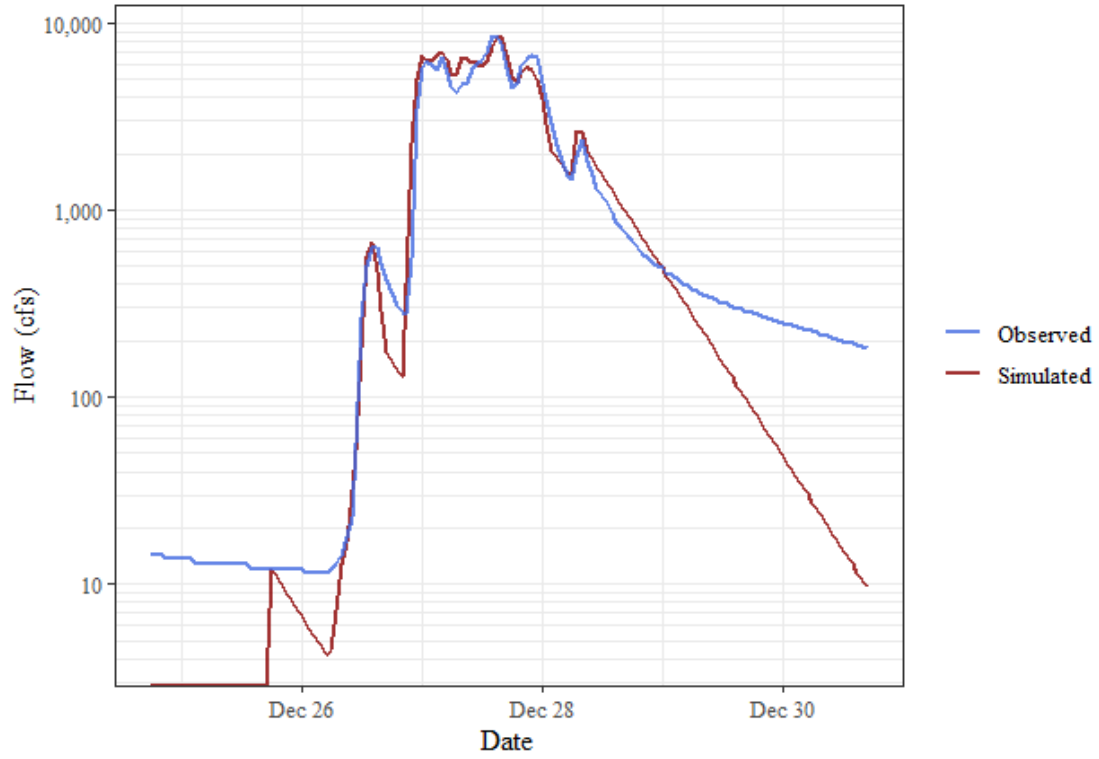
Baron Fork at Dutch Mills, AR, Time Series Comparison

Goodness of Fit Table

Time Step	MAE	Normalized RMSE (%)	PBIAS (%)	RSR	NSE	Modified NSE	R^2	Adjusted R^2
Hourly	257.81	20.4	1.3	0.2	0.96	0.85	0.96	0.94
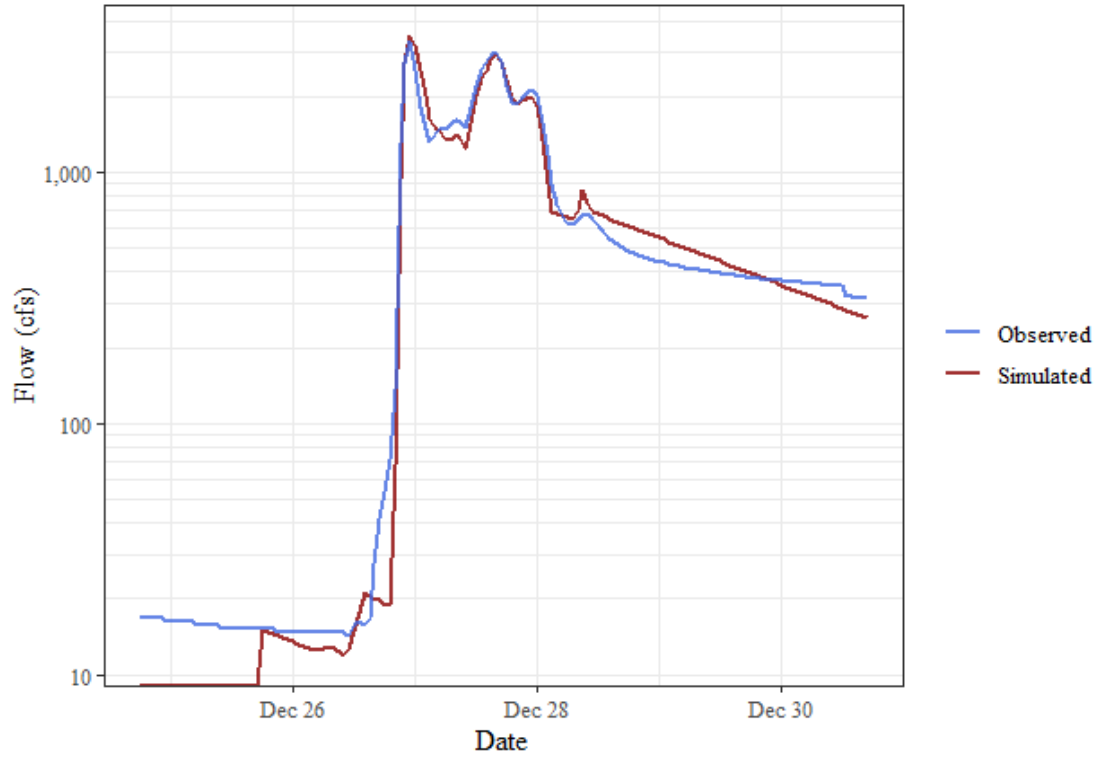
Flint Creek at Springtown, AR, Time Series Comparison

Goodness of Fit Table

Time Step	MAE	Normalized RMSE (%)	PBIAS (%)	RSR	NSE	Modified NSE	R^2	Adjusted R^2
Hourly	73.19	16.7	0.6	0.17	0.97	0.87	0.97	0.97
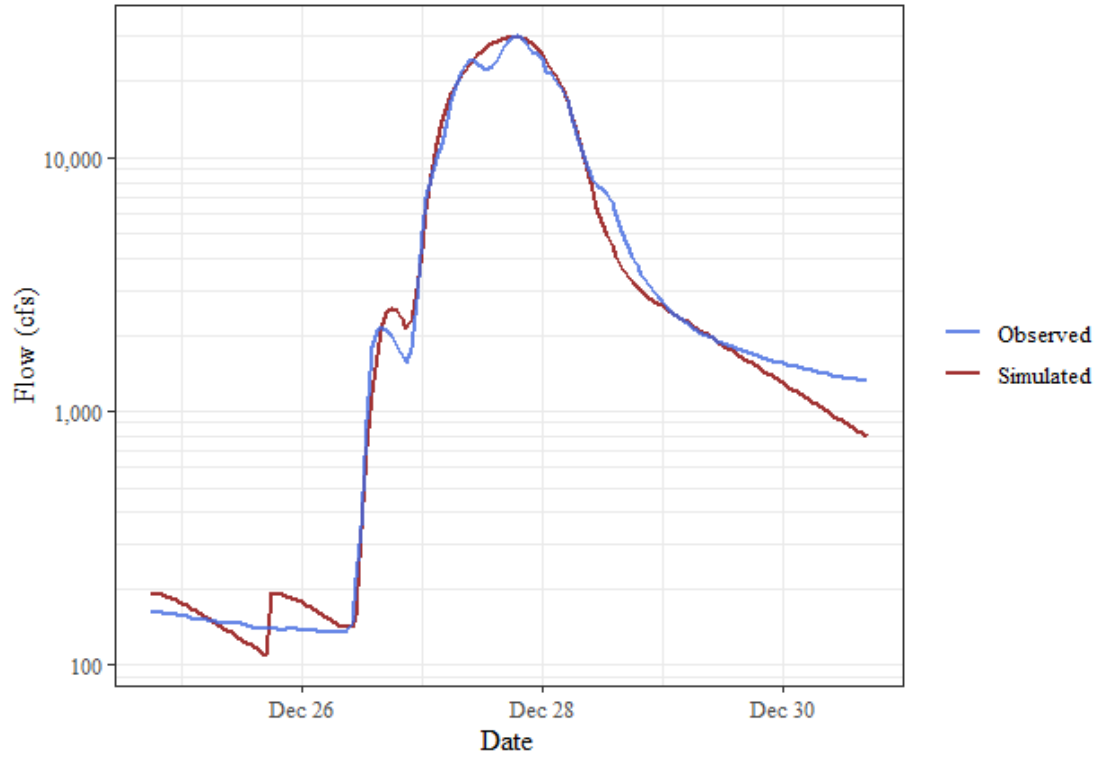
Illinois River at Savoy, AR, Time Series Comparison

Goodness of Fit Table

Time Step	MAE	Normalized RMSE (%)	PBIAS (%)	RSR	NSE	Modified NSE	R^2	Adjusted R^2
Hourly	534.21	12.3	2	0.12	0.98	0.92	0.99	0.94
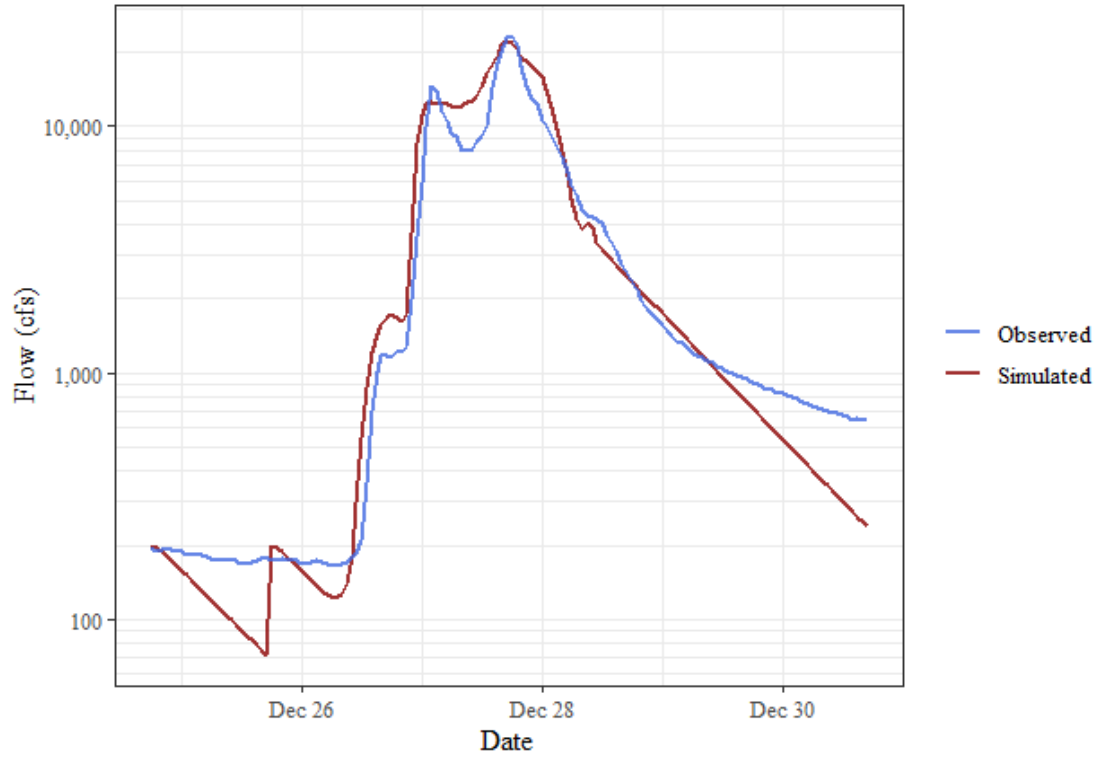
Osage Creek near Elm Springs, AR, Time Series Comparison

Goodness of Fit Table

Time Step	MAE	Normalized RMSE (%)	PBIAS (%)	RSR	NSE	Modified NSE	R^2	Adjusted R^2
Hourly	813.76	31.5	14.2	0.31	0.9	0.79	0.94	0.84
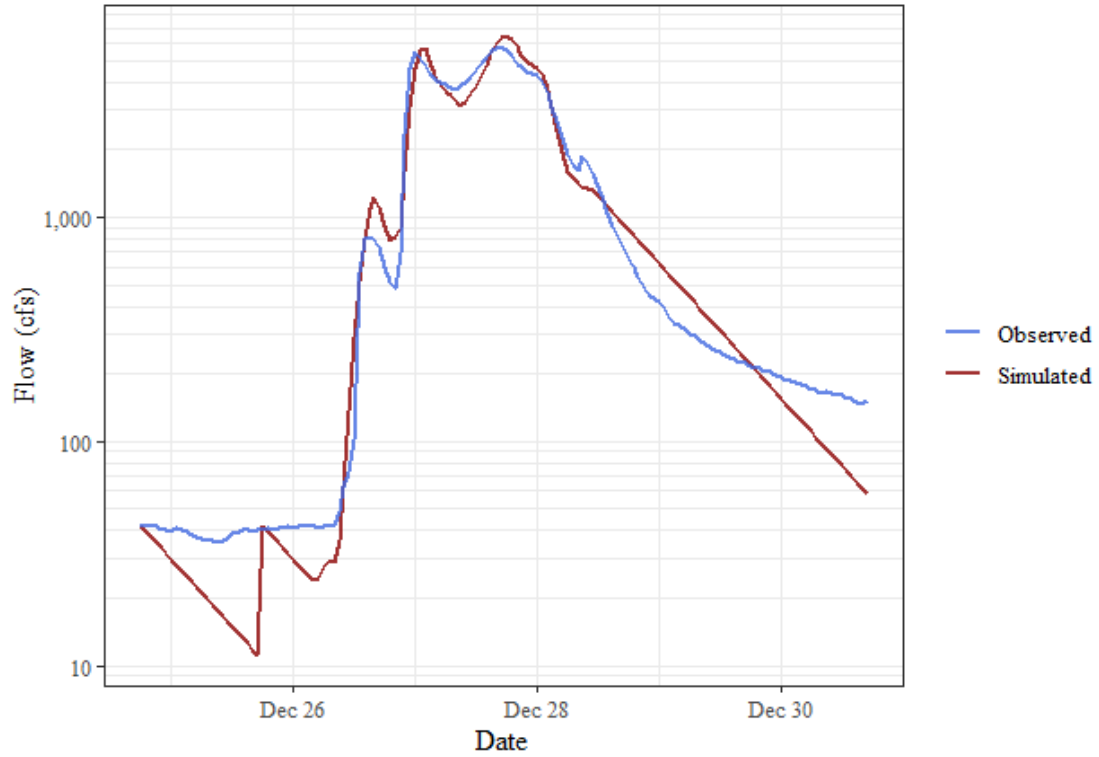
Osage Creek near Cave Springs, AR, Time Series Comparison

Goodness of Fit Table

Time Step	MAE	Normalized RMSE (%)	PBIAS (%)	RSR	NSE	Modified NSE	R^2	Adjusted R^2
Hourly	187.7	17.9	1.2	0.18	0.97	0.87	0.97	0.96

February 2018 Calibration Event

Illinois River near Tahlequah, OK, Time Series Comparison
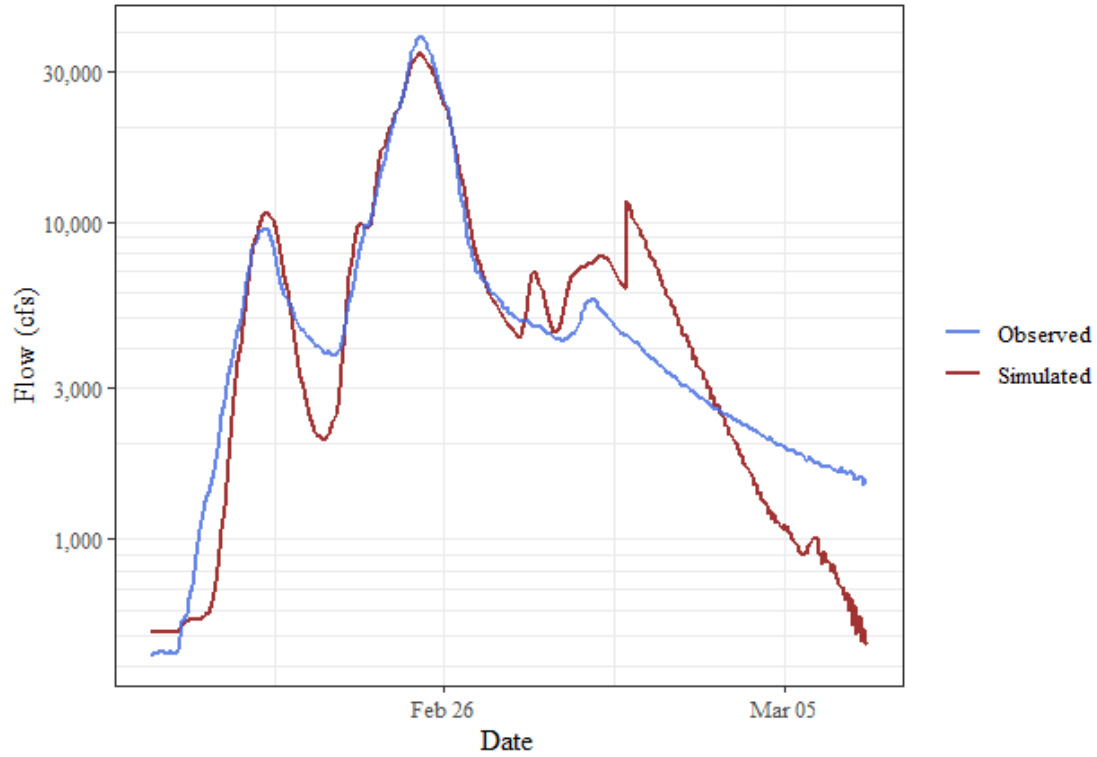
Goodness of Fit Table

Time Step	MAE	Normalized RMSE (%)	PBIAS (%)	RSR	NSE	Modified NSE	R^2	Adjusted R^2
Hourly	1,287.35	22.7	4	0.23	0.95	0.74	0.95	0.93
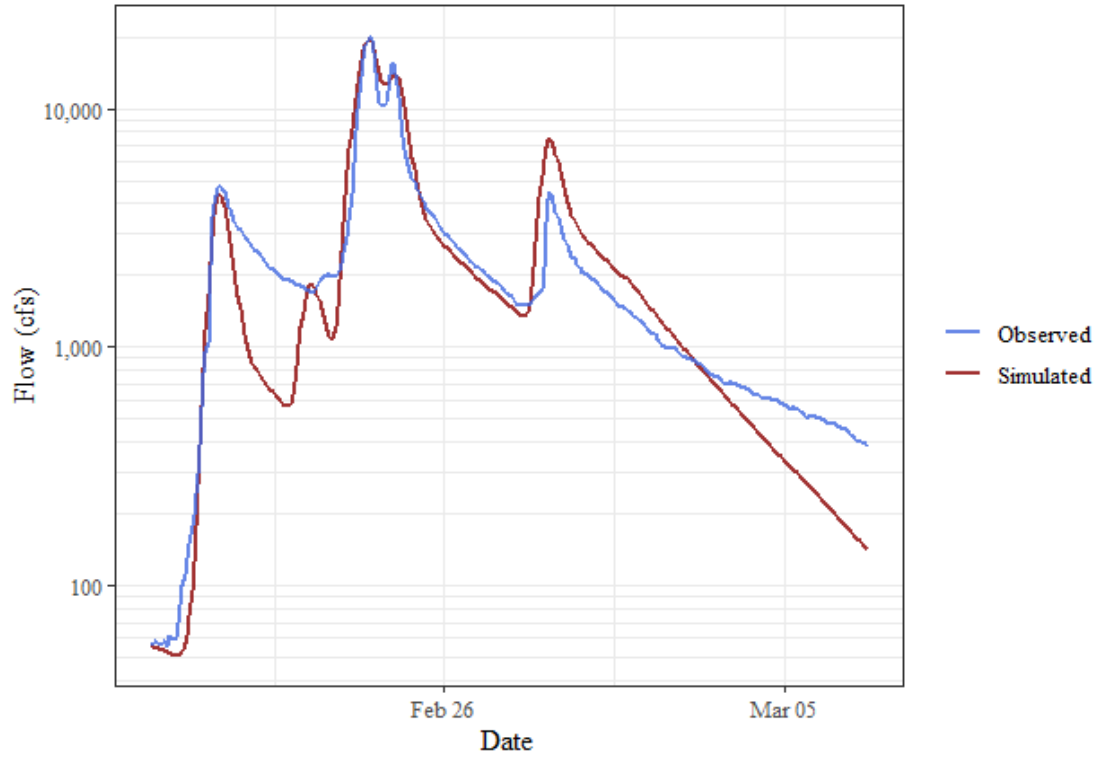
Baron Fork at Eldon, OK, Time Series Comparison

Goodness of Fit Table

Time Step	MAE	Normalized RMSE (%)	PBIAS (%)	RSR	NSE	Modified NSE	R^2	Adjusted R^2
Hourly	683.67	33.1	4.6	0.33	0.89	0.65	0.92	0.86
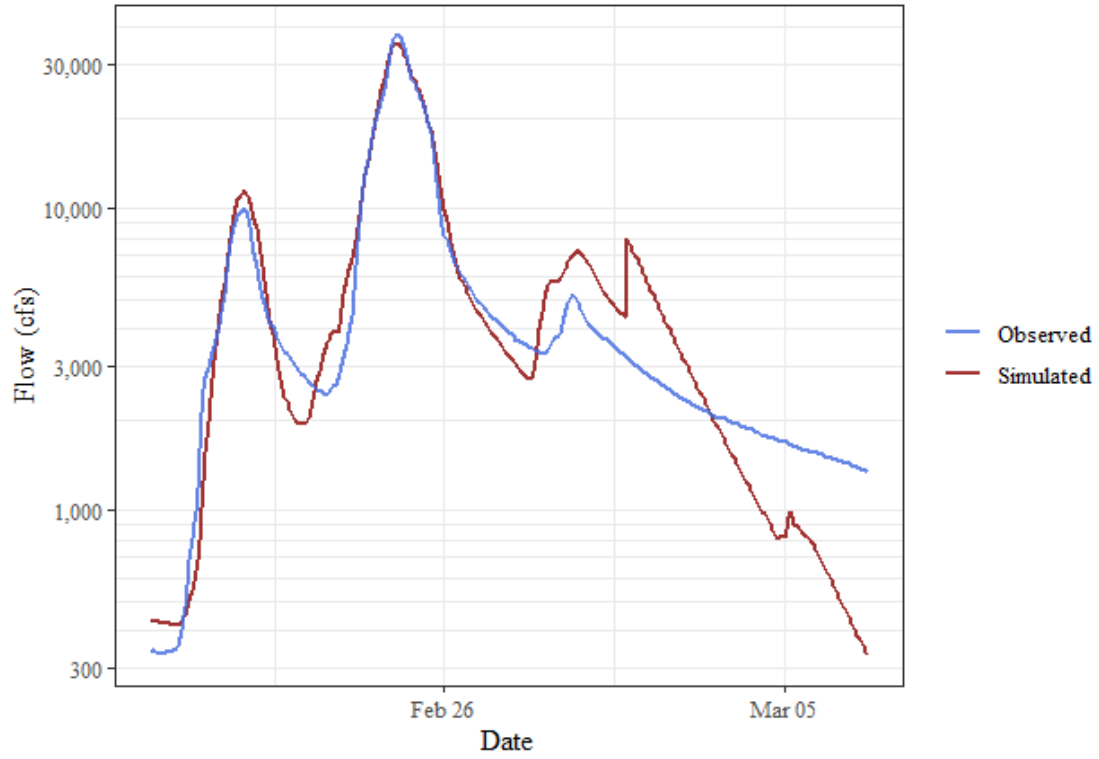
Illinois River at Chewey, OK, Time Series Comparison

Goodness of Fit Table

Time Step	MAE	Normalized RMSE (%)	PBIAS (%)	RSR	NSE	Modified NSE	R^2	Adjusted R^2
Hourly	1,072.23	18.4	6.3	0.18	0.97	0.77	0.97	0.95
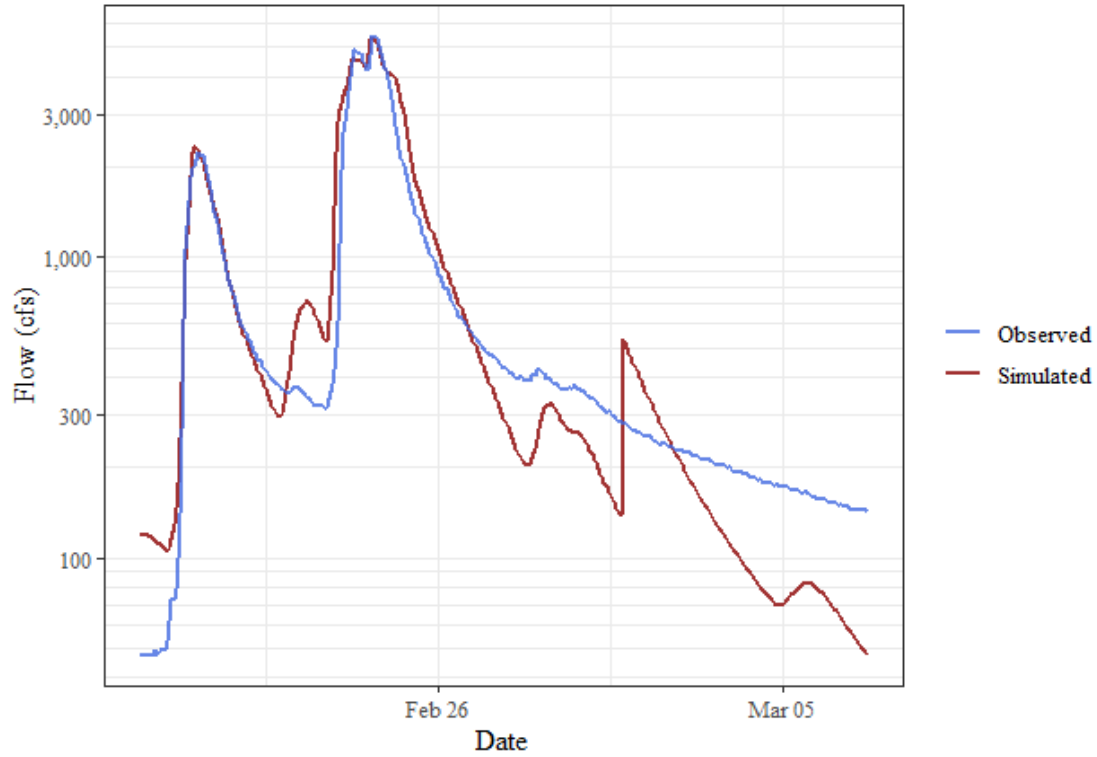
Flint Creek near Kansas, OK, Time Series Comparison

Goodness of Fit Table

| Time Step	MAE	Normalized RMSE (%)	PBIAS (%)	RSR	NSE	Modified NSE	R^2	Adjusted R^2
Hourly	166.26	27.6	6.7	0.28	0.92	0.77	0.94	0.89

Flint Creek near West Siloam Springs, OK, Time Series Comparison
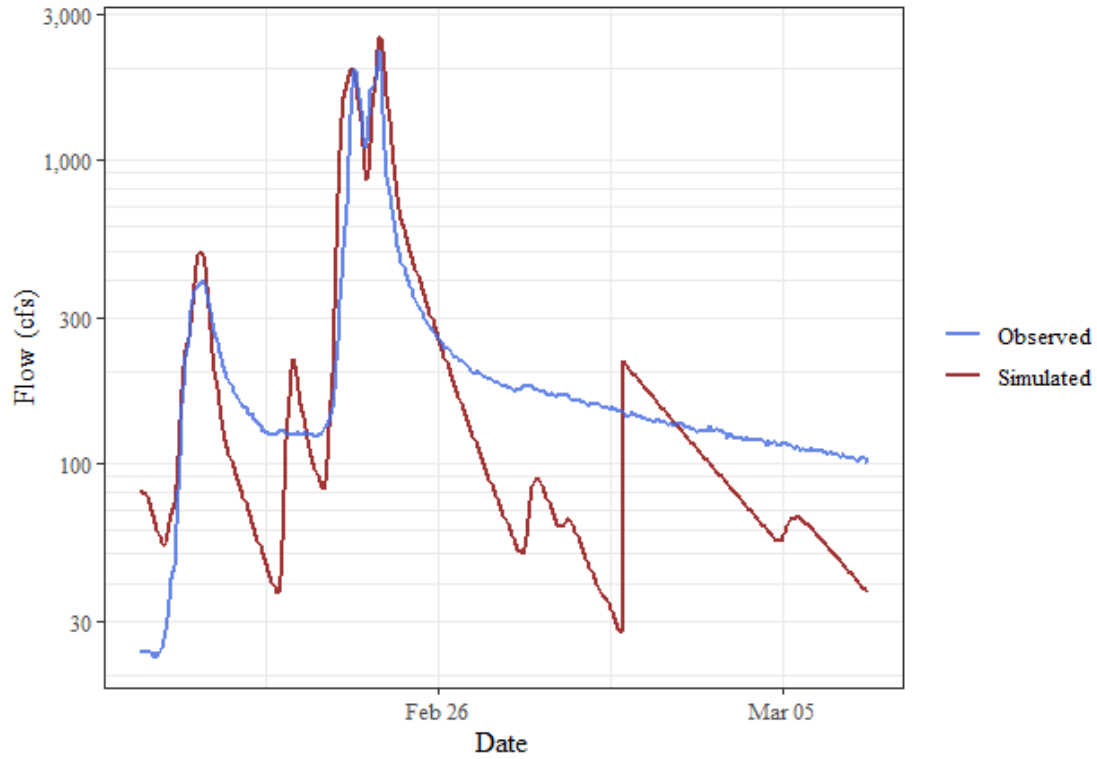
Goodness of Fit Table

Time Step	MAE	Normalized RMSE (%)	PBIAS (%)	RSR	NSE	Modified NSE	R^2	Adjusted R^2
Hourly	96.95	50.8	-2.2	0.51	0.74	0.46	0.85	0.78
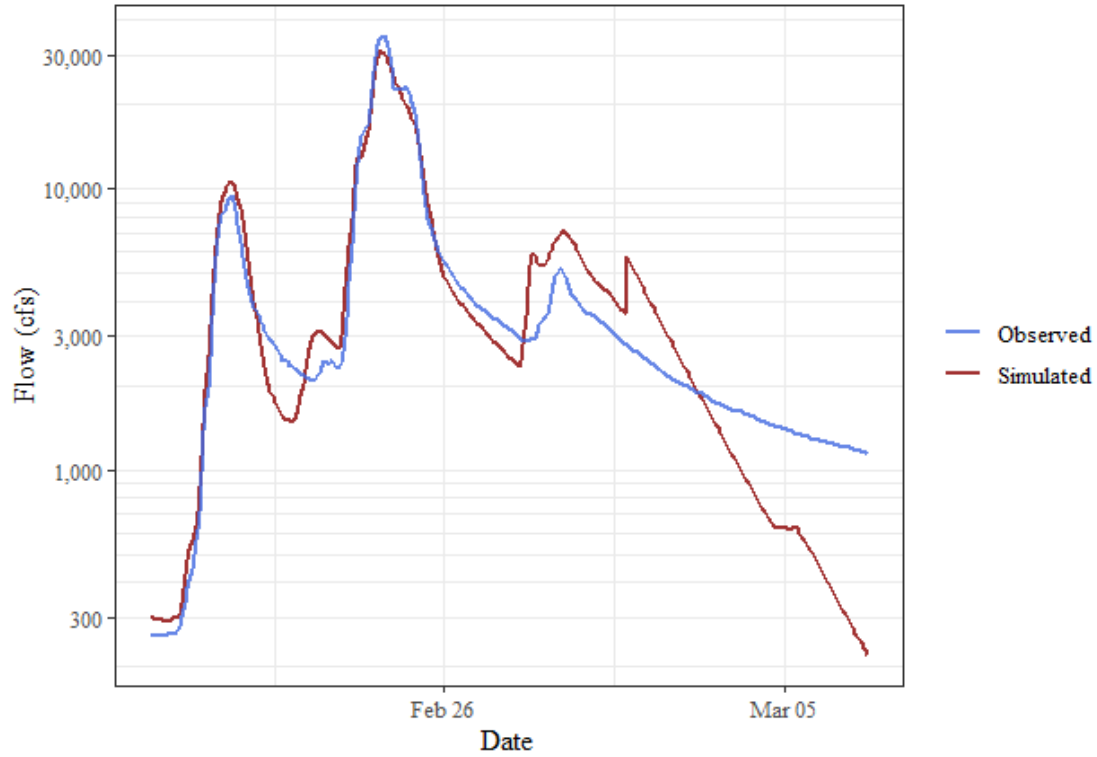
Illinois River near Watts, OK, Time Series Comparison

Goodness of Fit Table

Time Step	MAE	Normalized RMSE (%)	PBIAS (%)	RSR	NSE	Modified NSE	R²	Adjusted R²
Hourly	980.25	19.6	1.5	0.2	0.96	0.74	0.96	0. 92

Illinois River South of Siloam Springs, AR, Time Series Comparison
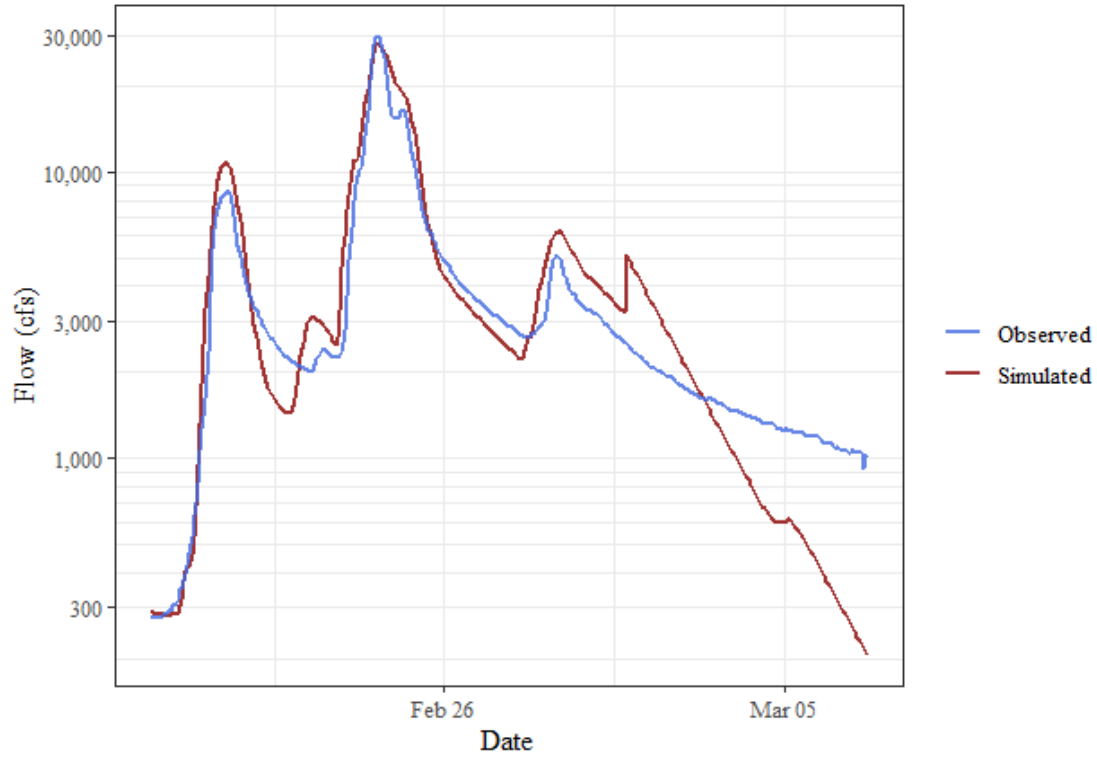
Goodness of Fit Table

Time Step	MAE	Normalized RMSE (%)	PBIAS (%)	RSR	NSE	Modified NSE	R^2	Adjusted R^2
Hourly	1,003.85	28.7	11.2	0.29	0.92	0.66	0.95	0.86

Illinois River at Hwy. 16 near Siloam Springs, AR,Time Series Comparison
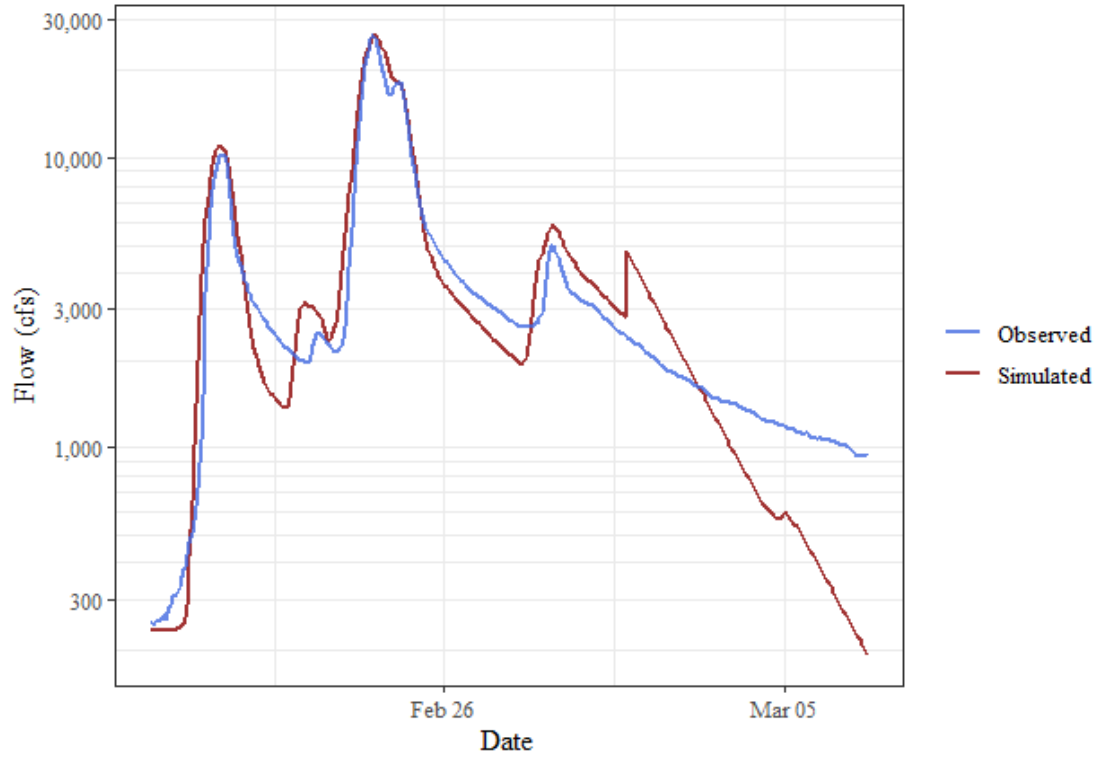
Goodness of Fit Table

Time Step	MAE	Normalized RMSE (%)	PBIAS (%)	RSR	NSE	Modified NSE	R^2	Adjusted R^2
Hourly	833.25	23	6.1	0.23	0.95	0.72	0.96	0.9
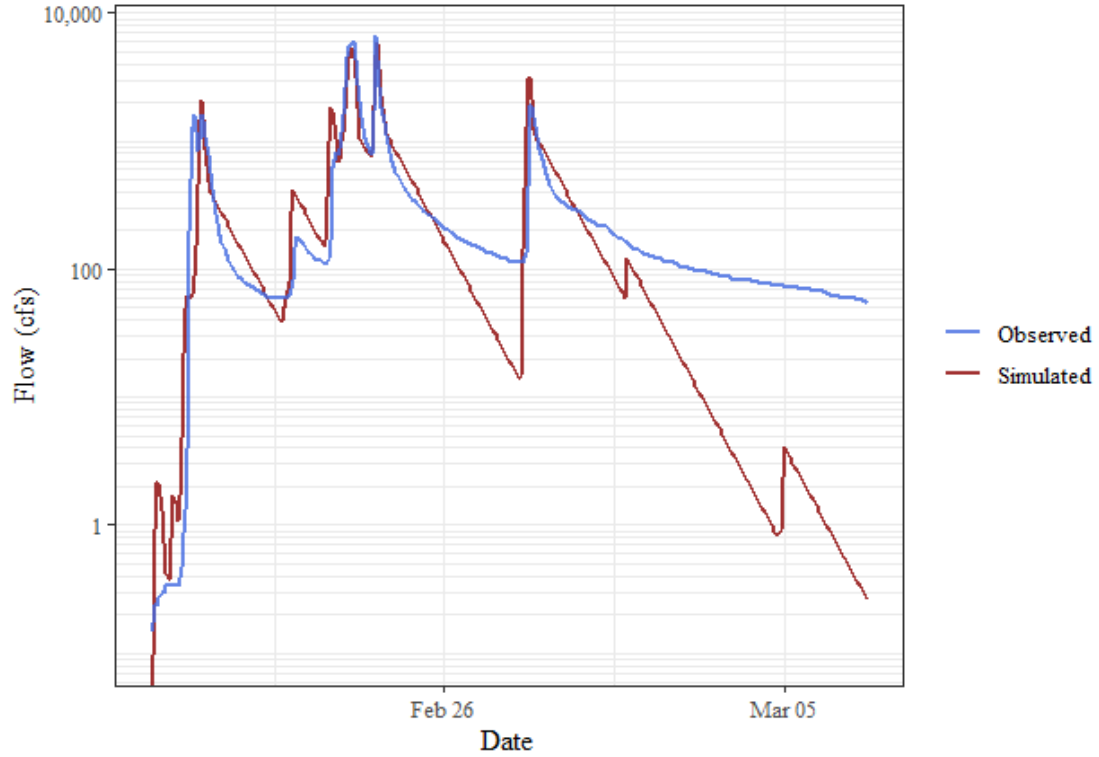
Baron Fork at Dutch Mills, AR, Time Series Comparison

Goodness of Fit Table

| Time Step	MAE	Normalized RMSE (%)	PBIAS (%)	RSR	NSE	Modified NSE	R^2	Adjusted R^2
Hourly	155.74	41.1	-6.5	0.41	0.83	0.62	0.83	0.72
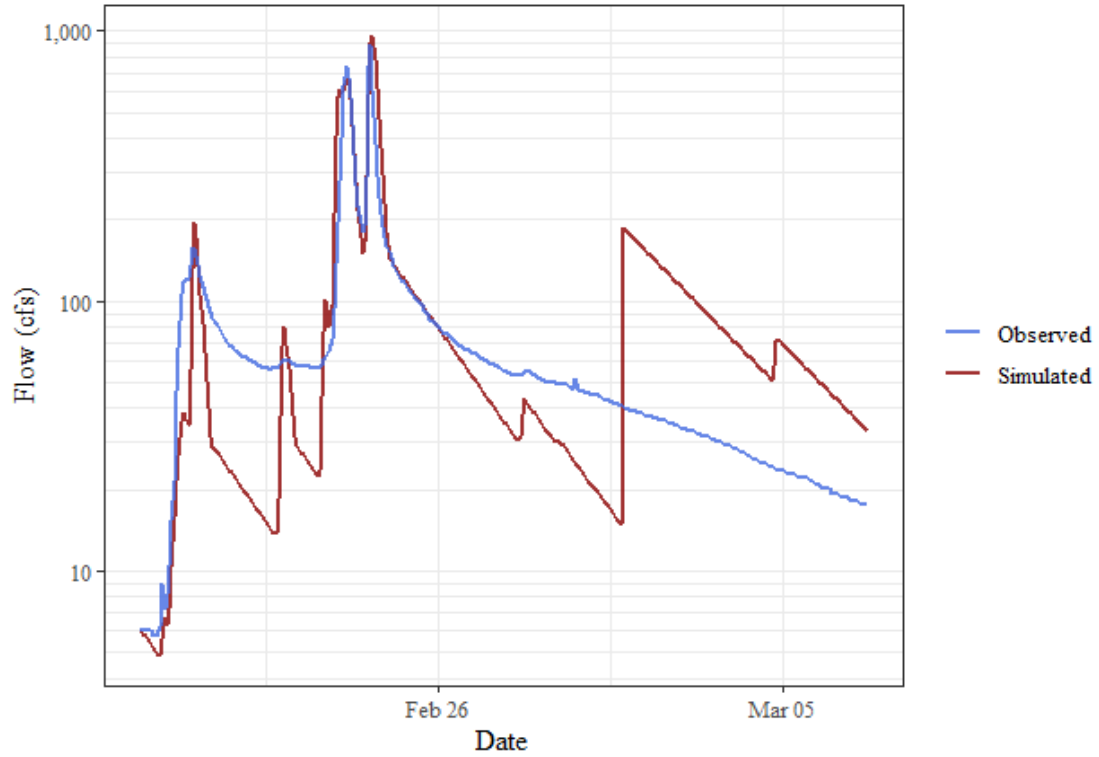
Flint Creek at Springtown, AR, Time Series Comparison

Goodness of Fit Table

Time Step	MAE	Normalized RMSE (%)	PBIAS (%)	RSR	NSE	Modified NSE	R^2	Adjusted R^2
Hourly	41.38	63	20.1	0.63	0.6	0.21	0.75	0.68
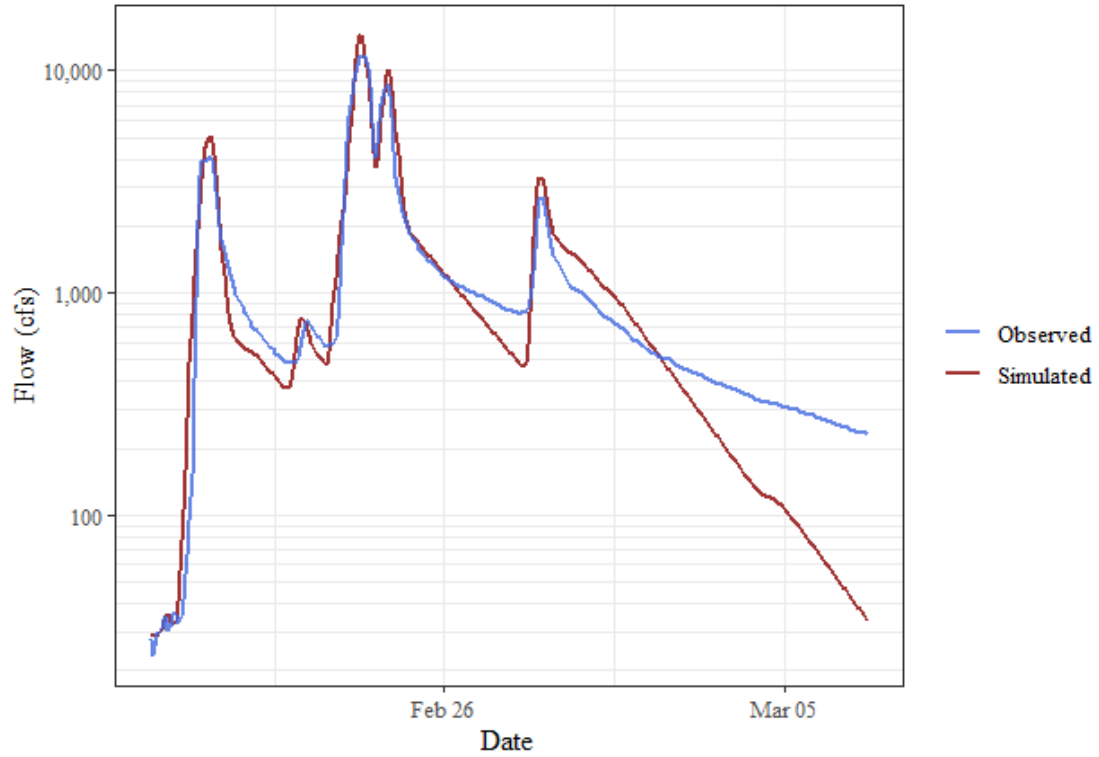
Illinois River at Savoy, AR, Time Series Comparison

Goodness of Fit Table

Time Step	MAE	Normalized RMSE (%)	PBIAS (%)	RSR	NSE	Modified NSE	R^2	Adjusted R^2
Hourly	291.73	24.4	1.9	0.24	0.94	0.75	0.96	0.9
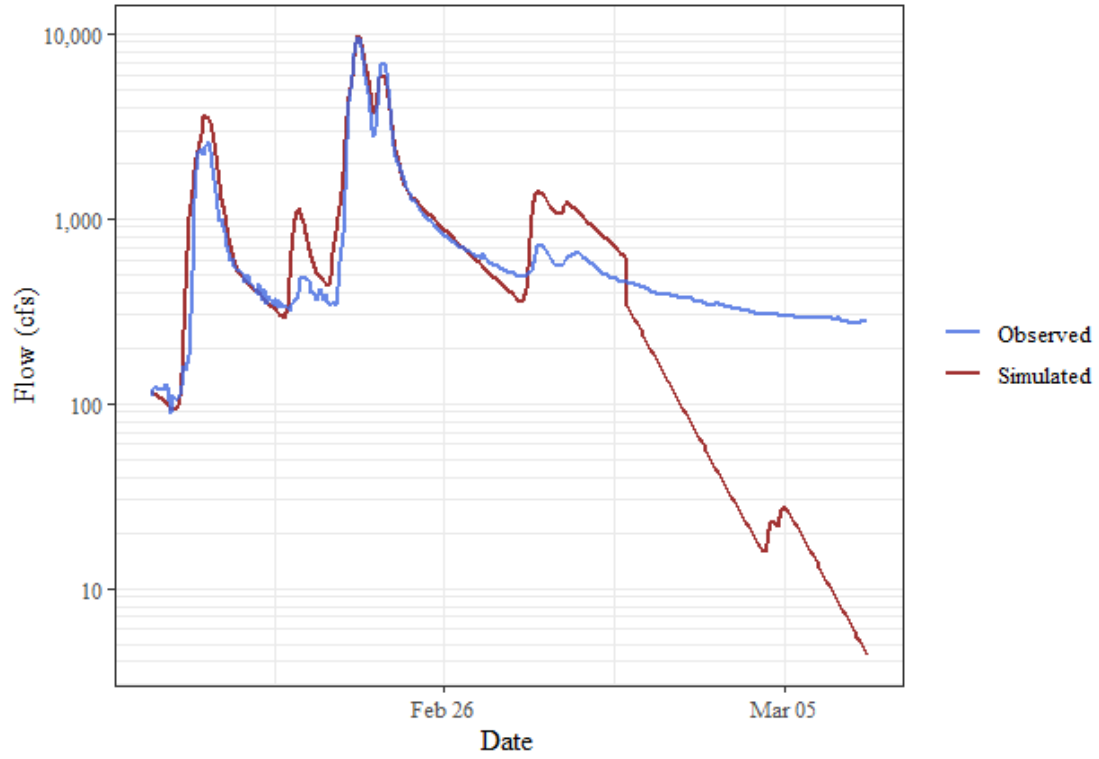
Osage Creek near Elm Springs, AR, Time Series Comparison

Goodness of Fit Table

Time Step	MAE	Normalized RMSE (%)	PBIAS (%)	RSR	NSE	Modified NSE	R^2	Adjusted R^2
Hourly	272.11	26	5.7	0.26	0.93	0.64	0.94	0.9

Osage Creek near Cave Springs, AR, Time Series Comparison
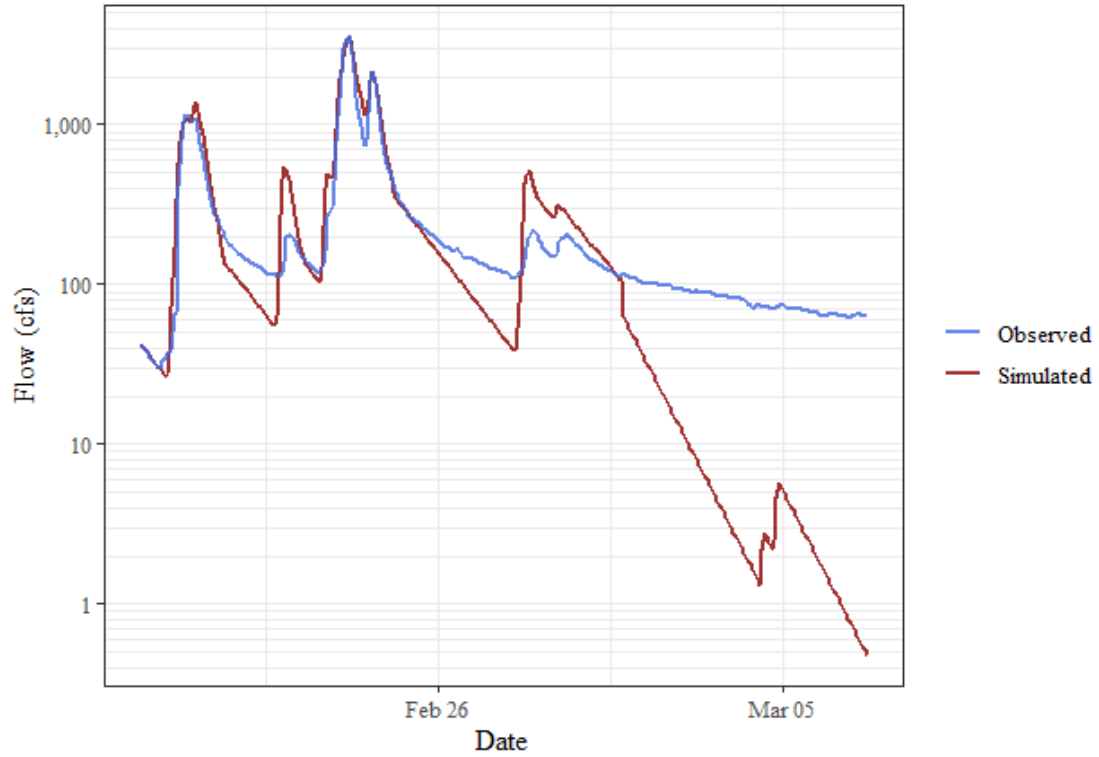
Goodness of Fit Table

Time Step	MAE	Normalized RMSE (%)	PBIAS (%)	RSR	NSE	Modified NSE	R^2	Adjusted R^2
Hourly	83.44	25	2.8	0.25	0.94	0.67	0.96	0.89

March 2008 Validation Event

Illinois River near Tahlequah, OK, Time Series Comparison
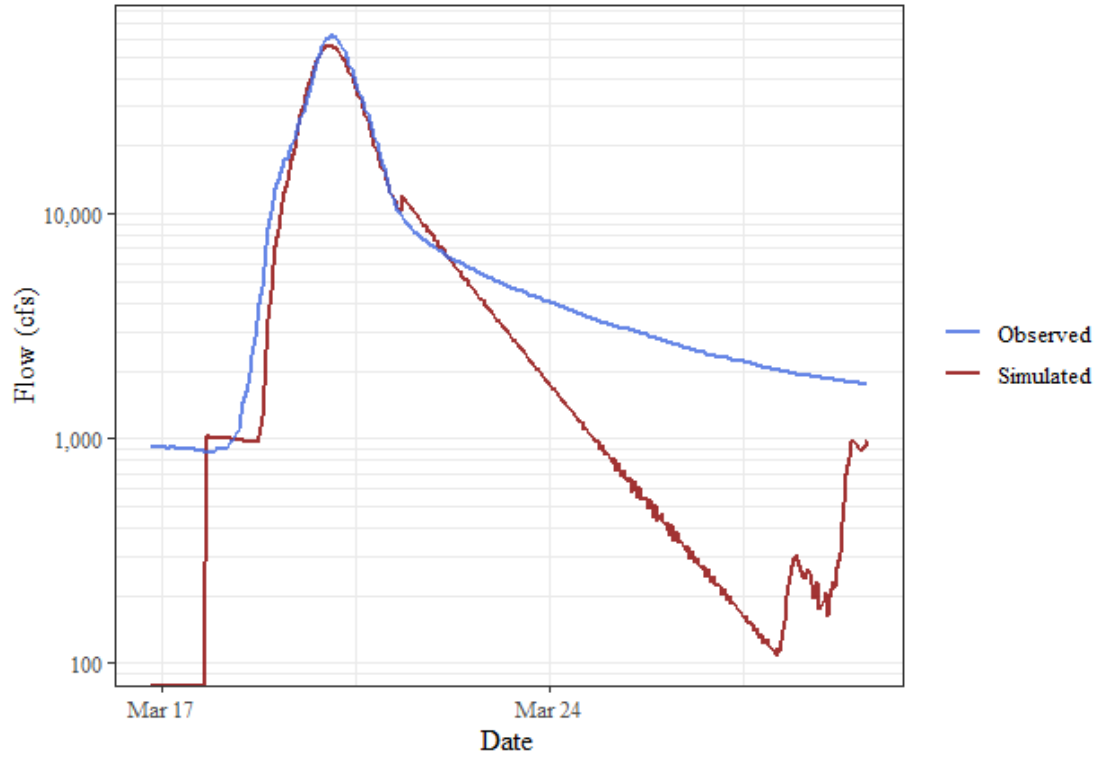
Goodness of Fit Table

Time Step	MAE	Normalized RMSE (%)	PBIAS (%)	RSR	NSE	Modified NSE	R^2	Adjusted R^2
Hourly	1,856.17	16.5	-18.8	0.17	0.97	0.78	0.99	0.92
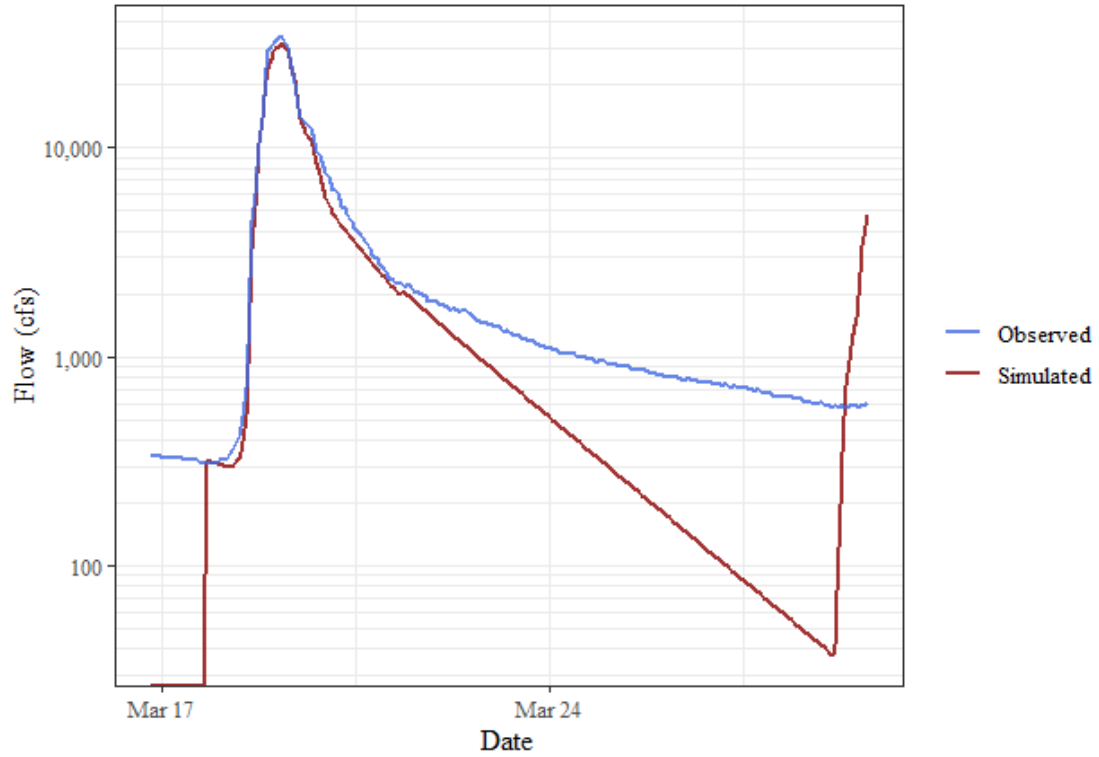
Baron Fork at Eldon, OK, Time Series Comparison

Goodness of Fit Table

Time Step	MAE	Normalized RMSE (%)	PBIAS (%)	RSR	NSE	Modified NSE	R^2	Adjusted R^2
Hourly	655.8	14.5	-17.6	0.14	0.98	0.81	0.99	0.9
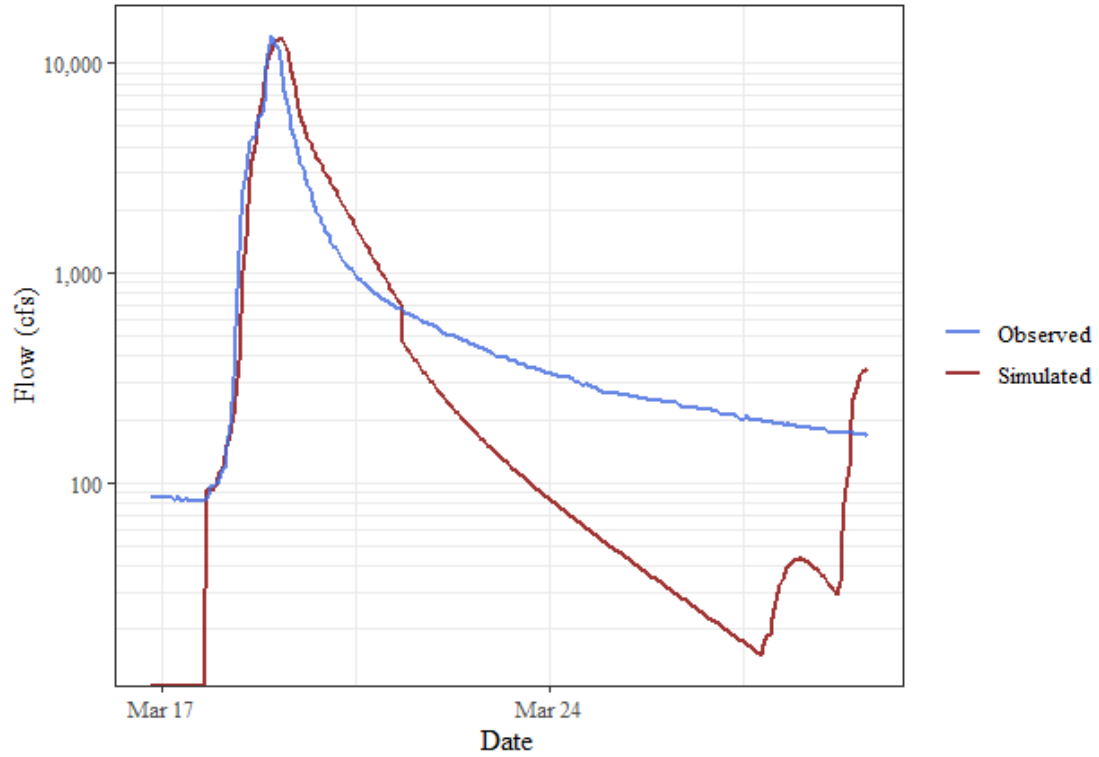
Flint Creek near Kansas, OK, Time Series Comparison

Goodness of Fit Table

Time Step	MAE	Normalized RMSE (%)	PBIAS (%)	RSR	NSE	Modified NSE	R^2	Adjusted R^2
Hourly	440.45	41.8	7.2	0.42	0.82	0.59	0.9	0.79

Flint Creek near West Siloam Springs, OK, Time Series Comparison
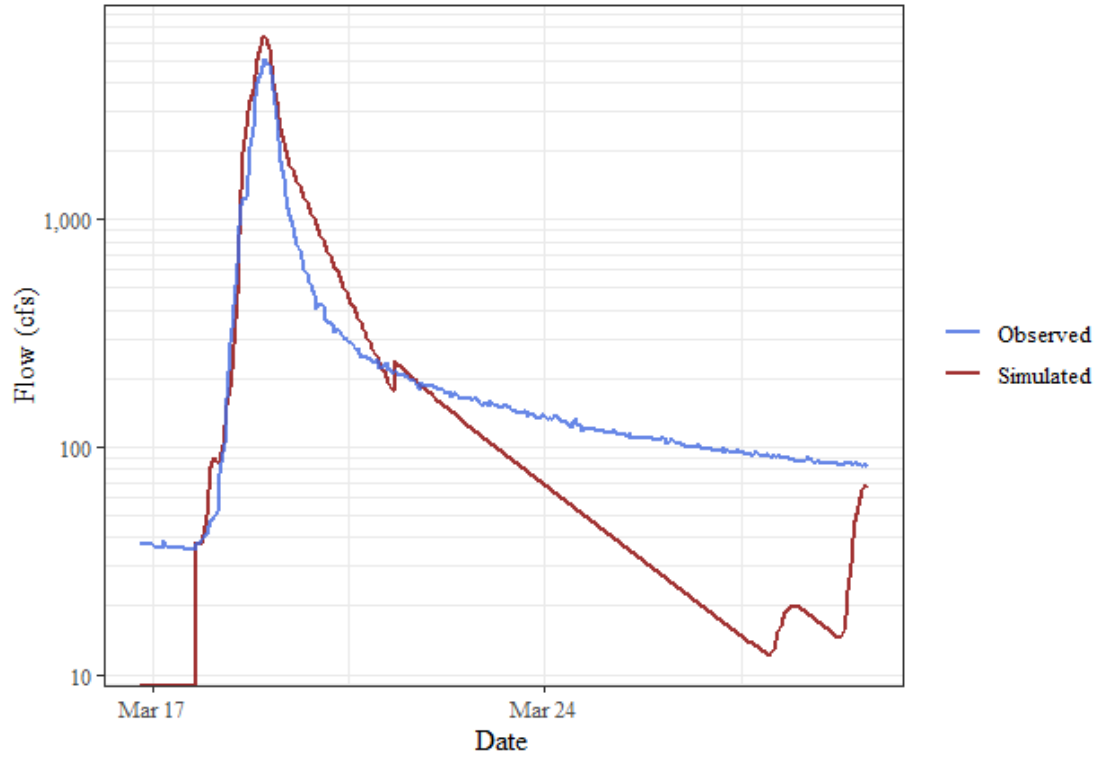
Goodness of Fit Table

Time Step	MAE	Normalized RMSE (%)	PBIAS (%)	RSR	NSE	Modified NSE	R^2	Adjusted R^2
Hourly	148.48	38.4	17.3	0.38	0.85	0.6	0.97	0.76
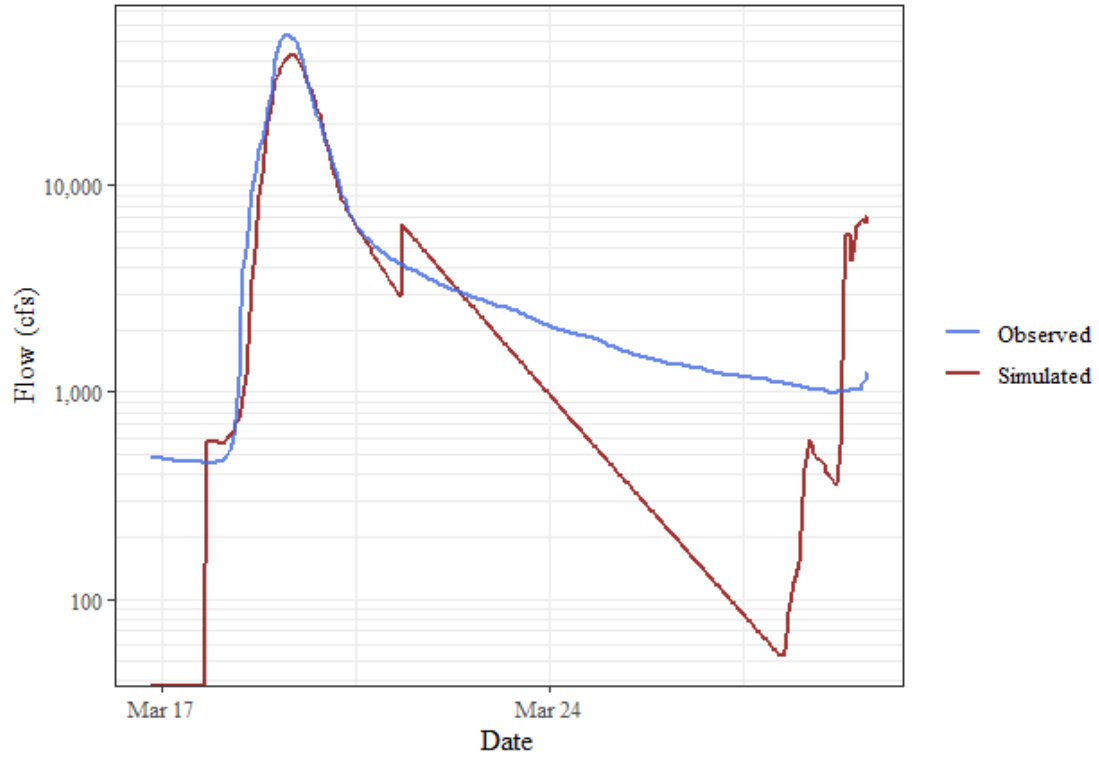
Illinois River near Watts, OK, Time Series Comparison

Goodness of Fit Table

Time Step	MAE	Normalized RMSE (%)	PBIAS (%)	RSR	NSE	Modified NSE	R^2	Adjusted R^2
Hourly	1,516.56	24.4	-17	0.24	0.94	0.75	0.96	0.81

Illinois River at Hwy. 16 near Siloam Springs, AR, Time Series Comparison
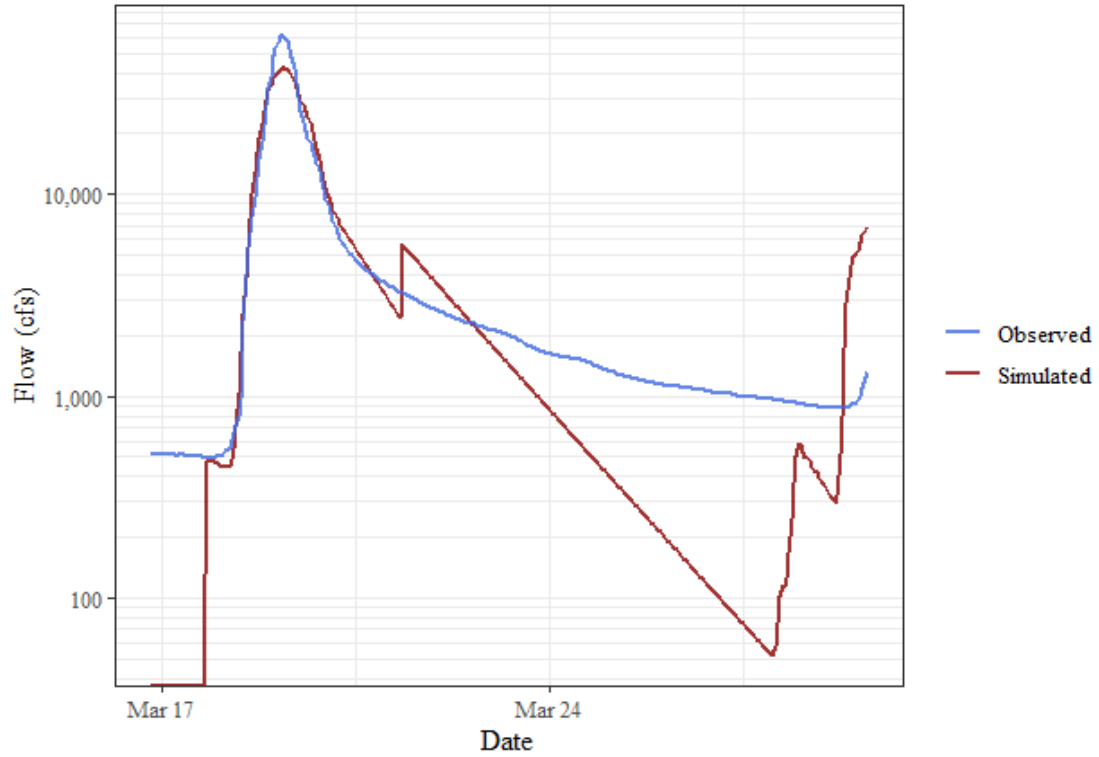
Goodness of Fit Table

Time Step	MAE	Normalized RMSE (%)	PBIAS (%)	RSR	NSE	Modified NSE	R^2	Adjusted R^2
Hourly	1,424.19	28.4	-9.3	0.28	0.92	0.74	0.94	0.78
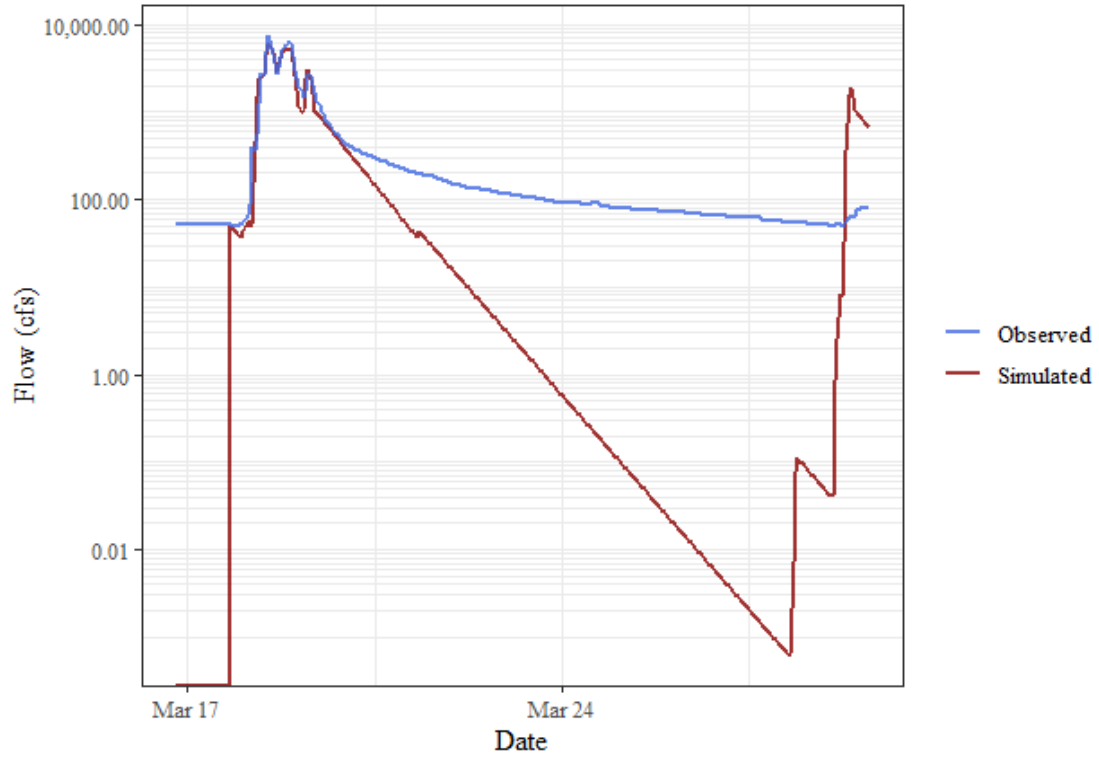
Baron Fork at Dutch Mills, AR, Time Series Comparison

Goodness of Fit Table

| Time Step	MAE	Normalized RMSE (%)	PBIAS (%)	RSR	NSE	Modified NSE	R^2	Adjusted R^2
Hourly	159.27	26.2	-15.5	0.26	0.93	0.71	0.94	0.84
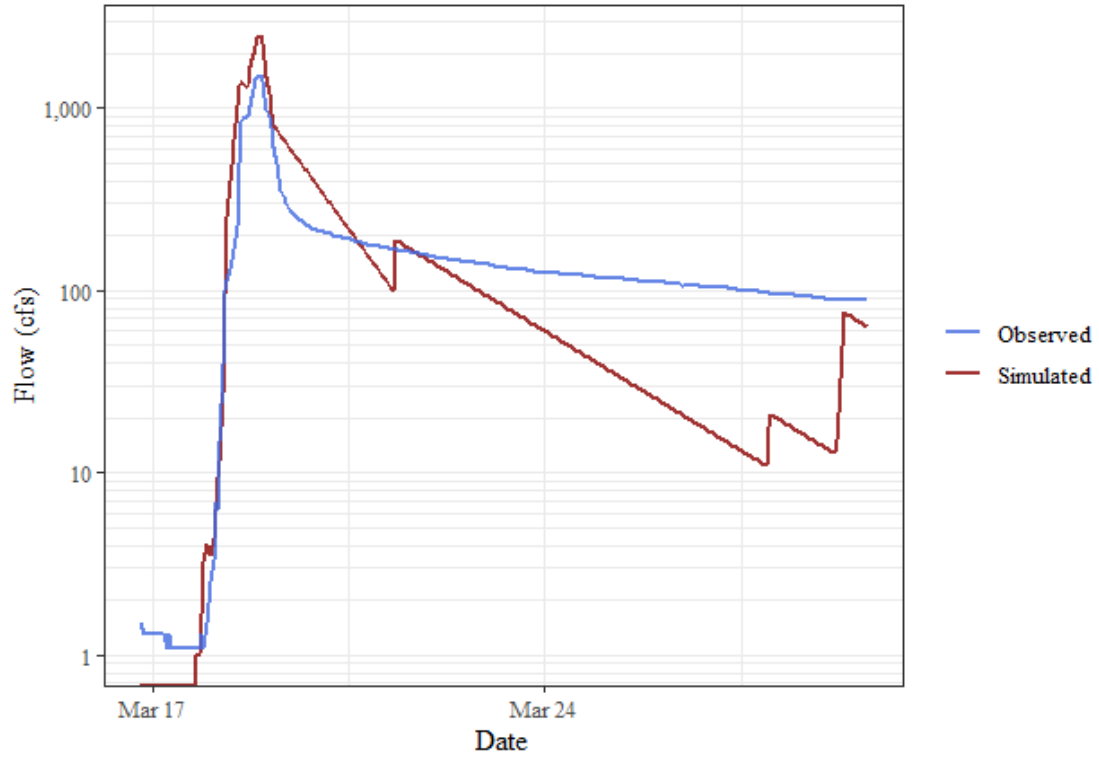
Flint Creek at Springtown, AR, Time Series Comparison

Goodness of Fit Table

Time Step	MAE	Normalized RMSE (%)	PBIAS (%)	RSR	NSE	Modified NSE	R^2	Adjusted R^2
Hourly	99.54	81.7	8.7	0.82	0.33	0.06	0.93	0.64
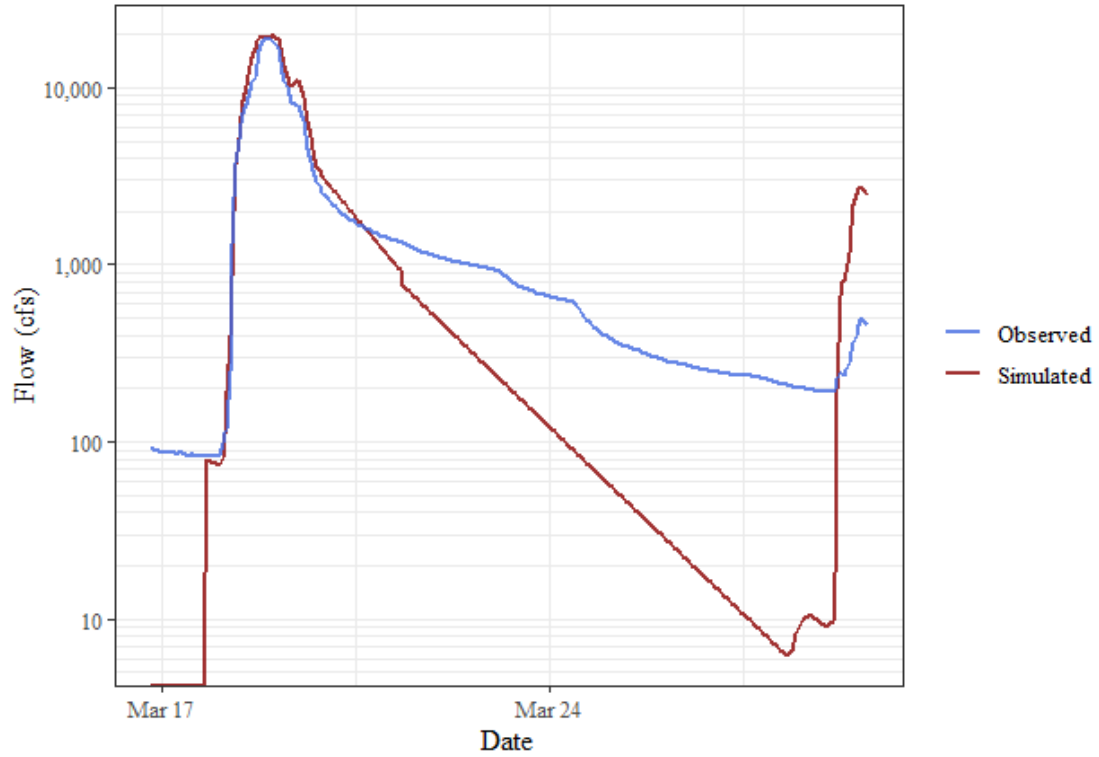
Illinois River at Savoy, AR, Time Series Comparison

Goodness of Fit Table

Time Step	MAE	Normalized RMSE (%)	PBIAS (%)	RSR	NSE	Modified NSE	R^2	Adjusted R^2
Hourly	572.47	25.7	2.9	0.26	0.93	0.72	0.97	0.85
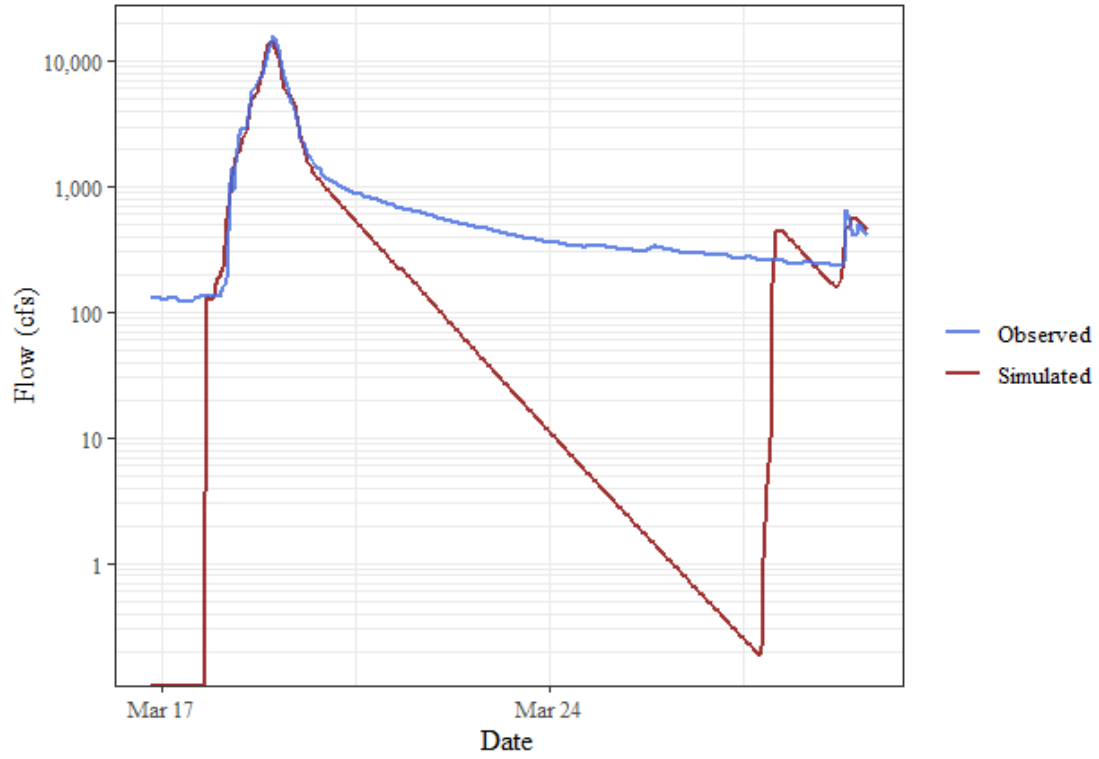
Osage Creek near Elm Springs, AR, Time Series Comparison

Goodness of Fit Table

Time Step	MAE	Normalized RMSE (%)	PBIAS (%)	RSR	NSE	Modified NSE	R^2	Adjusted R^2
Hourly	326.19	18.7	-25.5	0.19	0.96	0.71	0.98	0.9
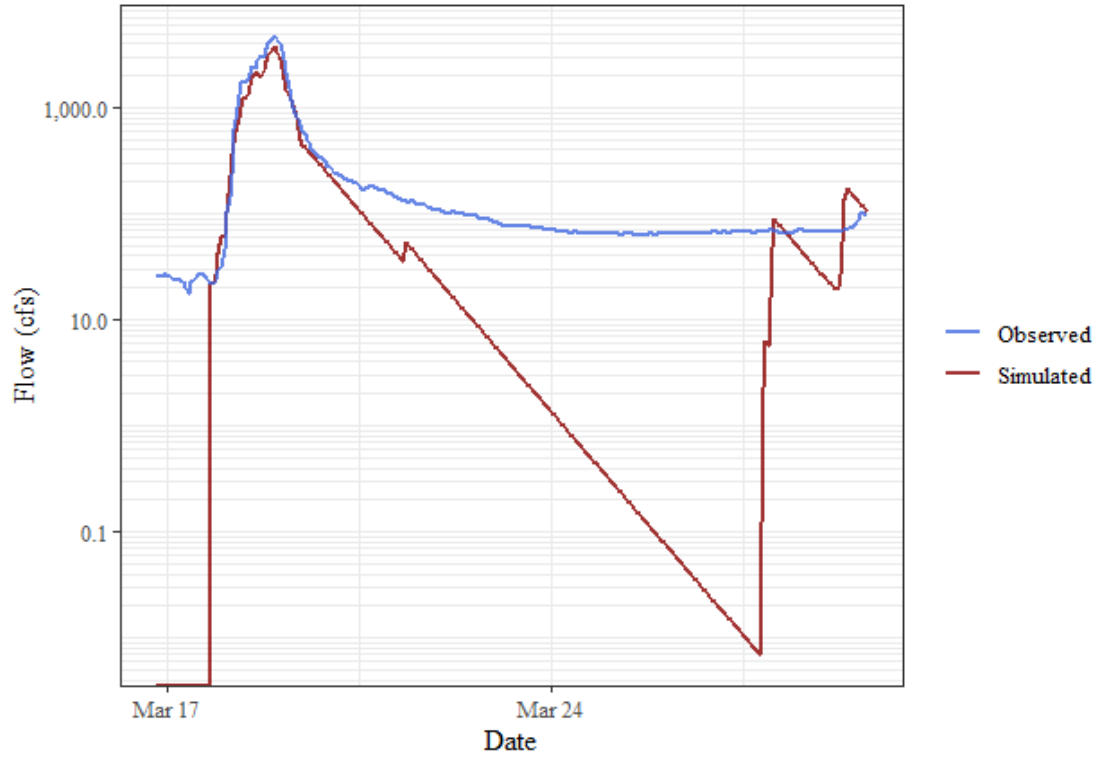
Osage Creek near Cave Springs, AR, Time Series Comparison

Goodness of Fit Table

Time Step	MAE	Normalized RMSE (%)	PBIAS (%)	RSR	NSE	Modified NSE	R^2	Adjusted R^2
Hourly	113.41	28.7	-33.5	0.29	0.92	0.72	0.99	0.74

April 2017 Validation Event

Illinois River near Tahlequah, OK, Time Series Comparison
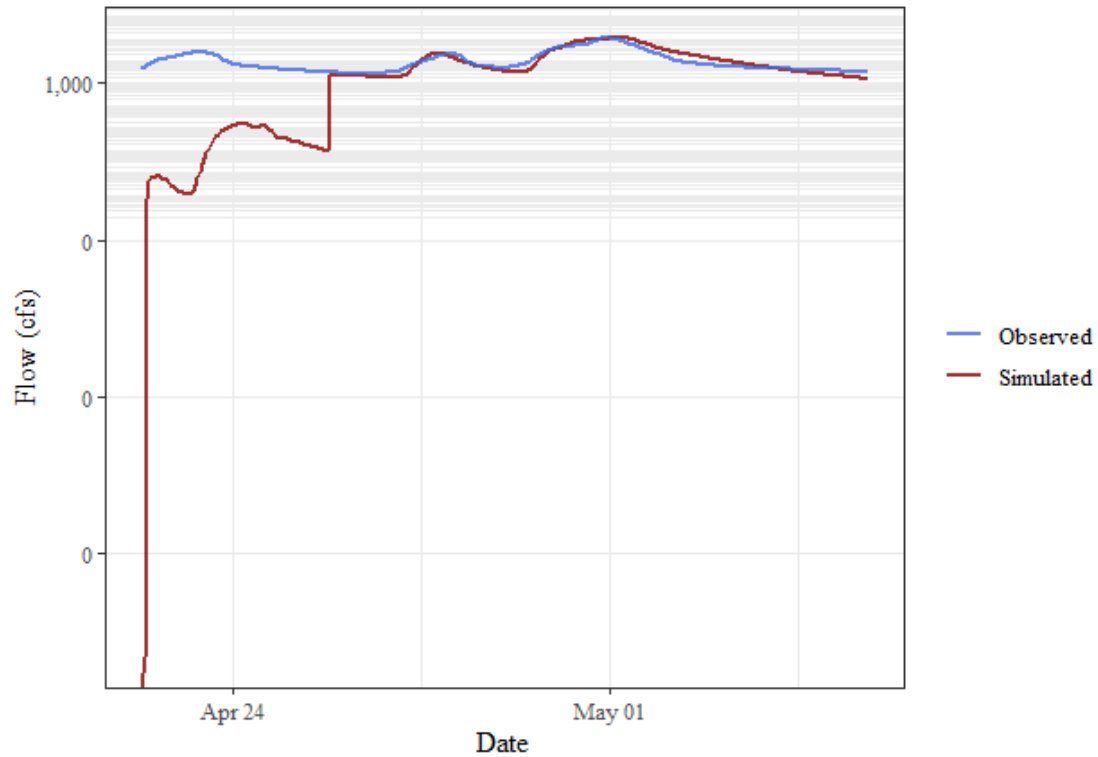
Goodness of Fit Table

Time Step	MAE	Normalized RMSE (%)	PBIAS (%)	RSR	NSE	Modified NSE	R^2	Adjusted R^2
Hourly	7,544.38	54	3.3	0.54	0.71	0.47	0.85	0.75
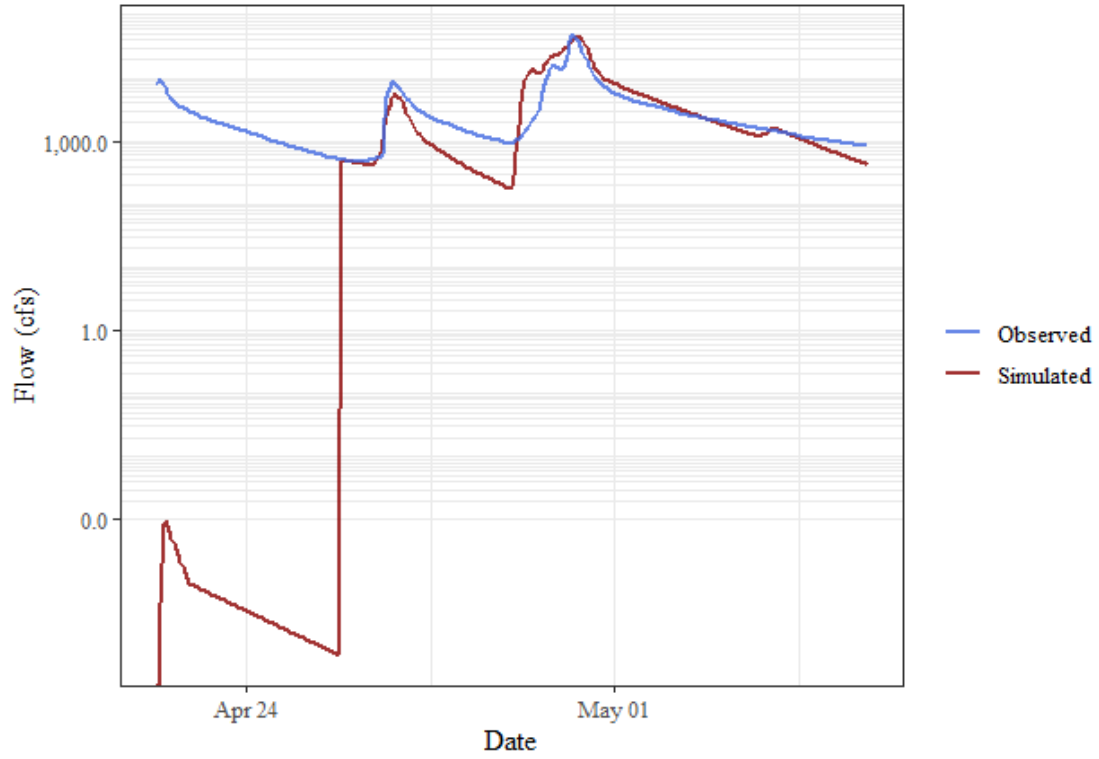
Baron Fork at Eldon, OK, Time Series Comparison

Goodness of Fit Table

Time Step	MAE	Normalized RMSE (%)	PBIAS (%)	RSR	NSE	Modified NSE	R^2	Adjusted R^2
Hourly	1,927.06	53.4	4.6	0.53	0.71	0.42	0.84	0.74
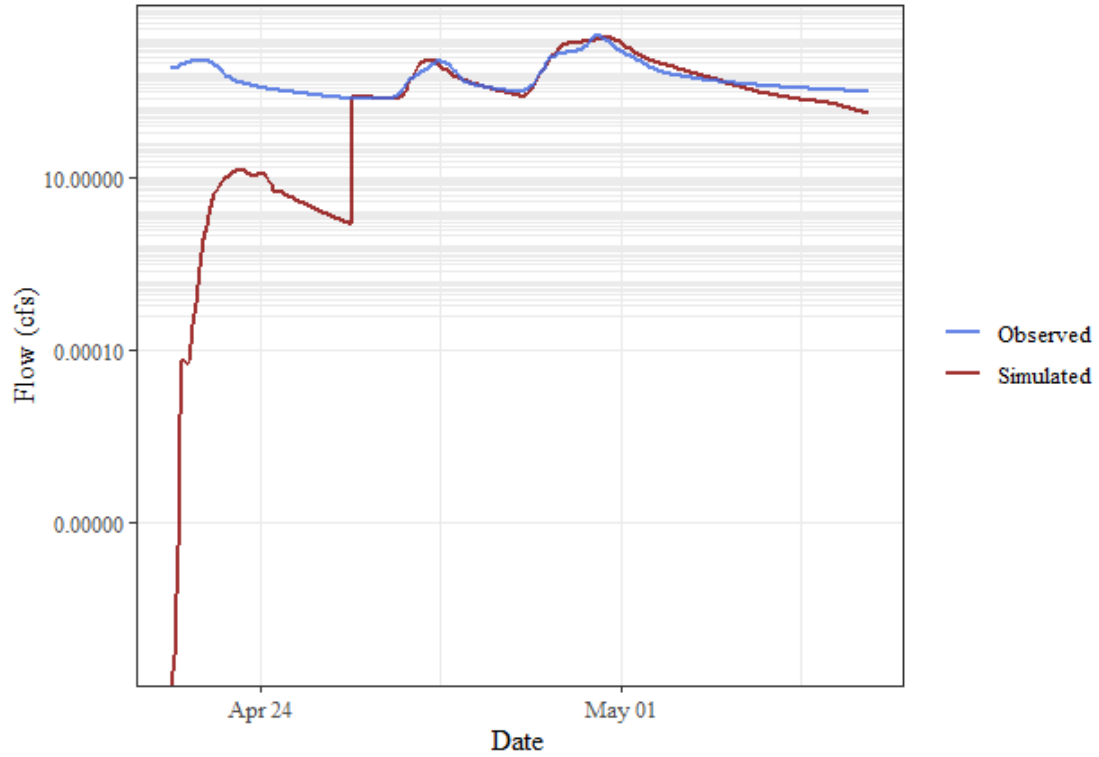
Illinois River at Chewey, OK, Time Series Comparison

Goodness of Fit Table

| Time Step	MAE	Normalized RMSE (%)	PBIAS (%)	RSR	NSE	Modified NSE	R^2	Adjusted R^2
Hourly	6,427.33	52.1	1.7	0.52	0.73	0.51	0.83	0.76
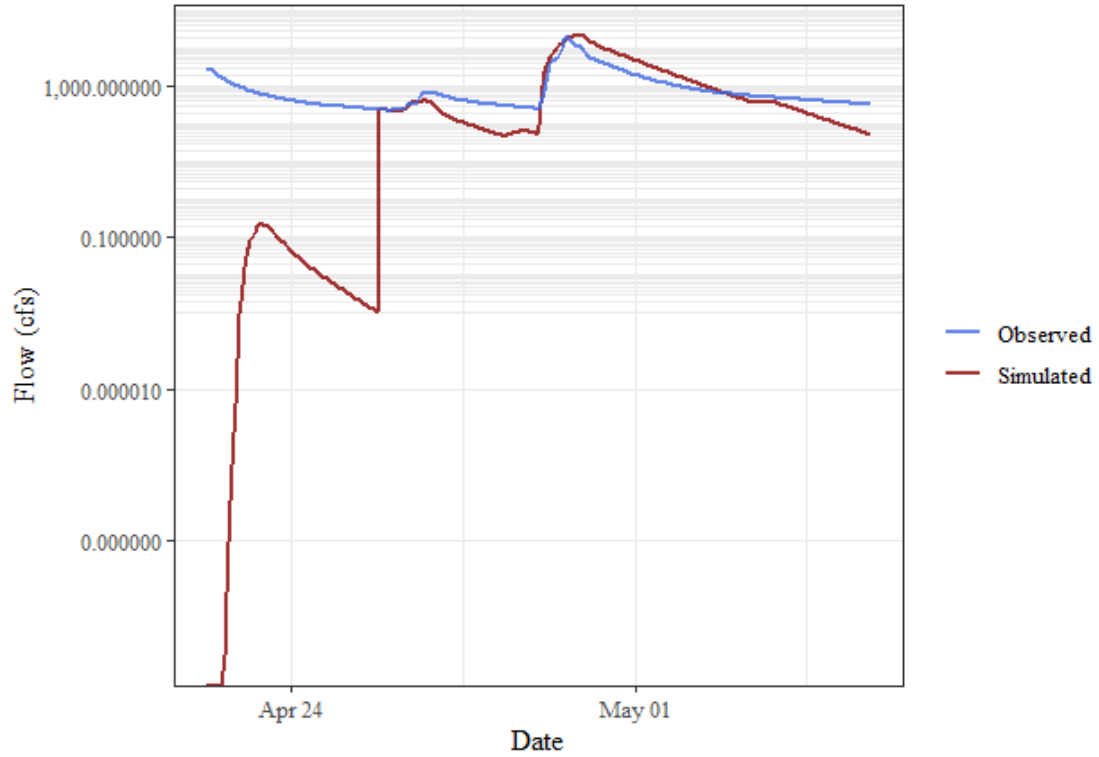
Flint Creek near Kansas, OK, Time Series Comparison

Goodness of Fit Table

Time Step	MAE	Normalized RMSE (%)	PBIAS (%)	RSR	NSE	Modified NSE	R^2	Adjusted R^2
Hourly	1,158.57	85.5	41.4	0.85	0.27	0.22	0.82	0.56

Flint Creek near West Siloam Springs, OK, Time Series Comparison
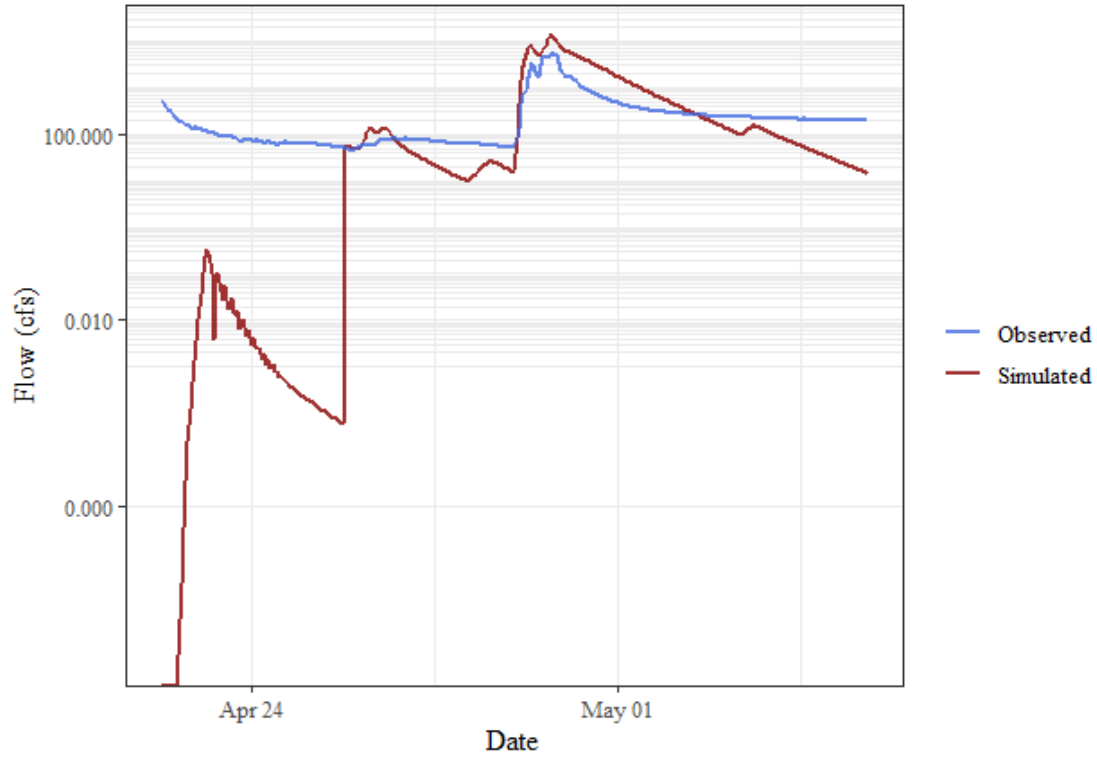
Goodness of Fit Table

Time Step	MAE	Normalized RMSE (%)	PBIAS (%)	RSR	NSE	Modified NSE	R²	Adjusted R²
Hourly	590.07	168.9	115.1	1.69	-1.86	-0.4	0.9	0.38

Illinois River near Watts, OK, Time Series Comparison
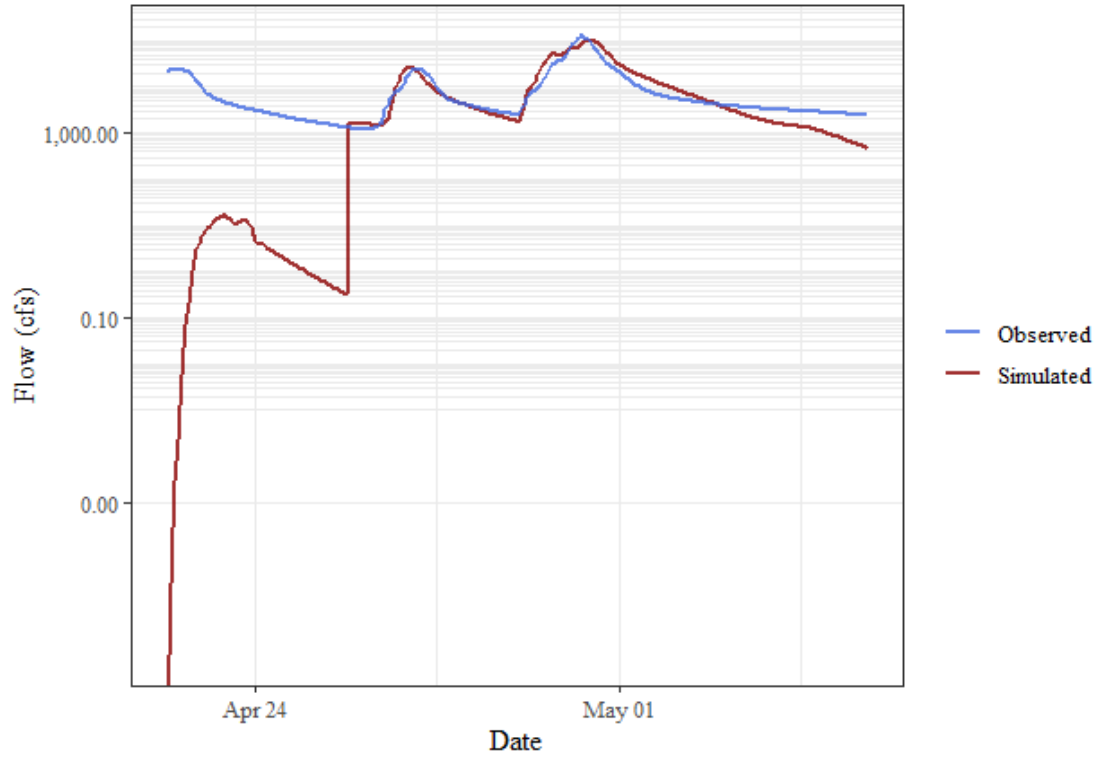
Goodness of Fit Table

| Time Step	MAE	Normalized RMSE (%)	PBIAS (%)	RSR	NSE	Modified NSE	R^2	Adjusted R^2
Hourly	5,330.06	45.8	-3.6	0.46	0.79	0.55	0.81	0.76

Illinois River South of Siloam Springs, AR, Time Series Comparison
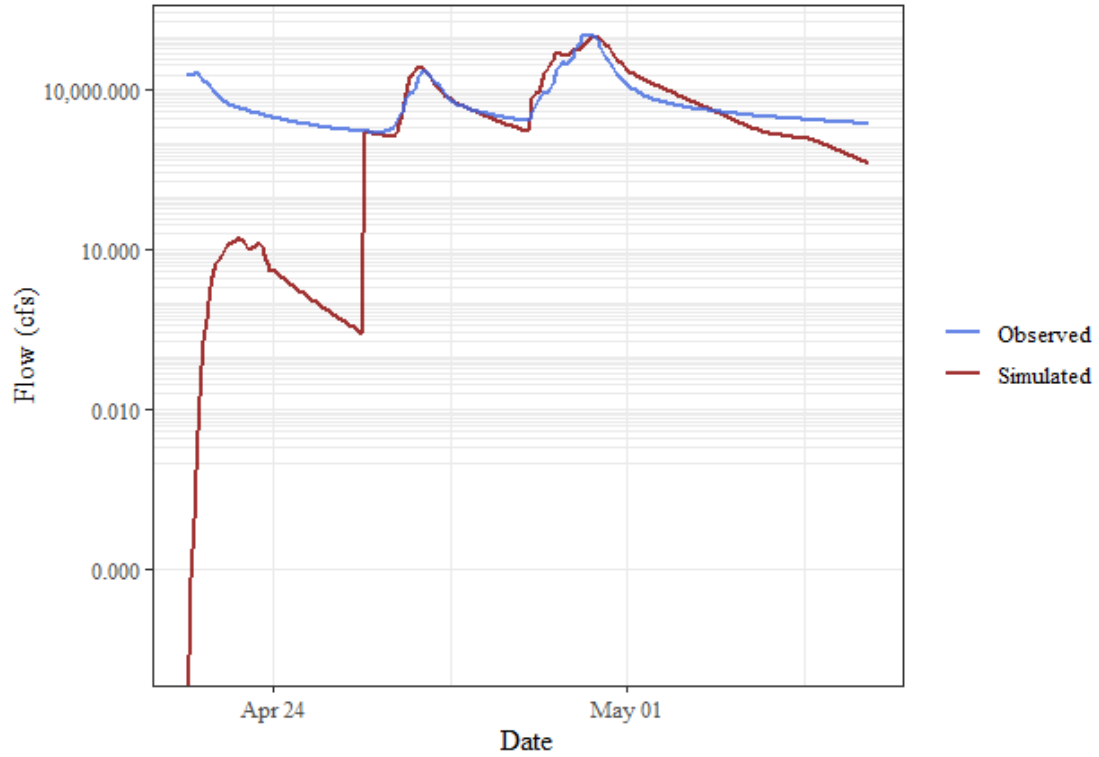
Goodness of Fit Table

Time Step	MAE	Normalized RMSE (%)	PBIAS (%)	RSR	NSE	Modified NSE	R^2	Adjusted R^2
Hourly	4,949.53	46.2	3	0.46	0.79	0.51	0.82	0.82

Illinois River at Hwy. 16 near Siloam Springs, AR, Time Series Comparison
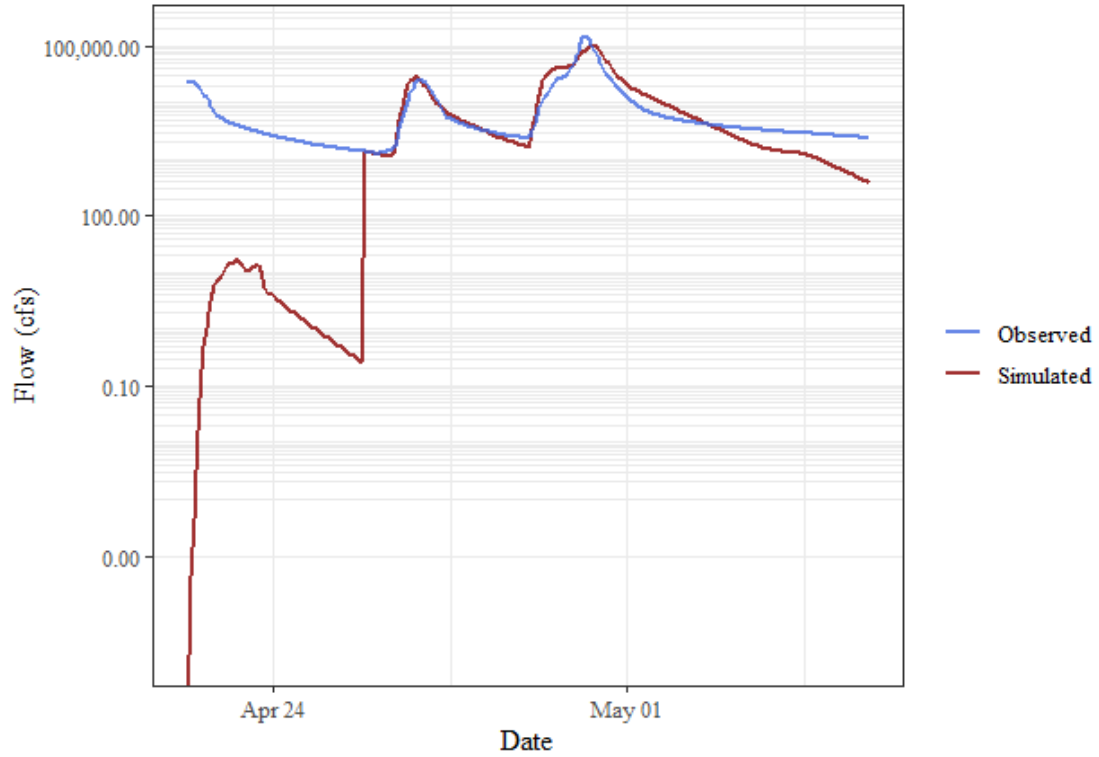
Goodness of Fit Table

Time Step	MAE	Normalized RMSE (%)	PBIAS (%)	RSR	NSE	Modified NSE	R^2	Adjusted R^2
Hourly	4,689.64	45.4	-4.2	0.45	0.79	0.56	0.8	0.68
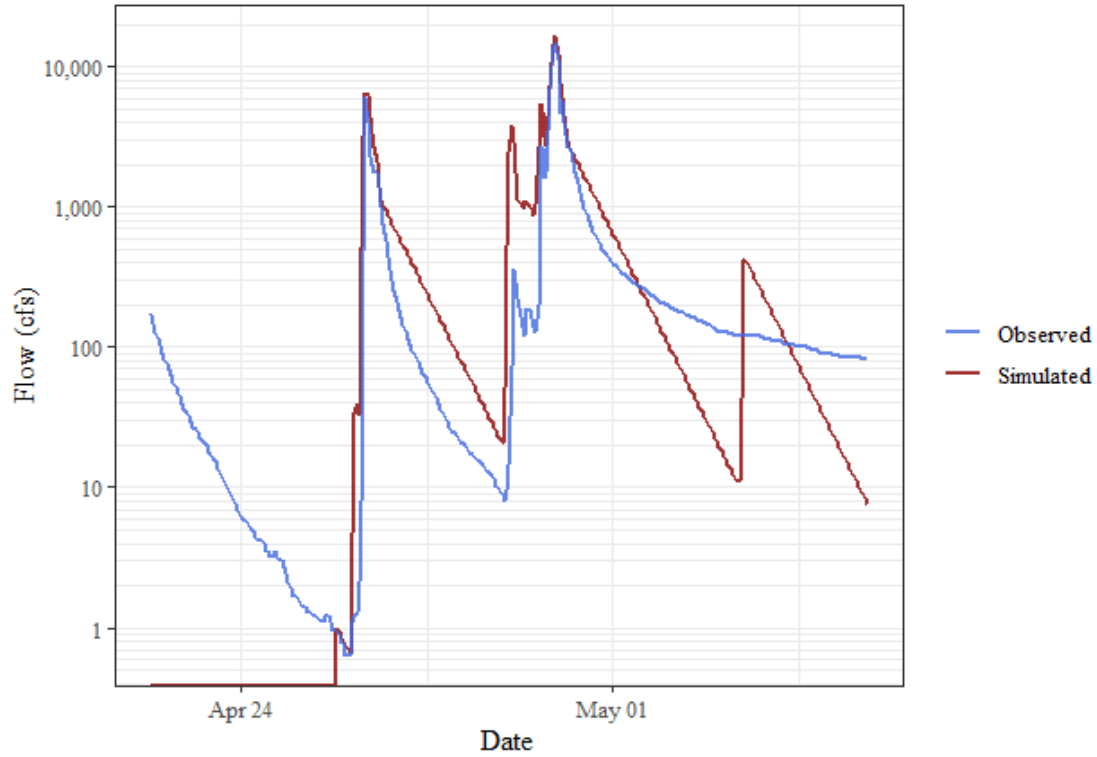
Baron Fork at Dutch Mills, AR, Time Series Comparison

Goodness of Fit Table

| Time Step	MAE	Normalized RMSE (%)	PBIAS (%)	RSR	NSE	Modified NSE	R^2	Adjusted R^2
Hourly	237.71	34.6	39.9	0.35	0.88	0.63	0.93	0.82
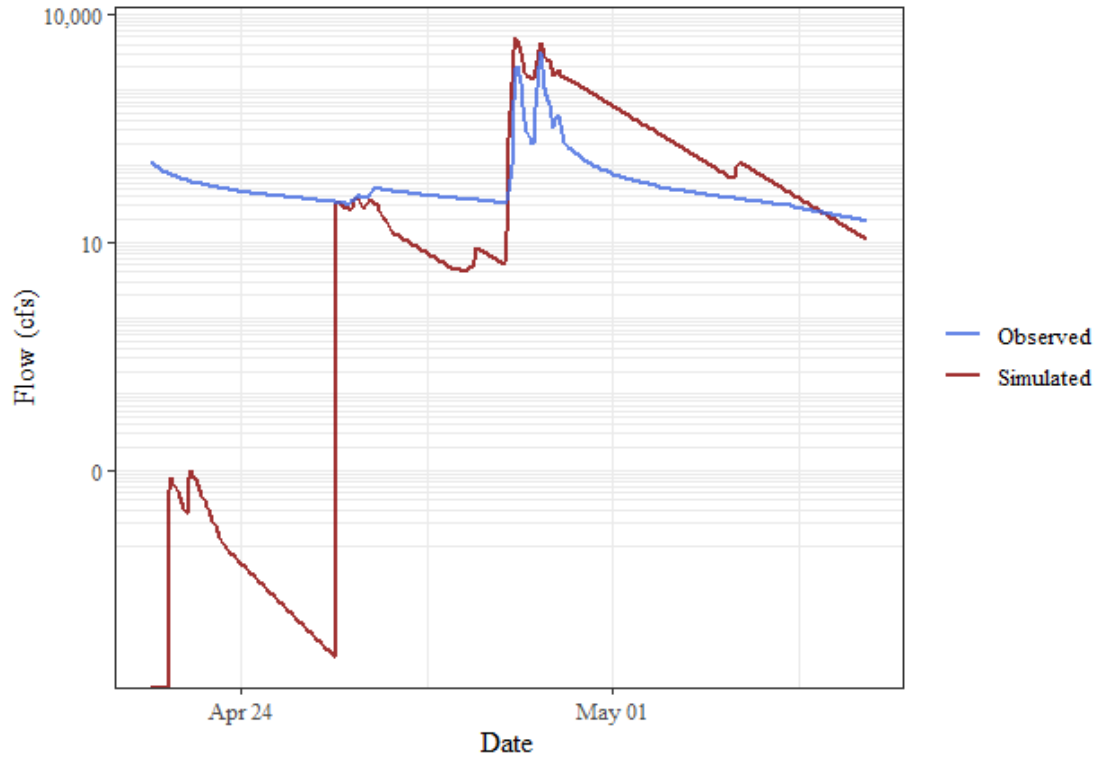
Flint Creek at Springtown, AR, Time Series Comparison

Goodness of Fit Table

Time Step	MAE	Normalized RMSE (%)	PBIAS (%)	RSR	NSE	Modified NSE	R^2	Adjusted R^2
Hourly	231.27	169.9	176.5	1.7	-1. 9	-1.04	0.76	0.35
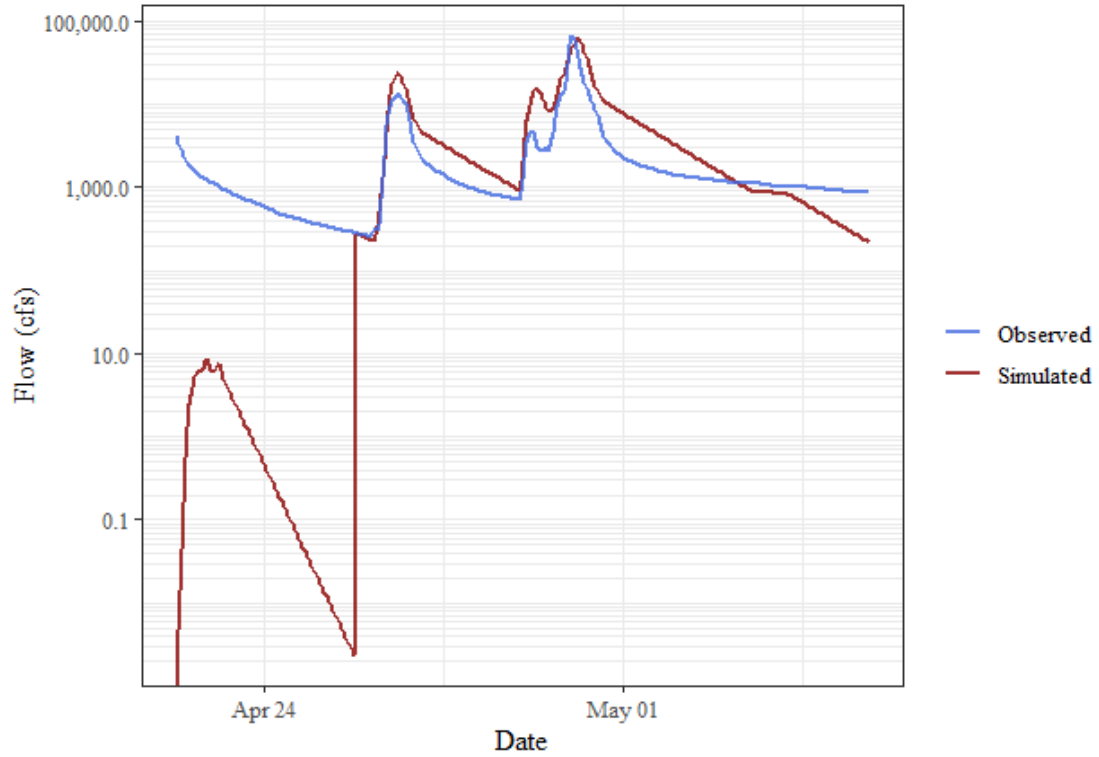
Illinois River at Savoy, AR, Time Series Comparison

Goodness of Fit Table

Time Step	MAE	Normalized RMSE (%)	PBIAS (%)	RSR	NSE	Modified NSE	R^2	Adjusted R^2
Hourly	2,395.78	65	52.9	0.65	0.58	0.27	0.79	0.65
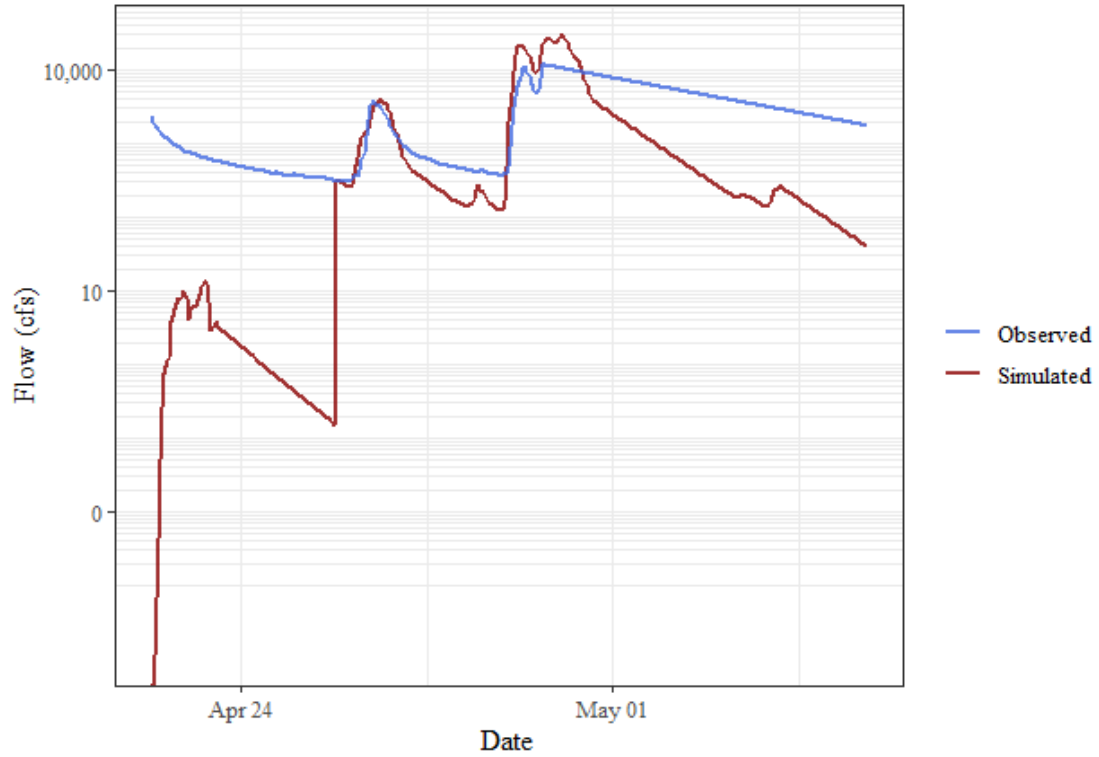
Osage Creek near Elm Springs, AR, Time Series Comparison

Goodness of Fit Table

Time Step	MAE	Normalized RMSE (%)	PBIAS (%)	RSR	NSE	Modified NSE	R^2	Adjusted R^2
Hourly	2,674.06	136.9	-21.2	1.37	-0.88	-0.06	0.53	0.49
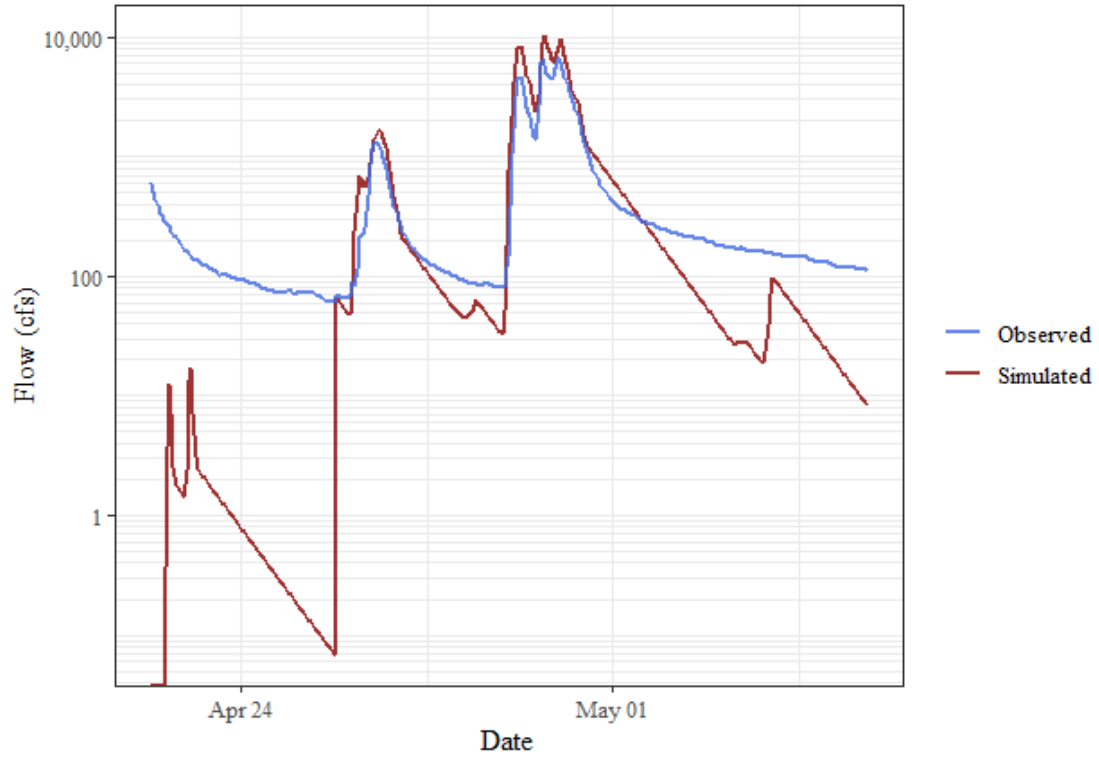
Osage Creek near Cave Springs, AR, Time Series Comparison

Goodness of Fit Table

Time Step	MAE	Normalized RMSE (%)	PBIAS (%)	RSR	NSE	Modified NSE	R^2	Adjusted R^2
Hourly	297.52	60.6	26.6	0.61	0.63	0.56	0.96	0.66

Appendix B: Simulated versus observed streamflow plots and goodness of fit statistics for the Illinois River HEC-RAS model calibration and validation events

April 2011 Calibration Event
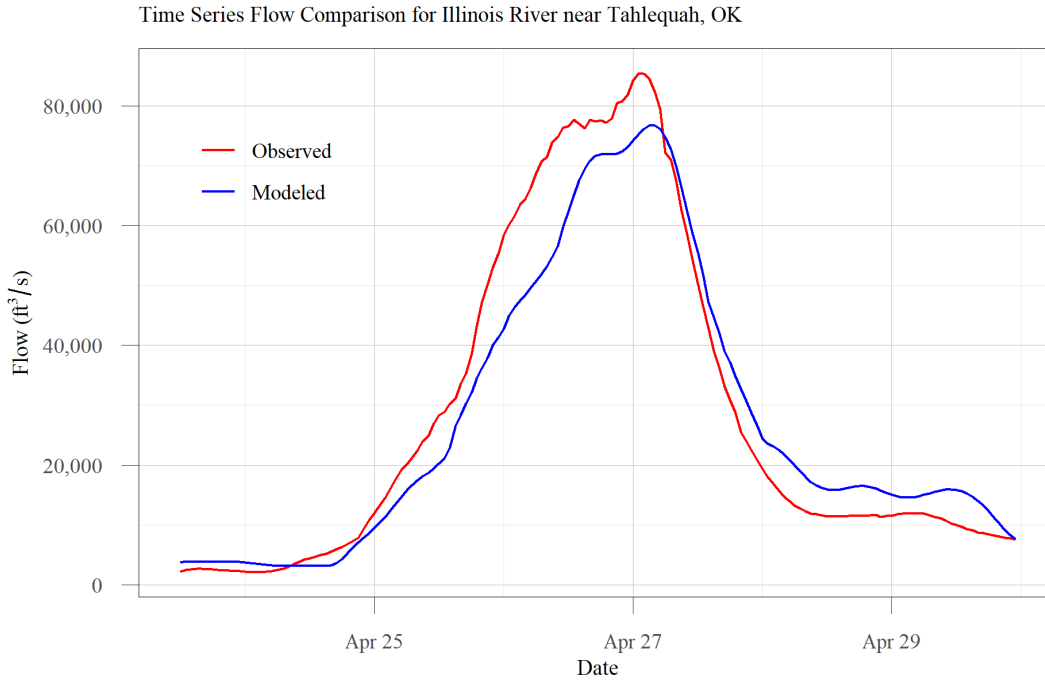
Illinois River near Tahlequah, OK, Time Series Comparison

Time Series Flow Comparison for Illinois River near Tahlequah, OK

Goodness of Fit Table

Parameter	Maximum Simulated (feet or cfs)	Maximum Observed (feet or cfs)	Normalized RMSE (%)	PBIAS (%)	RSR	NSE	R^2
Elevation	690.5	691.1	33.0	0.2	0.33	0.89	0.94
Flow	76,752	85,400	25.7	-4.5	0.26	0.93	0.95
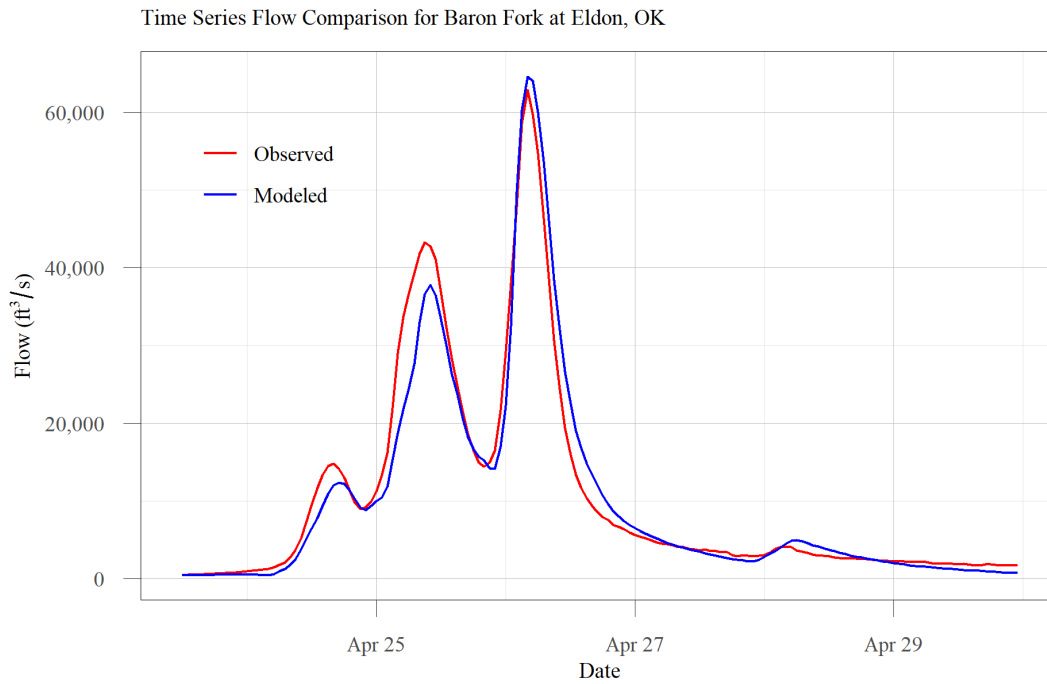
## Baron Fork at Eldon, OK, Time Series Comparison

Time Series Flow Comparison for Baron Fork at Eldon, OK

Goodness of Fit Table

Parameter	Maximum Simulated (feet or cfs)	Maximum Observed (feet or cfs)	Normalized RMSE (%)	PBIAS (%)	RSR	NSE	R^2
Elevation	729.7	729.7	24.2	0.0	0.24	0.94	0.95
Flow	64,644	62,900	22.6	-3.8	0.23	0.95	0.95

Illinois River at Chewey, OK, Time Series Comparison

Time Series Flow Comparison for Illinois River at Chewey, OK
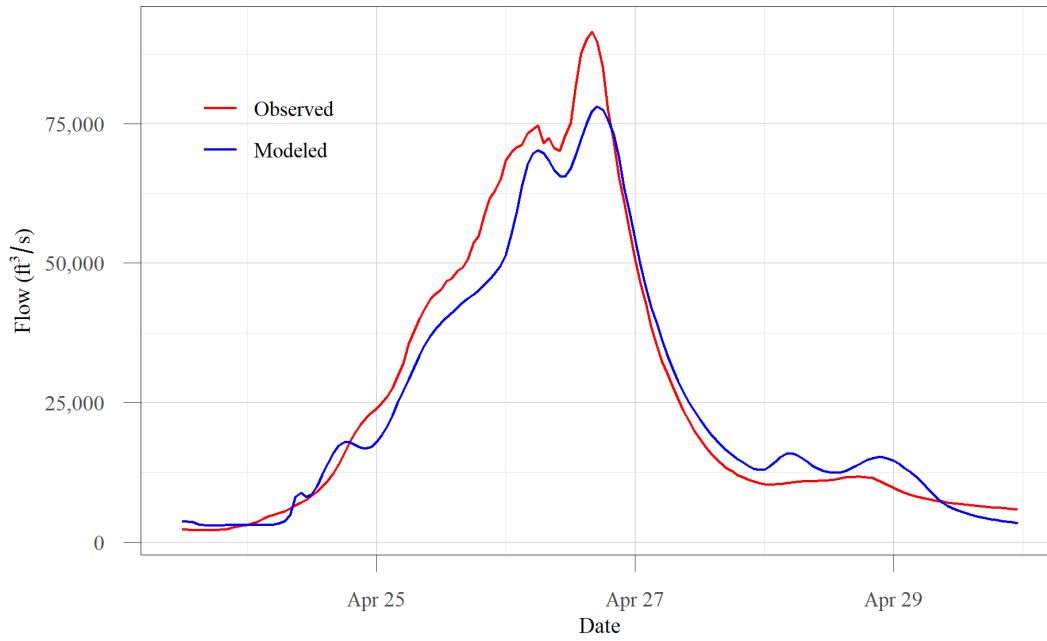
Goodness of Fit Table

Parameter	Maximum Simulated (feet or cfs)	Maximum Observed (feet or cfs)	Normalized RMSE (%)	PBIAS (%)	RSR	NSE	R^2
Elevation	828.5	830.4	21.7	-0.1	0.22	0.95	0.97
Flow	78,078	91,500	21.1	-4.6	0.21	0.96	0.97
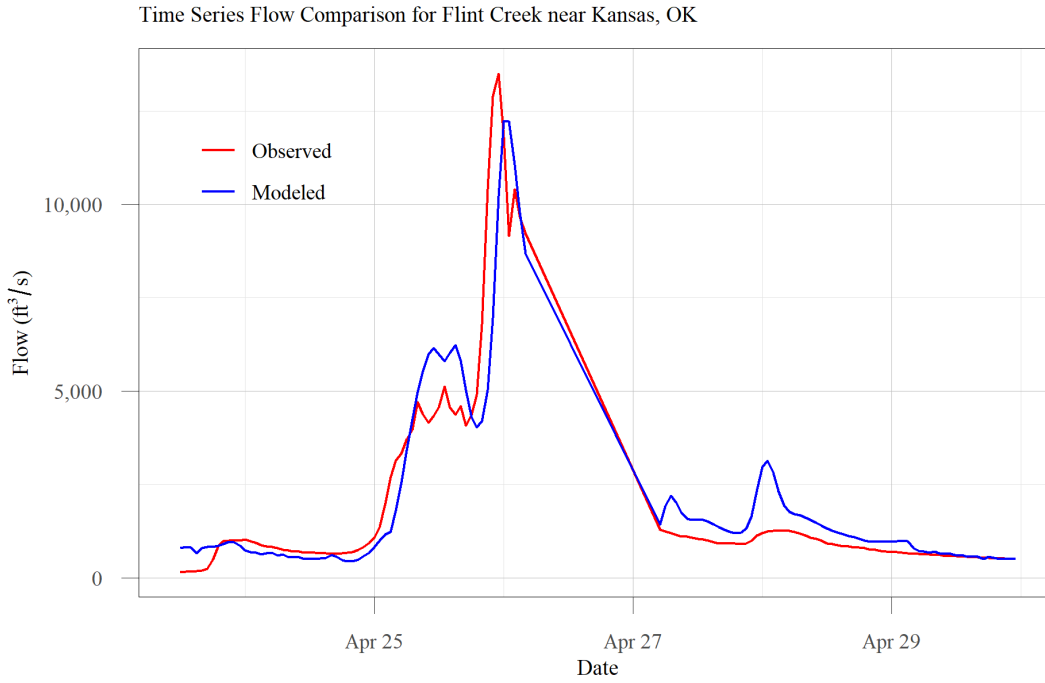
Flint Creek near Kansas, OK, Time Series Comparison

Time Series Flow Comparison for Flint Creek near Kansas, OK

Goodness of Fit Table

Parameter	Maximum Simulated (feet or cfs)	Maximum Observed (feet or cfs)	Normalized RMSE (%)	PBIAS (%)	RSR	NSE	R^2
Elevation	868.7	867.4	74.7	0.0	0.75	0.44	0.83
Flow	12,240	13,500	39.1	7.1	0.39	0.85	0.85

168

Flint Creek near West Siloam Springs, OK, Time Series Comparison

Time Series Flow Comparison for Flint Creek near West Siloam Springs, OK
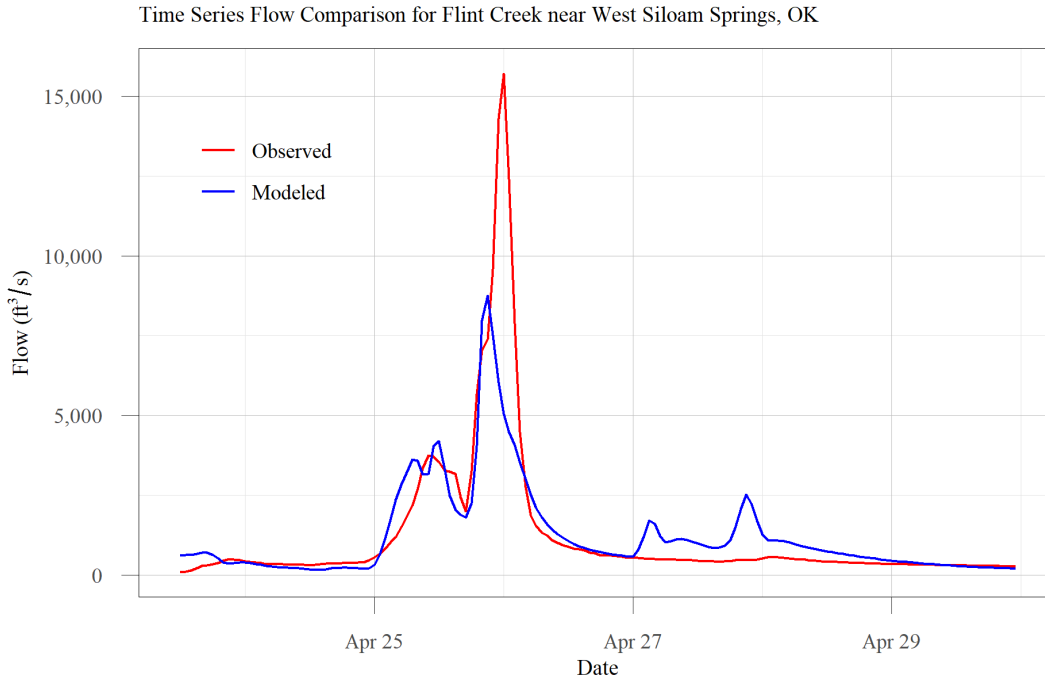

Goodness of Fit Table

Parameter	Maximum Simulated (feet or cfs)	Maximum Observed (feet or cfs)	Normalized RMSE (%)	PBIAS (%)	RSR	NSE	R^2
Elevation	970.7	970	61.1	0.1	0.61	0.62	0.79
Flow	8,748	15,700	60.2	0.9	0.6	0.64	0.67
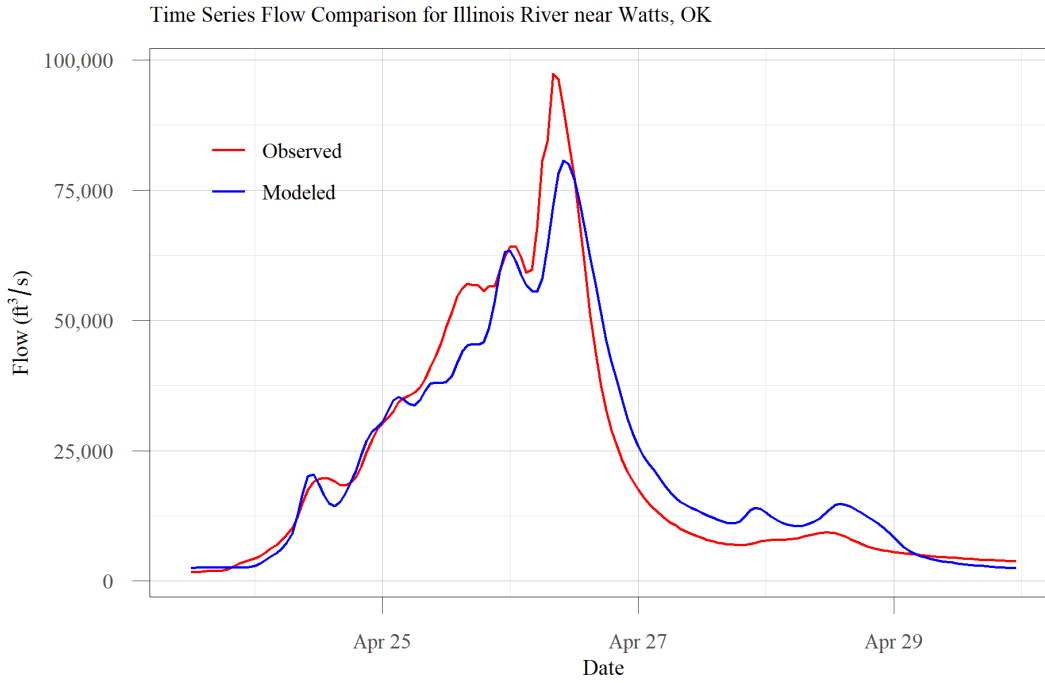
Illinois River near Watts, OK, Time Series Comparison

Time Series Flow Comparison for Illinois River near Watts, OK

Goodness of Fit Table

Parameter	Maximum Simulated (feet or cfs)	Maximum Observed (feet or cfs)	Normalized RMSE (%)	PBIAS (%)	RSR	NSE	R^2
Elevation	920.1	922.6	54.6	-0.3	0.55	0.7	0.88
Flow	80,719	974,00	27.1	2.3	0.27	0.93	0.93

## Illinois River South of Siloam Springs, AR, Time Series Comparison

Time Series Flow Comparison for Illinois River South of Siloam Springs, AR
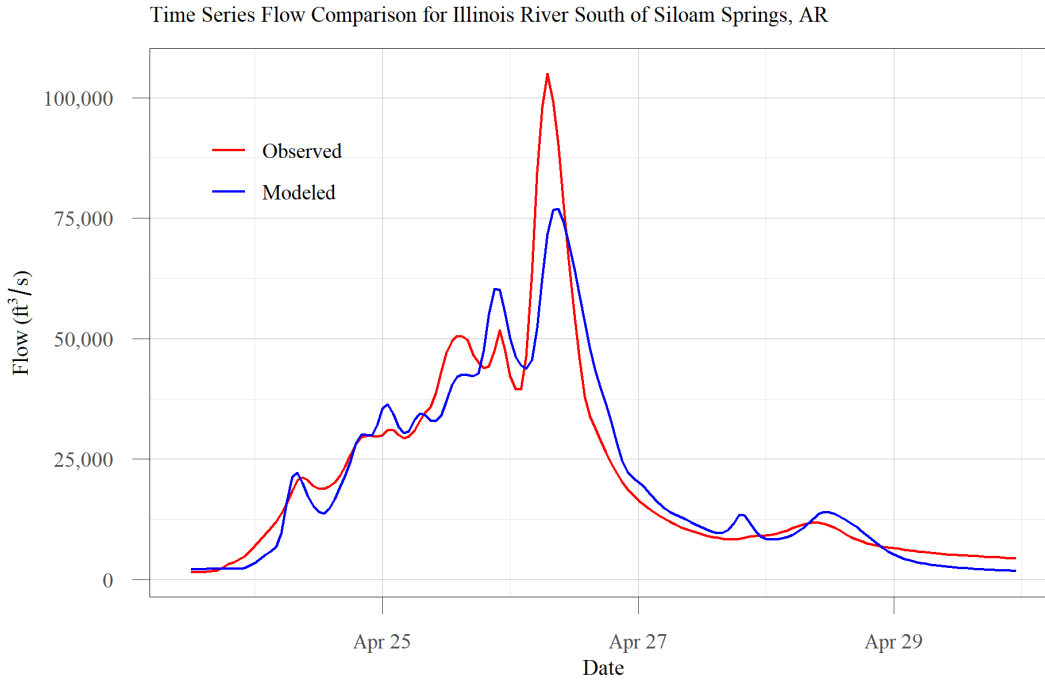
Goodness of Fit Table

Parameter	Maximum Simulated (feet or cfs)	Maximum Observed (feet or cfs)	Normalized RMSE (%)	PBIAS (%)	RSR	NSE	R^2
Elevation	937.9	940.8	36.0	0.0	0.36	0.87	0.87
Flow	76,975	105,000	33.4	-2.1	0.33	0.89	0.89

Illinois River at Hwy. 16 near Siloam Springs, AR, Time Series Comparison

Time Series Flow Comparison for Illinois River at Hwy. 16 near Siloam Springs AR
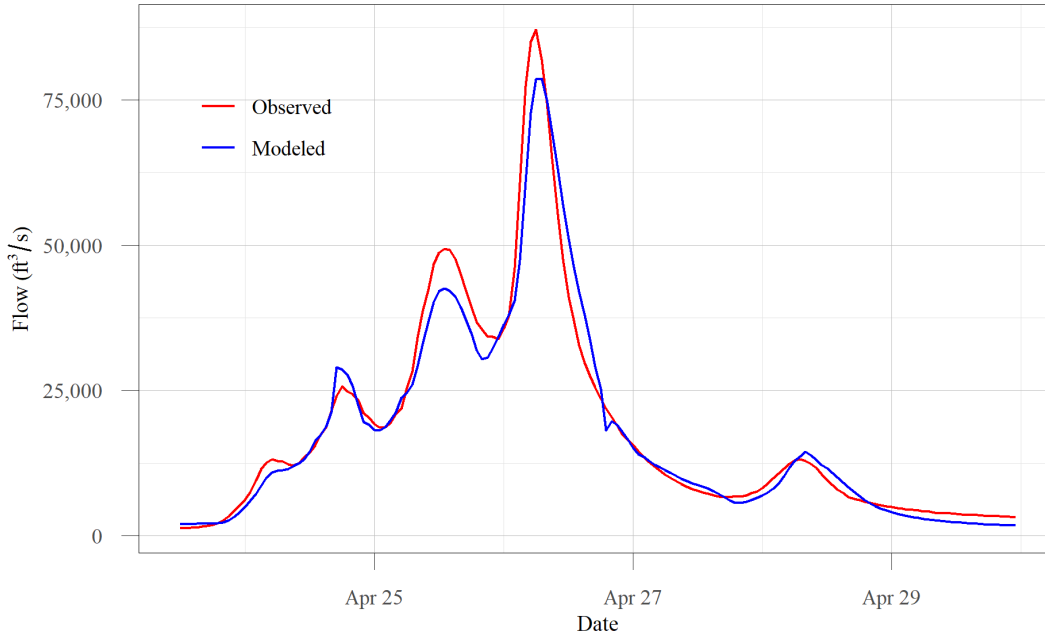
Goodness of Fit Table

Parameter	Maximum Simulated (feet or cfs)	Maximum Observed (feet or cfs)	Normalized RMSE (%)	PBIAS (%)	RSR	NSE	R²
Elevation	958.5	959.3	48.3	0.1	0.48	0.77	0.87
Flow	78,636	871,00	19.4	-3.6	0.19	0.96	0.96
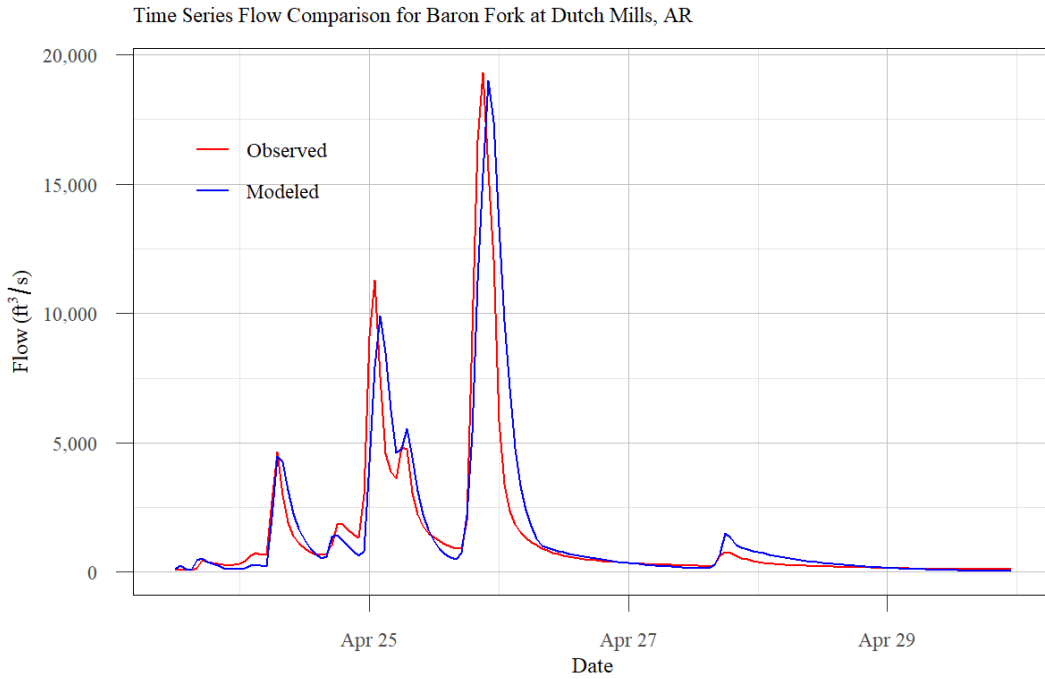
Baron Fork at Dutch Mills, AR, Time Series Comparison

Time Series Flow Comparison for Baron Fork at Dutch Mills, AR

Goodness of Fit Table

Parameter	Maximum Simulated (feet or cfs)	Maximum Observed (feet or cfs)	Normalized RMSE (%)	PBIAS (%)	RSR	NSE	R^2
Elevation	968.7	1001.3	1432.8	-3.4	14.33	-205.6	0.75
Flow	18,996	19,300	48.2	12.2	0.48	0.77	0.8
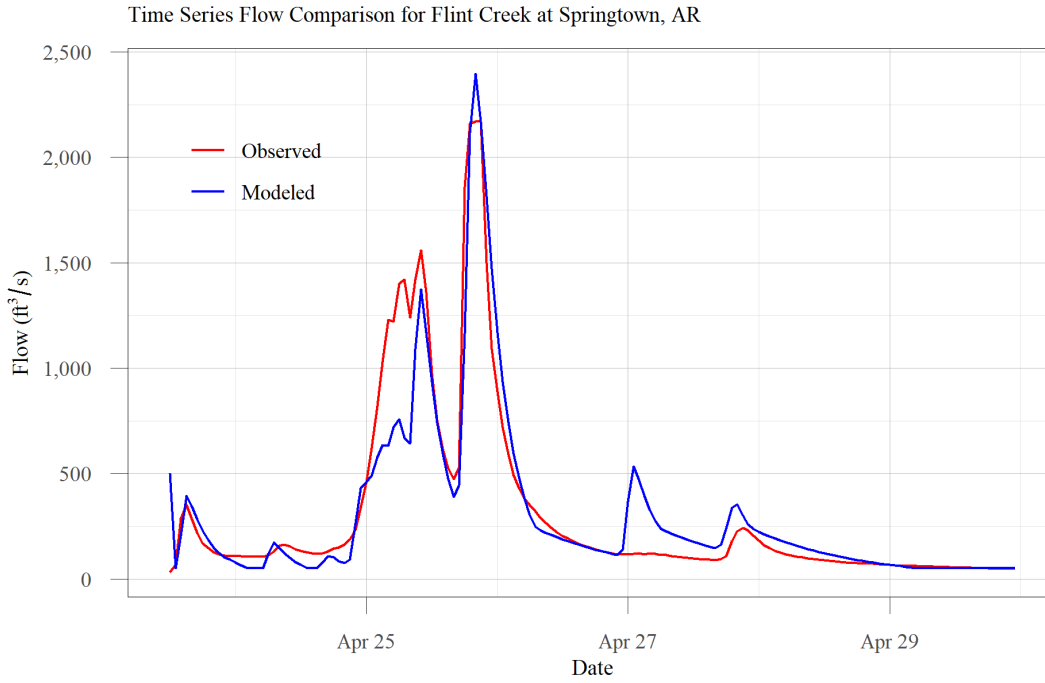
Flint Creek at Springtown, AR, Time Series Comparison

Time Series Flow Comparison for Flint Creek at Springtown, AR

Goodness of Fit Table

Parameter	Maximum Simulated (feet or cfs)	Maximum Observed (feet or cfs)	Normalized RMSE (%)	PBIAS (%)	RSR	NSE	R^2
Elevation	1,185.7	1,182.2	137.7	0.2	1.38	-0.91	0.83
Flow	2,397	2,170	37.4	-1.2	0.37	0.86	0.86
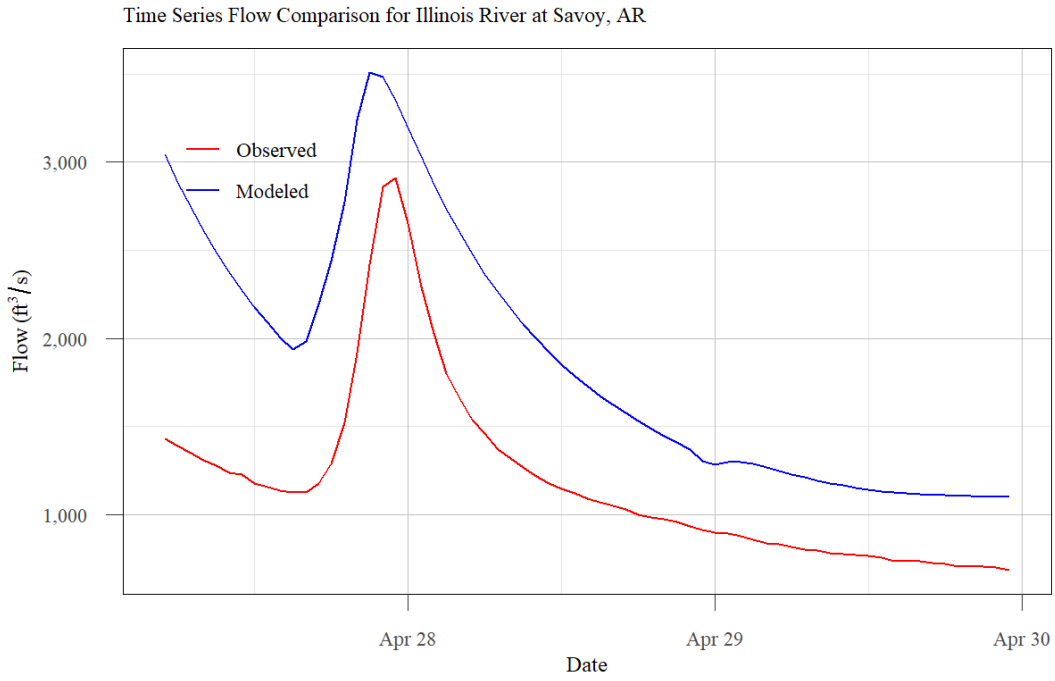
Illinois River at Savoy, AR, Time Series Comparison

Time Series Flow Comparison for Illinois River at Savoy, AR

Goodness of Fit Table

Parameter	Maximum Simulated (feet or cfs)	Maximum Observed (feet or cfs)	Normalized RMSE (%)	PBIAS (%)	RSR	NSE	R^2
Elevation	1,028.2	1,029.2	65.7	0.0	0.66	0.56	0.6
Flow	3505	2910	149.0	58.3	1.49	-1.25	0.83

Osage Creek near Elm Springs, AR, Time Series Comparison

Time Series Flow Comparison for Osage Creek near Elm Springs, AR
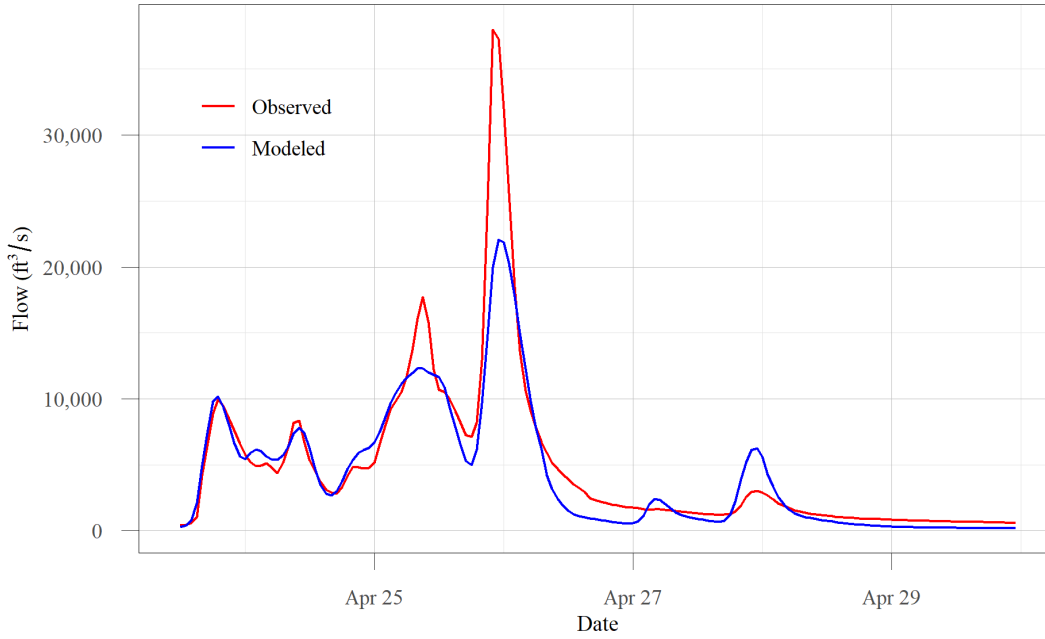
Goodness of Fit Table

Parameter	Maximum Simulated (feet or cfs)	Maximum Observed (feet or cfs)	Normalized RMSE (%)	PBIAS (%)	RSR	NSE	R^2
Elevation	1,070.8	1,072.8	71.1	-0.2	0.71	0.49	0.87
Flow	22,071	38,000	40.5	-13.1	0.4	0.83	0.88

December 2015 Calibration Event

Illinois River near Tahlequah, OK, Time Series Comparison

Time Series Flow Comparison for Illinois River near Tahlequah, OK
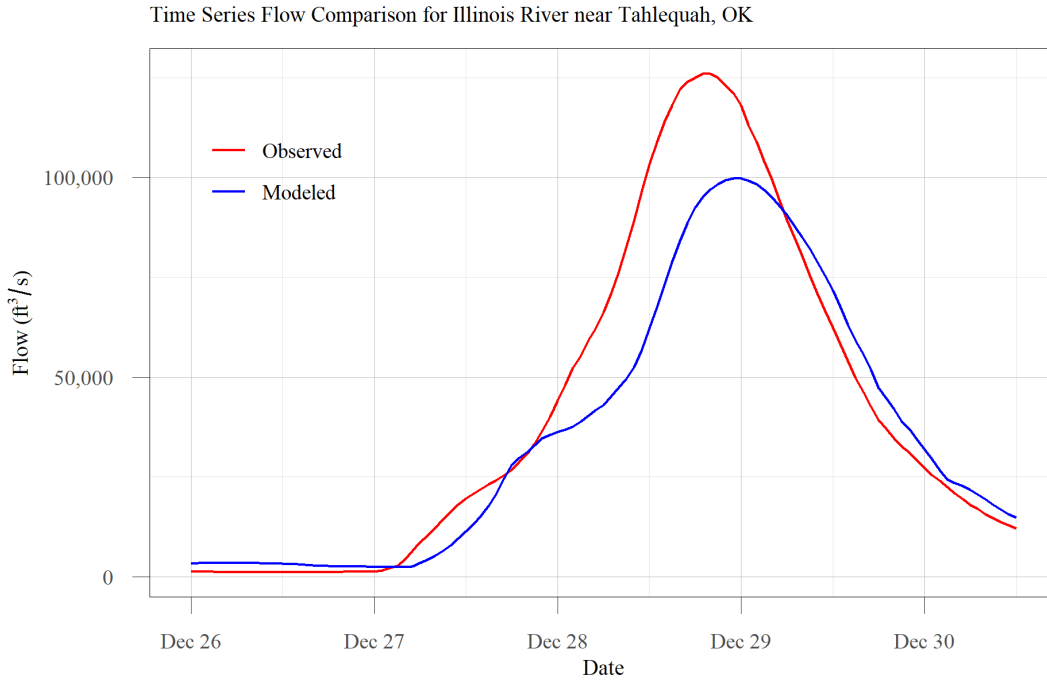
Goodness of Fit Table

Parameter	Maximum Simulated (feet or cfs)	Maximum Observed (feet or cfs)	Normalized RMSE (%)	PBIAS (%)	RSR	NSE	R^2
Elevation	693.3	695.8	25.4	-0.1	0.25	0.93	0.95
Flow	99,702	126,000	36.0	-13.1	0.36	0.87	0.91
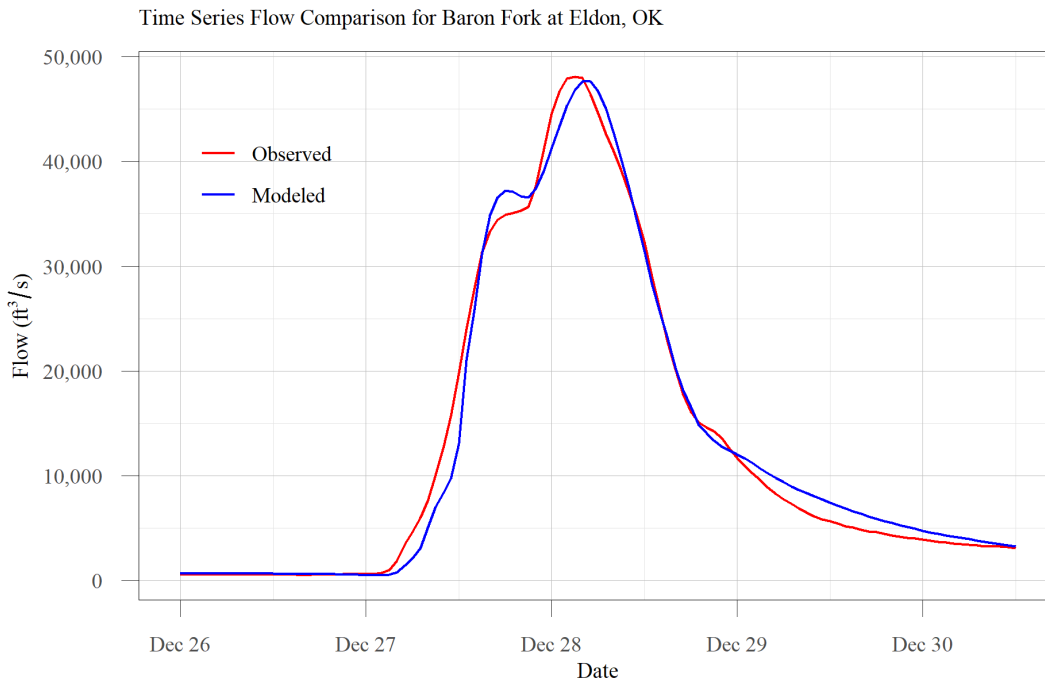
Baron Fork at Eldon, OK, Time Series Comparison

Time Series Flow Comparison for Baron Fork at Eldon, OK

Goodness of Fit Table

Parameter	Maximum Simulated (feet or cfs)	Maximum Observed (feet or cfs)	Normalized RMSE (%)	PBIAS (%)	RSR	NSE	R^2
Elevation	726.4	726.7	18.4	0.0	0.18	0.97	0.97
Flow	47,648	48,100	10.6	0.5	0.11	0.99	0.99
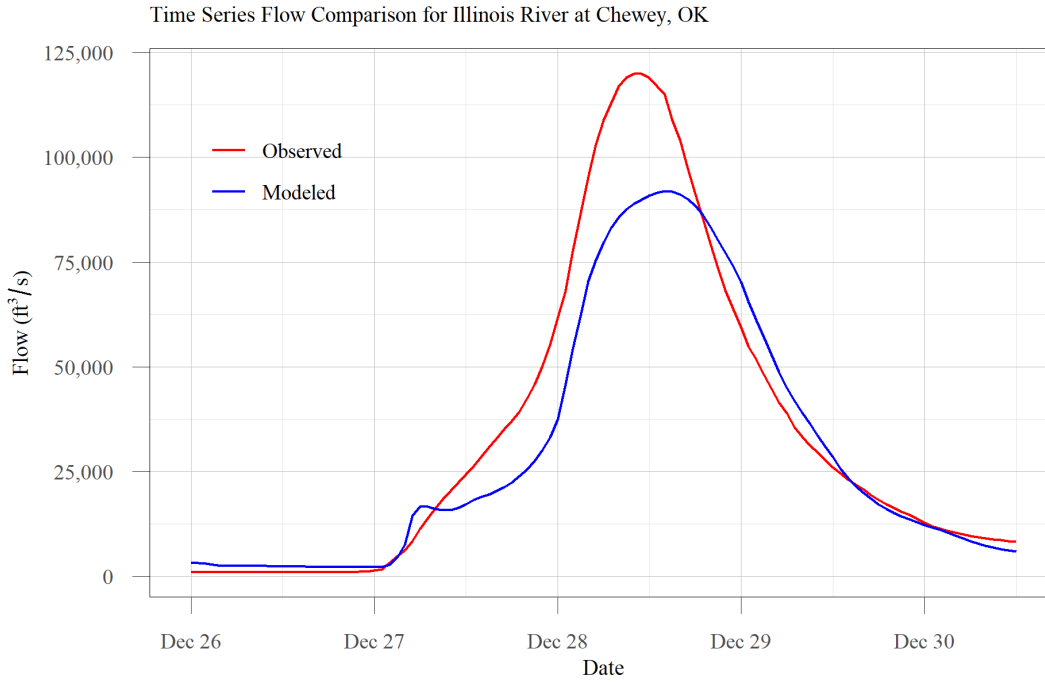
Illinois River at Chewey, OK, Time Series Comparison

Time Series Flow Comparison for Illinois River at Chewey, OK

Goodness of Fit Table

Parameter	Maximum Simulated (feet or cfs)	Maximum Observed (feet or cfs)	Normalized RMSE (%)	PBIAS (%)	RSR	NSE	R^2
Elevation	830.5	833.2	26.0	-0.1	0.26	0.93	0.95
Flow	91,939	120,000	32.6	-13.0	0.33	0.89	0.93
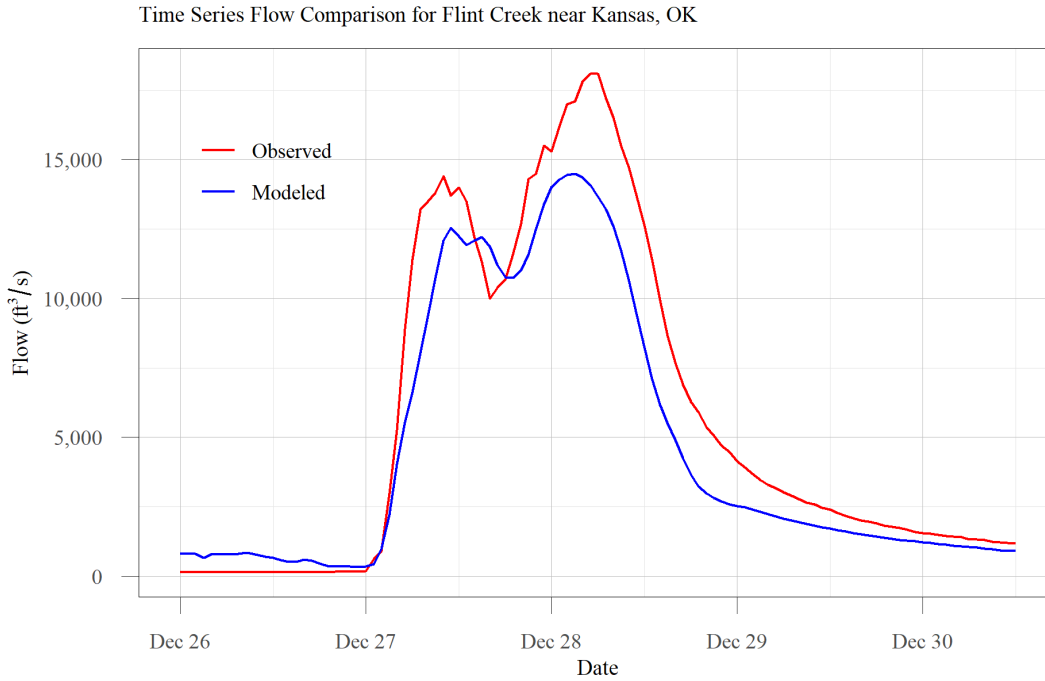
Flint Creek near Kansas, OK, Time Series Comparison

Time Series Flow Comparison for Flint Creek near Kansas, OK

Goodness of Fit Table

Parameter	Maximum Simulated (feet or cfs)	Maximum Observed (feet or cfs)	Normalized RMSE (%)	PBIAS (%)	RSR	NSE	R^2
Elevation	869.5	871	20.1	0.0	0.2	0.96	0.97
Flow	14,485	18,100	32.5	-19.6	0.32	0.89	0.95

Flint Creek near West Siloam Springs, OK, Time Series Comparison

Time Series Flow Comparison for Flint Creek near West Siloam Springs, OK
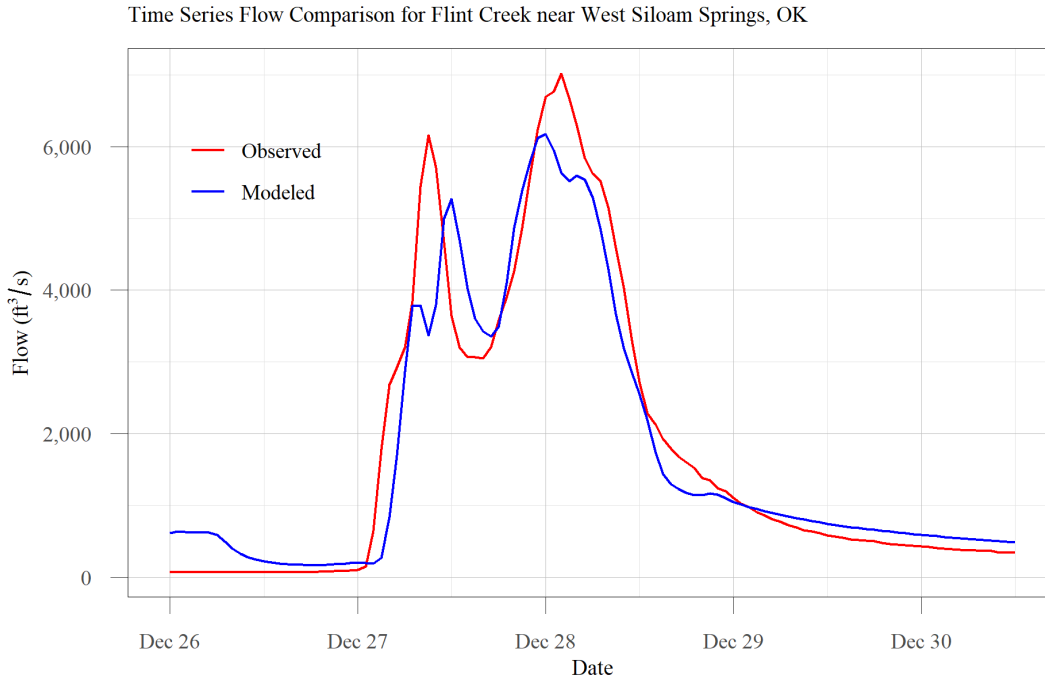
Goodness of Fit Table

Parameter	Maximum Simulated (feet or cfs)	Maximum Observed (feet or cfs)	Normalized RMSE (%)	PBIAS (%)	RSR	NSE	R^2
Elevation	969.2	970.2	36.8	0.0	0.37	0.86	0.89
Flow	6,175	7,020	29.7	-3.0	0.3	0.91	0.92
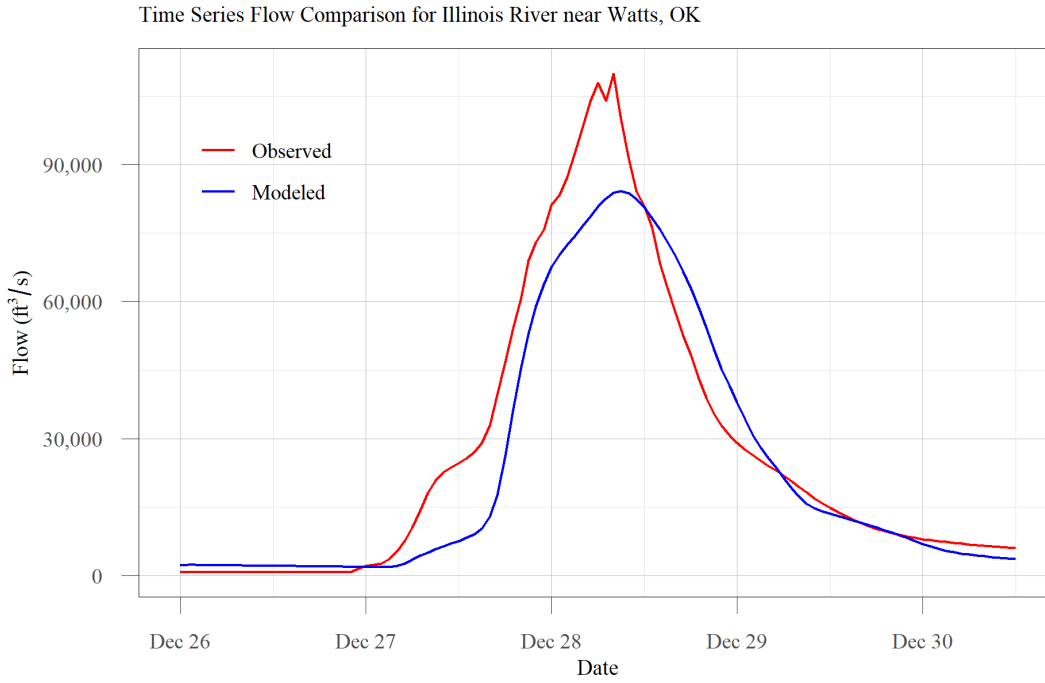
Illinois River near Watts, OK, Time Series Comparison

Time Series Flow Comparison for Illinois River near Watts, OK

Goodness of Fit Table

Parameter	Maximum Simulated (feet or cfs)	Maximum Observed (feet or cfs)	Normalized RMSE (%)	PBIAS (%)	RSR	NSE	R²
Elevation	920.5	922.6	64.6	-0.5	0.65	0.58	0.9
Flow	84,267	110,000	32.1	-12.1	0.32	0.9	0.91

Illinois River South of Siloam Springs, AR, Time Series Comparison

Time Series Flow Comparison for Illinois River South of Siloam Springs, AR
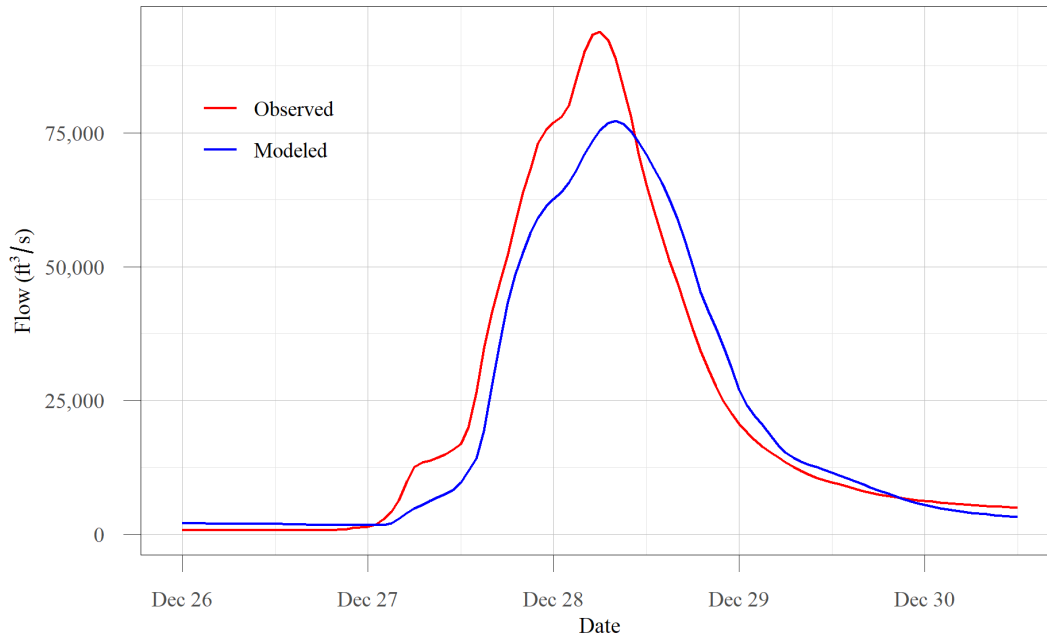
Goodness of Fit Table

Parameter	Maximum Simulated (feet or cfs)	Maximum Observed (feet or cfs)	Normalized RMSE (%)	PBIAS (%)	RSR	NSE	R^2
Elevation	938	940	28.0	-0.1	0.28	0.92	0.93
Flow	77,203	93,900	26.2	-6.7	0.26	0.93	0.94

Illinois River at Hwy. 16 near Siloam Springs, AR, Time Series Comparison

Time Series Flow Comparison for Illinois River at Hwy. 16 near Siloam Springs AR
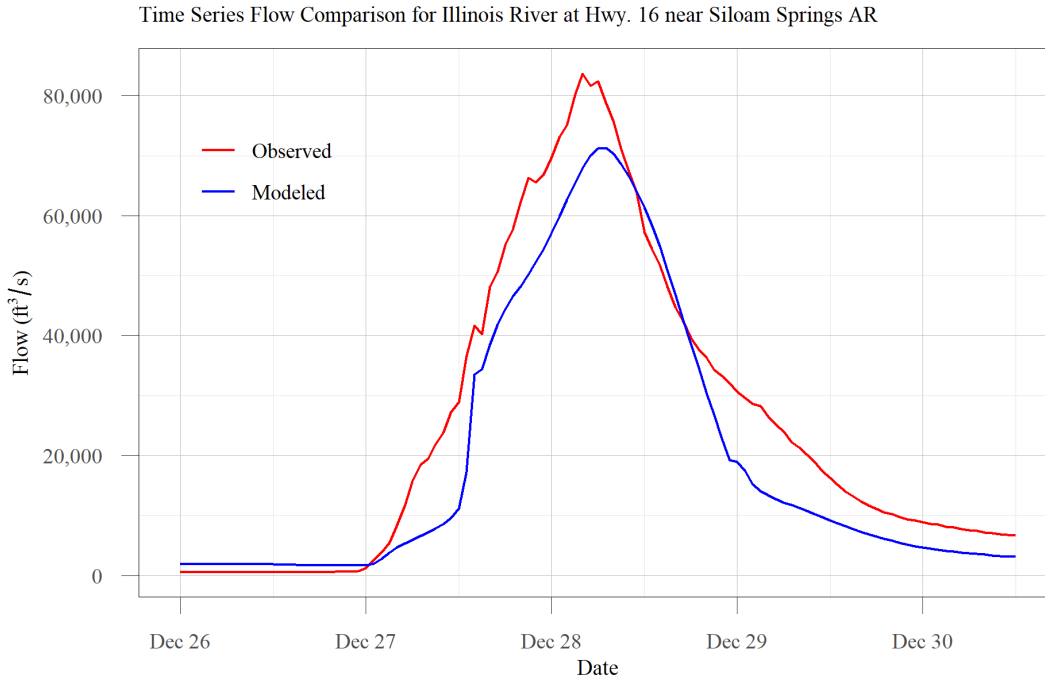
Goodness of Fit Table

Parameter	Maximum Simulated (feet or cfs)	Maximum Observed (feet or cfs)	Normalized RMSE (%)	PBIAS (%)	RSR	NSE	R^2
Elevation	957.9	959	19.2	0.0	0.19	0.96	0.96
Flow	71,270	83,700	31.8	-21.5	0.32	0.9	0.95
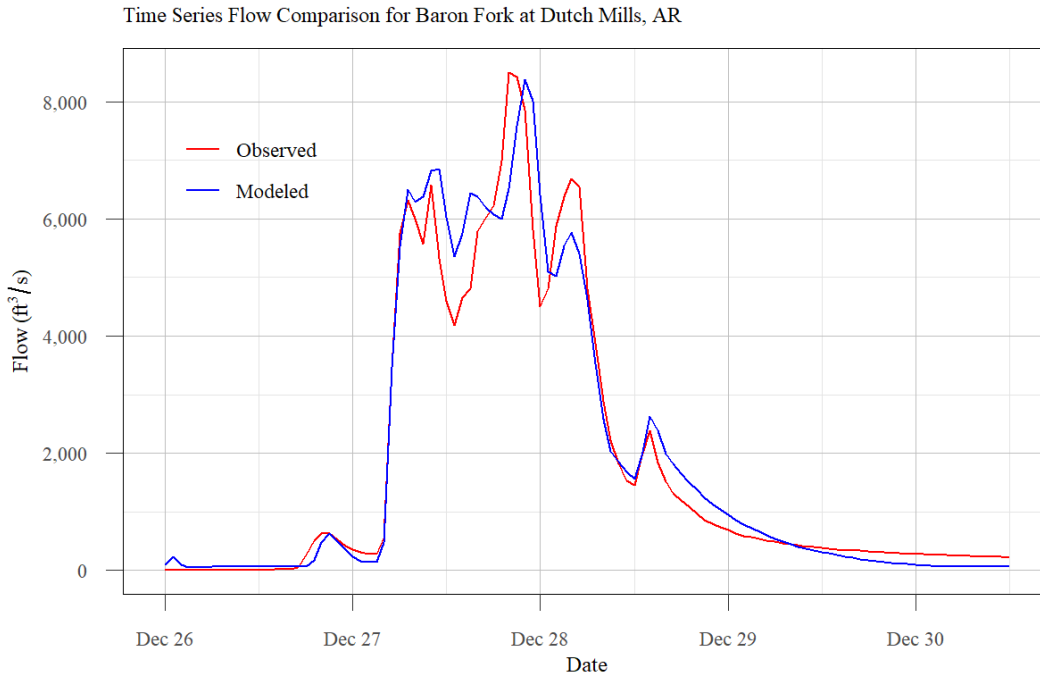
Baron Fork at Dutch Mills, AR, Time Series Comparison

Time Series Flow Comparison for Baron Fork at Dutch Mills, AR

Goodness of Fit Table

Parameter	Maximum Simulated (feet or cfs)	Maximum Observed (feet or cfs)	Normalized RMSE (%)	PBIAS (%)	RSR	NSE	R^2
Elevation	964.3	996.3	1394.1	-3.5	13.94	-195.2	0.87
Flow	8,376	8,490	22.5	3.1	0.22	0.95	0.95
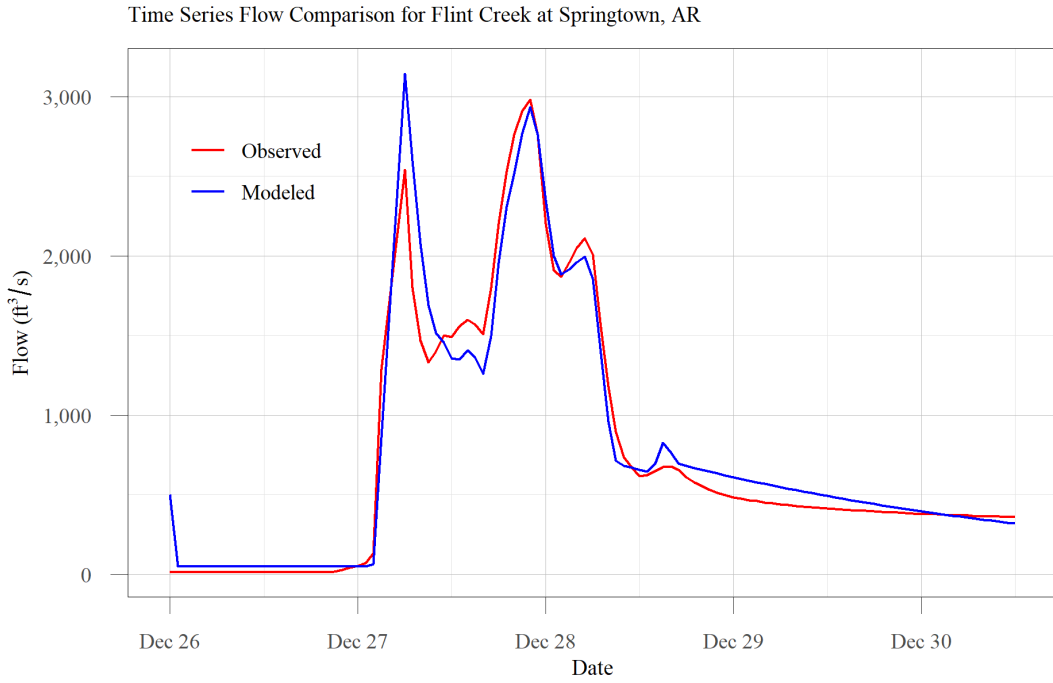
Flint Creek at Springtown, AR, Time Series Comparison

Time Series Flow Comparison for Flint Creek at Springtown, AR

Goodness of Fit Table

Parameter	Maximum Simulated (feet or cfs)	Maximum Observed (feet or cfs)	Normalized RMSE (%)	PBIAS (%)	RSR	NSE	R^2
Elevation	1,186.3	1,182.2	183.6	0.3	1.84	-2.4	0.91
Flow	3,145	2,980	21.1	3.7	0.21	0.95	0.96
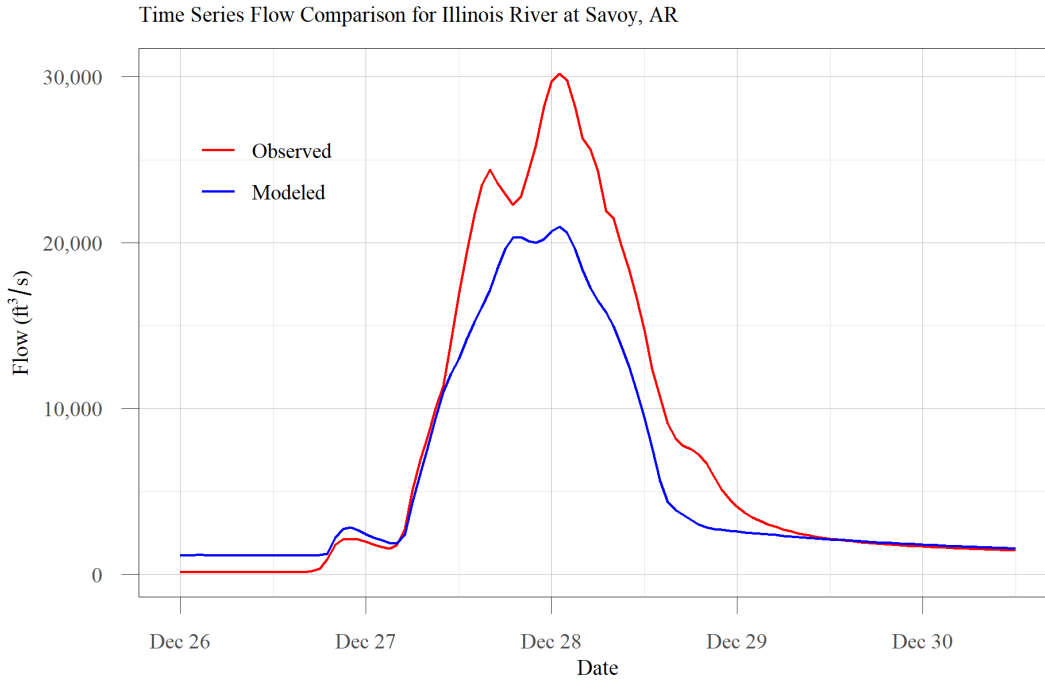
186

Illinois River at Savoy, AR, Time Series Comparison

Time Series Flow Comparison for Illinois River at Savoy, AR

Goodness of Fit Table

Parameter	Maximum Simulated (feet or cfs)	Maximum Observed (feet or cfs)	Normalized RMSE (%)	PBIAS (%)	RSR	NSE	R^2
Elevation	1,035.3	1,038.6	48.0	-0.1	0.48	0.77	0.87
Flow	20,972	30,200	37.2	-22.6	0.37	0.86	0.97

Osage Creek near Elm Springs, AR, Time Series Comparison
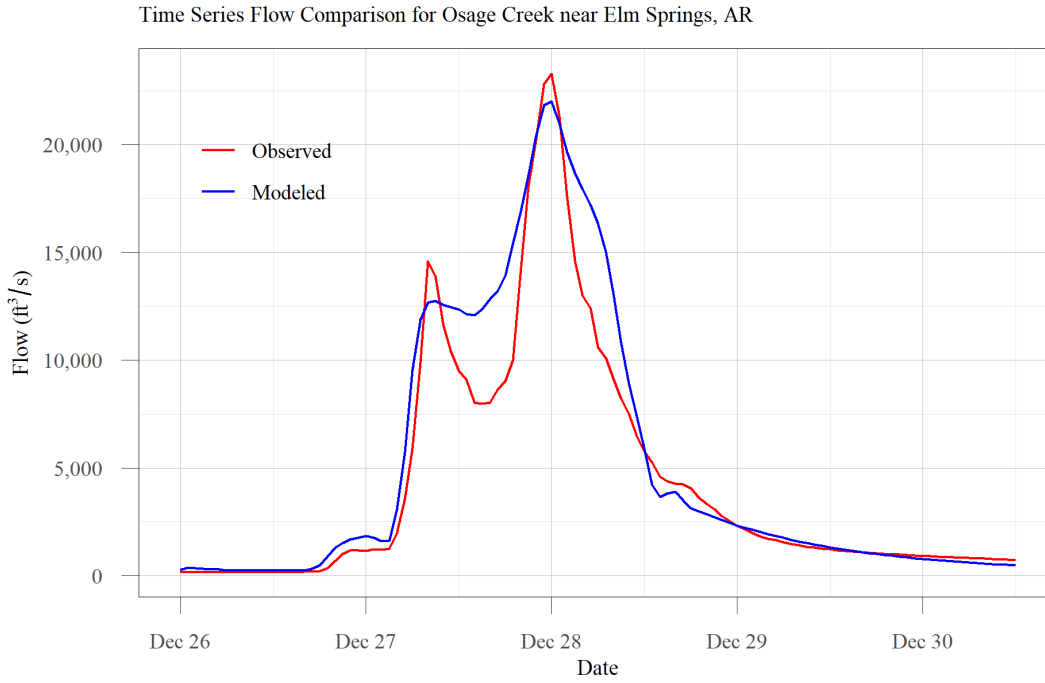
Time Series Flow Comparison for Osage Creek near Elm Springs, AR

Goodness of Fit Table

Parameter	Maximum Simulated (feet or cfs)	Maximum Observed (feet or cfs)	Normalized RMSE (%)	PBIAS (%)	RSR	NSE	R^2
Elevation	1,070.8	1,070.9	30.0	-0.1	0.3	0.91	0.97
Flow	22,000	23,300	32.1	16.4	0.32	0.9	0.94
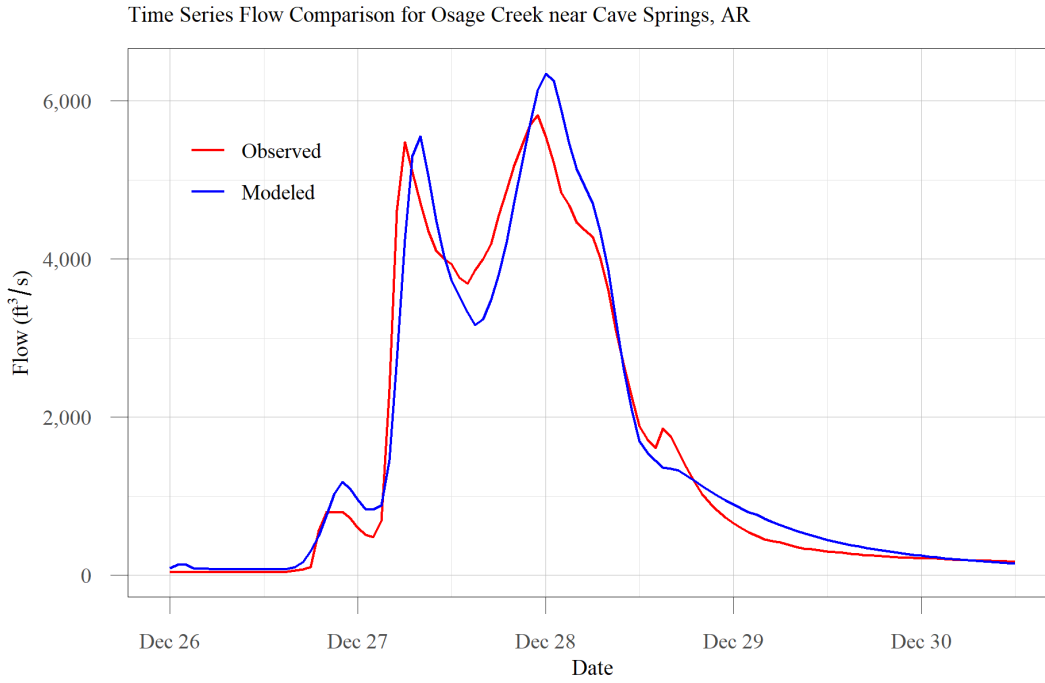
Osage Creek near Cave Springs, AR, Time Series Comparison

Time Series Flow Comparison for Osage Creek near Cave Springs, AR

Goodness of Fit Table

Parameter	Maximum Simulated (feet or cfs)	Maximum Observed (feet or cfs)	Normalized RMSE (%)	PBIAS (%)	RSR	NSE	R^2
Elevation	1,142	1,142.5	19.8	0.0	0.2	0.96	0.97
Flow	6,347	5,820	21.0	2.9	0.21	0.96	0.96

April 2017 Validation Event

Illinois River near Tahlequah, OK, Time Series Comparison

Time Series Flow Comparison for Illinois River near Tahlequah, OK
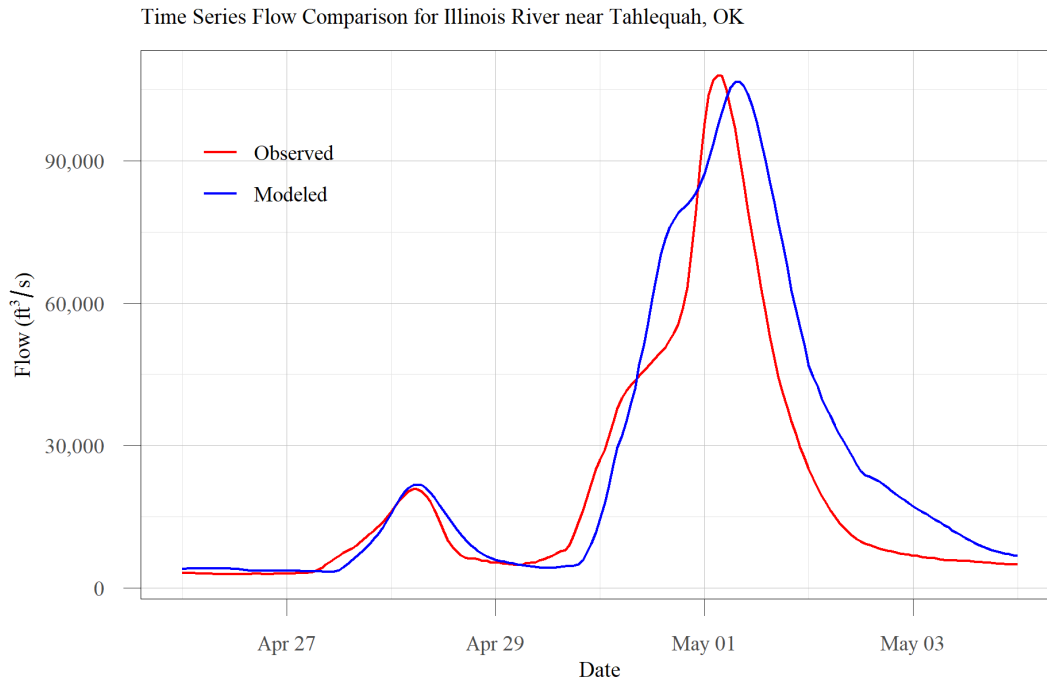
Goodness of Fit Table

Parameter	Maximum Simulated (feet or cfs)	Maximum Observed (feet or cfs)	Normalized RMSE (%)	PBIAS (%)	RSR	NSE	R^2
Elevation	694.1	694.4	45.7	0.2	0.46	0.79	0.86
Flow	106,792	108,000	45.0	24.9	0.45	0.8	0.88
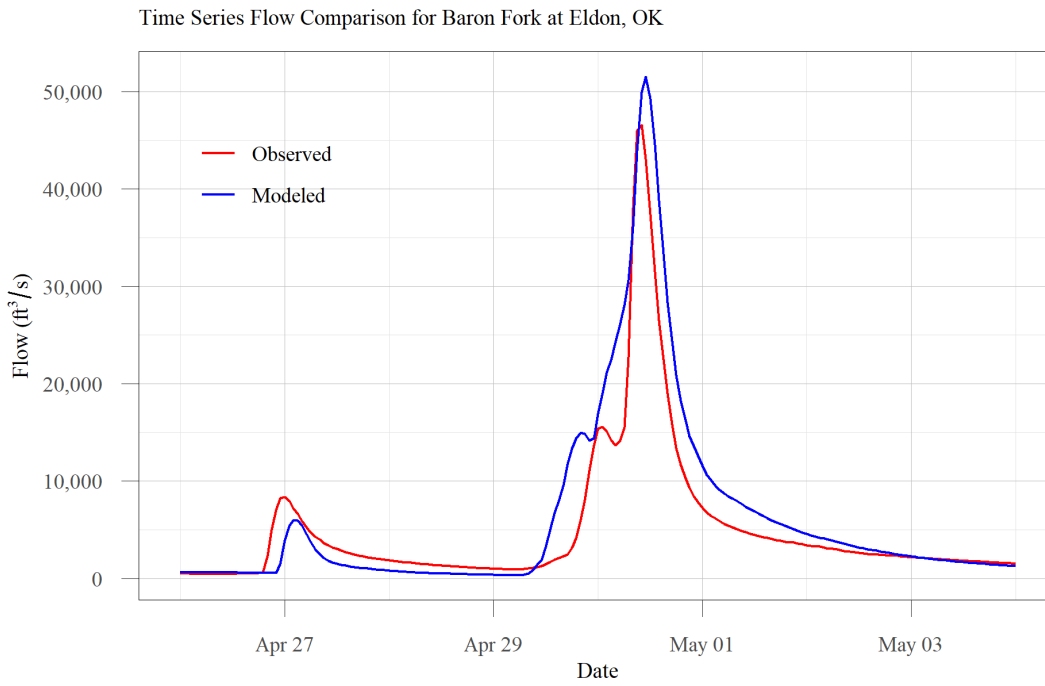
Baron Fork at Eldon, OK, Time Series Comparison

Time Series Flow Comparison for Baron Fork at Eldon, OK

Goodness of Fit Table

Parameter	Maximum Simulated (feet or cfs)	Maximum Observed (feet or cfs)	Normalized RMSE (%)	PBIAS (%)	RSR	NSE	R^2
Elevation	27.2	726.4	73.2	0.0	0.73	0.46	0.79
Flow	51,559	46,600	47.0	24.7	0.47	0.78	0.91
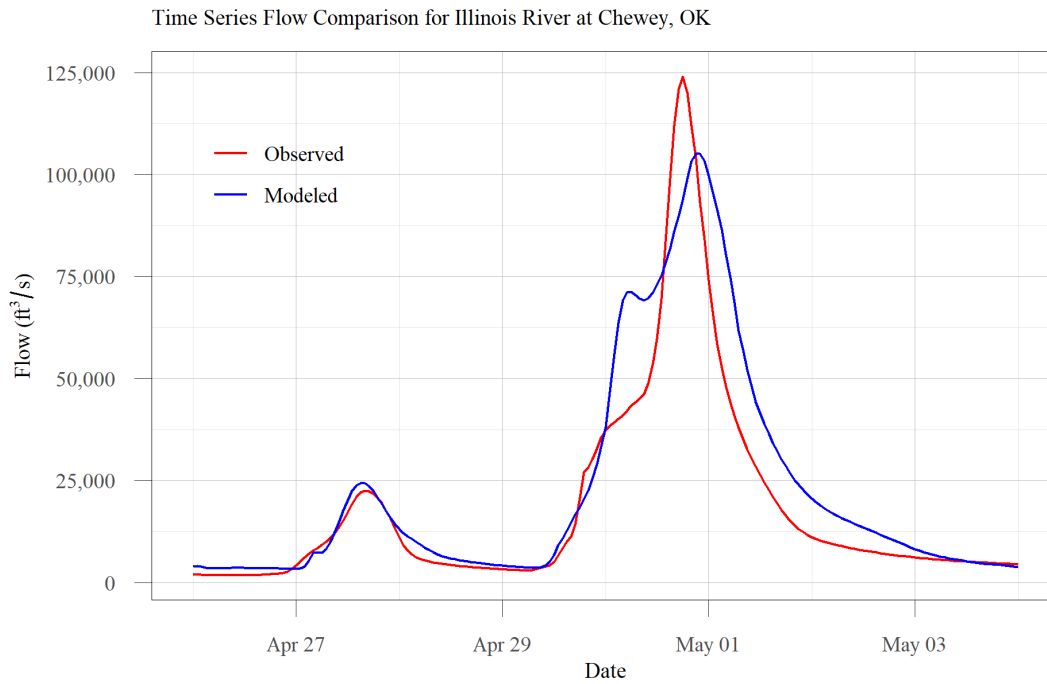
Illinois River at Chewey, OK, Time Series Comparison

Time Series Flow Comparison for Illinois River at Chewey, OK

Goodness of Fit Table

Parameter	Maximum Simulated (feet or cfs)	Maximum Observed (feet or cfs)	Normalized RMSE (%)	PBIAS (%)	RSR	NSE	R^2
Elevation	832.2	833.5	33.1	0.1	0.33	0.89	0.93
Flow	105,100	124,000	41.7	23.8	0.42	0.83	0.88
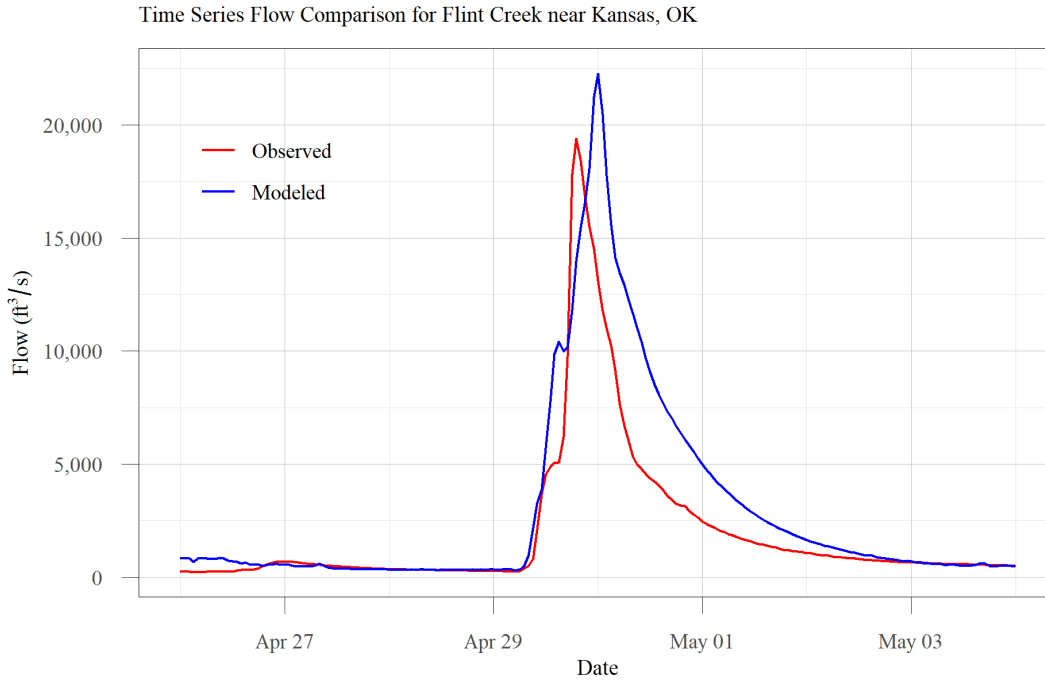
Flint Creek near Kansas, OK, Time Series Comparison

Time Series Flow Comparison for Flint Creek near Kansas, OK

Goodness of Fit Table

Parameter	Maximum Simulated (feet or cfs)	Maximum Observed (feet or cfs)	Normalized RMSE (%)	PBIAS (%)	RSR	NSE	R^2
Elevation	872.1	873.3	68.5	0.0	0.68	0.53	0.75
Flow	22,268	19,400	62.5	47.4	0.62	0.61	0.83

Flint Creek near West Siloam Springs, OK, Time Series Comparison

Time Series Flow Comparison for Flint Creek near West Siloam Springs, OK
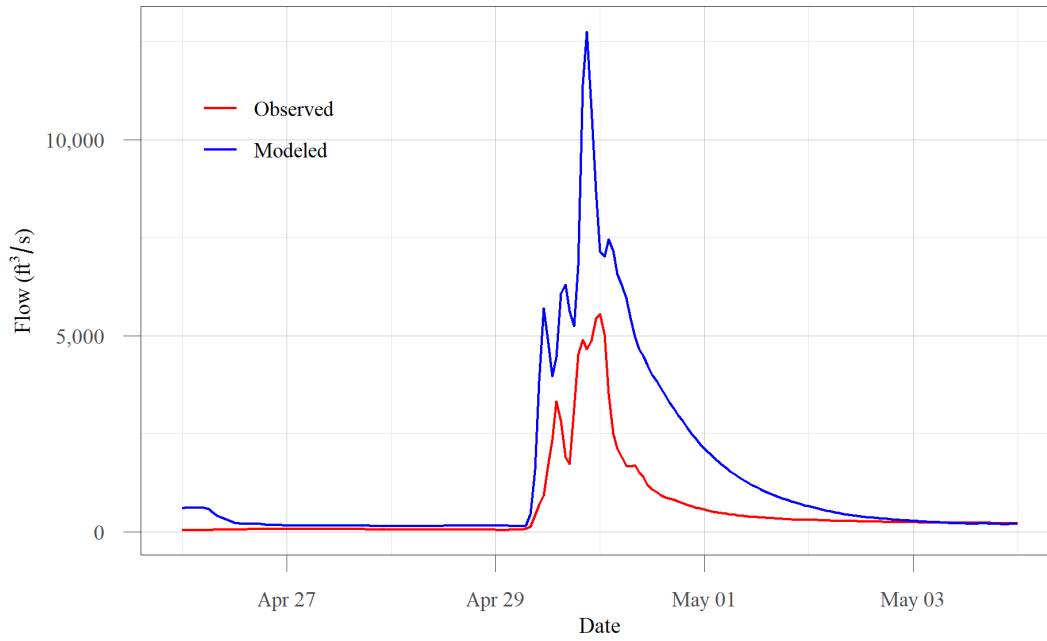
Goodness of Fit Table

Parameter	Maximum Simulated (feet or cfs)	Maximum Observed (feet or cfs)	Normalized RMSE (%)	PBIAS (%)	RSR	NSE	R^2
Elevation	972	969.3	77.7	0.1	0.78	0.39	0.9
Flow	12,753	5,560	152.4	145.6	1.52	-1.33	0.85
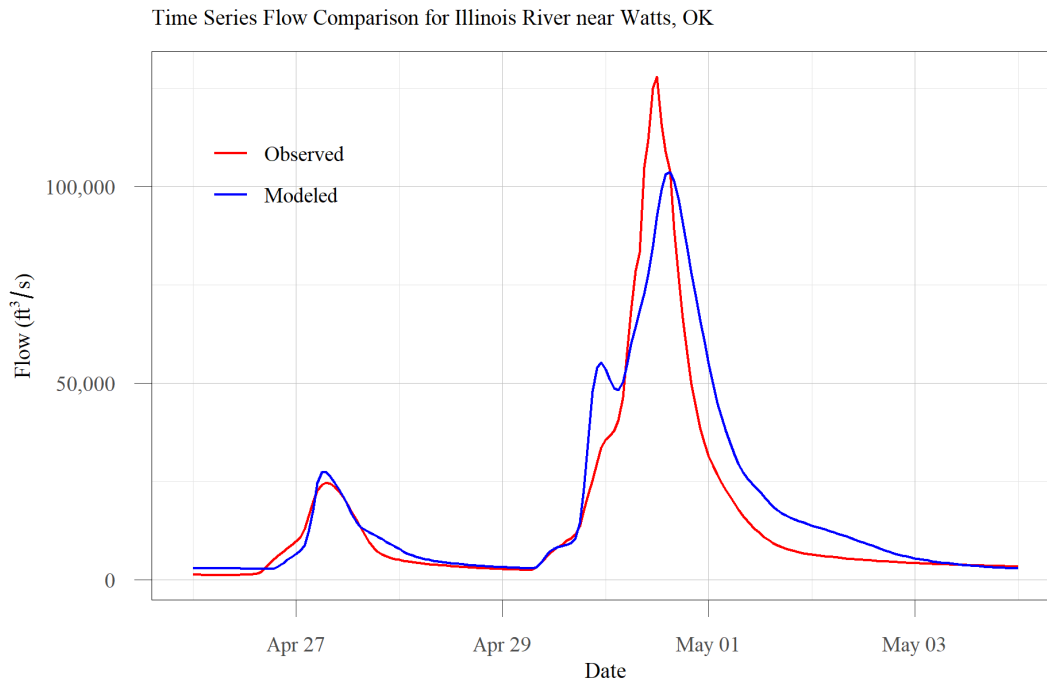
Illinois River near Watts, OK, Time Series Comparison

Time Series Flow Comparison for Illinois River near Watts, OK

Goodness of Fit Table

Parameter	Maximum Simulated (feet or cfs)	Maximum Observed (feet or cfs)	Normalized RMSE (%)	PBIAS (%)	RSR	NSE	R^2
Elevation	922.1	924.1	58.8	-0.2	0.59	0.65	0.87
Flow	103,695	128,000	38.5	18.8	0.39	0.85	0.87

Illinois River South of Siloam Springs, AR, Time Series Comparison

Time Series Flow Comparison for Illinois River South of Siloam Springs, AR
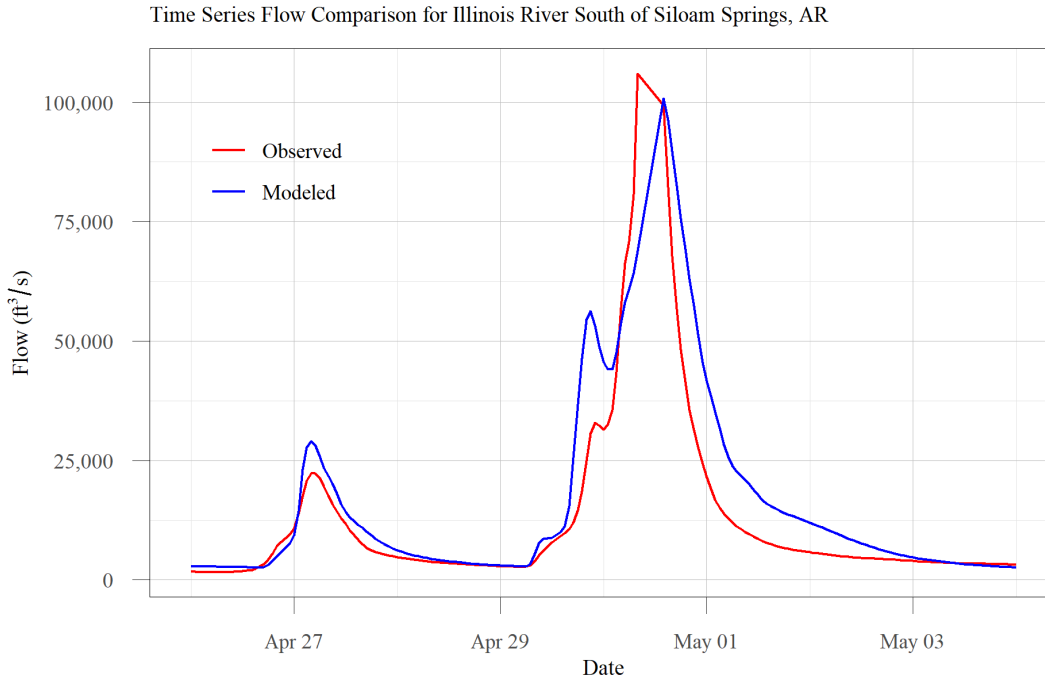
Goodness of Fit Table

Parameter	Maximum Simulated (feet or cfs)	Maximum Observed (feet or cfs)	Normalized RMSE (%)	PBIAS (%)	RSR	NSE	R^2
Elevation	940.2	941.7	41.2	0.2	0.41	0.83	0.9
Flow	100,811	106,000	52.3	36.4	0.52	0.72	0.84

Illinois River at Hwy. 16 near Siloam Springs, AR, Time Series Comparison

Time Series Flow Comparison for Illinois River at Hwy. 16 near Siloam Springs AR
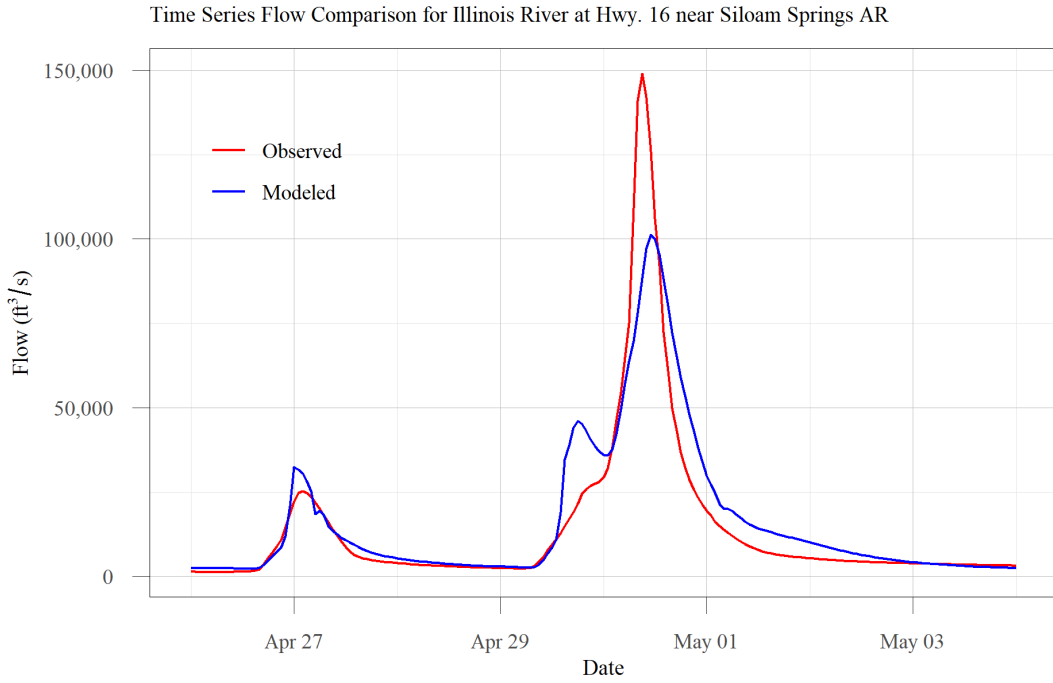

Goodness of Fit Table

Parameter	Maximum Simulated (feet or cfs)	Maximum Observed (feet or cfs)	Normalized RMSE (%)	PBIAS (%)	RSR	NSE	R^2
Elevation	960.3	961.8	47.3	0.2	0.47	0.78	0.9
Flow	101,191	149,000	41.1	13.8	0.41	0.83	0.84
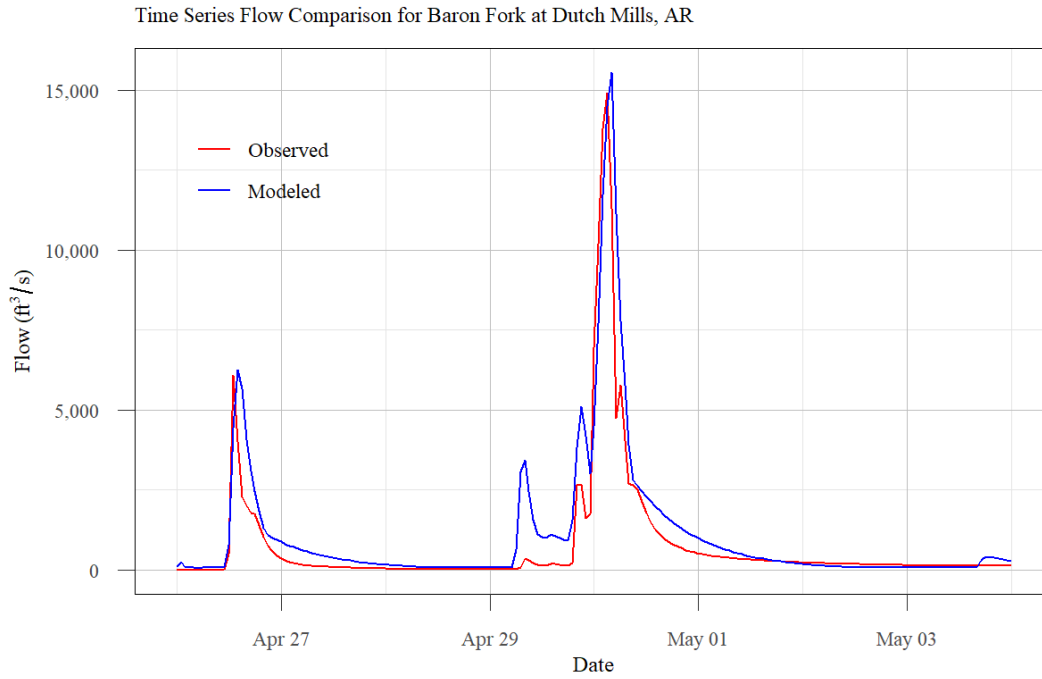
Baron Fork at Dutch Mills, AR, Time Series Comparison

Time Series Flow Comparison for Baron Fork at Dutch Mills, AR

Goodness of Fit Table

Parameter	Maximum Simulated (feet or cfs)	Maximum Observed (feet or cfs)	Normalized RMSE (%)	PBIAS (%)	RSR	NSE	R^2
Elevation	967.9	999.5	1900.2	-3.5	19	-361.9	0.68
Flow	15,539	14,900	46.2	44.9	0.46	0.79	0.85
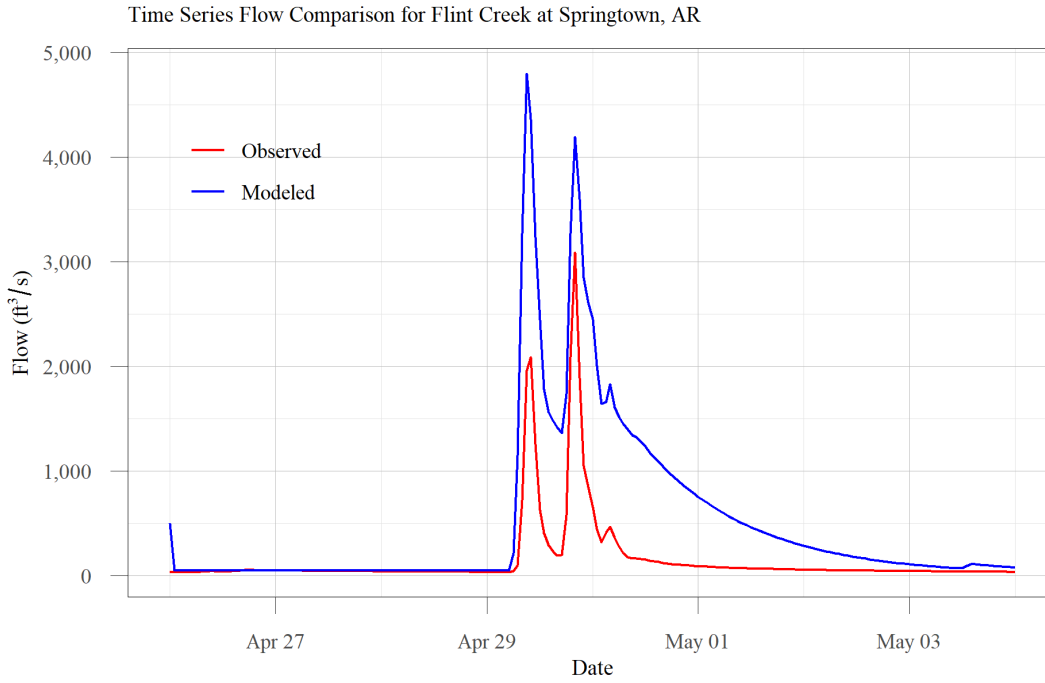
Flint Creek at Springtown, AR, Time Series Comparison

Time Series Flow Comparison for Flint Creek at Springtown, AR

Goodness of Fit Table

Parameter	Maximum Simulated (feet or cfs)	Maximum Observed (feet or cfs)	Normalized RMSE (%)	PBIAS (%)	RSR	NSE	R^2
Elevation	1,186.8	1,183.4	289.4	0.3	2.89	-7.42	0.63
Flow	4,801	3,090	173.4	235.6	1.73	-2.02	0.77
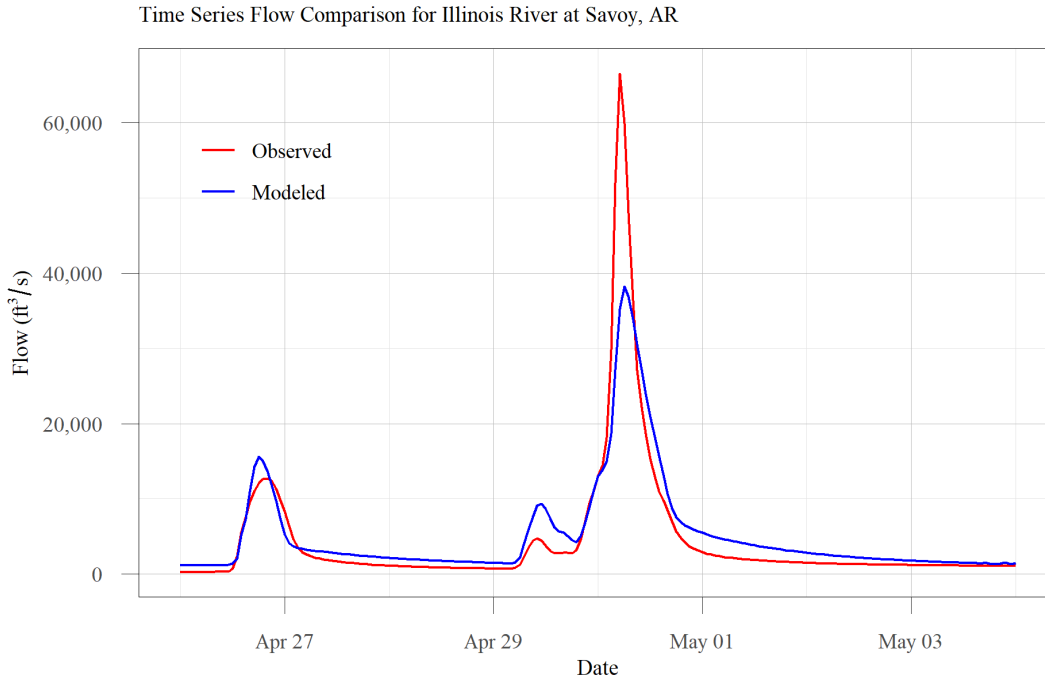
Illinois River at Savoy, AR, Time Series Comparison

Time Series Flow Comparison for Illinois River at Savoy, AR

Goodness of Fit Table

Parameter	Maximum Simulated (feet or cfs)	Maximum Observed (feet or cfs)	Normalized RMSE (%)	PBIAS (%)	RSR	NSE	R^2
Elevation	1,039.3	1,044.8	44.2	0.1	0.44	0.8	0.92
Flow	38,232	66,500	42.0	13.9	0.42	0.82	0.87
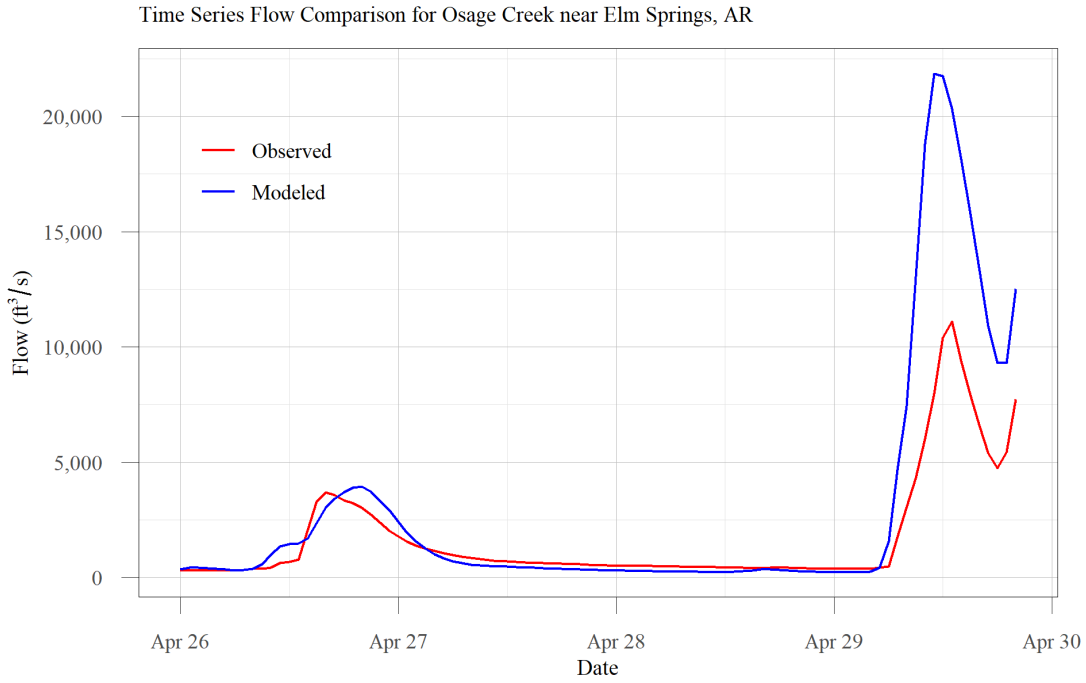
Osage Creek near Elm Springs, AR, Time Series Comparison

Time Series Flow Comparison for Osage Creek near Elm Springs, AR

Goodness of Fit Table

Parameter	Maximum Simulated (feet or cfs)	Maximum Observed (feet or cfs)	Normalized RMSE (%)	PBIAS (%)	RSR	NSE	R^2
Elevation	1,070.7	1,068.8	85.4	-0.1	0.85	0.26	0.92
Flow	21,858	11,100	132.8	64.9	1.33	-0.78	0.92

Osage Creek near Cave Springs, AR, Time Series Comparison

Time Series Flow Comparison for Osage Creek near Cave Springs, AR
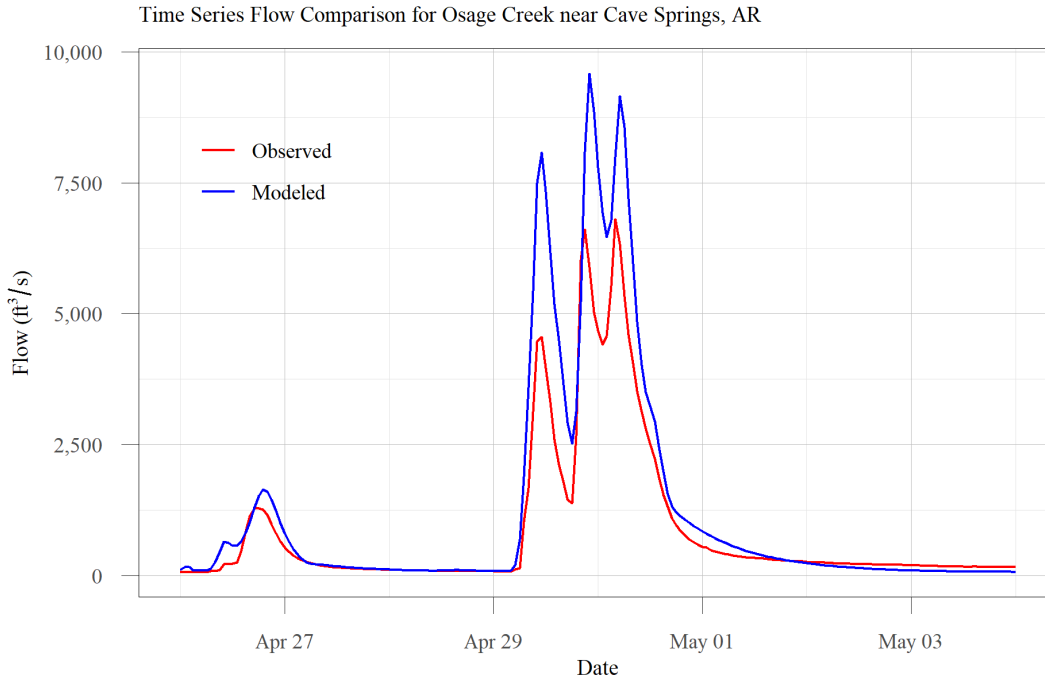
Goodness of Fit Table

Parameter	Maximum Simulated (feet or cfs)	Maximum Observed (feet or cfs)	Normalized RMSE (%)	PBIAS (%)	RSR	NSE	R^2
Elevation	1,143.4	1,143.5	35.4	0.0	0.35	0.87	0.94
Flow	586	6810	61.8	41.7	0.62	0.62	0.95

Appendix C

Scenario time-series plots using the 2017 gridded precipitation

2017 Event 07196900 Baron Fork at Dutch Mills, AR
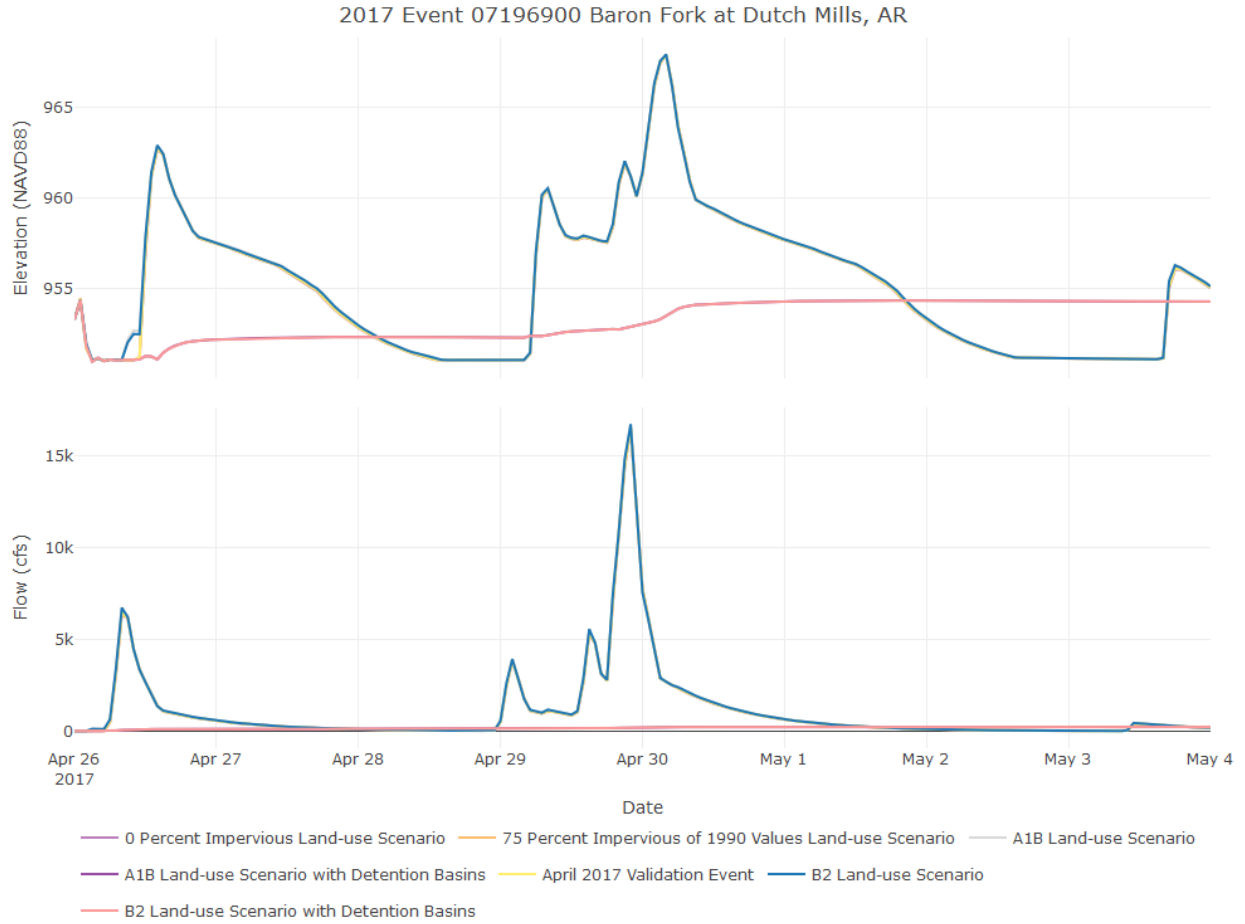
2017 Event 07197000 Baron Fork at Eldon, OK

Legend:
- 0 Percent Impervious Land-use Scenario
- 75 Percent Impervious of 1990 Values Land-use Scenario
- A1B Land-use Scenario
- A1B Land-use Scenario with Detention Basins
- April 2017 Validation Event
- B2 Land-use Scenario
- B2 Land-use Scenario with Detention Basins
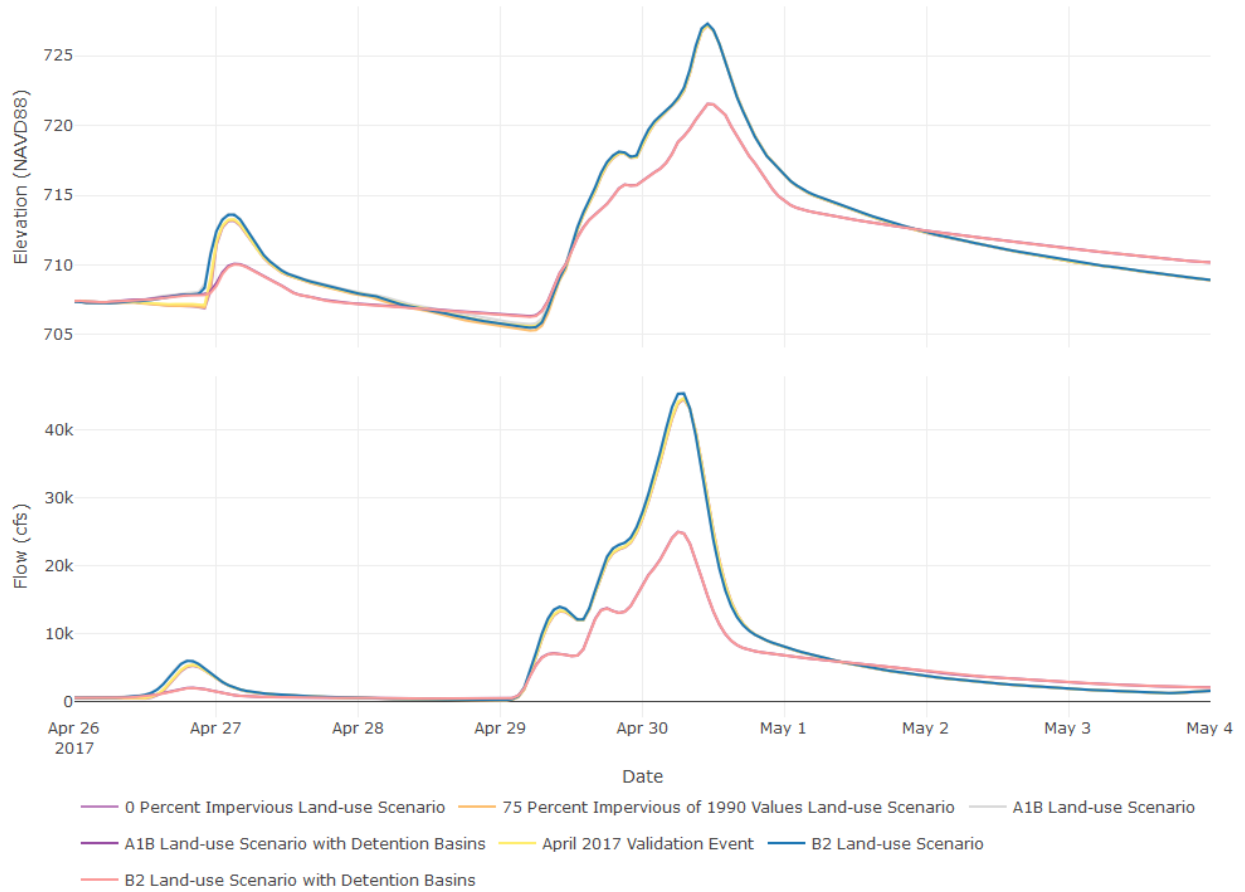
2017 Event 07196500 Illinois River near Tahlequah, OK
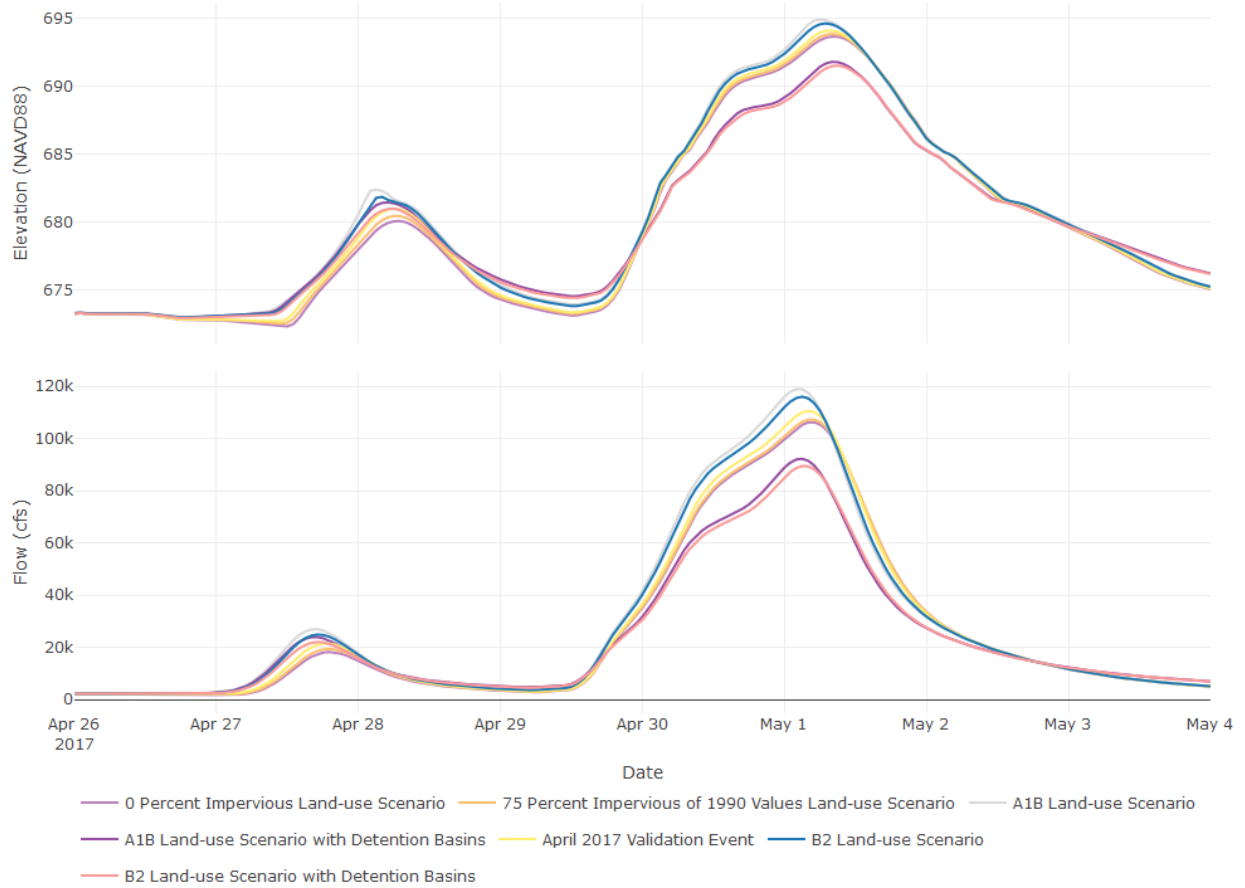
2017 Event 07195500 Illinois River near Watts, OK
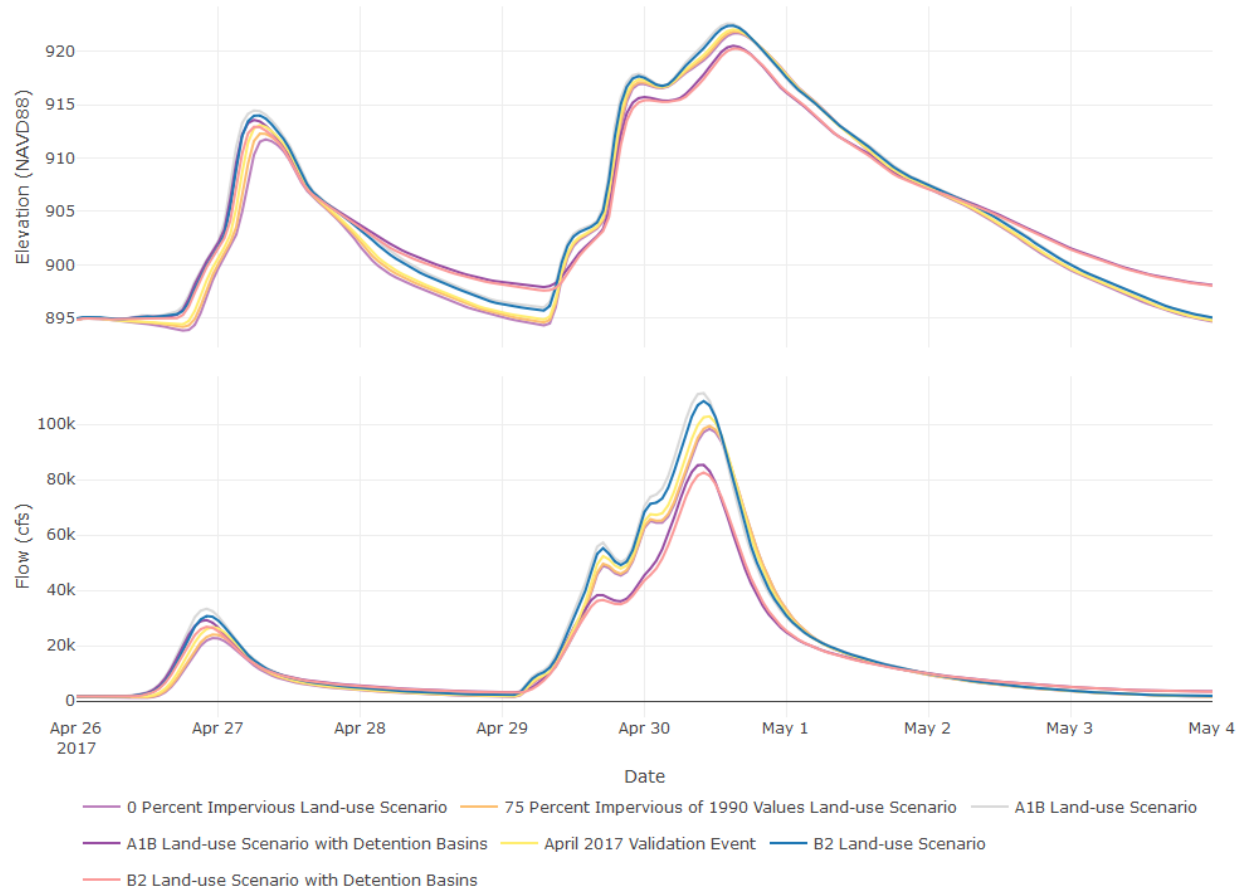
2017 Event 07195430 Illinois River South of Siloam Springs, AR
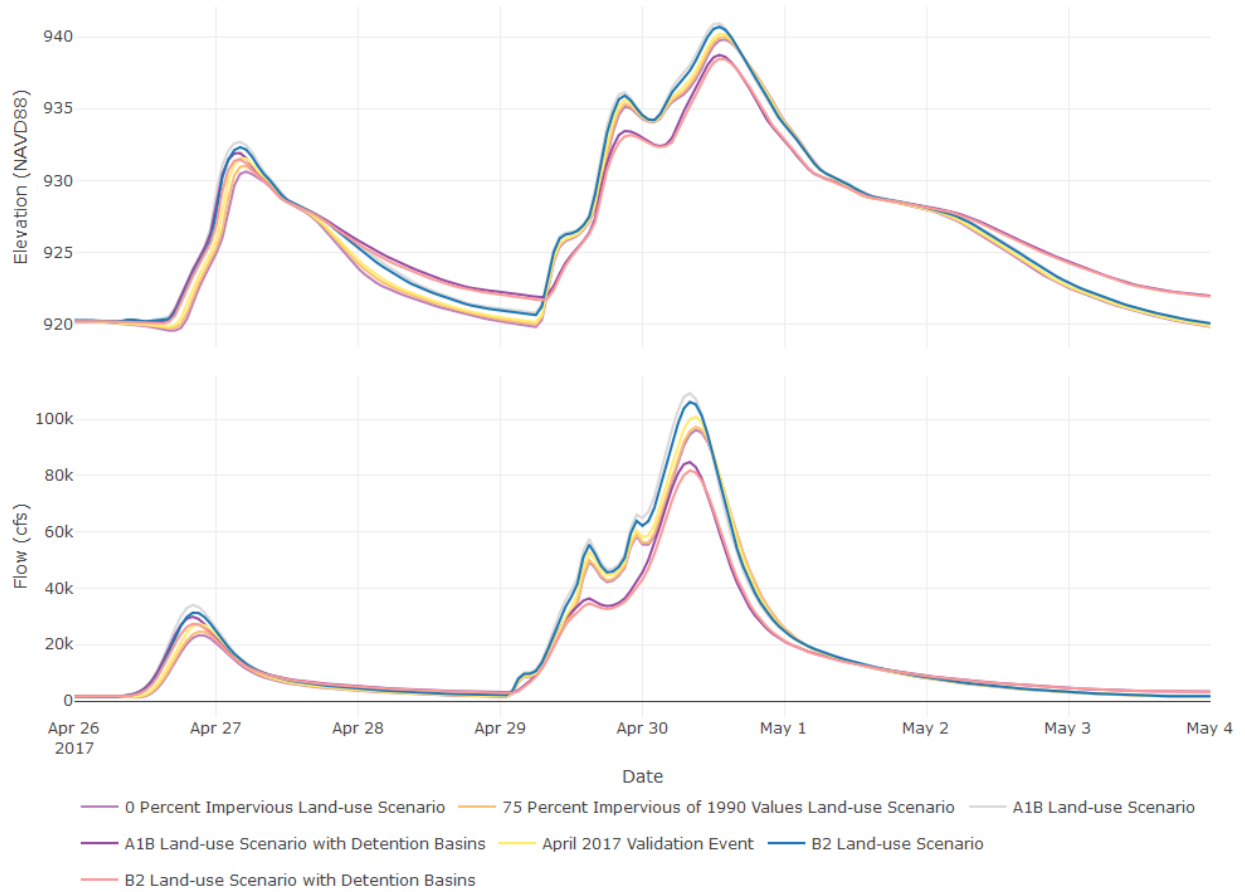
2017 Event 07194880 Osage Creek near Cave Springs, AR
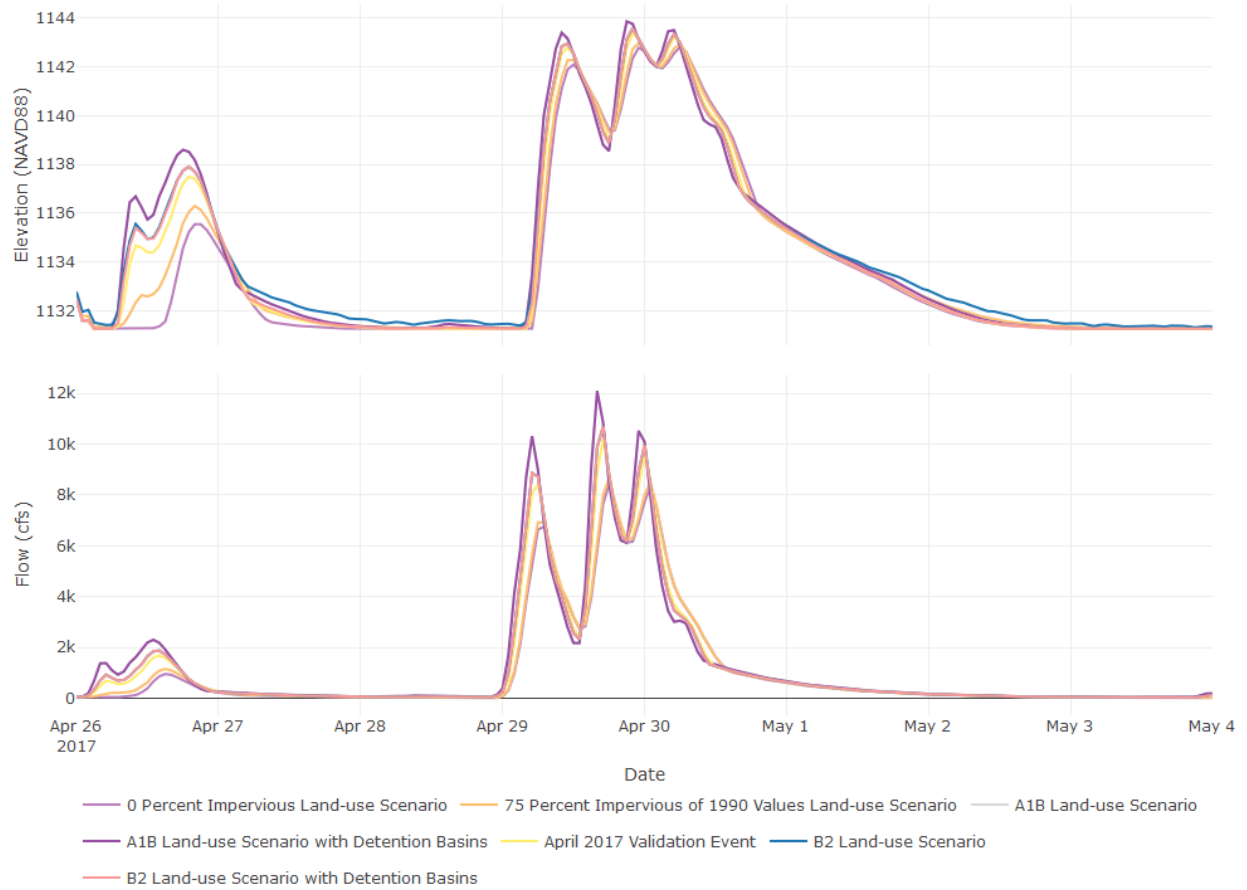
2017 Event 07195000 Osage Creek near Elm Springs, AR
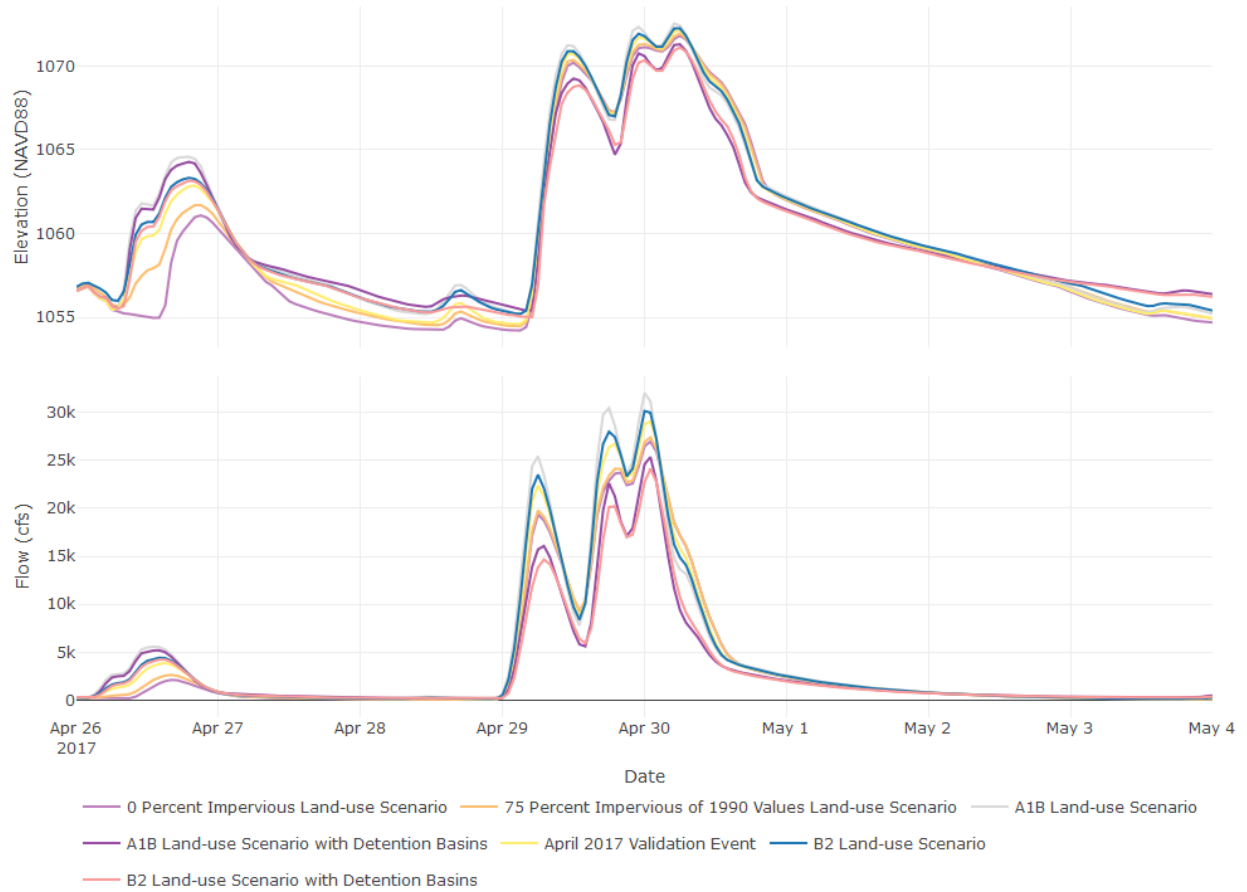
2017 Event 07195800 Flint Creek at Springtown, AR

Legend:
- 0 Percent Impervious Land-use Scenario
- 75 Percent Impervious of 1990 Values Land-use Scenario
- A1B Land-use Scenario
- A1B Land-use Scenario with Detention Basins
- April 2017 Validation Event
- B2 Land-use Scenario
- B2 Land-use Scenario with Detention Basins
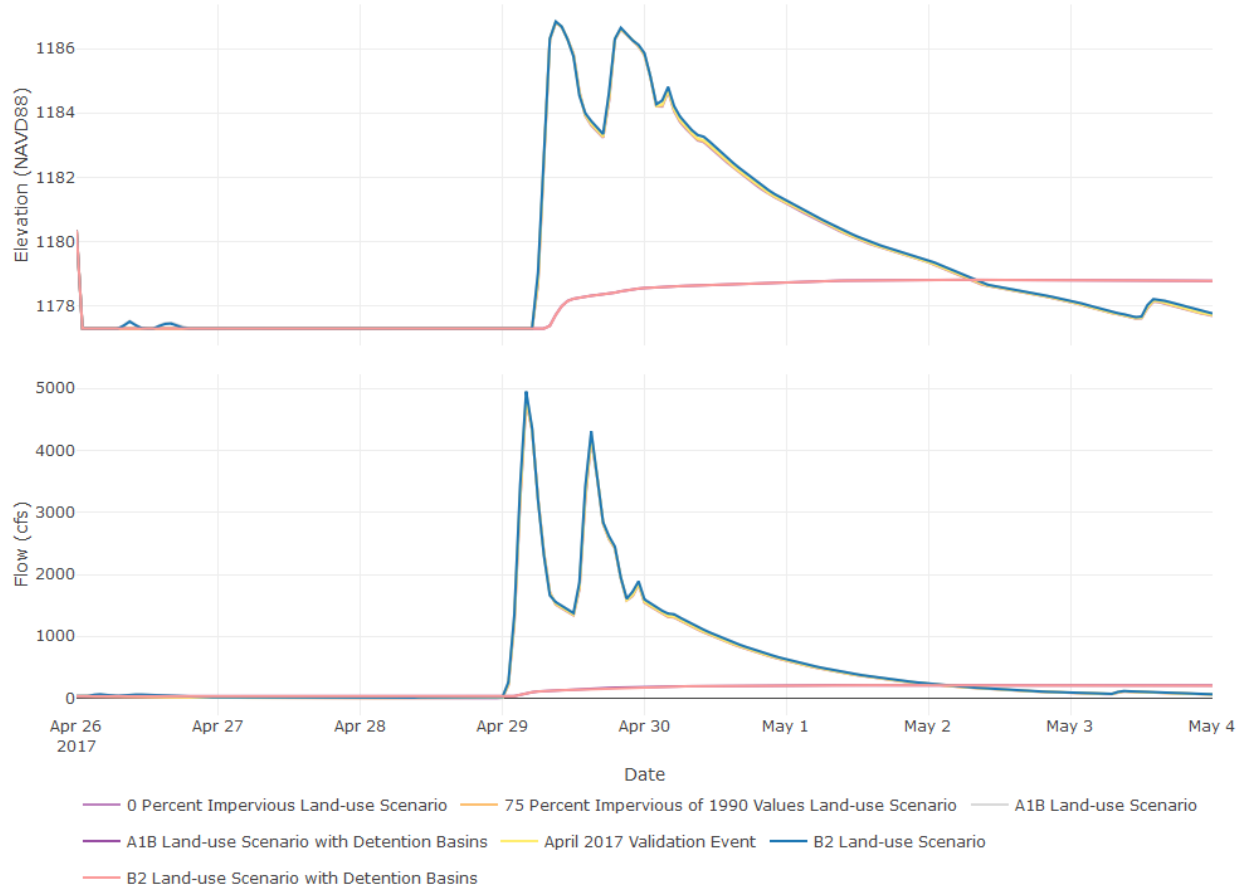
2017 Event 07196000 Flint Creek near Kansas, OK
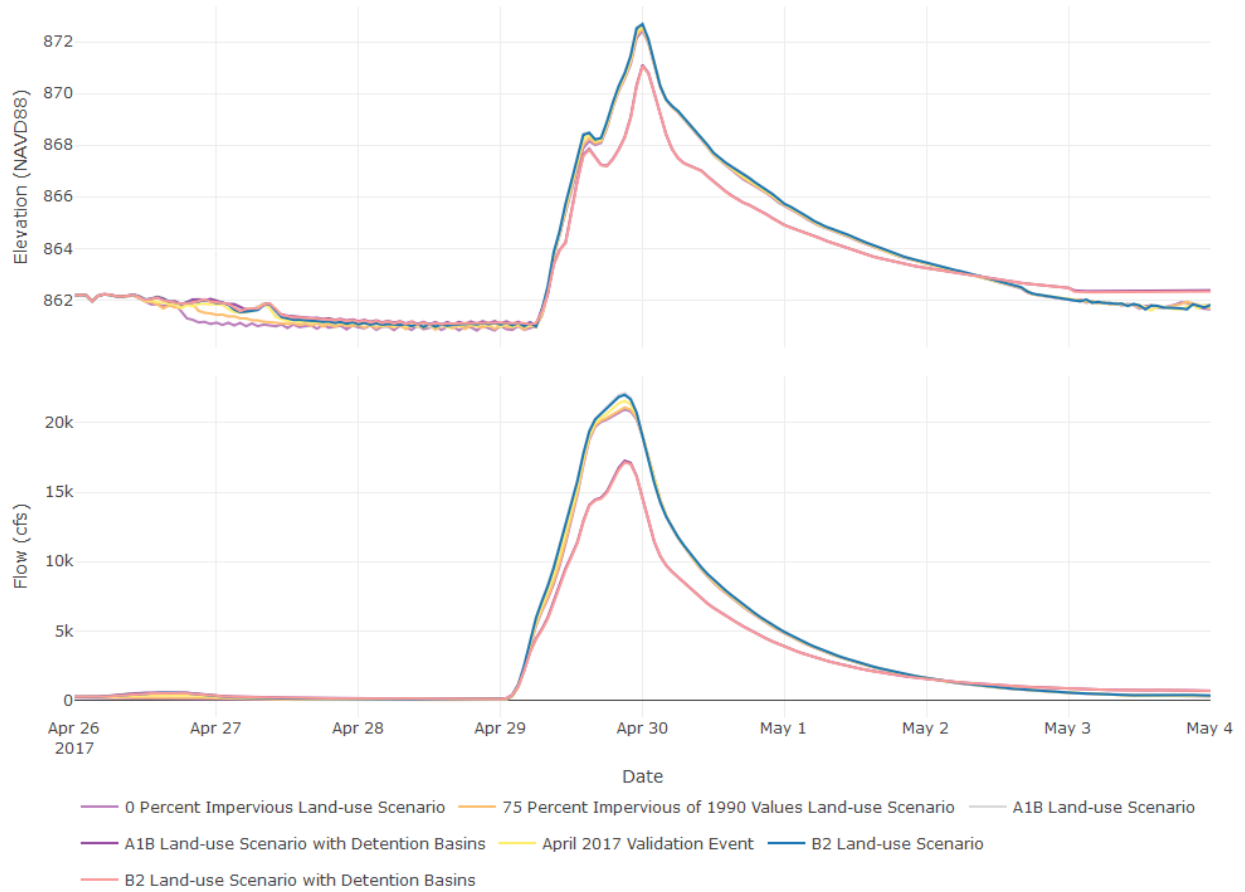
2017 Event 07195855 Flint Creek near West Siloam Springs, OK
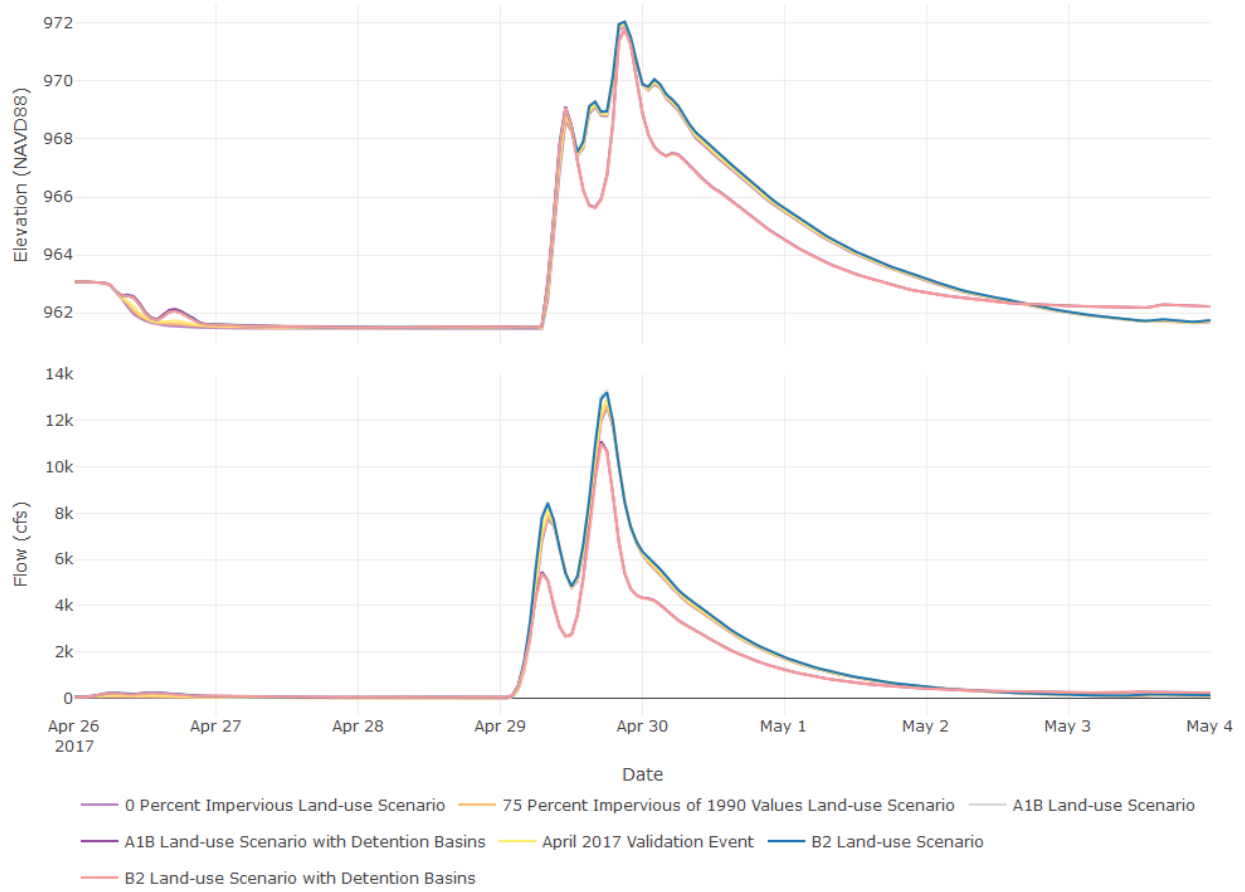
2017 Event 07196090 Illinois River at Chewey, OK
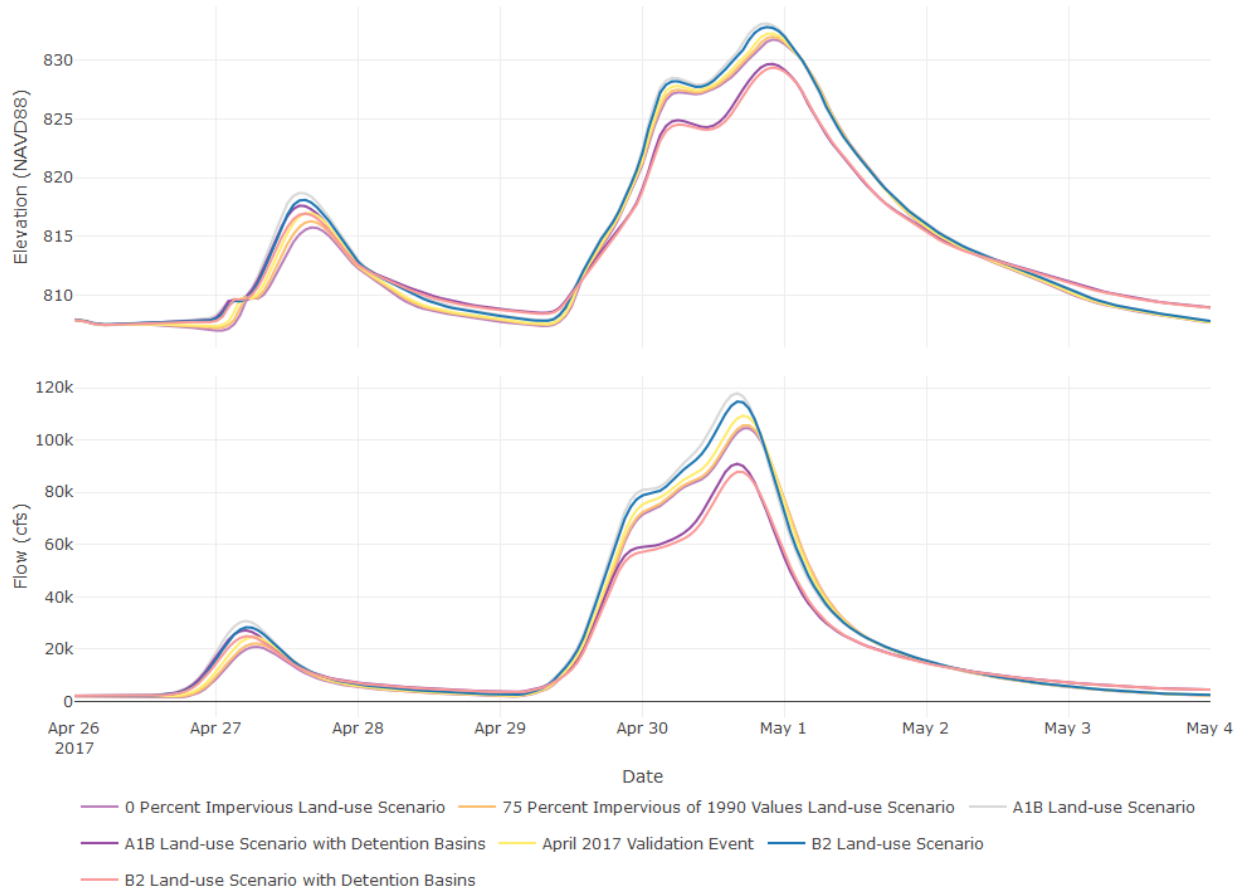
2017 Event 07195400 Illinois River at Hwy. 16 near Siloam Springs AR
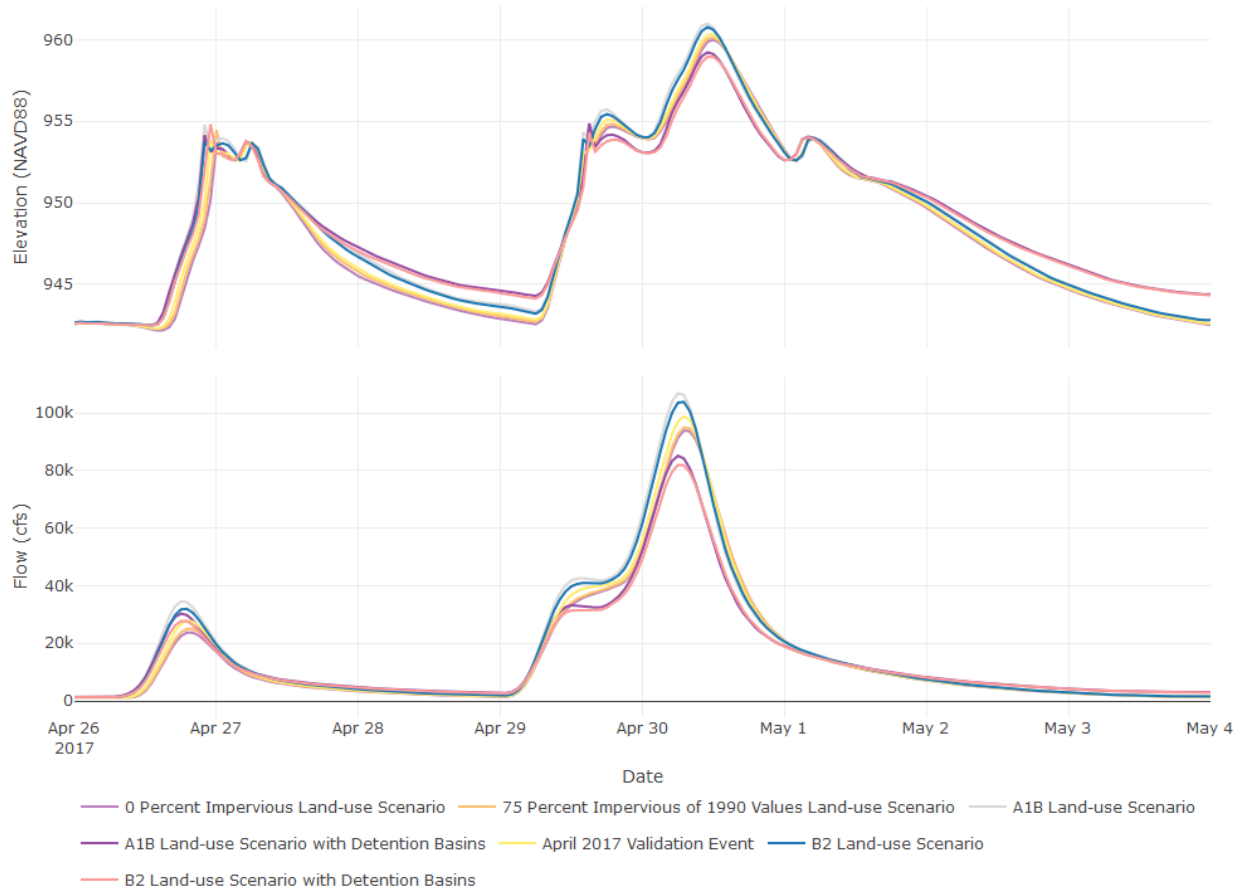
2017 Event 07194800 Illinois River at Savoy, AR

— 0 Percent Impervious Land-use Scenario — 75 Percent Impervious of 1990 Values Land-use Scenario — A1B Land-use Scenario
— A1B Land-use Scenario with Detention Basins — April 2017 Validation Event — B2 Land-use Scenario
— B2 Land-use Scenario with Detention Basins
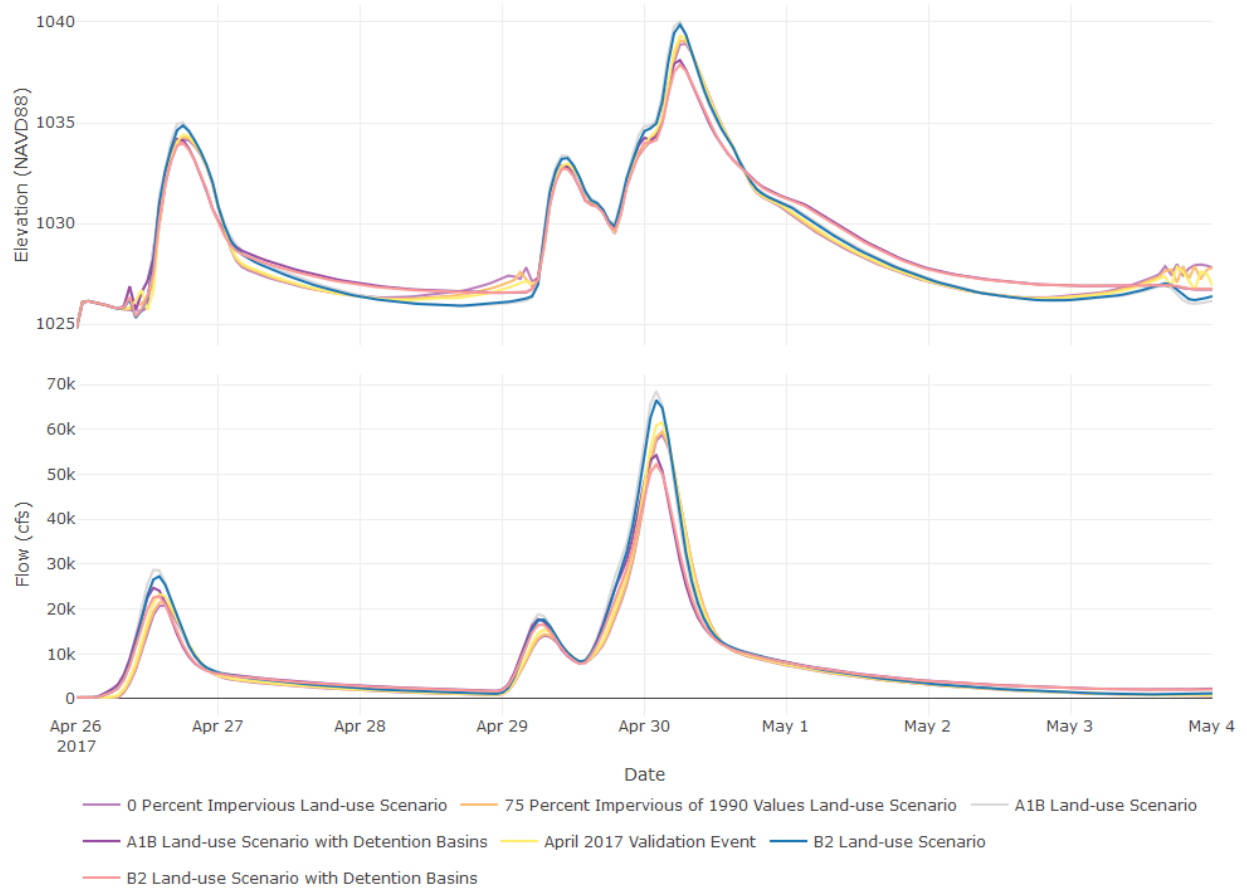
Scenario time-series plots using the 100-year frequency gridded precipitation

1% AEP Event (100-year) 07196900 Baron Fork at Dutch Mills, AR
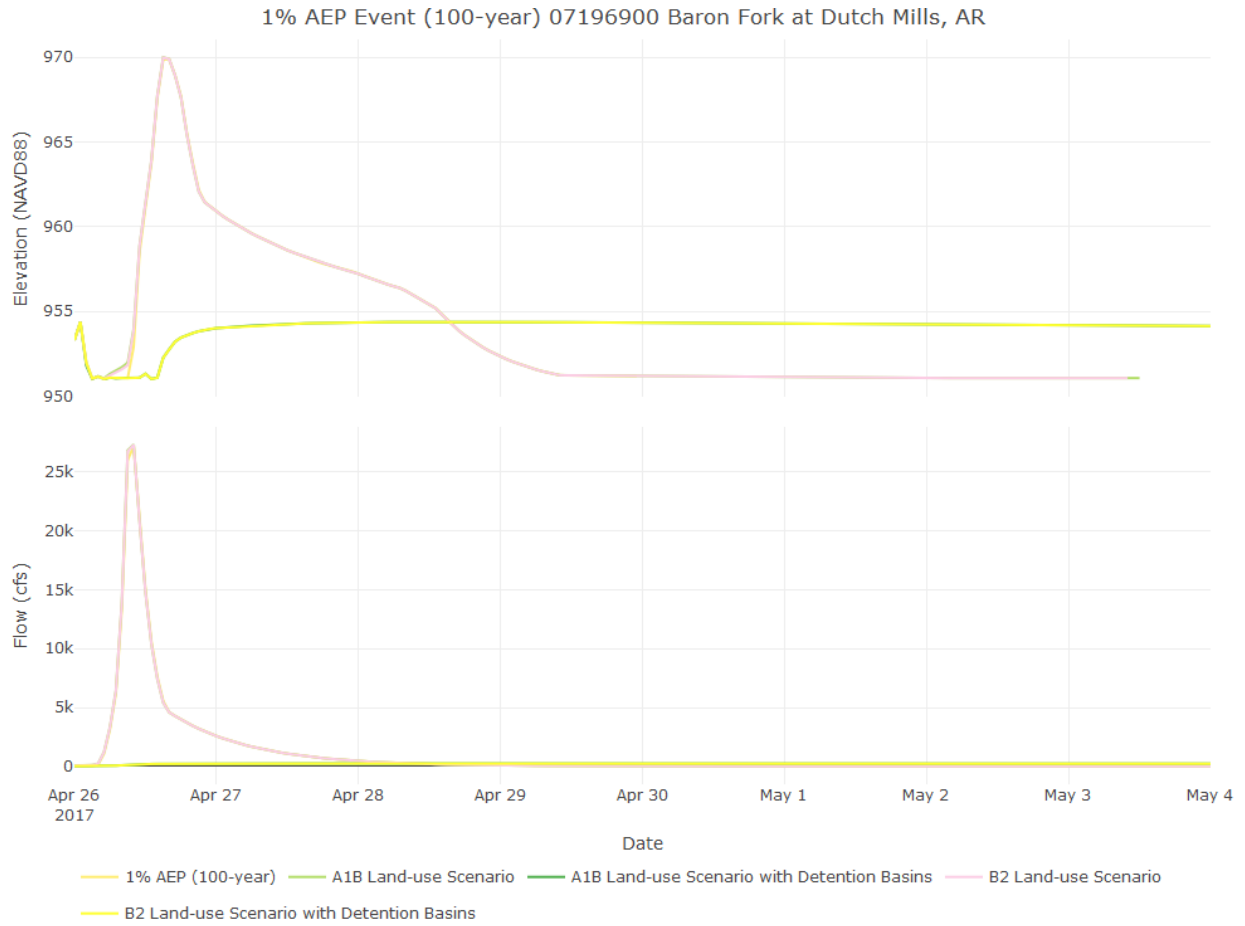
1% AEP Event (100-year) 07197000 Baron Fork at Eldon, OK

Legend: 1% AEP (100-year) — A1B Land-use Scenario — A1B Land-use Scenario with Detention Basins — B2 Land-use Scenario — B2 Land-use Scenario with Detention Basins
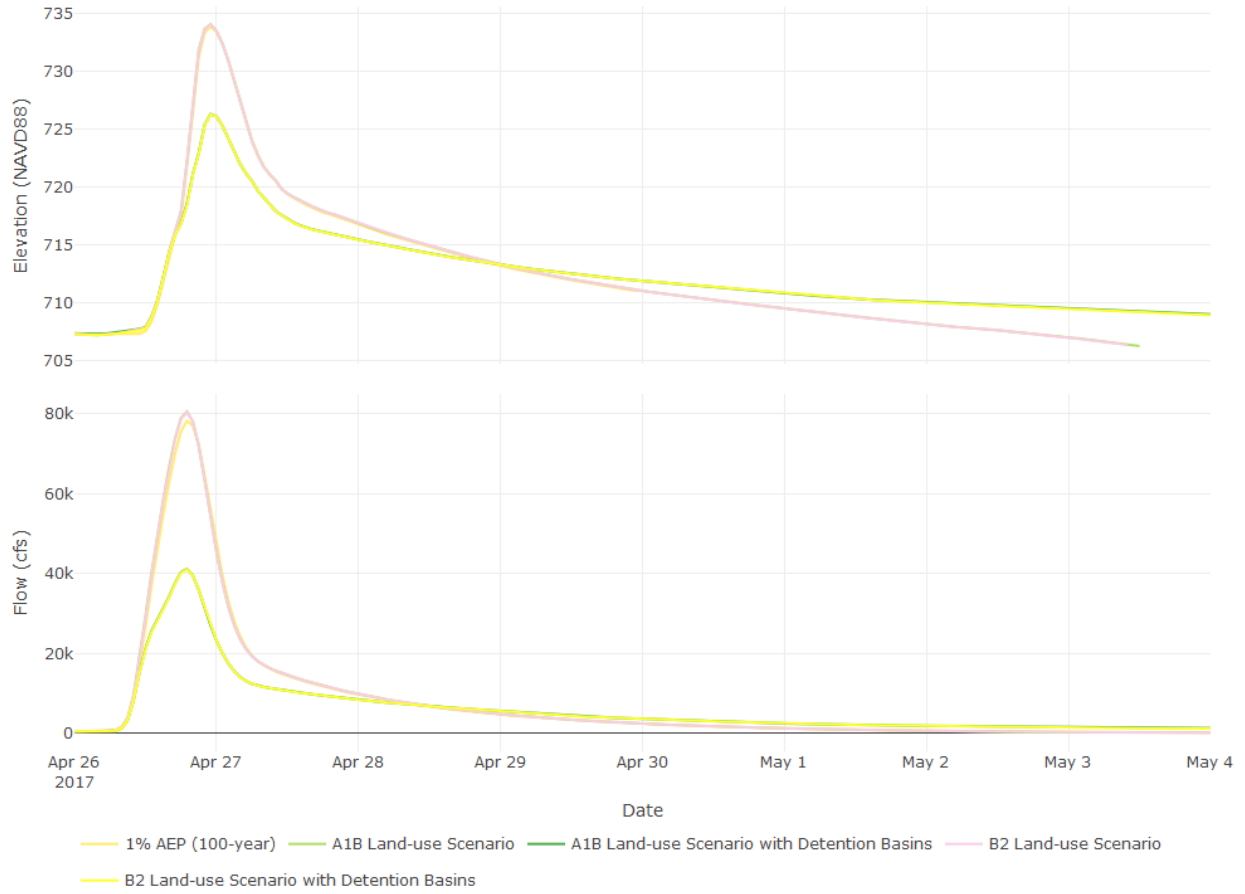
1% AEP Event (100-year) 07196500 Illinois River near Tahlequah, OK
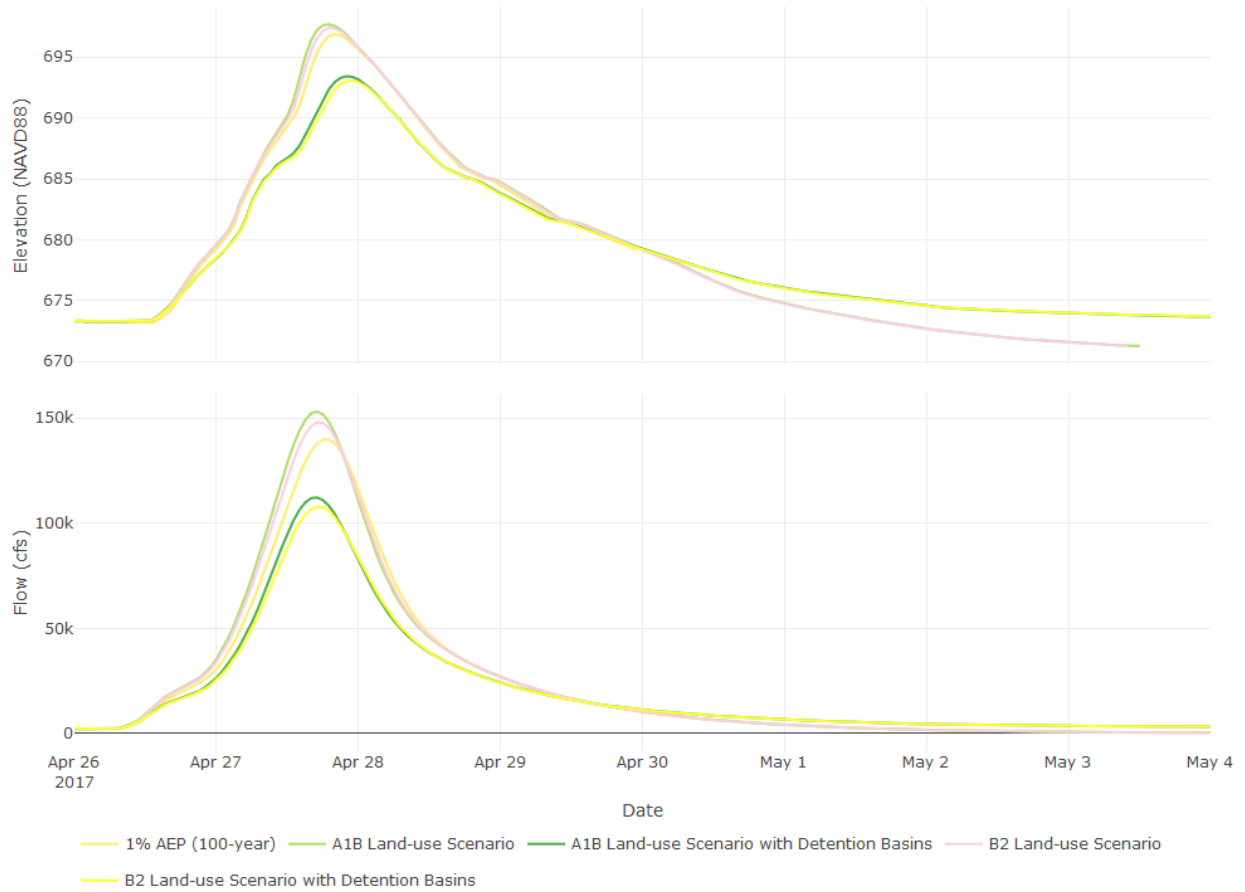
1% AEP Event (100-year) 07195500 Illinois River near Watts, OK
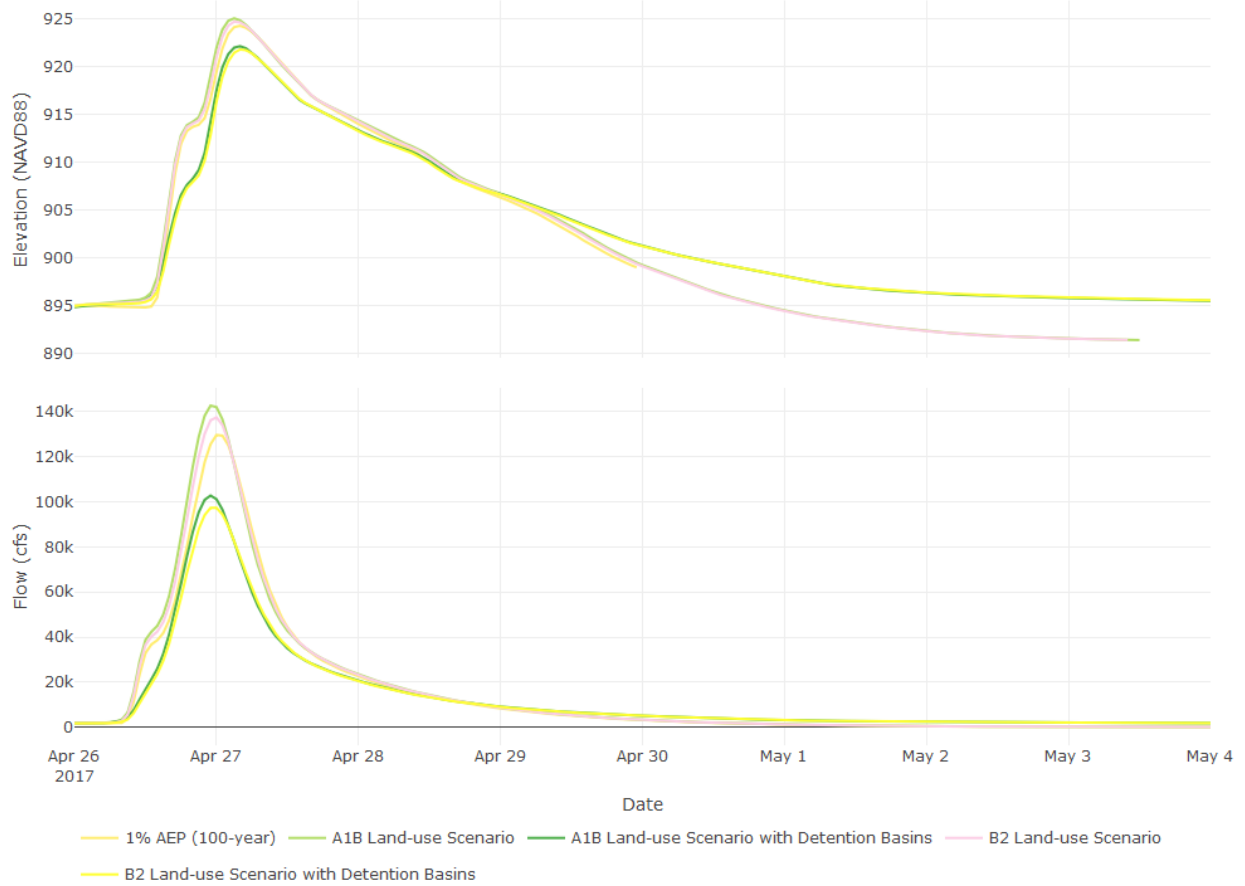
1% AEP Event (100-year) 07195430 Illinois River South of Siloam Springs, AR

1% AEP Event (100-year) 07194880 Osage Creek near Cave Springs, AR

Legend:
- 1% AEP (100-year)
- A1B Land-use Scenario
- A1B Land-use Scenario with Detention Basins
- B2 Land-use Scenario
- B2 Land-use Scenario with Detention Basins
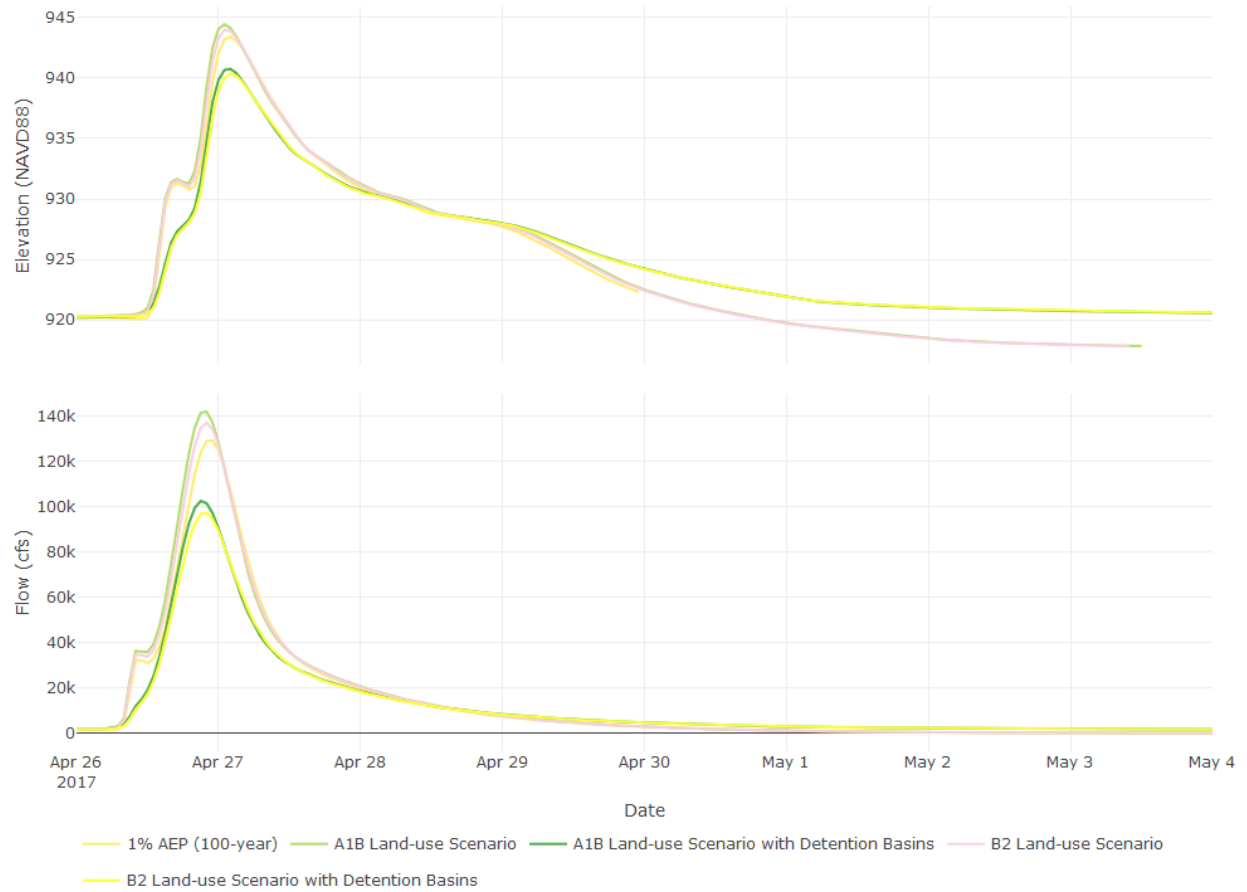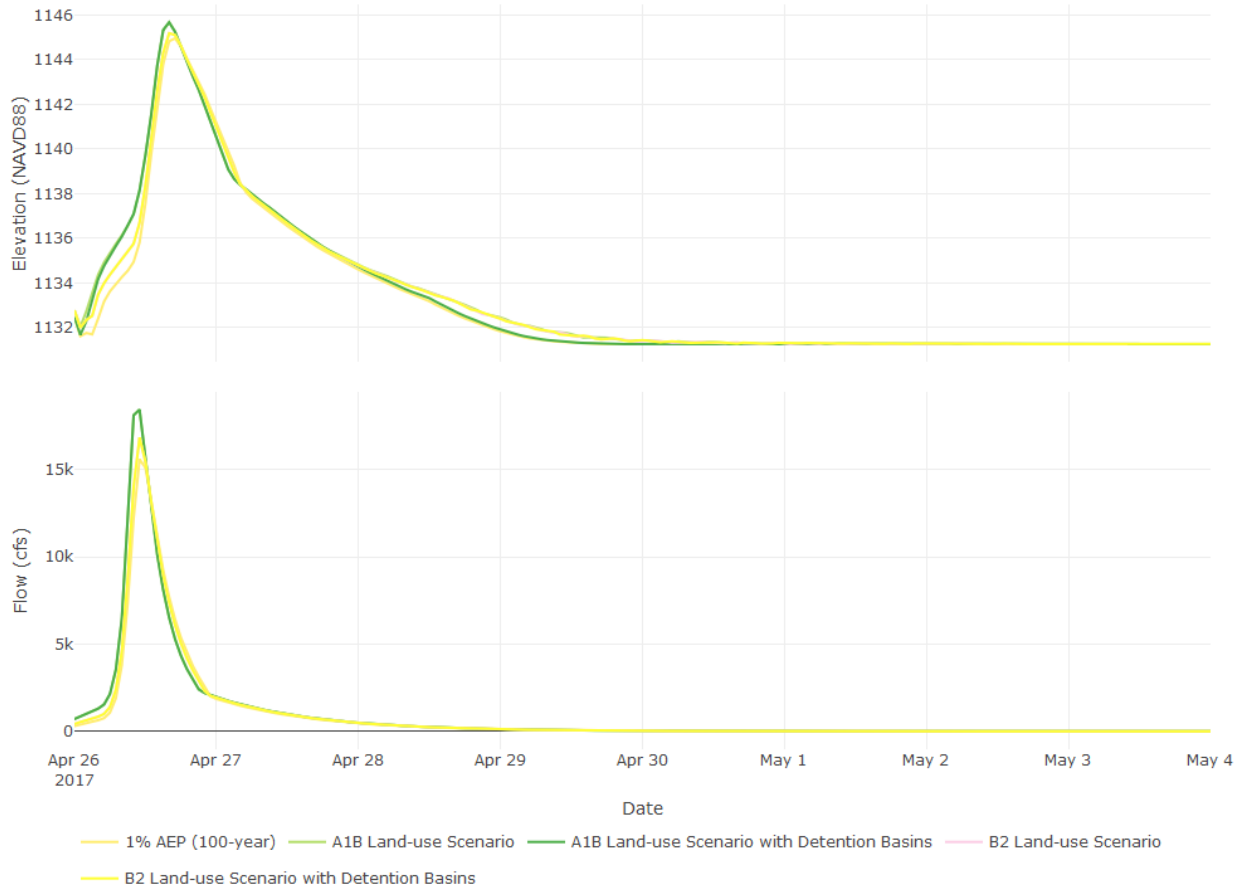
1% AEP Event (100-year) 07195000 Osage Creek near Elm Springs, AR
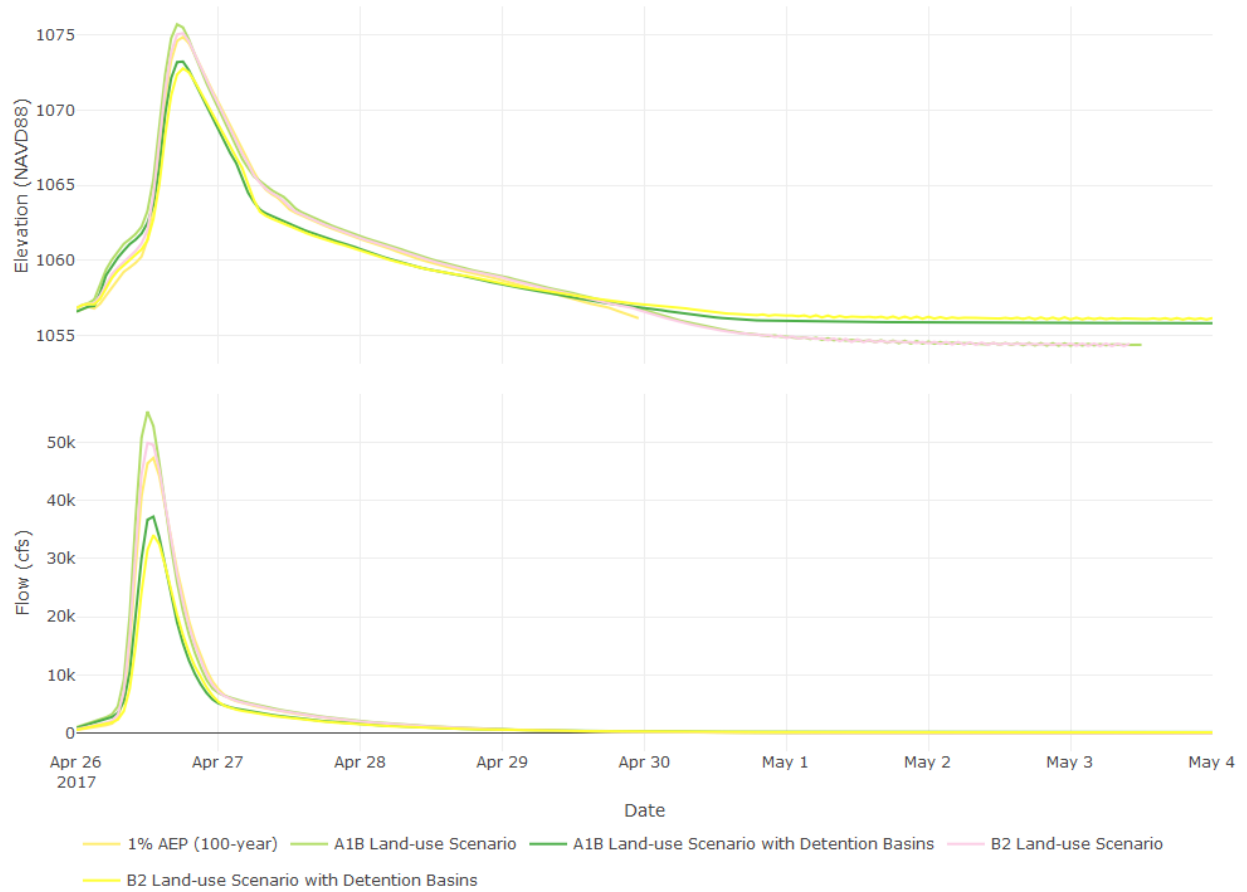
1% AEP Event (100-year) 07195800 Flint Creek at Springtown, AR

Legend:
- 1% AEP (100-year)
- A1B Land-use Scenario
- A1B Land-use Scenario with Detention Basins
- B2 Land-use Scenario
- B2 Land-use Scenario with Detention Basins
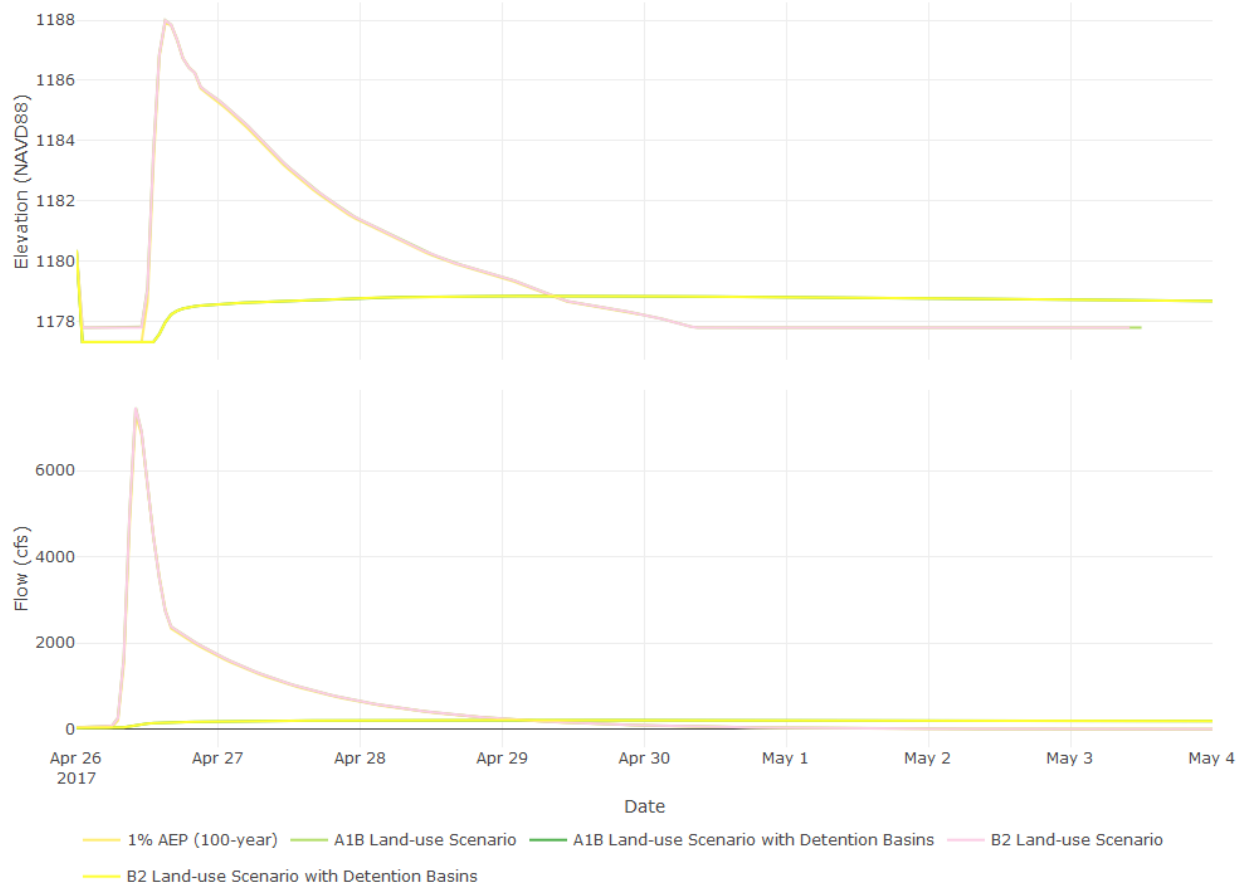
1% AEP Event (100-year) 07196000 Flint Creek near Kansas, OK
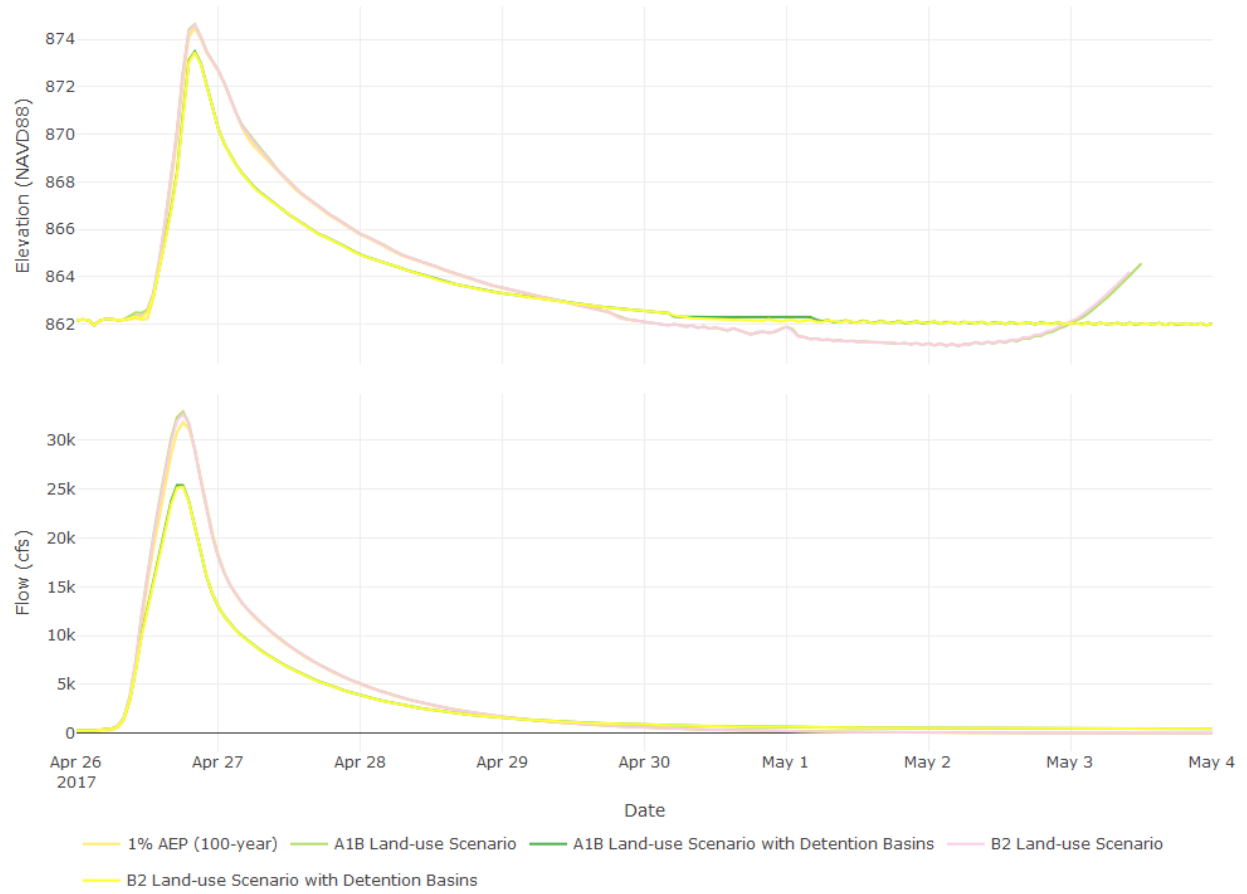
1% AEP Event (100-year) 07195855 Flint Creek near West Siloam Springs, OK
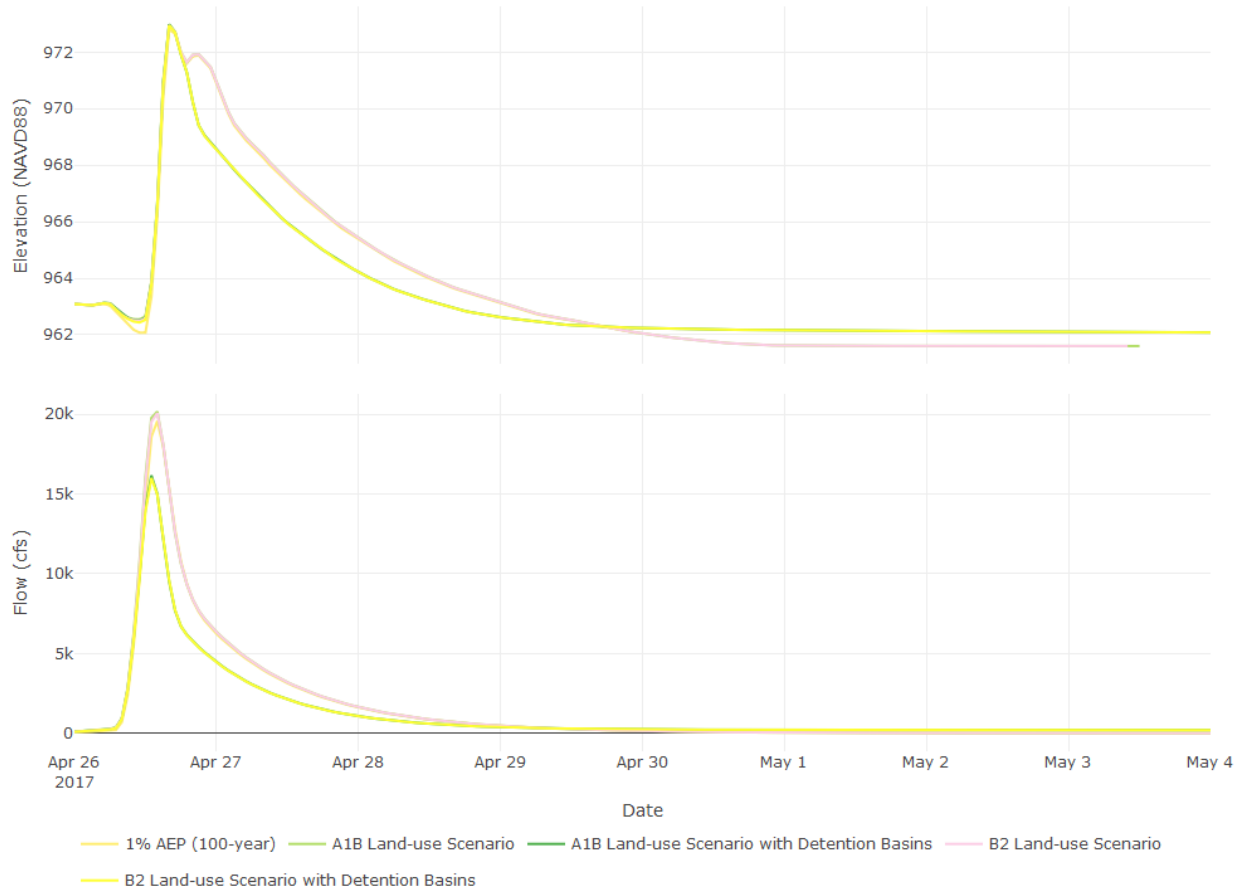
1% AEP Event (100-year) 07196090 Illinois River at Chewey, OK
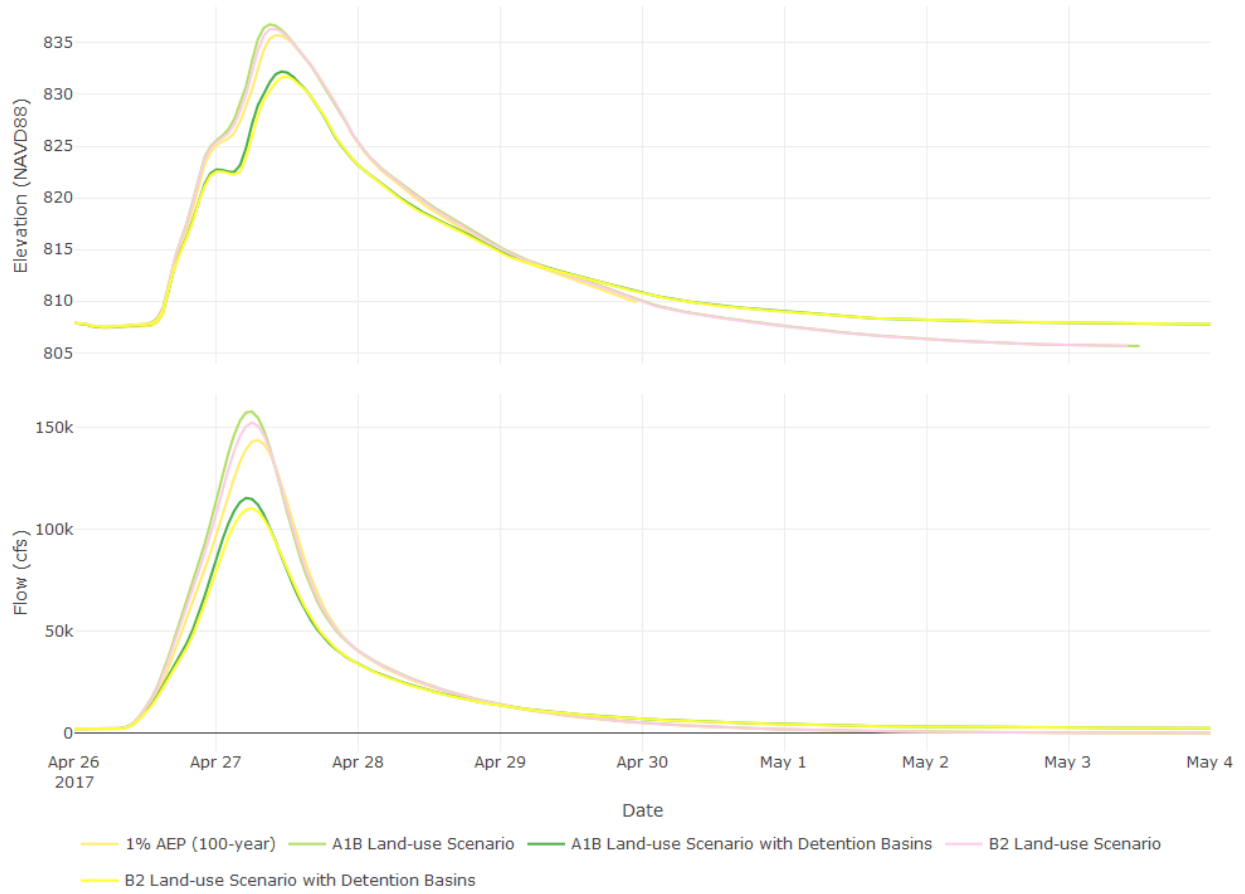
1% AEP Event (100-year) 07195400 Illinois River at Hwy. 16 near Siloam Springs AR
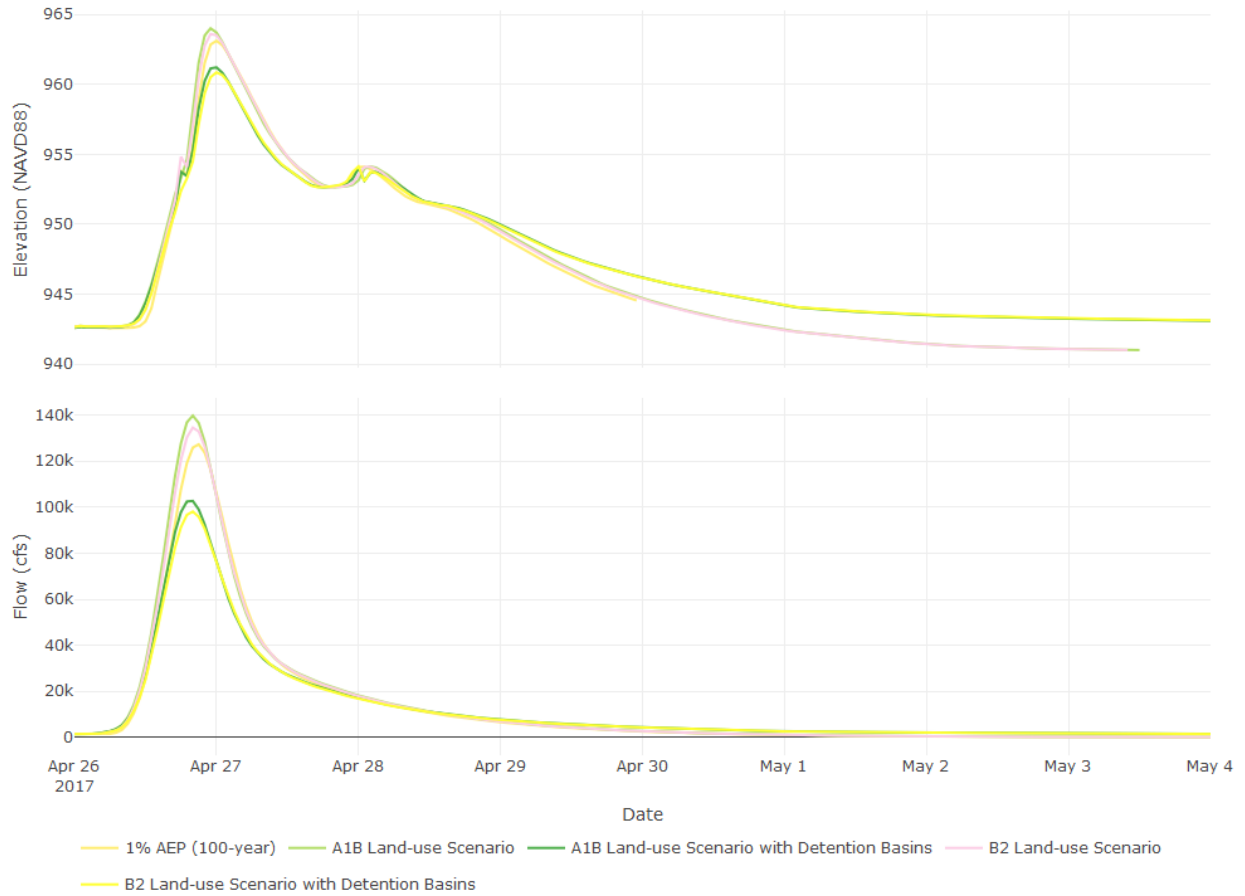
1% AEP Event (100-year) 07194800 Illinois River at Savoy, AR
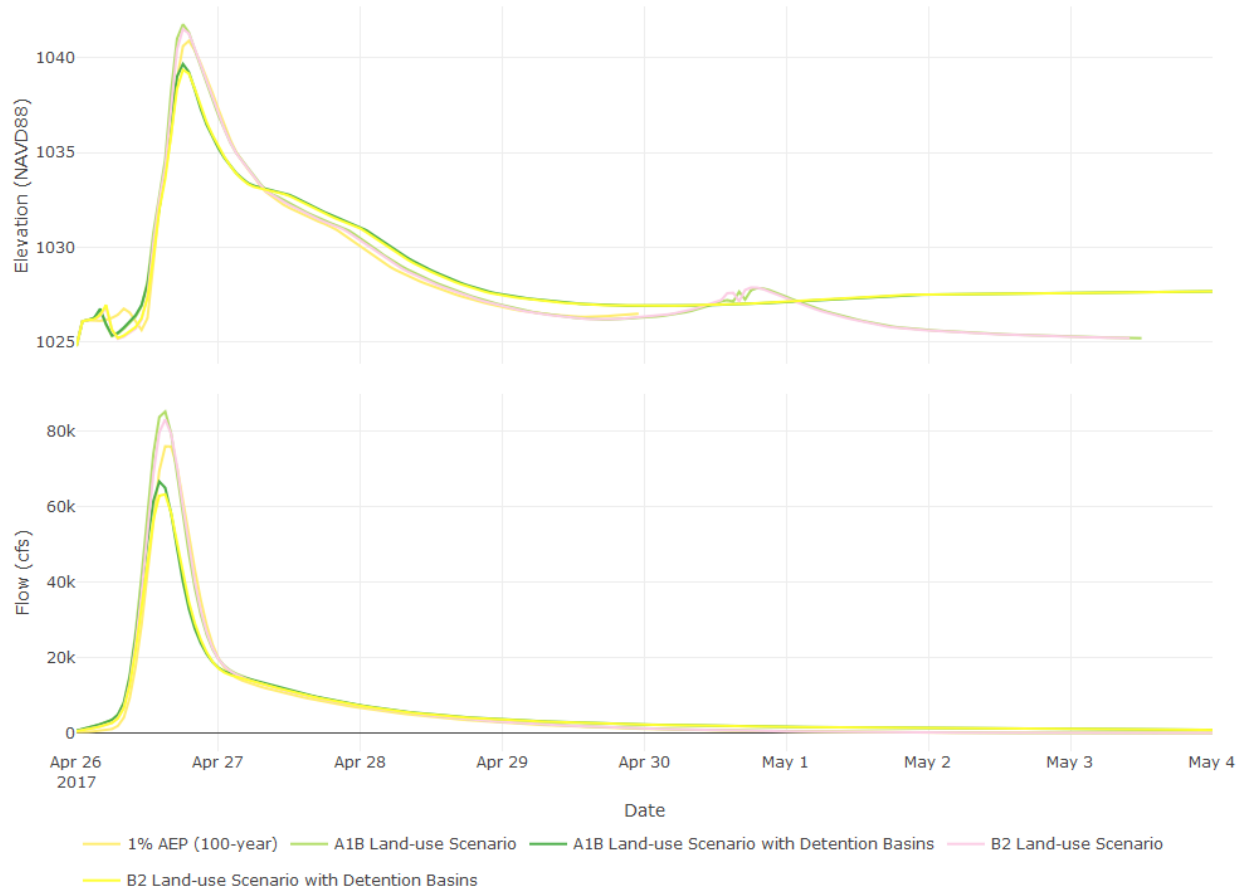
Annual Exceedance Probability (AEP) time-series plots

07196900 Baron Fork at Dutch Mills, AR

07197000 Baron Fork at Eldon, OK

Legend:
- 1% AEP (100-year)
- 10% AEP (10-year)
- 2% AEP (50-year)
- 20% AEP (5-year)
- 4% AEP (25-year)
- 50% AEP (2-year)

07196500 Illinois River near Tahlequah, OK

07195500 Illinois River near Watts, OK

07195430 Illinois River South of Siloam Springs, AR

Legend: 1% AEP (100-year), 10% AEP (10-year), 2% AEP (50-year), 20% AEP (5-year), 4% AEP (25-year), 50% AEP (2-year)
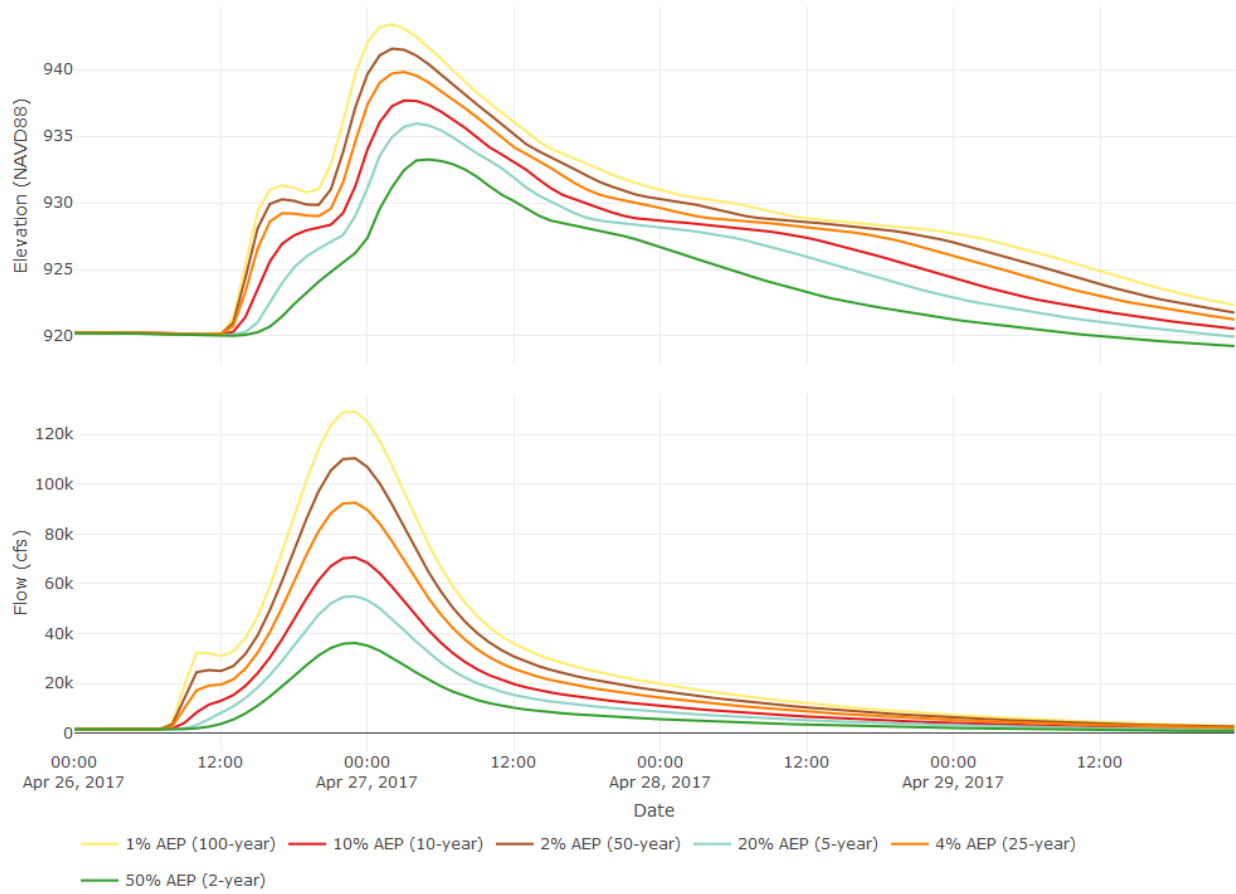
07194880 Osage Creek near Cave Springs, AR

07195000 Osage Creek near Elm Springs, AR

07195800 Flint Creek at Springtown, AR

07196000 Flint Creek near Kansas, OK

07195855 Flint Creek near West Siloam Springs, OK
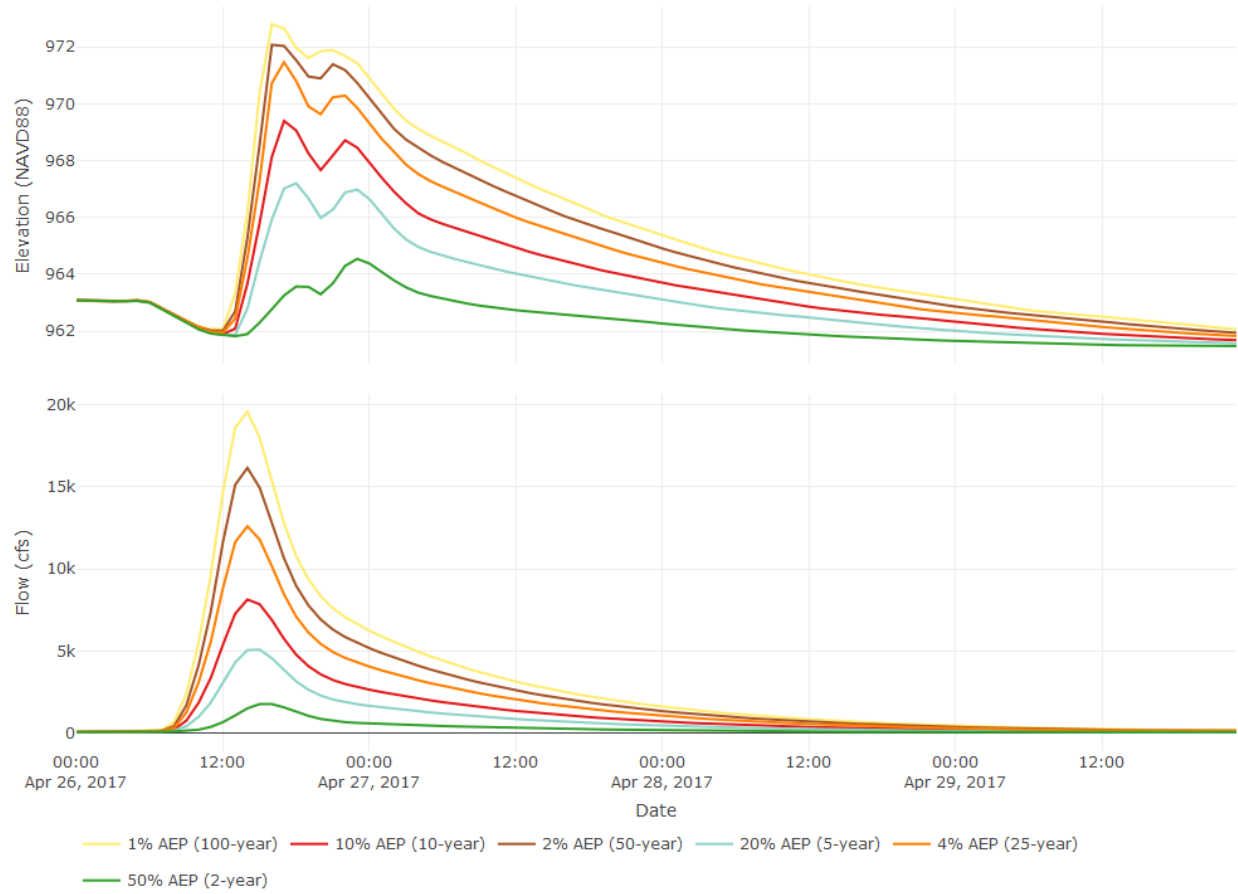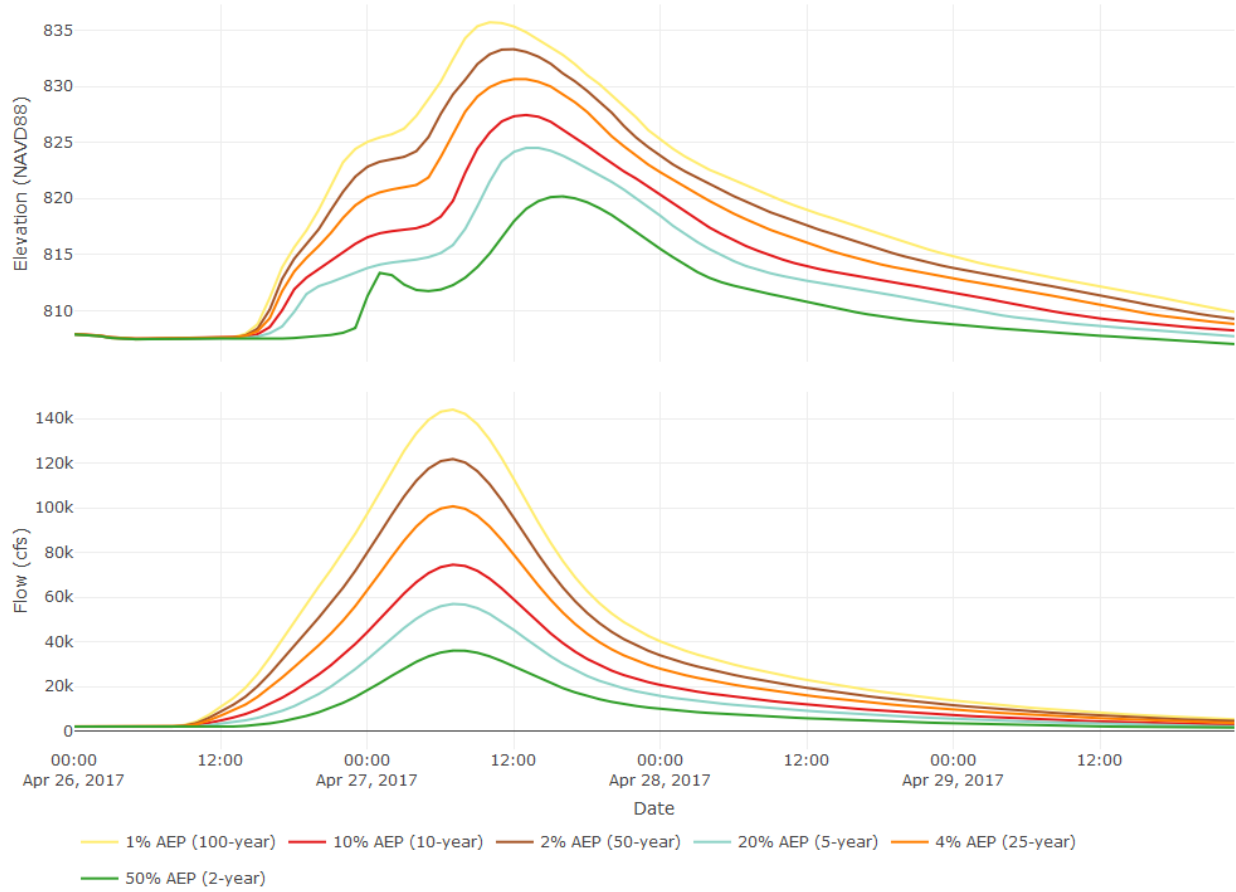
07196090 Illinois River at Chewey, OK

07195400 Illinois River at Hwy. 16 near Siloam Springs AR
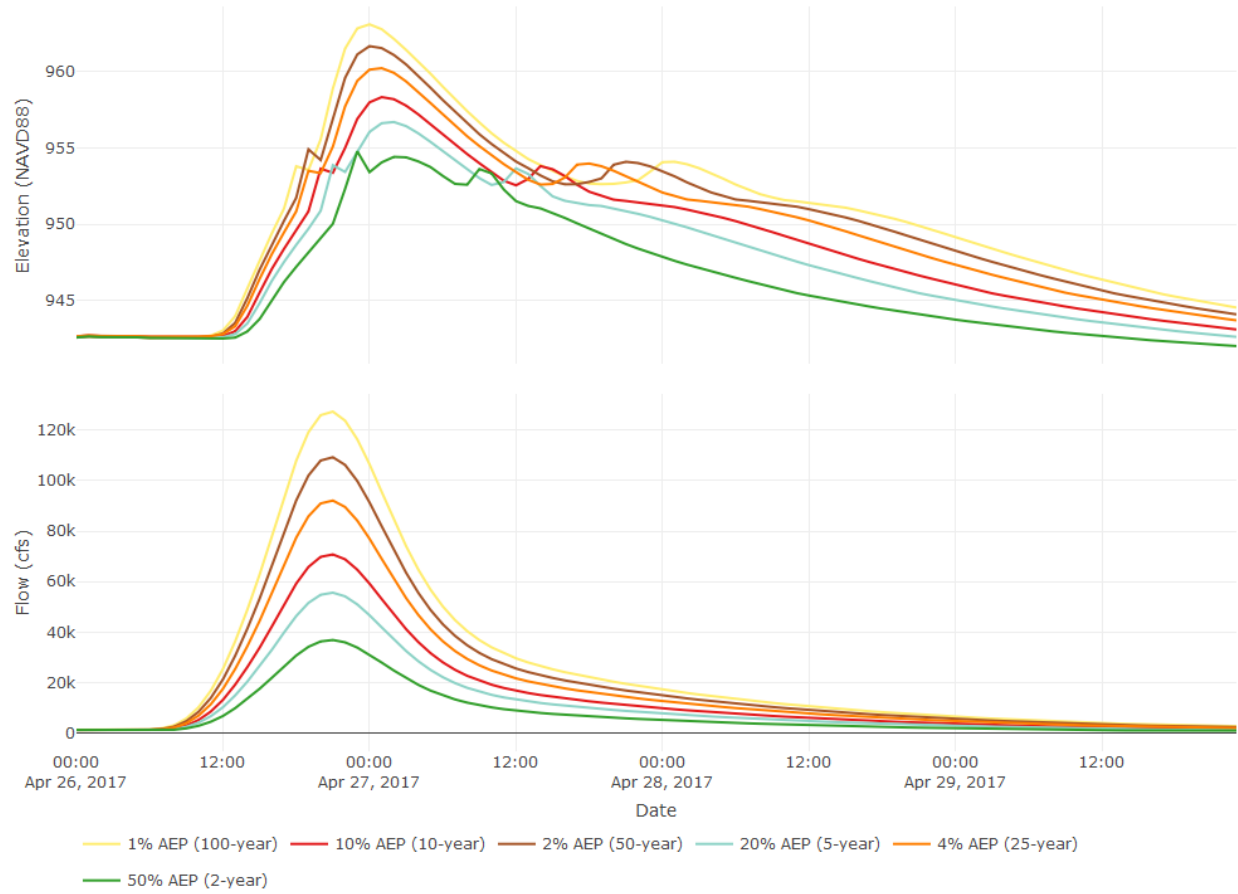
07194800 Illinois River at Savoy, AR
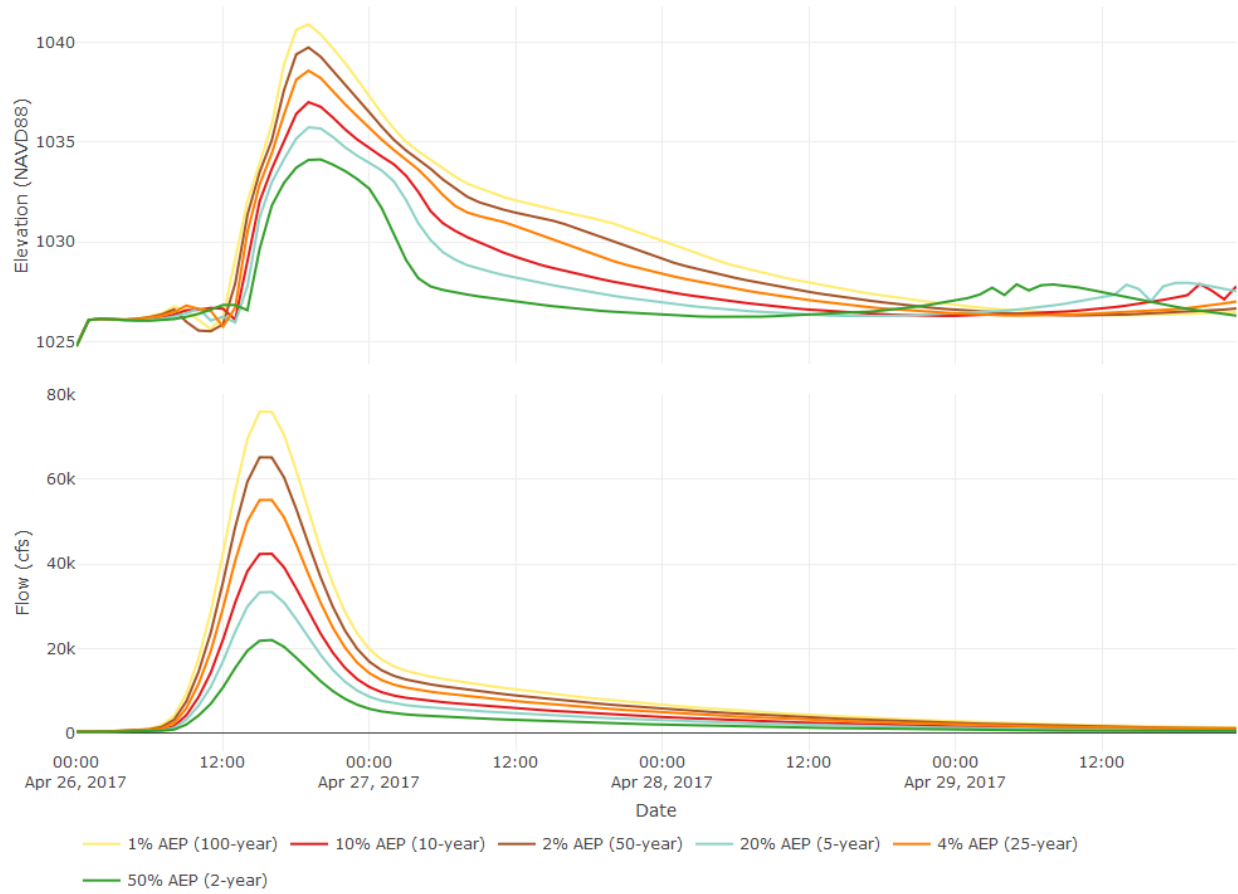
Scenario time-series plots with 100-foot riparian buffers
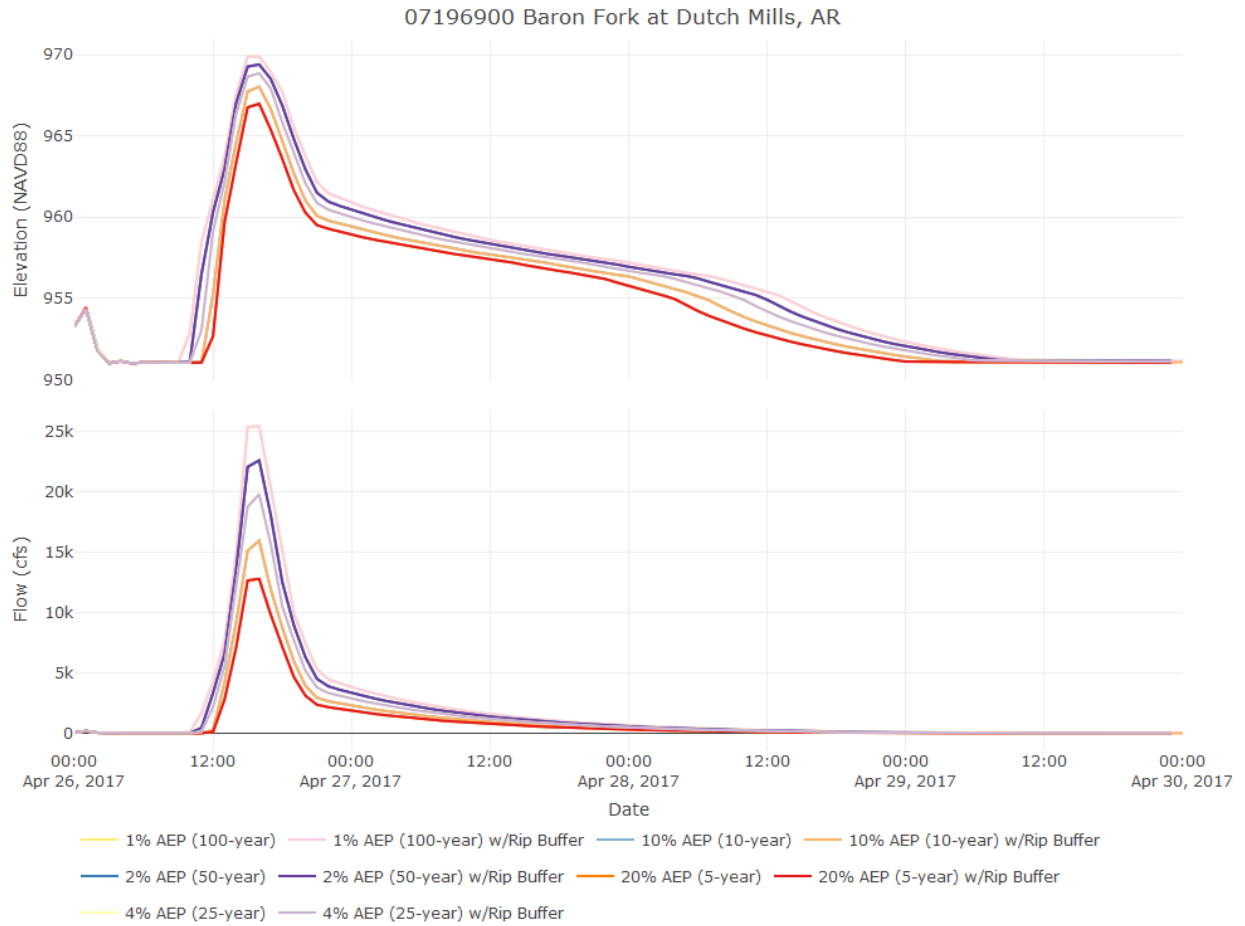
07196900 Baron Fork at Dutch Mills, AR
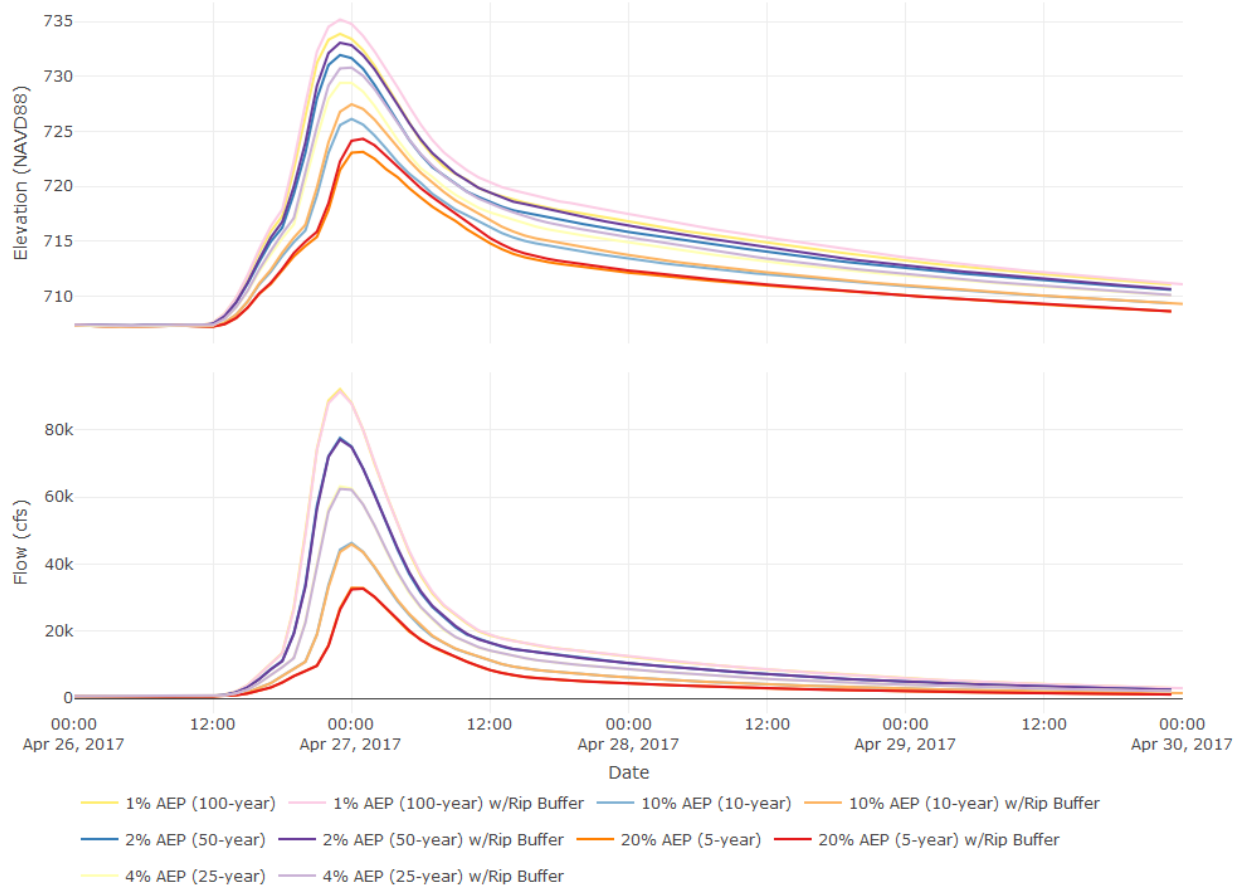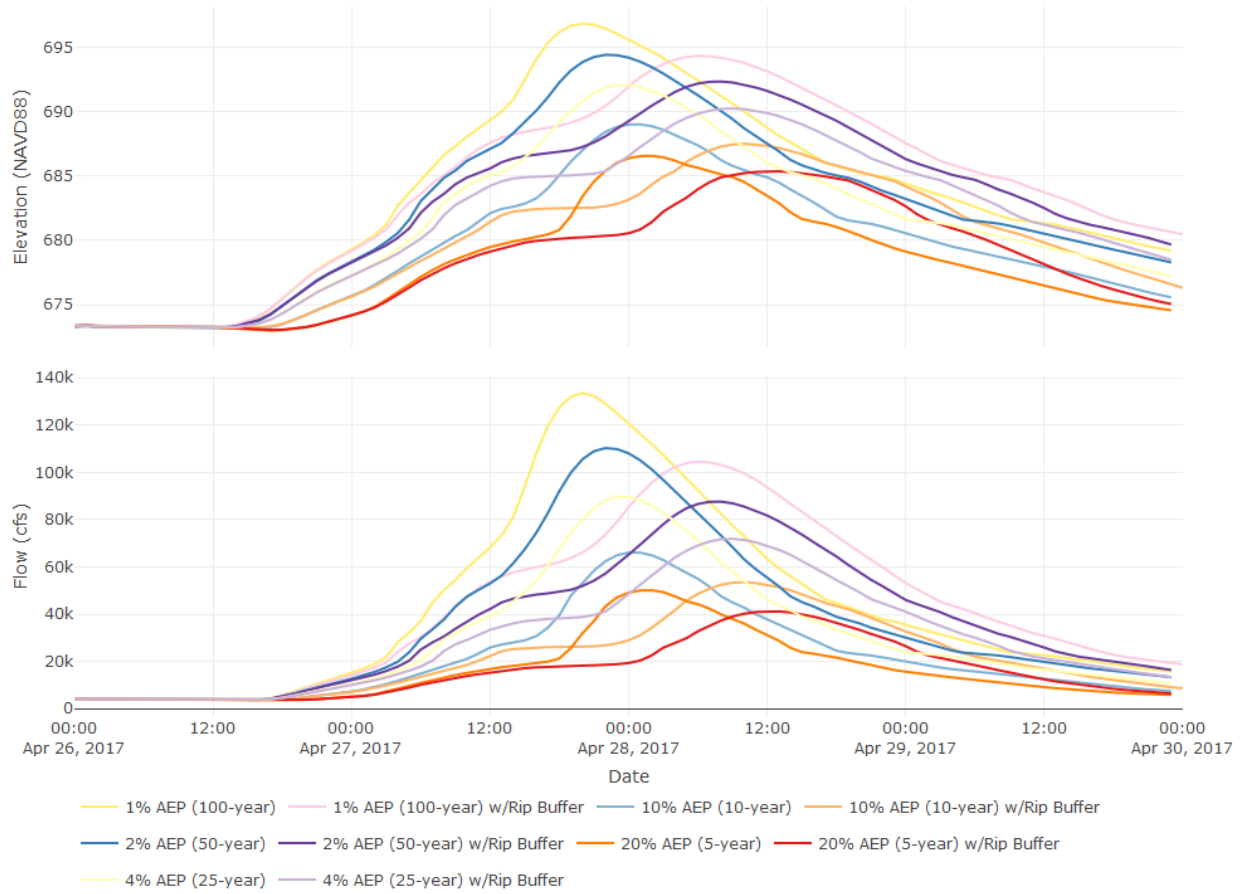
Legend:
- 1% AEP (100-year)
- 1% AEP (100-year) w/Rip Buffer
- 10% AEP (10-year)
- 10% AEP (10-year) w/Rip Buffer
- 2% AEP (50-year)
- 2% AEP (50-year) w/Rip Buffer
- 20% AEP (5-year)
- 20% AEP (5-year) w/Rip Buffer
- 4% AEP (25-year)
- 4% AEP (25-year) w/Rip Buffer

07197000 Baron Fork at Eldon, OK

Legend:
- 1% AEP (100-year)
- 1% AEP (100-year) w/Rip Buffer
- 10% AEP (10-year)
- 10% AEP (10-year) w/Rip Buffer
- 2% AEP (50-year)
- 2% AEP (50-year) w/Rip Buffer
- 20% AEP (5-year)
- 20% AEP (5-year) w/Rip Buffer
- 4% AEP (25-year)
- 4% AEP (25-year) w/Rip Buffer

07196500 Illinois River near Tahlequah, OK

07195500 Illinois River near Watts, OK
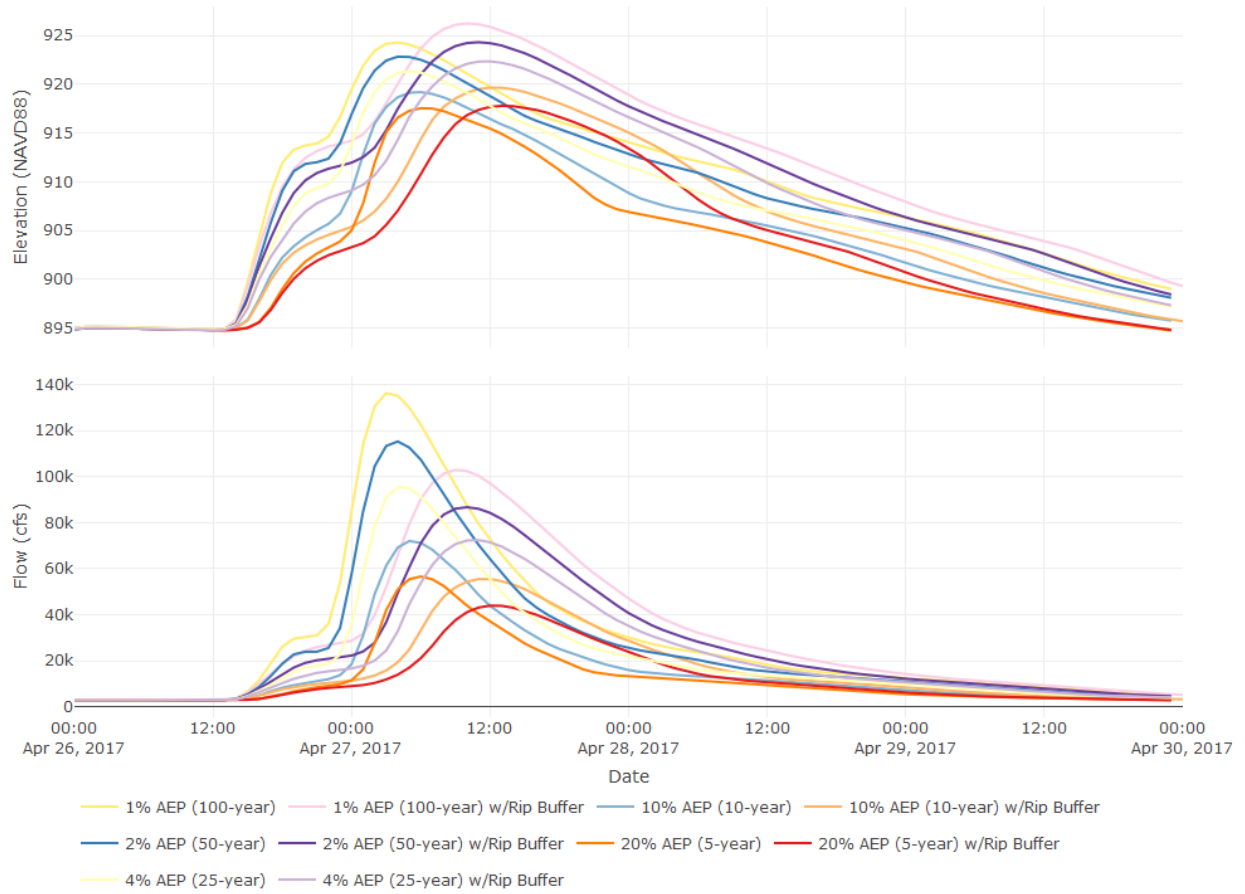
07195430 Illinois River South of Siloam Springs, AR

07194880 Osage Creek near Cave Springs, AR

07195000 Osage Creek near Elm Springs, AR

07195800 Flint Creek at Springtown, AR

07196000 Flint Creek near Kansas, OK

Legend:
- 1% AEP (100-year)
- 1% AEP (100-year) w/Rip Buffer
- 10% AEP (10-year)
- 10% AEP (10-year) w/Rip Buffer
- 2% AEP (50-year)
- 2% AEP (50-year) w/Rip Buffer
- 20% AEP (5-year)
- 20% AEP (5-year) w/Rip Buffer
- 4% AEP (25-year)
- 4% AEP (25-year) w/Rip Buffer

07195855 Flint Creek near West Siloam Springs, OK

07196090 Illinois River at Chewey, OK

07195400 Illinois River at Hwy. 16 near Siloam Springs AR

07194800 Illinois River at Savoy, AR